2022

Novel signalling pathways resolving the inflammatory response during peripheral nerve regeneration

Woodley, Patricia Kate

http://hdl.handle.net/10026.1/19594

http://dx.doi.org/10.24382/454
University of Plymouth

UNIVERSITY OF PLYMOUTH

Novel signalling pathways resolving the inflammatory response during peripheral nerve regeneration.

by **PATRICIA KATE WOODLEY**

A thesis submitted to the University of Plymouth in

partial fulfilment for the degree of

DOCTOR OF PHILOSOPHY

Peninsula Medical School

December 2021

Author's Declaration

At no time during the registration for the degree of Doctor of Philosophy has the author been registered for any other University award without prior agreement of the Doctoral College Quality Sub-Committee.

Work submitted for this research degree at the University of Plymouth has not formed part of any other degree either at the University of Plymouth or at another establishment.

Publications (or public presentation of creative research outputs):

- Dun, X. P., et al. (2019), 'Macrophage-Derived Slit3 Controls Cell Migration and Axon Pathfinding in the Peripheral Nerve Bridge', Cell Reports, 26 (6), 1458-+. DOI: 10.1016/j.celrep.2018.12.081
- Woodley, P. K., et al. (2019). "Distinct VIP and PACAP Functions in the Distal Nerve Stump During Peripheral Nerve Regeneration." Frontiers in Neuroscience 13(1326). DOI: 10.3389/fnins.2019.01326

Presentations at conferences:

- *Axon 2019 "Circuits Development & Axon Regeneration" – Poster presentation*

Word count of main body of thesis: 43,650

Signed: Patricia Kate Woodley

Date: 30/12/2021

Acknowledgements
I would like to thank my Director of Studies Xin Peng Dun for giving me the opportunity to undertake this PhD and for all his help, support and guidance through the process. Your expertise really helped me succeed, thank you for sharing it with me. I would also like to extend my thanks to David Parkinson your input has been immeasurable. Thank to Glenn at the EM unit for all your help processing the samples and producing the images required for part of this project.

My home friends have been both a source of support and security during these times, especially you Mel, thank you. I have also been extremely lucky to meet same fantastic lab mates during my time at the University of Plymouth, the chats, laughter and jokes got me through some particularly long and tough lab days. I was to give special thanks to my lab bestie Liyam, what a ride we have had. Not only have you helped me to work hard and play hard you also gave me hope and support when I needed it the most.

I have been lucky enough to have the most supportive family during this time. To my bothers, Tom and Phil, I cannot thank you enough for your support along the way especially on days you were subjected to my terrible moods, I could not have asked for better brothers. Dad, I would not have been able to complete the journey without your support and unconditional love, I know raising me has not been an easy journey, but I hope I make you proud.

Adam, how lucky I am to have you in my life. You might not necessarily get what I do but your unwavering support and motivation was exactly what I needed to get me to the end of this journey. You have been the light in my dark and have done everything you can to help me through some of difficulties I have faced during this time from providing unmeasurable amounts of love and laughs to finally allowing me to get our

pooch, Dudley. Adam and Dudley, words cannot describe how grateful I am for you and how much I love you both.

Finally, I dedicate this thesis to grandmother a journey you were here to see me embark upon but unfortunately not to see me finish.

Abstract
Novel signalling pathways resolving the inflammatory response during peripheral nerve regeneration.

by Patricia Kate Woodley

Introduction. The peripheral nervous system has the remarkable capacity to regenerate and restore function following damage or disease. Instrumental in this regenerative process are macrophages, Schwann cells and the production of inflammatory cytokines. The production of inflammatory cytokines from macrophages and Schwann cells needs to be tightly regulated to ensure efficient regeneration and to prevent chronic inflammation. Currently there is limited knowledge regarding which signalling pathways act to control both the inflammatory response and macrophage efflux that allows tissue homeostasis to resume within the peripheral nerves. This thesis aims to investigate the expression pattern and distinct function of VIP and PACAP and their receptors VPAC1, VPAC2 and PAC1 in the peripheral nerve post injury and how signalling through these receptors can act to promote resolution of the inflammatory response. Once macrophages have executed their function, they are required to leave the peripheral nerve to prevent chronic inflammation. There is only one macrophage efflux mechanism currently described in the peripheral nerves, where the NOGO receptors interacts with myelin to promote macrophage clearance. EphA5 has been shown to be upregulated in various RNA sequencing data sets and can induce contact dependent migratory behaviour within cells. EphA5-EphrinA signalling as a potential mechanism to induce macrophage migration and efflux out of the peripheral nerve was investigated.

Methods. This project uses a combination of in vitro, ex vivo and in vivo models, including primary macrophage and Schwann cell cultures and mouse sciatic nerve cut

and crush injury models to establish the function of VIP and PACAP and EphA5-EphrinA signalling at various time points throughout peripheral nerve regeneration.

Results. My results show VPAC1, VPAC2, and PAC1 to be up-regulated in the mouse distal nerve following peripheral nerve injury and are highly expressed in Schwann cells and macrophages within the distal sciatic nerve. VIP and PACAP can act on cultured rat Schwann cells, to promote myelin gene expression but can also inhibit the release of pro-inflammatory cytokines by Schwann cells. In addition to this, we show VIP and PACAP can act through macrophages to inhibit pro-inflammatory cytokine expression. EphA5 and EphrinA ligands expression is also upregulated after injury. EphA5 is expressed from macrophages and Schwann cells in the distal nerve stump and EphA5 global knock out (KO) leads to increased macrophage numbers in the distal nerve stump up to 60 days post injury and a decrease in axon regeneration into the nerve bridge. Additionally, migration assays further showed Schwann cell and macrophage migration to be decreased upon inhibition of EphA5 in vitro. Finally, following a crush injury, EphA5 KO mice have a slower recovery of sensory and motor function and decreased g-ratios at 28DPI suggesting a role for EphA5-dependent signalling in functional recovery.

Conclusions. This data provides evidence that VIP and PACAP have important functions in the distal nerve stump following injury to promote remyelination and regulate the inflammatory response. Consequently, VIP and PACAP receptors represent important potential targets to promote peripheral nerve repair following injury. In addition, my results also shows a novel function for the upregulated expression of EphA5 and EphrinA in injured peripheral nerves. EphA5 KO mice revealed that EphA5 signalling is important for both macrophage and Schwann cell migratory function following injury. EphA signalling through EphA5 expressed on

macrophages is revealed to be an important signalling pathway for macrophage efflux out of the peripheral nerve following peripheral nerve injury, whereas EphA5 signaliing through Schwann cells could act to promote Schwann cell elongation and migration into the nerve bridge

Abbreviations

Abbreviation	
BDNF	Brain-derived neurotrophic factor
BSA	Bovine serum albumin
CDIP	Chronic demyelinating inflammatory neuropathy
cDNA	Complementary deoxyribonucleic acid
CIL	Contact inhibition of locomotion
CMT	Charcot Marie Tooth
CNS	Central nervous system
DCC	Deleted in colorectal cancer
DMEM	Dulbecco's modified Eagle's medium
DNA	Deoxyribonucleic acid
DPI	Days post injury
DRG	Dorsal root ganglion
EDTA	Ethylenediaminetetraacetic acid
EM	Electron microscopy
Eph	Erythropoietin-producing hepatocellular carcinoma
Ephrin	Eph receptor-interacting protein
ERK	Extracellular signal-regulated kinase
FBS	Foetal bovine serum
GFP	Green fluorescent protein
HDAC	Histone Deacetylase
ICC	Immunocytochemistry
IHC	Immunohistochemistry
IL	Interleukin
KO	Knock out
LPS	Polyinosinic:polycytidylic acid
MAG	Myelin associated glycoprotein
MBP	Myelin basic protein
MCP-1	Monocyte chemoattraction protein
MPZ	Myelin protein zero
mRNA	Messenger ribonucleic acid
NCC	Neural crest cells
NCV	Nerve conduction velocity
Necl	Nectin like proteins
NF	Neurofilament
NGF	Nerve growth factor
NgR	Nogo receptor

Nrg	Neuregulin
NT	Neurotrophin
OCT	Optimal cutting temperature
PACAP	Pituitary adenylate cyclase-activating polypeptide
PBS	Phosphate buffered saline
PCR	Polymerase chain reaction
PI3K	Phosphatidylinositol3-kinase
PIP2	Phosphatidyli-nositol(4,5)-trisphosphate
PIP3	Phosphatidyli-nositol(3,4,5)-trisphosphate
PLL	Poly L Lysine
PMP22	Peripheral Myelin Protein 22
PNS	Peripheral nervous system
Poly IC	Lipopolysaccharide
PTEN	Phosphatase and tensin homolog
qRT-PCR	Quantitative real time polymerase chain reaction
ROBO	Roundabout
RT	Room temperature
SC	Schwann cells
SSI	Static sciatic index
TLR	Toll like receptor
TNF	Tumour necrosis factor
VEGF	Vascular endothelial growth factor
VIP	vasoactive intestinal peptide

1. Table of Contents

List of figures

List of Tables

1. Introduction

1.1 Peripheral nervous system

The PNS (peripheral nervous system) is made up of all nerves and cell bodies of neurones in the body, excluding the brain and spinal cord which belongs to the CNS (central nervous system). The peripheral nerves connect the body to the central nervous system allowing information to be sent between these two systems. Signals from the brain and spinal cord are sent through motor neurons to conduct limb movement and autonomic functions such as breathing and digestion. Signals can also be sent from the peripheral nerves to the CNS through sensory neurones. The peripheral nerves unlike the CNS are not protected and are therefore left open to both chemical and mechanical assault. Therefore, a break between the CNS and the PNS can occur and this can cause problems with both sensory and motor function.

Peripheral nerves are largely made up of two cell types, neurones and Schwann cells. Neurones are cells that are able to transfer information through electrical excitability between cells. Schwann cells on the other hand have multiple functions that range from controlling the speed of action potential to providing trophic support and producing factors that allow for neuronal survival and guidance (Figure 3).

1.2 Axons

Axons function to send electric impulses away from the nerve cell body. This allows for connections to be made throughout the body and information is then able to be sent to different muscles and organs. A proper functioning nervous system first depends upon axons being guided to the correct place during development. A growth cone, a large cytoskeletal organisation containing growing axons present during development and then again during regeneration enables axons to grow in response to chemoattractant. For axons to become functional they must grow towards and

connect with its target organ which requires many axon guidance signals for correct guidance, axons must then be able to efficiently produce an action potential for axons to be able to function and carry out their role (Fletcher 2016; Yu and Bargmann 2001).

1.2.1 Axon guidance and axon guidance molecules

Axons move through their environment during development and encounter cues which help guide axons to their correct targets, these cues are referred to as axon guidance molecules. The growth cone of extending axons are specialised cytoskeletal motile structures which move through the environment sensing guidance molecules which may repel or attract growing axons (Aberle 2019). Actin dynamics is central to axon extension. Actin polymerisation leads to the filopodia and lamellipodia extrusion which allow extension of growing axons. The dynamics of the growth cone is regulated by axon guidance cues. Both long range acting and short range acting signalling molecules are required for axon guidance during development. There are four categories of very well-defined axon guidance molecules, Ephrins, Semaphorins, Slits and Netrins (Egea and Klein 2007; Keynes and Cook 1995).

1.2.1.1 Ephrins

Eph receptors (Erythropoietin-producing human hepatocellular receptors) bind to Ephrins ligands (Eph receptor-interacting proteins) to initiate receptor tyrosine kinase signalling. Ephrins and their Eph receptors are divided into two categories EphA and EphB. EphA receptors preferentially bind to EphrinA1-5 ligands, which are attached to the membrane through GPI (glycosylphosphatidylinositol) linkage whereas EphB receptors preferentially bind to EphrinB ligands and are linked to the cell surface through a transmembrane domain (Lisabeth et al. 2013). Eph-Ephrin signalling is contact dependent and therefore requires cell-cell contact where protein interaction can induce bidirectional signalling into their respective cells. Bidirectional signalling is

where both receptor and ligands can transduce signals. Signalling from the Eph receptor into the cell is referred to as forward signalling, whereas Ephrin ligand signalling into the cell is referred to as reverse signalling (Kullander and Klein 2002). Both pathways are linked to downstream effectors such as Ras GTPases, Rho GTPases and Akt, forming complex signalling pathways (Arvanitis and Davy 2008). The signalling pathways activated are involved in actin cytoskeleton dynamics and Eph-Ephrin signalling can induce growth cone remodelling and cell migration. Eph/Ephrin signalling was first described as being important for axon guidance in the visual system where reverse signalling by EphB acts to direct retinal axons out of the eye through RhoA signalling (Birgbauer et al. 2000). EphA and EphrinA gradients are required for spinal motor neurones to innervate limbs where EphA4 expressing motor axon growth cones interact with EphrinAs to help guide motor axons to innervate dorsal muscles (Egea and Klein 2007). Absence of EphA4 causes axons destined for dorsal regions to become mis-targeted and project towards ventral regions (Helmbacher et al. 2000). Whereas interaction between EphA5 and EphrinA5 is needed for axon fasciculation with inhibition of EphA5 preventing the formation of axon bundles in vitro (Cooper et al. 2009). These examples highlight multiple examples and the importance of interactions between Eph/Ephrins for axon guidance (Caras 1997).

1.2.1.2 Semaphorins

Semaphorins are membrane bound and secreted signalling proteins. There are 8 classes of Semaphorins but those in class 3 a secreted Semaphorin, are of most importance for axon guidance (Koncina et al. 2007; Ng et al. 2013). Plexin are the binding receptors and Neurophilin 1 and Neurophilin 2 are co-receptors for Class 3 Semaphorins. Plexin-Neurophilin complexes form high affinity receptor complexes for

secreted Semaphorin (Sharma et al. 2012). Semaphorin 3A is a repulsive factor, has growth cone collapsing properties and have been shown to act on both motor and sensory neurones within the peripheral nervous system (Koncina et al. 2007). Knock out of Neurophilin 1 the Semaphorin 3A receptor causes afferent neurones of the mouse PNS to over shoot their targets and have abnormal trajectories (Kitsukawa et al. 1997).

1.2.1.3 Netrins

Netrin acts as a secreted long range axon guidance protein which can function as both a chemoattractant and a chemorepellent. Three secreted Netrins, Netrin-1, -3 and –4 and two GPI anchored membrane proteins Netrin G1 and G2 have been discovered in mammals. Receptors for Netrins include DCC (Deleted in colorectal cancer), UNC5 (Uncoordinated receptor 5), DSCAM (Down syndrome cell adhesion molecule) and Neogenin (Deiner et al. 1997; G. F. Liu et al. 2009). DCC and UNC5 receptors orchestrate remodelling of the cell membrane and cytoskeleton and is therefore crucial during axon guidance processes promoting axon outgrowth and growth cone navigation. UNC5 or homodimerised DCC receptors both mediate a chemoattractive reaction, whereas heterodimerization between DCC and UNC5 mediates a repulsive reaction (Boyer and Gupton 2018; Keleman and Dickson 2001). DSCAM function however is not as well understood but DSCAM knock down leads to netrin-dependent commissural axon outgrowth and pathfinding (G. F. Liu et al. 2009). Amongst axon guidance cues, Netrin-1 has the strongest ability to promote axon extension and has been the most well described in the literature in the context of axon guidance (Boyer and Gupton 2018; Serafini et al. 1996). During development, netrin is required for commissural axons to cross the midline and Netrin-$1^{-/-}$ (Bin et al. 2015). In the

peripheral nervous system, Netrin-1 receptors are expressed in Schwann cells, the cell bodies of sensory neurons and the axons of both motor and sensory neurons (Dun and Parkinson 2017; Madison et al. 2000).

1.2.1.4 Slit/Robo

Slit acts as a chemorepellent and binds to the transmembrane Robo (Roundabout) receptor (Brose et al. 1999; Yuan et al. 1999). Four different Robo receptors, Robo1-4, and 3 Slit ligands,Slit1-3, are expressed in mammals (Brose et al. 1999; Jen et al. 2004; Marillat et al. 2002). These receptors and ligands are expressed in complementary patterns throughout development of the peripheral nervous system (Carr et al. 2017). Slit-Robo signalling is particularly important for axon path finding and crossing of commissural axon at the midline during development (Dickson and Gilestro 2006). In Robo1 and Robo2 KO mice axons crossing the floor plate were severely misguided whereas Slit1-3 triple KO had disorganised commissural axons with many axons staying within the midline or recrossing the midline rather than extending towards their targets (Long et al. 2004). Secreted Slit ligands are also able to bind to DCC, which can silence Netrin mediated chemoattraction showing that different signalling pathways can act together to further guide axons towards their targets during development (Stein and Tessier-Lavigne 2001).

1.2.2 Action potentials

Action potentials occur when information in the form of an electrical current is sent down an axon away from the cell body. The resting potential for a neurone is around -30 to -70mV (Lodish 2000). In neurones potassium (K+) is found at a high concentration within the cell whereas sodium (Na+) and chloride (Cl-) are found at

higher concentration outside the cell. Neurones in a resting state are permeable to K+ and K+ flows down a concentration gradient. When an action potential is generated, the neuron becomes depolarised. As a result of an electrical stimulus voltage gated sodium ion channels open and Na+ moves into the cell to raise the charge from negative to positive. Once depolarization has occurred, Na+ ion channels close and due to the positive charge within the cell, K+ ion channel opens and K+ now moves down a gradient and out of the cell. The membrane potential falls and the membrane becomes repolarised (Fletcher 2016). Following an action potential neurones enter a refractory period where they cannot become depolarised, this means action potentials will only flow down the axon in one direction.

1.3 Schwann cells

Schwann cells were discovered in the early nineteenth century by Theodore Schwann who noticed certain cells, which were later called Schwann cells, to be wrapped around axons in the peripheral nervous system (Bhatheja and Field 2006). Schwann cells were later divided into two categories myelinating and non-myelinating. Schwann cells are derived from NCCs (neural crest cells) and go through two differentiation stages, first NCCs develop into highly proliferative precursor cells before turning into immature Schwann cells which radially sort axons from axon bundles (Figure 1) (Jessen et al. 2015; Muppirala et al. 2021). Schwann cells within the nerve stay in this immature state until birth. Following birth immature Schwann cells then further differentiate into myelinating or non-myelinating Schwann cells (Woodhoo and Sommer 2008). There are many factors that dictate Schwann cell lineage, this includes number of axons the Schwann cell is in contact with and transcription factors such as Sox10, Krox20 and Oct6. Schwann cells however are not terminally differentiated and

retain a high degree of plasticity throughout their lifetime, this is particularly important following injury and will be discussed further later.

1.3.1 Myelinating Schwann cells

The main function of myelinated Schwann cells is to allow saltatory conduction. Myelinated Schwann cells are essential for large complex nervous system as it allows for efficient rapid conduction of action potentials. Schwann cells form a myelin sheath which wraps around the axon to insulate it and thereby increases saltatory conduction speed (Lodish 2000). In the PNS myelinating Schwann cells wrap around axons larger than 1μm diameter and forms a 1:1 ratio between Schwann cell and axon that is that each Schwann cell myelinates a single axons which is in contrast to oligodendrocytes that can myelinate multiple axons. Each myelin sheath has an average internodal length of around 1mm which is interrupted by a 1μm gap of unmyelinated axon called a node of Ranvier adjacent to each myelin sheath. Axon potentials are able to jump from each node of Ranvier along the myelinated internode down to the axon terminal.

1.3.1.1 Myelin composition

The composition of the myelin sheath is essential for its function in insulating the nerve, generating rapid action potentials and allowing normal motor and sensory function. The myelin sheath plasma membrane has a very high lipid content of between 70-80% which is enriched with few proteins. These lipids include galactosphingolipids, saturated long-chain fatty acids and cholesterol which wrap around the Schwann cell membrane and are later compacted by myelin proteins to generate the compacted myelin sheath (Garbay et al. 2000). One of the most abundant proteins within the sheath is the protein MPZ (myelin protein zero) which accounts for around 50-70% of myelin proteins (Greenfield et al. 1973). MPZ is a transmembrane adhesion molecule and is required for protein myelin sheath assembly within the peripheral nervous

system. The extracellular domains of the MPZ protein form homotypic interactions to effectively glue together layers of the myelin sheath and help compact it (Lemke et al. 2008). MBP (Myelin basic protein) is another protein which helps compact myelin and makes up between 5-15% of total myelin proteins. MBP is mostly found in the major dense line which is a 3nm compartment between two cytoplasmic leaflets of stacked myelin membranes, here it binds to the cytoplasmic region of MPZ (Raasakka et al. 2017). Mutations within the MPZ gene are responsible for some cases of CMT1B (Charcot Marie Tooth) and the axonal form of CMT (Choi et al. 2011; Santoro et al. 2004). In mice deletion of both MBP and MPZ was lethal around 6 weeks postnatally, which highlights the importance for correct expression of both of these proteins (Martini et al. 1995; Santoro et al. 2004). Mice with deletion of just MPZ showed poor compaction and severe hypomyelination of the peripheral nerves where as deletion of just MBP lead to normal compaction and myelin sheaths (Martini et al. 1995). Other important proteins include PMP22 (peripheral myelin protein 22) which makes up around 2-5% of myelin proteins (Pareek et al. 1993). Its function in Schwann cells remains less clear than that of other proteins. It is however clear that it's role is important as a point mutation of C-to-G which corresponds to the substitution of cysteine for serine in the 79th codon (S79C) within PMP22 has been described as the cause for some cases of CMT1A where the more common cause of PMP22 gene duplication is not seen (Chance et al. 1992; Roa et al. 1993).

1.3.1.2 Signals that regulate myelination

1.3.1.2.1 Axonal contact

Interaction between Schwann cells and axons is essential for the development and formation of myelin. One important protein adhesion complexes for communication between Schwann cells and axons are Necl (Nectin like proteins). Axons express Necl1 and Necl2, Schwann cells express Necl2 and Necl4, Necl4 expression is up-regulated in Schwann cells as myelination is initiated (Perlin and Talbot 2007). Interaction between Necl1 and Necl4 mediates adhesion between Schwann cells and axons, this interaction appears to be the most important for initiation of myelination, with inhibition of myelination seen when this interaction is disrupted (Spiegel et al. 2007). Other systems include the Adam22 Lgi4 system, where Lgi4 is secreted by Schwann cells and binds Adam 22 on axons. This interaction triggers Schwann cells to enter a promyelinating state. Schwann cell specific deletion of Lgi4 or axonal deletion of Adam22 leads to hypomyelination (Ozkaynak et al. 2010; Sagane et al. 2005). Finally, PI3K (phosphatidylinositol3-kinase) signalling in Schwann cells that is activated by axonal contact is required for both Schwann cell survival and myelination. Inhibition of PI3K leads to shorter, thinner myelin sheaths (Maurel and Salzer 2000). Interaction between axons and Schwann cells is the crucial step before myelination can occur.

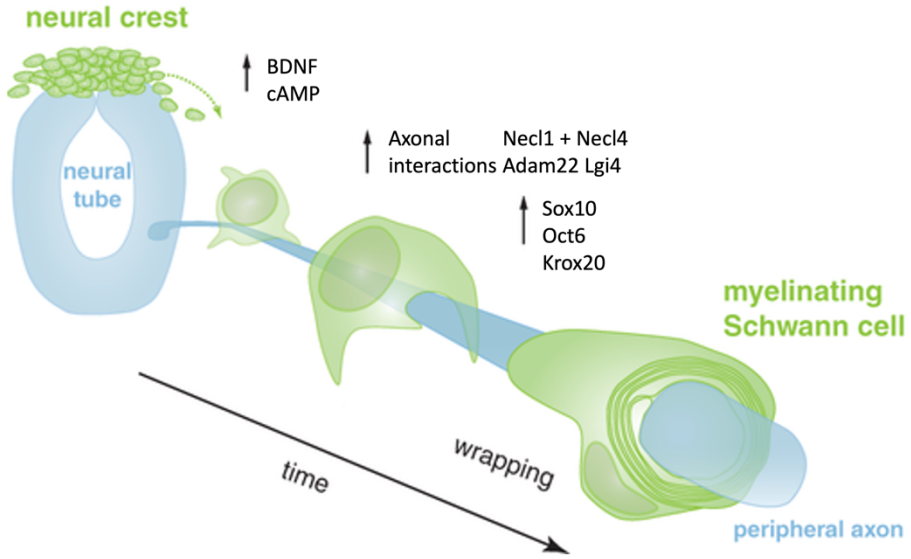

Figure 1 Schematic showings some of the signals that act to promote myelination of peripheral axons

There are many factors that promote the development of a neural crest cell into a myelinating Schwann cell. Myelinating Schwann cells then act to encompass axons with a myelinated sheath. Figure adapted from (Muppirala et al. 2021).

1.3.1.2.2 Nrg/ErbB

Neuregulins (Nrg) are a large family of epidermal like growth factors. Six Nrg genes have been identified, Nrg1-6 activate and signal through ErbB receptors of which there are 4, ErbB1-4. Of these ligand receptor combinations, Nrg1 (Neuregulin1) binding to ErbB provides a key signalling mechanism to establish Schwann cell myelination. Nrg1 treatment of Schwann cell cultures in vitro leads to Schwann cell survival and myelination, with the crucial Nrg being Type 3 Nrg (Dong et al. 1995). Activation of ErbB receptors leads to activation of PI3K, AKT, Erk and mobilises Ca^{2+} (Newbern and Birchmeier 2010). Nrg/ErbB signalling is also vital for Schwann cell development and ErbB2, ErbB3 and Nrg1 mutant mice all show the same pathology in that they all show a lack of Schwann cell progenitors in the peripheral nerve (Michailov et al. 2004). Upon Schwann cell development Nrg/ErbB signalling pathways can direct some Schwann

cells to myelinate, with axon derived levels of Nrg being linked to the fate of Schwann cells towards a myelinating phenotype (Leimeroth et al. 2002; Meyer and Birchmeier 1995). ErbB2 null mice show aberrantly projected motor and sensory neurones and a complete lack of Schwann cells in the peripheral nerves. They are however present in the DRG but due to the lack of ErbB2 are unable to migrate into the peripheral nerves (Morris et al. 1999). Disruption of ErbB2 or Nrg1 can lead to hypomyelination, reduced levels of myelination, highlighting the importance for precise levels of Nrg and ErbB (S. Chen et al. 2006; Michailov et al. 2004). ErbB3 null mice show a neuropathy like phenotype as motor and sensory axons form initially but then go on to undergo cell death in the embryonic stages (Riethmacher et al. 1997).

1.3.1.2.3 Sox10

Sox10 is the transcription factor in control of neural crest cell differentiation into peripheral nerve glia. Sox10 importance for the control of normally myelinated Schwann cells is highlighted in mice which hold mutations for Sox10 in neuronal cells. The $Sox10^{lacZ}$ mice died at birth as they could not breath. Here, dorsal root ganglions develop normally but Schwann cells are not developed which leads to significant disruption of motor and sensory function (Britsch et al. 2001). The Schwann cells in adult mice in which Sox10 has been deleted using a tamoxifen injection to cause ER-Cre recombination and gene KO, loose myelin within myelinated Schwann cells and mice show signs of peripheral neuropathy (Bremer et al. 2011). This shows Sox10 as a key signal for the maintenance of normally myelinated Schwann cells.

1.3.1.2.4 Oct6

Oct6, like Sox10 is a transcription factor required for normal myelination of myelinating Schwann cells. Oct6 is an important factor in the transitioning of Schwann cells to

myelinating Schwann cells (Blanchard et al. 1996). If Oct6 is deleted myelination in mature Schwann cells is impaired (Bermingham et al. 1996). Oct6 expression changes within the nerves of patients with peripheral neuropathy and injury. Axonal degradation leads to an upregulation of Oct6 within Schwann cells highlights a role for Oct6 in peripheral nerve regeneration as well as development of myelinated Schwann cells (Kawasaki et al. 2003). Oct6 is highly expressed from Schwann cells in the distal nerve stump 6DPI in WT mice and at 12DPI in Oct6 null Schwann cells myelination was delayed compared to WT with many Schwann cells still in their promyelin stage and axons that has regenerated has thinner myelin (Ghazvini et al. 2002).

1.3.1.2.5 Krox20

Krox20 also known as EGR2 (Early growth response protein 2) is a transcription factor containing two DNA binding domains. Krox20 comes from the Krüppel-like factors family, a group of proteins that contain a cytosine/histidine zinc finger that play a key role during differentiation and development (Bieker 2001). Krox20 has been dubbed the master regulator of myelination within the peripheral nervous system. A major piece of evidence for this is that Krox20 null mice completely fail to myelinate their axons, Schwann cells ensheath axons but are only able to wrap round a maximum of one and a half turns compared to the 250 to 300 turns seen in health. In humans Krox20 mutations are associated with various types of hypomyelination or demyelinating diseases such as hypomyelinating neuropathies and CMT1 (Le et al. 2005; Topilko et al. 1994). Once Schwann cells make contact with large axons, over 1-2μm in diameter Krox20 expression is activated. Krox20 is activated by the transcription factors Oct6/Sox10 which bind to the cis regulatory element (Bermingham et al. 1996; Ghislain and Charnay 2006). Krox20 then binds to many of

the regulatory regions on genes required for myelination and acts to recruit histone deacetylases to regulate and activate the gene expression of proteins important for myelination specifically MPB and MPZ (Jang et al. 2010; LeBlanc et al. 2006). In addition to Krox20 activating the expression of myelin related genes, it is also responsible for the repression of other genes such as cJun and Sox2 both of which are negative regulators of myelination. cJun is a regulator of Schwann cell plasticity and Krox20 inactivation of cJun will help drive Schwann cells into a matured myelinated state (Parkinson et al. 2004; Parkinson et al. 2008). Krox20 expression is not only required to myelinate Schwann cells during development, it is also required to maintain Schwann cells in this myelinated state in the adult nerve (Decker et al. 2006).

The transcription factors discussed above all work together to promote myelination of Schwann cells. Krox20 induction represents an example of a positive feed forward loop. Sox10 first induces Oct6 and then cooperates with Oct6 to activate Krox20 expression. This leads to amplified and maintained Krox20 expression and consequently myelination (Decker et al. 2006; Topilko et al. 1994)

1.3.1.2.6 Neurotrophins

Neurotrophins are a group of proteins involved in survival, development and function of peripheral nerves. There are currently four neurotrophins characterized that have a similar structure and function and are derived from the same gene, named NGF (nerve growth factor), BDNF (brain-derived neurotrophic factor), NT-3 (neurotrophin-3) and NT-4 (neurotrophin-4) (Barde et al. 1982; Campenot 1977; Ernfors et al. 1990; Hallbook 1999; Maisonpierre et al. 1991). There are two receptor classes characterised for neurotrophins: trk (the tropomyosin-related kinase) tyrosine

kinase receptors and $p75^{NTR}$ (p75 neurotrophin receptor), the latter of which will bind all neurotrophins (J. H. Xiao et al. 2009). Different neurotrophin-receptor combinations help to control myelination during development. NT3 action through trk3 inhibits myelination during development, whereas BDNF promotes myelination in developing Schwann cells. In vivo application of BDNF to developing mouse sciatic nerve enhanced myelination (Chan et al. 2001). Blocking of $p75^{NTR}$ using blocking antibodies during myelination results in the inhibition of MBP and MPZ expression.

It is now known that BDNF acts through $p75^{NTR}$ to enhance myelination and ensheathment of Schwann cells during development (Cosgaya et al. 2002). In addition to this, mice embryos with a global loss of $p75^{NTR}$ have peripheral neural development defects in which neurite outgrowth is impaired. Neurite outgrowth is required before Schwann cells can act to myelinate axons. In addition to neurite outgrowth $p75^{NTR}$ may also have a role in Schwann cell migration and elongation prior to myelination as p75 null mice show no s100 staining in the peripheral nerves of developing embryos (Bentley and Lee 2000).

1.3.1.2.7 PI3K/Akt

The PI3K-Akt-mTORC signalling controls the onset of myelination. PI3K catalyses the reaction of PIP2 (phosphatidyli-nositol(4,5)-trisphosphate) to PIP3 (phosphatidyli-nositol(3,4,5)-trisphosphate); PTEN (phosphatase and tensin homolog) catalyses the opposite reaction. Growth factors typically act to stimulate PI3K, resulting in activation of Akt which in turn actives mTORC1. In vitro experiments show that activation of PI3K in Schwann cell-DRG cultures increased expression of MAG (myelin associated glycoprotein) (Ogata et al. 2004). Before the onset of myelination mTORC1 activates S6K which actually acts to block Krox20 expression in the peripheral nervous system, this allows Schwann cells to transition from a pro myelinating state to a myelinating

state and ensure correct and appropriate timing of myelination (Figlia et al. 2017). In Schwann cells that have already started wrapping axons, high mTORC1 expression resulted in axons being wrapped in thicker myelin sheaths, whereas absence of mTORC1 resulted in hypomyelination (Norrmen et al. 2014; Sherman et al. 2012). This shows that PI3K-Akt-mTORC signalling has a major role in controlling the transition of Schwann cells from a pro-myelinating to myelinating state. PI3K-Akt-mTORC then continues to signal to promote normal myelin formation during development.

1.3.1.2.8 cAMP

cAMP is a crucial second messenger molecule in the promotion of differentiation and myelination of Schwann cells. It acts downstream of Rac1 and acts to induce the expression of the transcription factor Krox20 and block expression of cJun. cAMP has been shown in various in vitro cell culture experiments to be important for pushing Schwann cells into a differentiated state. Forskolin for example elevates cAMP and induces the expression of myelin proteins such as MBP and MPZ (Bacallao and Monje 2015). Further studies by Gomis-Coloma et al., 2018 showed that cAMP can act to shuttle HDAC3 (Histone Deacetylase 3) and HDAC4 (Histone Deacetylase 4) into the nucleus where it inhibits expression of cJun and halts proliferation. Halting proliferation and the expression of cJun can then push Schwann cells into a differentiated state by the upregulation of Krox20 and myelin gene expression (Gomis-Coloma et al. 2018). Rac1 has been shown to control myelination where cAMP acts downstream of Rac1. Rac1 conditional KO mice where Rac1 is specifically removed from Schwann cells leads to a decrease in cAMP second messenger production and a deficiency in myelin protein expression (Guo et al. 2012).

GPR126 has been shown as a crucial G Proteins coupled receptor that cAMP acts through to drive Schwann cell myelination. Monk et al 2009, first showed that myelination in GPR126 KO zebra fish did not occur. Schwann cells associated with axons but myelination did not progress and Schwann cells were arrested in the pro myelinating stage. This could however be rescued by treating nerves with forskolin to elevate cAMP levels (Monk et al. 2009). This induced Oct6, Krox20 and consequently myelination and dubbed cAMP as one of the master regulators in myelination. GPR126 KO mice further highlighted the importance of GPR126 in myelination, where these mice showed a similar phenotype to zebra fish, Schwann cells were able to associate with axons but became stuck in a promyelinating state. Many of these GPR126 mice did not survive to birth, those mice that did showed functional limb abnormalities and MBP was not expressed in the peripheral nerves of GPR126 mice (Monk et al. 2011). GPR126 conditional KO mice were mice that has GPR126 knocked out of Schwann cells using a Cre recombinase system under the control of dessert hedgehog. Nerves in these mice were shown to have lower levels of cAMP second messenger levels in their peripheral nerves along with defects in myelination. This phenotype could be rescued by inducing cAMP in nerves which attenuated defective myelination and lead to the expression of MBP (Mogha et al. 2013). This directly linked GPR126 induced cAMP production and highlighted the importance of cAMP for normal myelination of peripheral nerves. cAMP is an important second messenger in inducing the expression of myelin protein both in vitro and in vivo.

1.3.2 Non myelinating (Remak) Schwann cells

Multiple small diameter axons are bundled together into Remak bundles by non myelinating Schwann cells. Here, up to 20 axons can be grouped together. Non myelinated Schwann cells make up group C fibers, which are unmyelinated small diameter axons with low conduction velocity. These include postganglionic autonomic and nociceptor axons. Axons ensheathed by non-myelinating Schwann cells are able to jump between Remak bundles and are therefore not found within the same bundles along the whole length of the nerve. (Griffin and Thompson 2008).

Non myelinating Schwann cells are less well characterized than myelinating Schwann cells due to the lack of lineage-specific drivers and appropriate mouse models with gene and protein loss only in these cells. However, non myelinating Schwann cells like myelinating Schwann cells are able too provide metabolic support to axons. The serine/threonine kinase LKB1 (also known as serin/threonine kinase 11) is involved in many metabolic processes and is crucial for small diameter axon stability. Mice models lacking LKB1 in their Schwann cells show degeneration of Remak bundles and multiple sensory defects (Beirowski et al. 2014). To further link Remak bundles closely with metabolism and axonal support, knock out of Tfam a mitochondrial transcription factor specificly in Schwann cells saw the preferential loss of C-fiber axons (Viader et al. 2011). Non myelinating Schwann cells, like myelinating Schwann cells have have a high degree of plasticity, this is important during injury and allows for C-fiber axons to regenerate and reinnervate their targets faster. There has recently been shown to be an emerging role for non myelinating Schwann cells in the onset of diabetic neuropathy. C fibers can become prone to injury in diabetic patients where dysregulation of glucose metabolism causes glucose to become toxic leading to diabetic neuropathy within some patients (Stino and Smith 2017).

1.3.3 Repair Schwann cells

Upon injury both non-myelinating and and myelinating Schwann cells are able to re-program into specialised cells termed repair Schwann cells (Arthur-Farraj et al. 2012; Arthur-Farraj et al. 2017; Jessen et al. 2015; Jessen and Arthur-Farraj 2019; Mindos et al. 2017; Napoli et al. 2012; Nocera and Jacob 2020). The function of these schwann cells go from maintenance of myelin and axonal ensheathment to promoting regeneration and repair following peripheral nerve injury. In order to do this Schwann cells are required to undergo an extensive change in gene expression to down regulate genes associated with myelination such as Krox20 and upregulate the expression of genes associated with Schwann cell plasticity and neuronal survival such as p75 and genes involved in cell motility, morphological flexibility, epithelial mesenchymal transition (EMT) and stemness such as TGFβ (Jessen and Mirsky 2016; Jessen and Arthur-Farraj 2019).

Upon receiving injury signals from injured axons, Schwann cells down regulate gene expression for myelin genes such as Krox20 and MBP and start to clear their myelin sheaths. Associated with down regulation of pro-myelination genes is a concurrent increase in the production of trophic factors to support axon survival such as such as NGF, BDNF, GDNF, NT-3, NT-4, TrkA and p75 (Bunge 1994; Frostick et al. 1998). Schwann cells are reprogrammed to undergo the process of phagocytosis and also activates an immune response by upregulating the expression of cytokines which act to recruit macrophages and that further aids in myelin phagocytosis (Dubovy et al. 2014). Schwann cells also undergo structural reorganisation where they become elongated with parallel processes. These long processes between cells overlap to create tracts called Bands of Bungner that axons can regenerate along (Gaudet et al.

2011). Finally, repair Schwann cells are able to differentiate back into myelinating Schwann cells and remyelinate regenerated axons if appropriate (Rotshenker 2011).

1.3.3.1 Signals that regulate repair Schwann cells

After nerve injury techniques such as RNAs seq and microarray have shown there are over 4000 differentially expressed RNAs further confirming the large number of transcriptional changes peripheral nerves undergo following injury (Barrette et al. 2010; Bosse et al. 2006; Jessen and Arthur-Farraj 2019). Not all of these changes can be discussed but some of the most well described pathways will be discussed below.

1.3.3.1.1 c-Jun

c-Jun a transcription factor is a negative regulator of myelination and is upregulated following peripheral nerve injury where it activates repair programming (Parkinson et al. 2008). c-Jun has been shown to be the master regulator in the control of re-programming of myelinating and Remak Schwann cells into a repair-competent phenotype. Microarray data has shown c-Jun to regulate serval genes crucial to peripheral nerve repair (Arthur-Farraj et al. 2017; Fontana et al. 2012). Mice with a conditional KO for c-Jun in Schwann cells develop normally, with normal peripheral nerve architecture and function (Arthur-Farraj et al. 2012). However, following injury Schwann cells in KO animals failed to reprogram into a repair phenotype and failed to upregulate factors associated with trophic support such as BDNF and GDNF. c-Jun KO animals also failed to efficiently clear myelin with myelin break down being substantially delayed from c-Jun KO Schwann cells compared to WT. c-Jun KO animals also showed dysregulation in the structure of both Bands of Bungner and Schwann cells, where Schwann cells were shown to have reduced processes. This in turn leads to reduced axon regeneration and reinnervation into targets and

substantially less motor and sensory recovery in c-Jun conditional KO animals (Arthur-Farraj et al. 2012). Further importance of c-Jun in promoting the repair phenotype was shown in a model overexpressing c-Jun in Schwann cells. Axons having undergone a crush injury showed accelerated demyelination. Remyelination was delayed but functional and sensory recovery was eventually fully restored (Fazal et al. 2017). It is therefore of note that low c-Jun levels blocks Schwann cells from entering a repair phenotype and has neuroprotective effects. Conversely, high c-Jun levels can prevent efficient remyelination following regeneration. Therefore the levels of c-Jun have to be tightly controlled in repair Schwann cells the enable their correct function (Figlia 2018). Merlin originally discovered as a tumour suppressor, has been described to control Schwann cell repair capacity following injury. The mP0TOTA-CRE (P0-CRE) line was used to specifically remove Merlin in Schwann cells. Analysis of Schwann cells showed that removal of merlin showed transient hypomyelination during development. Following a crush injury, Merlin null nerves showed a large decrease in regenerating axons and an increase in G ratio compared to WT controls. This poor regeneration and remyelination was observed up to 60DPI. Merlin null nerves always showed decreased c-Jun induction up to 11 days post injury. However, at 21DPI weak c-Jun expression was maintained which stopped repair Schwann cells from remyelinating and differentiating back into a myelinating Schwann cell (Mindos et al. 2017).

1.3.3.1.2 Erk1/2

Following a transection injury in a rat model, Erk1/2 within the peripheral nerve is phosphorylated within 30 minutes and phosphorylation of Erk1/2 remains elevated until around day 16 (Sheu et al. 2000). Erk is also rapidly activated in mouse peripheral nerves following injury (Napoli et al. 2012). Activation of Ras/Raf/Erk signalling is one of the key pathways in regulating Schwann cell plasticity and can act to promote

Schwann cells to dedifferentiate (Harrisingh et al. 2004). The transgenic mouse which targeted the tamoxifen (Tmx)-inducible Raf-kinase/estrogen receptor fusion protein (RafTR) in myelinating Schwann cells allowed Raf/MEK/Erk pathway to be assessed in adult myelinating Schwann cells in vivo by selectively activating it through taxoxifen injection. RafTR activation lead to increased Erk activity in Schwann cells and caused a progressive weakness and impairment of co-ordination in mice (Napoli et al. 2012). Analysis of Schwann cells in tamoxifen injected mice revealed that Schwann cells had entered into a dedifferentiated state where expression of myelin genes were down regulated and Schwann cell had begun to proliferate. In the peripheral nerves 10 days post tamoxifen injection there was widespread breakdown of myelin and axons had began to demyelinate. A pro-inflammatory response with large numbers of macrophages within the peripheral nerves was also observed. This showed that activation of Erk within myelinating Schwann cells in this model drove Schwann cells to loose myelin and dedifferentiate (Napoli et al. 2012).

Erk is activated by upstream kinases and therefore its expression can be regulated by the levels and activity of these kinases. MEK1DD is one of these kinases and phosphorylates Erk to activate it. Mice harbouring a gain of function mutation for MEK1DD specifically in Schwann cells using a Cre recombinase system produced sustained activation of Erk and Schwann cells displayed defects in repair and functional recovery upon peripheral nerve injury. Although Wallerian degeneration occured faster, repair of injured nerves was delayed and the myelin surrounding remyelinated axons was much more unstable compared to controls at 4 weeks post injury. EM images showed smaller myelinated axons, decreased myelin compaction and myelin loops. In addition to this, functional and sensory recovery showed delayed reactions to pin prick tests and decreased ability to successful complete beam and

rotarod tests compared to WT. This again shows the importance for strict control of the Erk/MAPK signalling axis in Schwann cells following injury to enable successful peripheral nerve repair (Cervellini et al. 2018).

1.3.3.1.3 TGF-β1

As mentioned above, when Schwann cells dedifferentiate they enter into a state of which promotes EMT and increased motility. EMT is the process in which cells loose their polarity and cell contacts and become migratory, this process requires the activation of transcription factors, secretion of matrix metalloproteases (MMP) and reorganisation of the actin cytoskeleton (Kalluri and Weinberg 2009). TGF-β1 is a cytokine which has been described to act on Schwann cells to promote mesenchymal transitioning and migration. In the injured peripheral nerves of mice with a Schwann cell specific KO of TGF-β1 Schwann cell migration from the proximal stump is reduced and Schwann cell cords are shorted 6DPI (Clements et al. 2017). It has since been shown that TGF-β1 is able to induce the expression of MMP2 and MMP9 and cell invasion in vitro (Muscella et al. 2020). MMPs also have a role within Schwann cell dedifferentiation where it helps to initiate myelin degradation (Kobayashi et al. 2008). The ability of Schwann cells to migrate is particularly important after cut injuries where Schwann cells are required to migrate into the nerve bridge.

1.4 Connective tissue in the peripheral nerves

Connective tissue in the peripheral nerve functions to protect nerves, bundle nerve fascicles together and provide support to the blood vessels and lymphatic system of the peripheral nervous system. There are three different layers of connective tissue, the epineurium the outermost layer, the perineurium encapsulates fascicles and nerve fibres and the endoneurium which surrounds myelinated axons.

1.4.1 Epineurium

The epineurium is the permeable outermost layer of the nerve and ensheaths nerve fascicles together to form one peripheral nerve (**Figure 2**) (Peltonen et al. 2013). The epineurium is made up from dense connective tissue, mainly collagen, but also contains extracellular matrix macromolecules comprising of elastin called elastic fibres, adipocytes, fibroblasts and blood vessels. The extracellular collagen matrix of the epineurium contributes to the tensile strength of the nerve and allows for the nerve to be able to stretch and twist without damaging the axons.

1.4.2 Perineurium

The perineurium envelops each nerve fascicle (**Figure 2**). The perineurium is made up of perineurial cells and extracellular matrix containing fibronectin and collagen. Perineural cells are large and flat, tight junctions are formed between the neighbouring perineurial cells and each row of cells can form layers, with the larger fascicles containing more layers (Peltonen et al. 2013). The perineurial layer is a diffusion barrier between the endoneurium and extra fascicular tissue as heparin sulphate chains are arranged within the basement membrane and prevents molecules of more than 12nm in diameter diffusing through the barrier which could cause damage to the nerves (Olsson and Kristensson 1973; Peltonen et al. 2013).

1.4.3 Endoneurium

The endoneurium is the innermost layer and envelopes myelinated and non myelinated axons (**Figure 2**). Endoneurium forms around Schwann cells and contains basal lamina comprised of collagen, perlecan and laminin-2 as well as blood vessels, fibroblasts and macrophages (Graham and Muir 2016). Endoneurial vessels also form a capillary network which supplies nerves with oxygen. The endoneurium contains liquid referred to as endoneurial fluid, which is similar in composition to the cerebrospinal fluid in the central nervous system. The endoneurium is relatively impermeable and functions to prevent harmful molecules from entering into endoneurial fluid and to prevent rapid fluctuations in the concentration of potentially harmful plasma solutes which could affect the function of both Schwann cells and axons (Mizisin and Weerasuriya 2011).

1.5 Vasa nervorum

The vasa nervorum consists of the small arteries that provide the peripheral nerve with blood. The blood vessels run along the epineurium before entering the perineurium and endonerium to form a capillary network (**Figure 2**). This provides nutrients to the long axons within the peripheral nerves and waste products are removed in corresponding veins (Ubogu 2020).

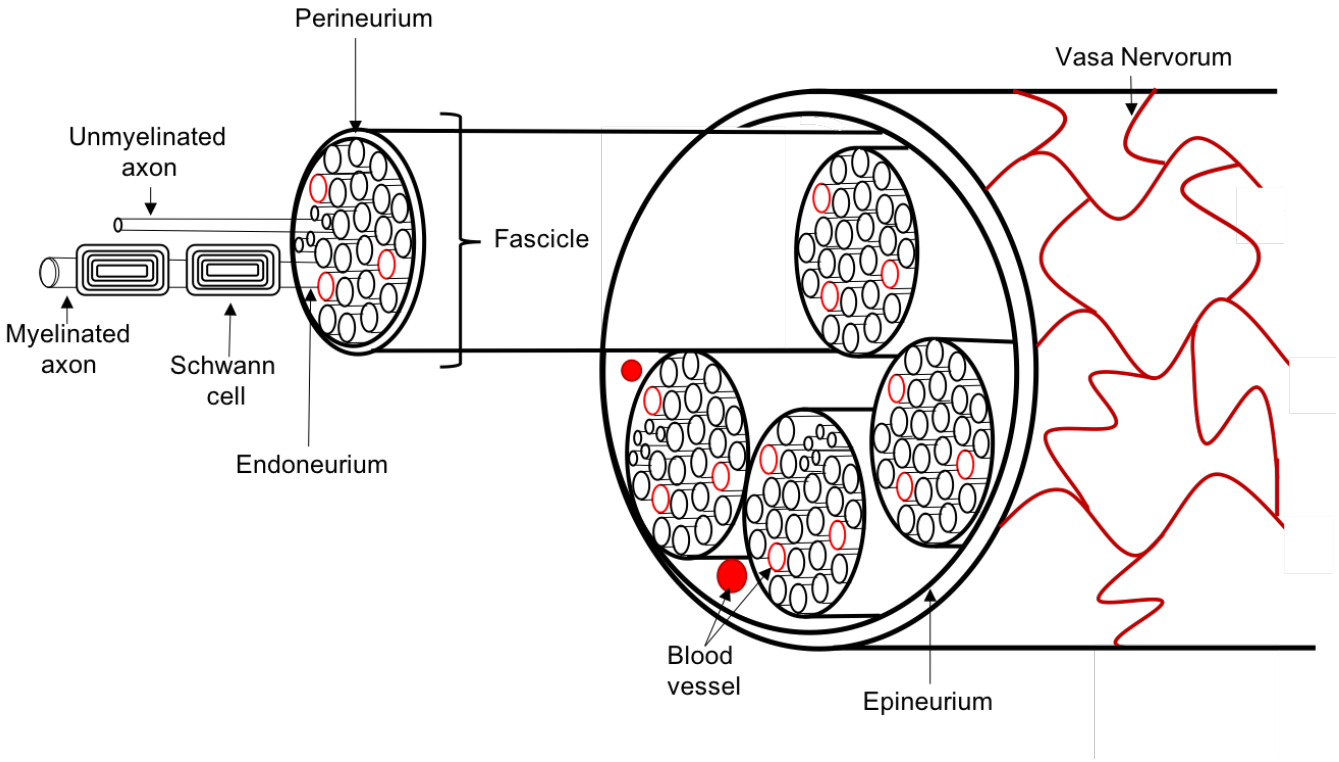

Figure 2 - Schematic of intact peripheral nerve

The epineurium is the outermost layer of connective tissues and binds nerve fascicles together. The epineurium is formed of connective tissue, collagen fibres and fibroblasts. The perineurium bundles axons together in nerve fascicles and is formed extracellular matrix composed of collagens and fibronectin. The perineurium's envelopes each nerve fascicle and main function is to control entry and exit of fluid. The endoneurium surrounds functional axons. Endothelial cells within the capillaries form the main blood nerve barrier. There are both myelinated axons where by Schwann cells form a myelin sheath and unmyelinated axons. The vasa nervorum are the small arteries that provide the peripheral nerve with blood.

1.6 Peripheral nerve injury epidemiology

Peripheral nerve injuries range from physical damage to the nerve where the nerve is crushed or transected to damage to nerves secondary to diseases such as diabetes or chemotherapy induced nerve damage. Various epidemiological studies show that men are much more likely to obtain peripheral nerve damage through injury than women. The mean age of which nerve injuries occurred is around 34 years old (Miranda and Torres 2016; Taylor et al. 2008). The most common nerve to be damaged was the brachial plexus which is in the upper region of the body, with sciatic and peroneal nerve most likely to be damaged in the lower regions of the body (Ciaramitaro et al. 2010). These injuries were often obtained through motor vehicle crashes although other common causes are sport injuries and combat wounds. A major cause of crush injuries also came as a result of bone dislocation. As peripheral nerve injury can cause significant pain and disability leading to decreased quality of life, it is becoming increasingly important to discover new ways to promote efficient and successful nerve repair.

Damage to peripheral nerves were classified into three categories by Seddon in 1972 and Sunderland in 1978, Neurapraxia, Axonotmesis and Neurotmesis (Robinson 2000). Neurapraxia is a mild injury to the nerve with a good prognosis. It occurs when a small part of the nerve is injured leading to interruption of conduction and temporary paralysis. During this type of injury there is no loss of axon continuity, the endoneurium, perineurium and epineurium remain intact and no Wallerian degeneration occurs. The temporary paralysis occurs due to no conduction occurring in the area of the injury as demyelination occurs following injury. Full recovery occurs following remyelination of the injured portion of the axon.

Axonotmesis is a severe injury as a result of more serious trauma or compression of the nerve. The epineurium and the perineurium remain intact however the axon and myelin are disrupted and Wallerian degeneration occurs distal to the injury site. Often both motor and sensory function are lost and muscles can undergo atrophy if injured nerve cannot repair well or quickly enough. Axons often regenerate fully as they are able to regenerate through to the distal portion of the nerve through bands of Bungner which creates a permissive growth environment. Successful regeneration is however dependent on a number of factors including the time and distance of which a regenerating axon has to cover (Radic et al. 2018).

Neurotmesis is the most severe nerve injury, a full transection, where the entire nerve structure is severed and this disrupts the endoneurium, perineurium, epineurium, Schwann cells and axons (Radic et al. 2018). This disruption leads to Wallerian degeneration in the distal nerve stump and the generation of a nerve bridge which lies between the proximal and distal stump and is made up of nerve fibroblasts, endothelial cells and Schwann cells to bridge the gap between the proximal and distal ends of the cut nerve (**Figure 3).** For recovery axons are required to regenerate from the proximal nerve stump, negotiate through the nerve bridge, an area of which new tissue must be formed for the regenerating axon to cross, before muscles can be innervated. Complete functional and sensory recovery is often incomplete (Campbell 2008).

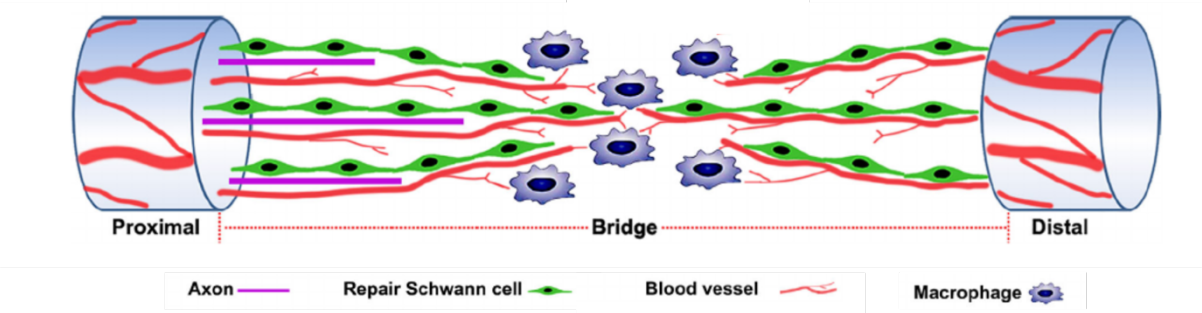

Figure 3 - Nerve bridge connecting the proximal and distal nerves

Schematic showing the nerve bridge that connects the proximal and distal nerve stumps. Many different cell types including nerve fibroblasts, endothelial cells, macrophages and Schwann cells enter into the nerve gap to form new tissue called the nerve bridge. The formation of this nerve bridge then generates a substrate that axons are able to migrate through from the proximal end and connect to the distal end. Figure adapted from (Min et al. 2021)

1.7 Current treatments for peripheral nerve injury

There are several treatment options for treating injured peripheral nerves depending on the degree of damage. Peripheral nerves do regenerate over time on their own although this process is slow with nerves only regenerating a maximum of around 1mm per day in humans. Therefore, if a large nerve such as the sciatic nerve is injured, regeneration through to its target may take many months to successfully occur. Often regeneration is incomplete and full functional recovery does not occur. Consequently, there are some treatments to enhance axonal regeneration and improve functional recovery.

If the nerve gap is <5mm the nerve can be directly sutured back together (R. J. Li et al. 2014b). For larger gaps, nerve grafts or artificial nerve conduits are used. Nerve grafts are currently considered the gold standard technique for repair. This technique requires the need for a second surgical procedure where a donor nerve is taken. The donor nerve is then ligated into the site of injury between the proximal and distal stumps where it can provide axon guidance through the graft and into the distal nerve

and trophic support from Schwann cells within the graft. This technique does however have its downfalls. Obtaining a nerve graft can in itself cause problems, in which removal of the donor nerve can create motor and sensory dysfunction at the donation site and it is not always possible to obtain a graft of the correct size or structure (Grinsell and Keating 2014; Sullivan et al. 2016). However, when these issues can be overcome, the advantages of such an auto-graft is that a true biological substrate is provided for axon regeneration, remyelination and the potential for functional recovery (R. J. Li et al. 2014b).

As a result of the potential problems associated with the use of a biological nerve graft, the use of artificial nerve conduits have been investigated. Conduits help guide axons and direct them towards their targets therefore allowing reinnervation and gain of functional recovery (Deal et al. 2012; R. J. Li et al. 2014b). Conduits provide a tube and a scaffold for structural support for regenerating axons. Traditionally, non biodegradable materials such as silicone or plastic which later in the regenerative process may be recognised as a foreign body and cause problems such as inflammation were used, the focus recently has been on natural, biodegradable materials such as collagen, fibrin and ECM (S. Klein et al. 2016; Lundborg et al. 1982). Scaffolds were also historically made out of synthetic materials but a move towards a mix of gel like structures and ECM is showing more promise in repairing large nerve gaps (L. L. Huang et al. 2018; G. C. Li et al. 2014a). Substances such as poly(lactide-co-glycolide) (PLGA) has been used to fill conduits with conductive fibre like structure to help guide axons to their peripheral targets and have been successful in animal studies (Jing et al. 2018). Recently research focus has been on introducing Schwann cells and growth factors into these conduits to further promote nerve repair (Ikeda et al. 2014; Muangsanit et al. 2020).

As discussed above, a nerve autograft is the gold standard in patients with larger gaps as they provide Schwann cells and the desired architecture required for successful repair. Nerve conduits currently show some success in patients but these lack Schwann cells and therefore the trophic support provided through the production of molecules such as growth factors and neurotrophins that is integral to nerve repair. Therefore there has been extensive research into the differential potential of stem cells into Schwann cells and their use in peripheral nerve repair. Human dental pulp stem cells (hDPSC) were obtained from human patients having their third molars removed and their differential potential was assessed. hDPSC were able to differentiate into Schwann cell like cells when treated first with betamercaptoethanol for 24h, followed by trans-retinoic acid for 72h and then with forskolin, basic fibroblast growth factor, platelet-derived growth factor and NRG. These Schwann cell like cells had a bipolar morphology and expressed p75 and GFAP like Schwann cells. In addition to this they were able to express neurotrophic factors BDNF, NGF, NT-3 and GDNF. Finally, these Schwann cell like cells were able to guide neurites and myelinate neurites in vitro (Martens et al. 2014). This has been assessed for use in conduits in a rat model. Nerve repair was enhanced with a greater number of neurites observed in conduits containing these Schwann cell like cells (Sanen et al. 2017). There is therefore great potential for use clinically in patients with peripheral nerve injuries, although currently no human trials have taken place with these cells or other stem cell derived cells (Z. Huang et al. 2020).

1.8 Biological response to peripheral nerve injury

Following injury, nerves undergo a now well characterised series of events. Axonal degradation in the distal portion of the nerve and back to the closest node of Ranvier occurs, this is called Wallerian degeneration, after Augustus Volney Waller who first observed these events (Waller 1850). Wallerian degeneration triggers a neuroinflammatory response which leads to the degeneration of axons and clearance of myelin and axonal debris proximally to the closest node of Ranvier and down through the length of the distal nerve. Axonal degeneration is accompanied by non-neuronal cellular events which help clear debris and then promote a permissive growth environment. If axon degeneration and the promotion of a permissive growth environment is successful degeneration is followed by axon regeneration and remyelination.

1.8.1 Neuronal response to injury

The first event to occur following a transection or crush nerve injury is axonal break down which occurs 24-48 hours post injury. Due to axonal damage intracellular calcium and proteases such as phospholipases and calpains quickly are expressed locally to the site of injury which leads to axon retraction and the formation of axon bulbs this is called acute axonal degradation (Knoferle et al. 2010). Calcium levels within the distal nerve stump rise and the axon goes into a period of latency where it is still able to conduct electrical signals. At around 72h post injury, rapid distal nerve degeneration occurs with microtubule disassembly and degradation of the axonal cytoskeleton (Hall 2005; Knoferle et al. 2010; Schlaepfer 1974). Chromomatolysis also takes place, which is the process in which the Nissl granules from the rough endoplasmic reticulum and site of protein synthesis within axons break up (Gaudet et

al. 2011). The degree in which axons degenerate in the proximal stump depends on the severity of the injury, in some case degradation is only back to the first node of Ranvier however in more severe cases, such as neurotmesis degeneration can occur all the way back to the cell body (Neukomm and Freeman 2014).

1.8.2 Schwann cell response to injury

The loss of Schwann cell-axon contact causes Schwann cells distal to the site of injury to undergo extensive changes to gene expression causing Schwann cells to dedifferentiate and then proliferate (Nocera and Jacob 2020). The expression of genes associated with myelin production such as MBP, MPZ and PMP22 is downregulated in myelinating Schwann cells and the expression of markers associated with immature Schwann cells and genes involved in processes promoting cell proliferation and survival are upregulated (Jessen and Arthur-Farraj 2019). This change in phenotype transforms Schwann cells into specialised cells, namely repair Schwann cells, some of the signalling pathways crucial to repair Schwann cell programming were discussed above. In this repair phenotype Schwann cells initiate the breakdown of compact myelin by undergoing a form of autophagy termed myelinophagy, where the myelin from myelinating Schwann cells is degraded to aid the clearance of debris (**Figure 4**) (Gomez-Sanchez et al. 2015). Schwann cells undertaking myelinophagy clear 40-50% of myelin themselves in the first 7 days post injury. In damaged nerves undergoing Wallerian degeneration myelin is fragmented into small ovid like structures where it loses its connection with the cell surface (Jung et al. 2011). As levels of myelin proteins decline, levels of genes associated with autophagy are induced such Autophagy related protein 9 and Autophagy related protein 7 (Gomez-Sanchez et al. 2015). Myelinophagy is inhibited upon treatment with

JNK/cJun inhibitors thereby highlighting this pathway as important for the activation of the myelinophagy pathway.

Products of axon degeneration and myelin breakdown are activators of Toll Like Receptors (TLR) on Schwann cells. TLR expression has been characterised within the peripheral nerves. TLR3, TLR4, and TLR7 are all highly expressed on Schwann cells in the intact peripheral nerves of rodents and their expression is suggested to play a role in immune surveillance (H. H. Zhang et al. 2018). TLR1 expression is upregulated following axotomy and may play a role in axonal degeneration following injury (Goethals et al. 2010). Activation of TLR signalling leads to the production of pro-inflammatory cytokines such as tumour necrosis factor alpha (TNF-α), Monocyte chemoattraction protein (MCP-1), Interleukin 1 alpha (IL-1α) and Interleukin 1 beta (IL-1β) from Schwann cells through NF-κB transcription factor signalling (Boivin et al. 2007). IL-1α and TNF-α for example is rapidly upregulated by Schwann cells that have lost their contact with axons and can be detected as soon as 6 hours post injury whereas IL-1β could be detected 1 day post injury and IL-6 mRNA as little as 2 hours posy injury (Reichert et al. 1996; Rotshenker et al. 1992; Shamash et al. 2002; Wagner and Myers 1996). In rats injection with recombinant IL-6 induces inflammation and severe demyelination indicating IL-6 role in both inflammatory cell recruitment (Deretzi et al. 1999).

1.8.2.1 Schwann cell migration

As part of the Schwann cell response to injury they become highly motile. Not only do Schwann cells migrate into the area of damage to help clear debris as previously described. In a transection injury where there is the formation of a nerve bridge, they also migrate into the peripheral nerve bridge. This migration into the nerve bridge allows the formation of Schwann cell cords which acts to link the proximal and distal

nerve stumps **(Figure 3).** These Schwann cell cords then act to direct regenerating axons from the proximal nerve stump, through the nerve bridge and into the distal stump promoting functional nerve repair (Min et al. 2021). In a mouse transection model, Schwann cells migrate out of the injury site on day 4 and on day 5 their migratory capacity exceeds that of axons and overtakes regenerating axons. Next, on day 6 axons migrate along Schwann cell chords following them across the nerve bridge and into the distal nerve stump (B. Chen et al. 2019). This mechanism shows an essential role for migratory Schwann cells and their role in axon guidance. ErbB2 signalling has been described to promote the migration of rat primary Schwann cells in vitro through activation of the GTPases Rac1 and Cdc42 highlighting this as one of the signalling pathway that may be responsible for repair Schwann cells migratory capacity (Yamauchi et al. 2008).

1.8.3 Macrophage response to nerve injury.

Signalling from axonal degeneration products through TLR signalling and the expression of pro-inflammatory cytokines from Schwann cells and resident macrophages, in association with the breakdown of the blood-nerve barrier, leads to the recruitment of haematogenous macrophages (Boivin et al. 2007; Rosenberg et al. 2012). These macrophages migrate into the peripheral nerves in response to cytokines and chemokines such as TNF-α, MCP-1, IL-6, IL-1α and IL-1β (Gaudet et al. 2011). Macrophages begin to accumulate 2-3 days following injury and peak in number at around day 14 in rodents (**Figure 4**) (Avellino et al. 1995; Bendszus and Stoll 2003; Mueller et al. 2003; Ydens et al. 2012).

The major cytokine responsible for macrophage recruitment is MCP-1 (also known as CLL2) which acts on the CCR2 receptor. The use of neutralising antibodies for MCP-

1 led to decreased macrophage accumulation within the peripheral nerves following injury (Perrin et al. 2005; Siebert et al. 2000; Zigrnond and Echevarria 2019). Another of these cytokines is TNF-α. TNF-α is expressed by Schwann cells and acts to recruit macrophages to the site of injury, rats with a global TNF-α KO show reduced macrophage recruitment and axon regeneration at 1 week post injury Correspondingly, injection of TNF-α into the nerves lead to break down of the blood nerve barrier and inflammatory cell infiltration (Shubayev et al. 2006; Uncini et al. 1999). Once macrophages enter the peripheral nerve, they themselves secrete TNF-α to continue to promote a pro-inflammatory environment within the nerve and their function has been cited as one of the factors responsible for neuropathic pain post injury (Shubayev and Myers 2000). IL-1β also has a role in recruiting macrophages into the peripheral nerves. The use of IL-1β blocking antibodies in the injured peripheral nerve significantly reduced macrophage recruitment and myelin clearance (Perrin et al. 2005). IL-6 has been reported to be primarily secreted from macrophages and not only promotes myelin phagocytosis, but also has a role in the generation of neuropathic pain (Murphy et al. 1999; Reichert et al. 1996; van Rossum et al. 2008). Under a pro-inflammatory environment as early as 2 days post injury, macrophages act to assist Schwann cells with the second phase of axonal and myelin debris removal, in which macrophages accumulate around injured axons and phagocytose myelin constituents (Avellino et al. 1995; Bruck et al. 1996). Constituents of myelin debris such as MAG are inhibitory to axonal regeneration (Hirata and Kawabuchi 2002; McKerracher et al. 1994). Therefore, the removal of myelin by macrophages is essential to axon regeneration and acts to clear the way for newly regenerating axons (Perry et al. 1987). When macrophages are inhibited through ingestion of liposomes

containing dichloromethylene diphosphonate myelin degradation in the peripheral nerves is reduced (Bruck et al. 1996).

After carrying out their pro-inflammatory phagocytic function, macrophages then undergo a transition. This transition is from a pro-inflammatory, phagocytic M1 state which predominately acts to digest cellular debris, to an anti-inflammatory M2 state which acts to promote tissue remodelling and subsequent regeneration (P. W. Chen et al. 2015; Kigerl et al. 2009; Mantovani et al. 2004). During this transition, macrophages switch from undergoing their role in actively removing debris to secreting cytokines and trophic factors that promote and support axon growth and tissue regeneration (David and Kroner 2011; Novak and Koh 2013). These secreted growth factors are essential to axon regeneration, in culture, neurones treated with macrophage conditioned media is enough to promote their survival and stimulate their outgrowth (Shibata et al. 2003).

Pro-inflammatory cytokines with a well defined roles within the peripheral nerve are IL-10, IL-4 and IL-13. IL-4 expression is upregulated around 10 days post-injury and has been described to directly promote axon regeneration following a transection injury (Mokarram et al. 2012; Opal and DePalo 2000). Whereas IL-10 expression can be detected from day four post-injury, its expression peaks at day 7 and continues to remain elevated up until day around day 14 in rodents (Be'eri et al. 1997). IL-10 acts to resolve the inflammatory response by inhibiting pro-inflammatory cytokine expression at the later stages of Wallerian degeneration following myelin clearance. IL-6 on the other hand can be detected within the first 2 hours following injury and remains expressed up to 21 days post-injury when it is suggested to act to reduce the expression of TNF-α, further polarising the peripheral nerve towards an M2 environment (Reichert et al. 1996; Xing et al. 1998). In a rat model of peripheral nerve

transection injury, a conduit containing IL-4 was placed at the injury site to initially polarise macrophages into an M2 state; this led to enhanced Schwann cell migration and axon regeneration (Mokarram et al. 2012). From all these findings, it is therefore clear that macrophages and the cytokines they express need to be carefully regulated to help support peripheral nerve regeneration and any dysregulation of their expression can be detrimental to repair.

1.8.3.1 Macrophage function in Schwann cell guidance and maturation following peripheral nerve injury

In addition to the production of cytokines, macrophages in injured peripheral nerves also have other characterised functions. Following peripheral nerve transection injury, Schwann cells are required to cross the nerve bridge to enable axon regeneration from the proximal through to the distal nerve. Schwann cells expressing Robo1 can be guided through the nerve bridge to the distal stump following macrophage secreted Slit3 (Dun et al. 2019). Schwann cells use blood vessels in the nerve bridge as tracts and this enables regenerating axons to cross through the bridge, guided to the distal nerve. For the process to occur multiple cell types are required to work together. Macrophages sense hypoxia in a nerve bridge and begin to produce VEGF (Vascular endothelial growth factor), a pro-angiogenic factor. This promotes endothelial cell migration from the nerve stump into the bridge and the formation of new vascularisation consequently enabling Schwann cell migration and axon regeneration through the distal nerve stump (Cattin et al. 2015).

Macrophages have also been described play a role in Schwann cell maturation post injury. The ablation of macrophages in a mouse model following peripheral nerve injury had been described to cause an increase in proliferating Schwann cells in the

peripheral nerves 3 days post injury (Bruck et al. 1996). At two weeks post-peripheral nerve injury where Schwann cell should begin to differentiate back into myelinating Schwann cells and remyelinate axons, Schwann cells were less differentiated, still showing markers for immature Schwann cells. As a result of a delay in Schwann cell differentiation into a myelinated Schwann cell, there was a significant reduction in the number of remyelinated axons. Gas6 (growth arrest specific gene 6) is one of the molecules involved in this process and is expressed from macrophages and acts on Schwann cells promoting Schwann cell differentiation, Schwann cell remyelination and ultimately efficient axon regeneration (Stratton et al. 2018).

1.8.4 Axon regeneration

During the regeneration stage, around 4 days post injury growth factors are produced from both macrophages and Schwann cells that provide a permissive growth environment to support axonal growth and neuronal survival (Barrette et al. 2008). Growth factors such as: NGF, BDNF, GDNF, NT3, NT4 and receptors TrkA and p75 play major roles during development (E. J. Huang and Reichardt 2001). Growth factor expression from neurons and Schwann cells is high during development but their expression is barely detectable in mature intact peripheral nerves. However, growth factor expression is strongly induced following peripheral nerve injury (Frostick et al. 1998; Gordon 2014) . The production of these factors in both the early and later time points of axon regeneration is critical for successful peripheral nerve regeneration (**Figure 4**). Neurotrophins initially act to promote the survival of injured axons proximal to the site of injury. Later following debris clearance, they act to promote axon elongation, growth and remyelination in the distal part of the nerve. GDNF and NT-4 produced by Schwann cells, have been reported to promote axon regeneration by acting to support regenerating axons and remyelination of axons in the rat facial nerve

(Barras et al. 2002). NGF and BDNF expression from macrophages is high following injury and acts to promote axon survival and outgrowth (Heumann et al. 1987). IL-4 and IL-6 have also both been described to act together with neurotrophic factors to increase neuron outgrowth, providing additional evidence that the cytokine expression and the inflammatory status within the peripheral nerve is crucial to successful peripheral nerve regeneration.

1.8.5 Reinnervation and resolution of the inflammatory response

In addition to myelin clearance and growth factor production, dedifferentiated Schwann cells act to provide structural support for axon regeneration. Bipolar Schwann cells join together in basal lamina tubes to form tracks known as bands of Bungner. These bands help to provide a growth environment that supports and guides axons regenerating through the distal nerve towards peripheral targets (Gaudet et al. 2011; Jessen and Mirsky 2016).

In order for peripheral nerve repair to become completed, axons must transverse the site of injury and reinnervate their targets, Schwann cells must remyelinate and haematogenous macrophages must leave the peripheral nerve. In a crush injury, the structure of the peripheral nerve is often retained and axons regenerate readily. In a transection injury, the proximal and distal ends of the nerve retract and a nerve bridge is formed. Axons must then navigate through the nerve bridge and down through the distal nerve stump to reinnervate their targets. Anti-inflammatory cytokines such as IL-10 are able to switch off the pro-inflammatory response from macrophage which allows them to transverse out of the peripheral nerves. IL-10 null mice show defective inflammatory resolution and impaired motor and sensory functional recovery (Mietto

et al. 2015). The switch to an anti-inflammatory cytokine expression profile limits further immune cell infiltration and prevents further myelin phagocytosis.

Remyelination occurs by signalling through PI3K-Akt-mTORC1 axis which activates transcription factors such as Krox-20, ultimately leading to the expression of myelin proteins and myelinated axons(Figlia et al. 2017; Topilko et al. 1994). Axonal derived Nrg1 is one of the signals that acts to promote myelination of regenerated axons. In mice with a Cre mediated KO of Nrg1 in the motor and sensory neurones, peripheral nerves showed decreased remyelination and increased G ratios after a crush injury compared to controls (Fricker et al. 2011; Mindos et al. 2017). Although axons that have reconnected with peripheral targets do remyelinate, myelin is often thinner than that in the proximal nerve (**Figure 4**).

1.8.6 Failure to reinnervate

Although axons do have the remarkable ability to regenerate, it is not always successful and axon regeneration is not always synonymous with functional recovery. This can be due to multiple reasons: hindrance or slow axon growth, small numbers of axons passing through the bridge and distal nerve stump, mis- directed axons and inability to support regenerating axons over a long period of time (Jessen and Mirsky 2019).

One of the biggest problems is the slow growth of axons. As nerve regeneration in humans occurs at a slow rate over a long distance, patients with peripheral nerve injury often see chronic denervation and muscle wasting (Menorca et al. 2013). Full functional recovery can only be reached if the end tissue is well maintained and is able to be reinnervated.

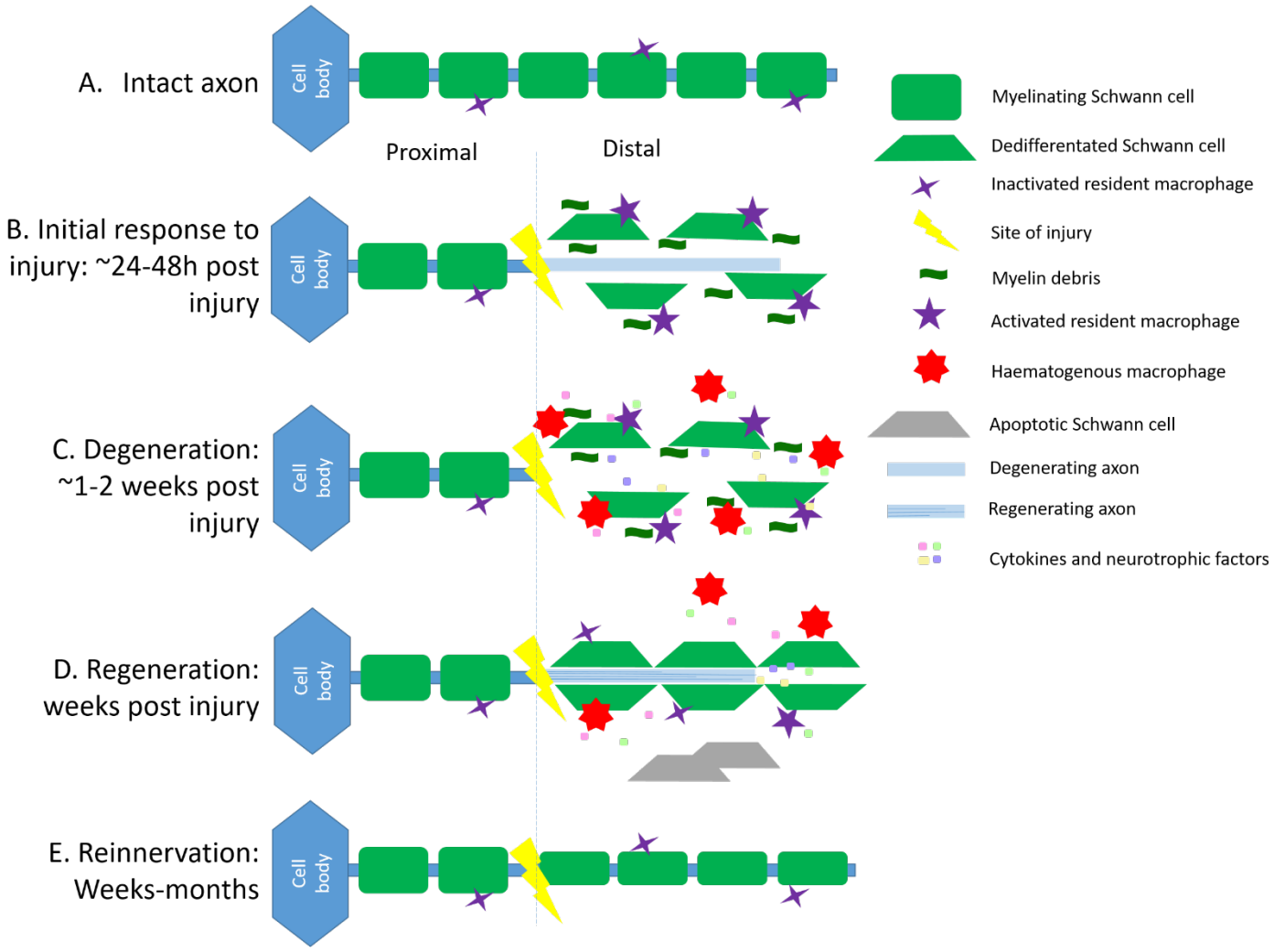

Figure 4 - Schematic illustration of events that occur following peripheral nerve damage

Schematic summarising the main series of events which occur during Wallerian degeneration in injured mouse peripheral nerve. A. uninjured nerve. B. Initial response to injury where axons begins to degenerate and myelin is broken down in the distal nerve stump. SCs and resident macrophages become activated and begin to secrete cytokines. SCs begin to dedifferentiate. C. In response to cytokine secretion, haematogenous macrophages infiltrate into injured nerves and work with SCs and resident macrophages to phagocytose myelin debris. Haematogenous macrophages contribute to the production of cytokines and also act to secrete neurotrophic factors. D. When SCs and macrophages successfully clear myelin debris macrophages switch to secrete anti-inflammatory factors and SCs realign to form tracts called bands of Bungner through which axons can regenerate. Macrophages start to clear from the site of injury. E. If axons' can successfully innervate their peripheral targets SCs can begin to re-myelinate, although myelin surrounding injured axons is often thinner than myelin in the proximal stump. The time scale of regeneration if much longer in humans compared to rodent systems, taking months to years for successful re-innervation (Gaudet et al. 2011)

1.9 Macrophage clearance mechanisms

After nerve regeneration macrophages are required to further down-regulate the expression of pro-inflammatory cytokines expression and up-regulate the expression of anti-inflammatory cytokines before macrophages are ready to leave the distal nerve stump (F. C. Zhang et al. 2020). Whilst the majority of macrophages are known to migrate out of peripheral nerves back into the blood stream, some macrophages are known to undergo apoptosis (Kuhlmann et al. 2001). Although macrophage efflux has been extensively described, the mechanisms which fully control this have not been discovered (Mueller et al. 2003). There is currently only one well defined mechanism controlling macrophage clearance, namely the role of the Nogo receptor (NgR) (Fry et al. 2007; Martini et al. 2008). NgR1 and NgR2 are expressed on the surface of macrophages present within the peripheral nerve within the first week following injury. These receptors can interact with MAG and other myelin proteins that make up newly synthesised myelin. The presence of new myelin around re-myelinated nerves interacts with NgRs to mediate repulsive signalling via Rho-A within macrophages and initiates macrophage migration. Macrophages then migrate towards blood vessels and enter back into the blood stream. Additional signals that can initiate repulsive signalling and promote macrophage migration may be important players in macrophage clearance from the distal nerve stump during peripheral nerve regeneration.

1.10 Neuropathic pain

If macrophages fail to leave the distal nerve stump this can lead to chronic inflammation and the development of neuropathic pain. Pro-inflammatory cytokine production is not downregulated and leads to prolonged macrophage recruitment and consequently chronic inflammation (Opree and Kress 2000). High levels of TNF-α and interlukin-2 (IL-2) have been correlated to patients with painful neuropathies, indicating

that neuropathic pain is at least in part due to the presence of pro-inflammatory cytokine producing macrophages (Uceyler et al. 2007). In a model of diabetic neuropathy in rats, depleting macrophage numbers within the peripheral nerves using liposome-encapsulated clodronate lead to a decrease in neuropathic pain (Mert et al. 2009).

1.11 Peripheral neuropathies

Peripheral neuropathies are caused by damage or disease to peripheral nerves. Peripheral neuropathies can be secondary to other diseases such as diabetes, cancer or infection, induced as a result of toxic chemotherapies or due to somatic or germline mutations within axons or Schwann cells leading to neuropathies (Brown et al. 2019; R. Singh et al. 2014; Willison et al. 2016). Neuropathy leads to the degeneration of peripheral nerves and consequently symptoms such as muscle wasting, skeletal deformities, and sensory problems such as weakness and pain.

There are major similarities within the nerves of those with a peripheral nerve injury and those with a peripheral neuropathy, with the most striking similarities seen being demyelination and macrophage recruitment into the peripheral nerves (Martini et al. 2013). Although Wallerian degeneration is crucial for nerve regeneration, Wallerian degeneration and macrophage recruitment taking place in uninjured nerves can have catastrophic effects on an individual (Rotshenker 2011). In the peripheral nerves of those with peripheral neuropathies, haematogenous macrophages enter the peripheral nerves in response to cytokines being expressed from Schwann cells and begin phagocytosing myelin (**Figure 5**).

1.11.1 Charcot Marie Tooth disease

CMT disease is the most common inherited peripheral neuropathy and has an occurrence in the population of around 1:2500. CMT occurs as a result of mutations within Schwann cells and axons and to date more than 40 gene mutations have been identified (Finsterer et al. 2018; Santoro et al. 2004; Saporta et al. 2011). There are many different types of CMT and these have been categorised based on the major changes or mutations found within the disease, demyelinating (CMT1/CMT4), Axonal (CMT2) or X-linked (CMTX).

CMT1 is the most common form of CMT and inherited in an autosomal dominant pattern. CMT1 is due to dysfunction in Schwann cells and the formation and maintenance of myelinated sheath. CMT1 type A (CMT1A) is caused by duplication or point mutation in the PMP22 gene whereby too much PMP22 is produced which results in inefficient protein folding, mutated protein and a lack of functional PMP22 protein. A 1.4Mb duplication of the PMP22 gene on chromosome 17p11.2 is the most common and accounts for up to 80% of cases (Chance et al. 1992; Krajewski et al. 2000). CMT1 usually presents in adolescence and is a slow progressive disease; patients have a normal lifespan. When patients first present, they often show slow conduction velocities usually in the lower legs , associated with muscle weakness and atrophy in the legs and this is followed by weakness and decreased sensation in the hands. CMT1A can be diagnosed through nerve conduction velocity (NCV) tests, genetic testing and nerve biopsies. Biopsies taken from patients show signals of demyelination, remyelination, the presence of onion bulbs and axon loss (Saporta et al. 2011).

CMT2 is caused by direct damage to the axons within the peripheral nerves. CMT2 can be inherited in both an autosomal dominant and autosomal recessive pattern.

CMT2A is the most common subtype of CMT2 which accounts for 20% of the cases of axonal CMT and is caused by defects in the MFN2 (mitofusin 2) gene (Finsterer et al. 2018). MFN2 is a dynamin-like GTPase an functions to regulate mitochondrial fusion and cell metabolism. In the axon MFN2 is expressed in mitochondria and has the role of energy sensing and promoting axon integrity. MFN2 mutation has been described to lead to defects in mitochondrial distribution along the axon which lead to the metabolic needs to the axons not being met and consequently axonal degeneration (Misko et al. 2012). CMT2 is less severe than CMT1 and onset is a bit later in life around 30 years of age (Bienfait et al. 2006). Patients presenting with CMT2 show distal weakness, atrophy and sensory loss. CMT2 can be diagnosed through NCV tests, electromyograph (which measures electrical activity within muscles) and genetic testing (Saporta et al. 2011).

CMTX is an X-Linked CMT caused by a mutation on the X chromosome and inherited in a dominant pattern. As a result of this it is much more common and severe in men than women (Y. Wang and Yin 2016). CMTX is caused by mutations in the connexin-32 gene located on the X-chromosome. Connexin 32 is located in Schwann cells, specifically in the gap junctions between layers of myelin and function to allow the flow of ions between layers of non compact myelin. It also interacts with components of myelin such as MAG and acts to help maintain the myelin sheath (Cisterna et al. 2019). Symptoms of CMTX are similar to those seen in CMT1 and CMT2. CMTX can be diagnosed using NCV tests, genetic testing and nerve biopsies which show prominent axonal changes (Saporta et al. 2011).

The pathogenesis of CMT1, CMT2 and CMTX diseases all lead to inflammation within the peripheral nerve (Bienfait et al. 2006; Groh et al. 2010; Martini et al. 2013). The expression of inflammatory cytokines within the peripheral nerves leads to

macrophage recruitment through the blood nerve barrier; Macrophages then act to phagocytose myelin and axonal debris, similar to what is seen following peripheral nerve injury (Hanemann and Muller 1998). Macrophages in the peripheral nerve following peripheral nerve injury usually act to clear debris, which would allow for nerve regeneration, however in CMT patient nerves macrophage recruitment is continuous which therefore leads to continuous damage. The presence of macrophages and their phagocytic activity within the nerves therefore means that there is a constant cycle of inflammation and macrophage recruitment and consequently the inability to resolve this inflammatory response (Ip et al. 2006). Mouse models of CMT1 in particular sees macrophage mediated myelin disruption, whereby macrophages act to phagocytose morphologically normal myelin sheathes (Kobsar et al. 2005). Inhibiting inflammatory cytokine expression and recruitment of macrophages may break the inflammatory cycle and allow Schwann cells to myelinate axons.

MCP-1 appears to be a major signal in the pathogenesis of peripheral neuropathies. In animal models of CMT1X, an inherited neuropathy, MCP-1 KO mice can block macrophage recruitment and subsequent myelin phagocytosis (Groh et al. 2010). Therefore, this work showed that eliminating MCP-1 expression from Schwann cells and macrophages in these diseases, where expression within the peripheral nerve is inappropriate, could lead to better disease outcomes. With macrophages being the major immune cell type being found within the peripheral nerves of patients with neuropathies, blocking macrophage recruitment into the nerves and prevention of myelin phagocytosis may also be an effective treatment strategy.

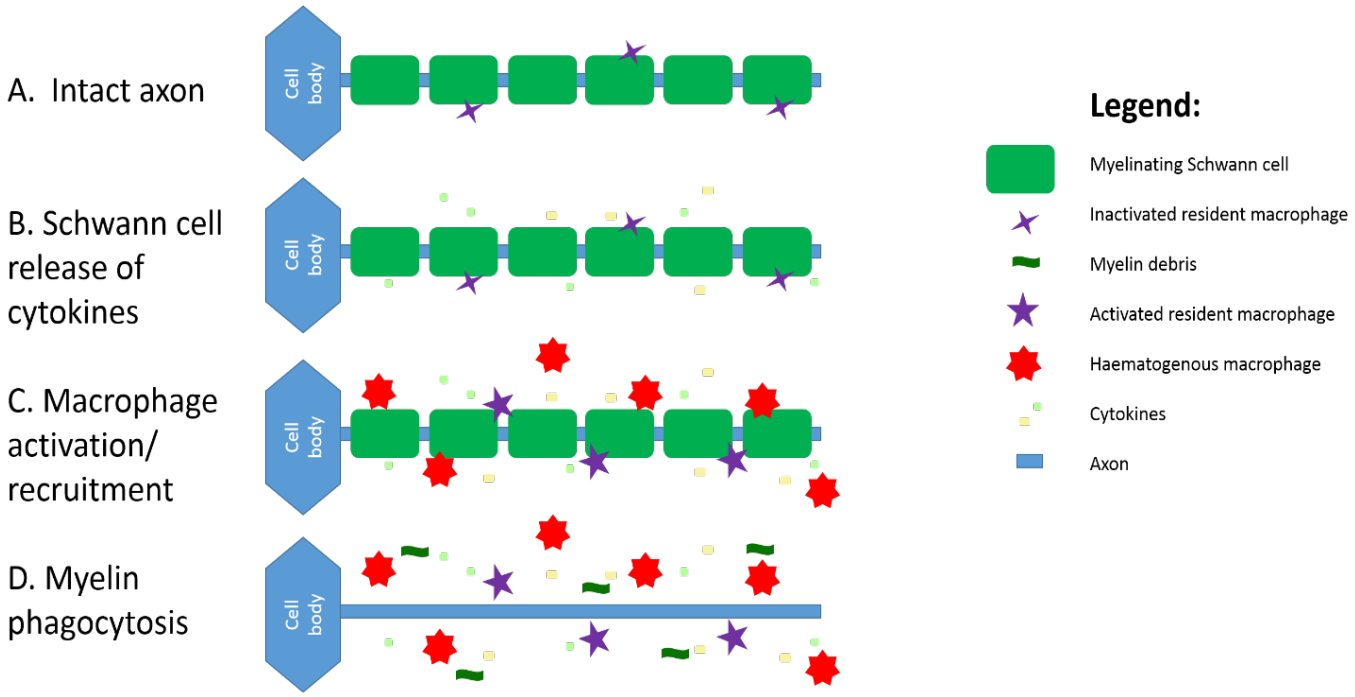

Figure 5 - Schematic of events that occur within the peripheral nerve of a peripheral neuropathy patient

Schematic events within nerve of peripheral neuropathy patient. A. Intact axon. B. SCs release cytokines within the peripheral nerves. C. In response to cytokine products resident macrophages become activated and haematogenous macrophages infiltrate into the peripheral nerves. D. Macrophages and SCs phagocytose myelin leaving intact but demyelinated axons which leads to the pathogenesis of peripheral neuropathies.

1.11.2 Guillain Barre Syndrome

Guillain Barre syndrome is a polyneuropathy that has two major subtypes, an acute demyelinating polyneuropathy which accounts for around 95% of cases and an axonal subtype which accounts for the remaining 5% of cases in Europe (Hadden et al. 1998). Guillain Barre syndrome is often caused secondary to an infection where the body's immune system malfunctions and immune cells begin the attack the nerves. Infections that can lead to Guillain Barre Syndrome include *Campylobacter jejuni* infection, HIV, glandular fever, Zika virus and cytomegalovirus although it can come secondary to more common illnesses such as food poisoning or flu (Leonhard et al. 2019; Leonhard et al. 2020; McCarthy and Giesecke 2001; Vellozzi et al. 2014). Symptoms are usually

muscle weakness, pain and problems with both balance and coordination. Diagnosis is through NCV tests, electromyography testing and lumbar puncture analysis where cerebral spinal fluid can be assessed for infection (Hadden et al. 1998). During Guillain Barre syndrome macrophages enter the peripheral nerves in response to pro-inflammatory cytokines TNFα, IL1β, IL12, IL18, IFNγ and MCP1 (Nicoletti et al. 2005; Sharief et al. 1993). Acute demyelinating polyneuropathy is the most common type of Guillain Barre syndrome and occurs when macrophages attack the myelin sheath, in axonal forms macrophages attack the axons. Both of these subtypes have the same pathogenesis and leads to increased inflammation and production of toxic species such as reactive oxygen species which leads to the peripheral nerve damage observed (Hartung and Toyka 1990). Although Guillain Barre Syndrome can be treated, there are some residual effects of the disease which can lead to decreased quality of life such as muscle weakness due to damaged axons and neuropathic pain (van den Berg et al. 2014). Inhibiting pro-inflammatory cytokine expression in peripheral nerves during the onset or early stages of Guillain Barre syndrome may act to inhibit macrophage recruitment into the nerves and prevent myelin and axon loss. During later stages of the disease polarising macrophages into an anti-inflammatory state, which promotes tissue regeneration and macrophage migration out of the peripheral nerves, may be useful to help resolve disease (Shen et al. 2018).

1.12 VIP and PACAP

Vasoactive Intestinal Peptide (VIP), a 28 amino acid peptide was first isolated from porcine intestine in 1970 and was first shown to have potent vasodilation properties (Said and Mutt 1970, 1972). Pituitary Adenylyl Cyclase Activating Peptide (PACAP), a 38 amino acid peptide, was later in 1989 and first isolated from ovine hypothalamic tissues (Miyata et al. 1989). PACAP and VIP share 68% amino acid homology at the N-terminus and both belong to the secretin-growth hormone-releasing hormone-glucagon superfamily. VIP and PAPCAP are neuropeptides, small polypeptides secreted by neuronal cells, and are key mediators in the communication between neurons and effector cells such as immune cells. Three receptors have been identified for VIP and PACAP: VPAC1, VPAC2 and PAC1. Both VIP and PACAP can act through VPAC1 and VPAC2, whereas PAC1 selectively binds PACAP (**Figure 6**) (Harmar et al. 1998; Vaudry et al. 2009; Waschek 2013). To allow functional differentiation between the effects of receptor specific signalling, receptor specific agonists and antagonists have been designed (Harmar et al. 1998). VPAC1, VPAC2 and PAC1 are G-Protein-Coupled Receptors (GPCRs) and ligand-receptor signalling primarily induces cAMP dependent signalling. These peptides have now been discovered to be widely expressed in a range of tissues and process a range of biological functions, one of these being immunomodulatory actions.

A

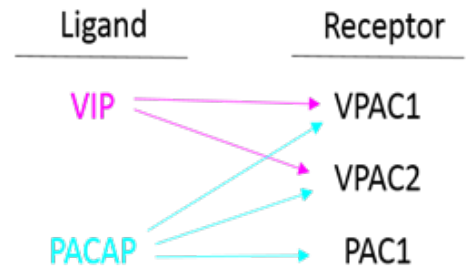

B

Receptor	Agonist	Antagonist
VPAC1	[Ala^{11,22,28}]VIP and [Lys^{15},Arg^{16},Leu^{27}]VIP(1-7)/ GRF(8–27)-NH_2	PG97-269
VPAC2	BAY 55-9837/Ro25-1553	PG99-465 (not completely selective)
PAC 1	Maxadilan	PACAP(6–38)

Figure 6 - VIP/PACAP receptor-ligand interactions

Schematic detailing receptor specificity. VPAC1 and VPAC2 recognise both VIP and PACAP whereas PAC1 is selective for PACAP (13). B. Table showing known receptor-specific agonist and antagonists for VPAC1, VPAC2 and PAC1 receptors. (Ganea and Delgado 2002)

Both VIP and PACAP can modulate the release of cytokines by inhibiting NF-κB signalling and down-regulating the release of pro-inflammatory cytokines such as TNF-α and MCP-1 (Delgado and Ganea 2000, 2001b; Delgado et al. 2002). VPAC1, VPAC2 and PAC1 have all been described to be expressed on both human and mouse macrophages (Burian et al. 2010; Calvo et al. 1994; Carrion et al. 2016; Delgado et al. 1999b; Delgado and Ganea 2001a; Storka et al. 2013). VPAC1 and VPAC2 have been shown to be expressed on macrophages with VPAC1 expression higher than VPAC2 expression (Burian et al. 2010; Carrion et al. 2016; Delgado et al. 1999c). PAC1 expression is less well described but appears to be expressed to a lower levels than that of VPAC1 and VPAC2 (Delgado and Ganea 2001a; Martinez et al. 2002). VPAC1 and PAC1 have been shown to be constitutively expressed on macrophages whereas VPAC2 expression is induced by stimulation of a pro-inflammatory environment using LPS in vitro (Carrion et al. 2016; Delgado et al. 1999c). VIP and PACAP have well described functions in inhibiting the expression of pro-inflammatory cytokines. VIP and PACAP actions on macrophages in both the blood and within other tissues have been described to inhibit the expression of pro-inflammatory cytokines (Delgado et al. 1999c; Delgado and Ganea 2001a; Ran et al. 2015; W. Sun et al. 2000). In macrophages stimulated with LPS to induce the expression of pro-inflammatory cytokines, VIP treatment was able to inhibit the expression of pro -inflammatory cytokines IL-12, IL-6 and TNF-α (Delgado et al. 1999c). VIP has also been reported to inhibit TGF-β expression from mouse macrophages and the cell line Raw 264.7 (W. Sun et al. 2000; C. X. Sun et al. 2017).

VIP and PACAP can act to inhibit pro-inflammatory cytokine expression through both cAMP-dependent (**Figure 7**) and -independent pathways (**Figure 8**). There are multiple cAMP dependent pathways for VIP and PACAP inhibition of cytokine

expression. In a cAMP dependent manner VIP has been shown to inhibit NFκB activity through phosphorylation of CREB, which binds to its cofactor CREB binding protein; this prevents interaction of CREB with NFκB which leads to its inhibition through its subsequent inability to translocate to the nucleus (Delgado and Ganea 2001a). The cAMP dependent pathway can also cause inhibition of phosphorylation of the MEKK (MAP/ERK kinase kinase), which leads to inhibition of p38 and inhibition of phosphorylation of TBP (TATA-box protein) (Delgado and Ganea 2000). This phosphorylation leads to TBP having reduced affinity for NFκB and therefore less ability of NFκB translocation into the nucleus. cAMP dependent pathways for VIP and PACAP signalling can also activate PKA which inhibits the phosphorylation of the JAK/STAT (Janus kinase/signal transduction and activator of transcription) pathway inhibiting the production of nitric oxide and consequently inhibiting inflammation (**Figure 7**) (Ran et al. 2015; W. Sun et al. 2000). In a cAMP independent manner VIP and PACAP binding to their receptors may inhibit the activity of IκK enzyme complex that is involved in propagating the cellular response to inflammation. IκK then is unable to phosphorylate IκB, a protein that is bound to NFκB and inhibits its function (**Figure 8**). This leads to stabilisation of the NFκB- IκB complex and NFκB remains inactive in the cytoplasm. VIP/PACAP signalling has therefore been investigated as a potential treatment for many chronic inflammatory diseases such as arthritis and in experimental autoimmune encephalomyelitis (a model for multiple sclerosis), where it has been seen to reduce the severity of such diseases (Delgado et al. 2001; Gonzalez-Rey et al. 2006b; Gonzalez-Rey et al. 2006a; Tan et al. 2009).

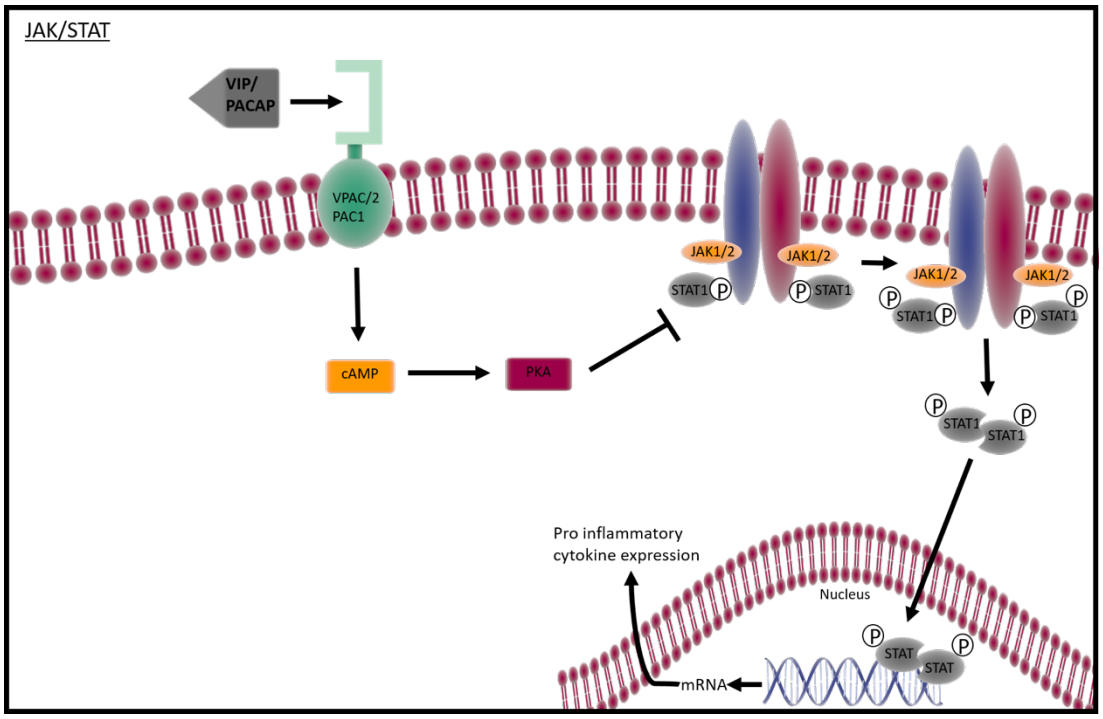

Figure 7 - VIP and PACAP inhibition of JAK/STAT pathway

VIP and PACAP can act through their receptors to increase intracellular cAMP and activate PKA. PKA can then inhibit JAK/STAT phosphorylation and their translocation into the nucleus. This prevents the transcription of pro-inflammatory cytokines.

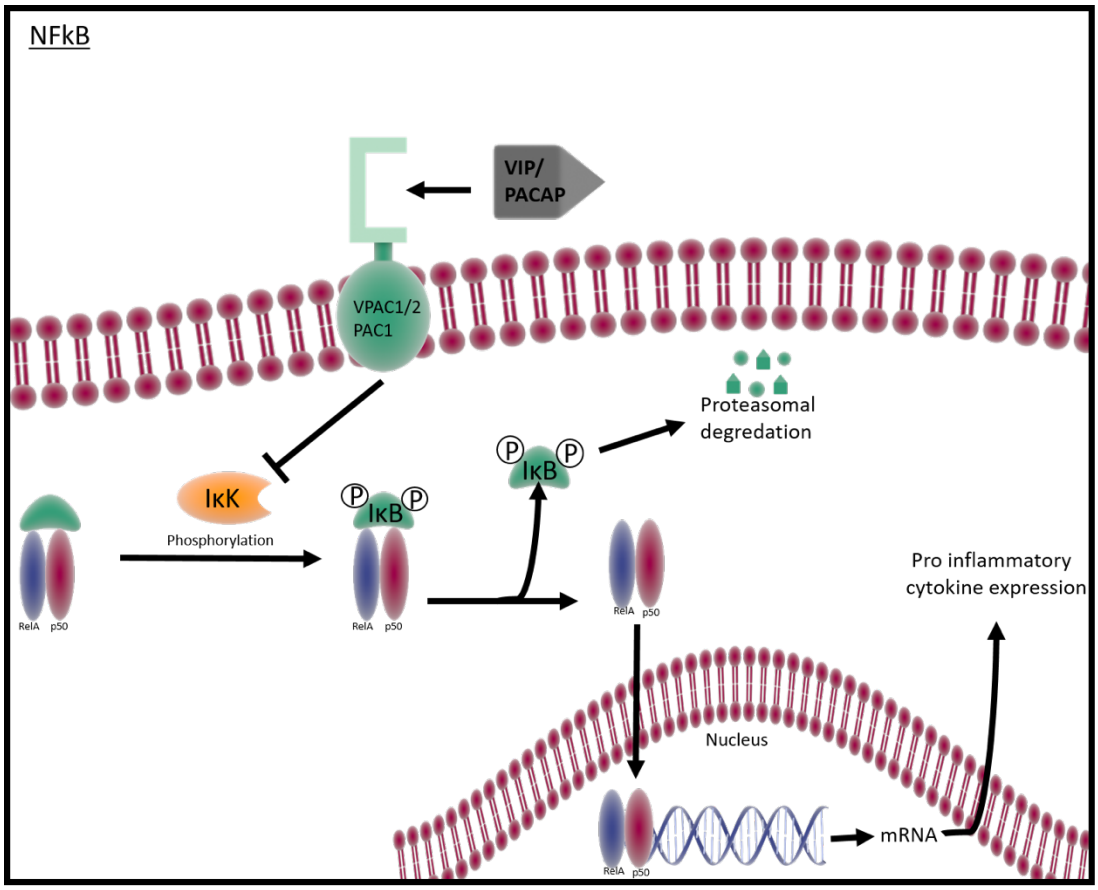

Figure 8 - VIP and PACAP inactivation of NFκB pathway

VIP/PACAP can act through VPAC1/VPAC2/PAC1 to inhibit the NFκB pathway through a cAMP independent manner. Peptide binding to receptor can inhibit activity of IκK. IκK cannot phosphorylate IκB. IκB complex remains in the cytoplasm and RelA/p50 cannot translocate to the nucleus for pro-inflammatory cytokine expression.

VIP and PACAP expression is up-regulated in the peripheral nerves following injury and has been specifically described to be upregulated in the both motor and sensory axons post injury (Zhou et al. 1999). VIP mRNA is detectable in motor neurons 6 h post peripheral nerve injury and reaches a maximum level up-regulation on day 7. Thereafter, the mRNA level of VIP begins to decrease but VIP expression remains upregulated up to 30 days post-injury (Armstrong et al. 2003). cDNA microarray analysis in dorsal root ganglion (DRG) at 2, 7, 14, and 28 days following nerve injury also showed at least a 10 fold VIP up-regulation at all investigated time points (H. S. Xiao et al. 2002). The up-regulation of PACAP mRNA in motor neurons is detectable 6 h after injury and PACAP peaks at 48 h where it shows a more than 20-fold up-regulation. PACAP levels in motor neurons then decrease slightly from day 2 following injury, but remain elevated 10-fold for as long as 30 days post injury and therefore throughout the regeneration process (Zhou et al. 1999). Previous studies have confirmed that VIP and PACAP are secreted by regenerating axons which acts to promote neuronal survival and axon outgrowth via receptors localized on the growth cone of regenerating axons acting in an autocrine fashion (Armstrong et al. 2003; Armstrong et al. 2008; Lioudyno et al. 1998; Zhou et al. 1999).

After peripheral nerve injury VIP has been reported to act on Schwann cells to inhibit the release of nitric oxide, which reduces neuronal cell death and simultaneously promotes the growth of regenerating axons (Lee et al. 2009; Q. L. Zhang et al. 2002). Other studies have shown PACAP KO animals to have reduced axon regeneration following injury. This impaired regeneration in PACAP KO animals is associated with an increase in pro-inflammatory factors (Armstrong et al. 2008). VIP treatment on rat schwannoma cells increases intracellular cAMP and the production of laminin and

myelin proteins (Castorina et al. 2014). This could indicate that VIP/PACAP could also act on Schwann cells to induce myelin gene expression.

1.13 EphA5

Erythropoietin-producing human hepatocellular receptors (Eph) bind to Eph receptor-interacting proteins (Ephrins) to initiate receptor tyrosine kinase signalling. Eph receptors were first cloned from an erythropoietin producing hepatoma cell line in 1987 (Hirai et al. 1987). EphA receptors preferentially bind to EphrinA1-5 ligands, which are attached to the membrane through glycosylphosphatidylinositol (GPI) linkage. Eph-Ephrin signalling is contact-dependent and therefore requires cell-cell contact where protein interaction can induce bidirectional signalling through the cells (**Figure 9**). Both receptors and ligands can transduce signals. Signalling through the Eph receptor into the cell is referred to as forward signalling, whereas Ephrin ligand signalling into the cell is referred to as reverse signalling (Pasquale 2008). Both pathways are linked to downstream effectors such as Ras GTPases, Rho GTPases, RAC and Akt, forming complex signalling pathways (Miao and Wang 2012).

Eph-Ephrin signalling has been extensively characterised and is active in a variety of physiological processes and diseases. These processes include a major role in control of the actin cytoskeleton and migration in processes such as angiogenesis, tumour cell migration and cancer metastasis and directing neuronal and vascular network formation during development (Beauchamp and Debinski 2012; Egea and Klein 2007; Miao and Wang 2009; Pasquale 2008). Alterations in actin cytoskeleton dynamics through Eph/Ephrin signalling can control migration and consequently plays a major role in axon guidance and synaptogenesis (R. Klein 2004; Xu and Henkemeyer 2012). For example, EphrinA reverse signalling has been described to mediate axon path

finding (J. B. Wang et al. 2016). Axons in the developing nervous system undergo repulsive signalling through the formation of Eph-Ephrin protein complexes either through cell-cell or cell-axon contacts. This helps guide growth cones to their peripheral targets. During development of the midbrain, EphA5 interaction with EphrinA5 regulates dopaminergic axon outgrowth (Cooper et al. 2009). In vitro assays where dopaminergic neurones were cultured on NIH 3T3 (fibroblast cell line) control cells or NIH 3T3 cells expressing EphrinA5 showed that neurite length was increased in the presence of EphrinA5 ligand indicating its importance as a ligand for neurite out growth. EphrinA5 activity was shown to be mediated though the EphA5 receptor as neurite outgrowth was not observed when EphA5 mutant dopaminergic neurons were cultured on cells in the presence of EphrinA5 (Cooper et al. 2009). EphA5 is expressed in the developing hippocampus in a medial to lateral gradient (Yue et al. 2002). EphA5 mutation, that leads to a truncated and subsequently inactive EphA5, causes hippocampal axons which would normally terminate in the lateral septum to mistarget and move ventrally and laterally indicating a role for EphA5 in hippocampus axon targeting (Yue et al. 2002).

EphA5 have been extensively described to play a role in retinal plasticity following superior colliculus injury. After injury, EphrinA2 expression increases in the superior colliculus followed by increase in EphA5 expression in the retina (Rodger et al. 2001). The upregulation of EphA5 and EphrinA2 expression may act to guide retinocollicular projection following injury. EphA5 expression has been shown to be upregulated within the peripheral nerve following injury, and coupled with EphA5 having a prominent role in axon guidance during development and its role in retinal plasticity following injury suggest that EphA5 could play a function in the peripheral nerves following injury (Barrette et al. 2010; Pan et al. 2017).

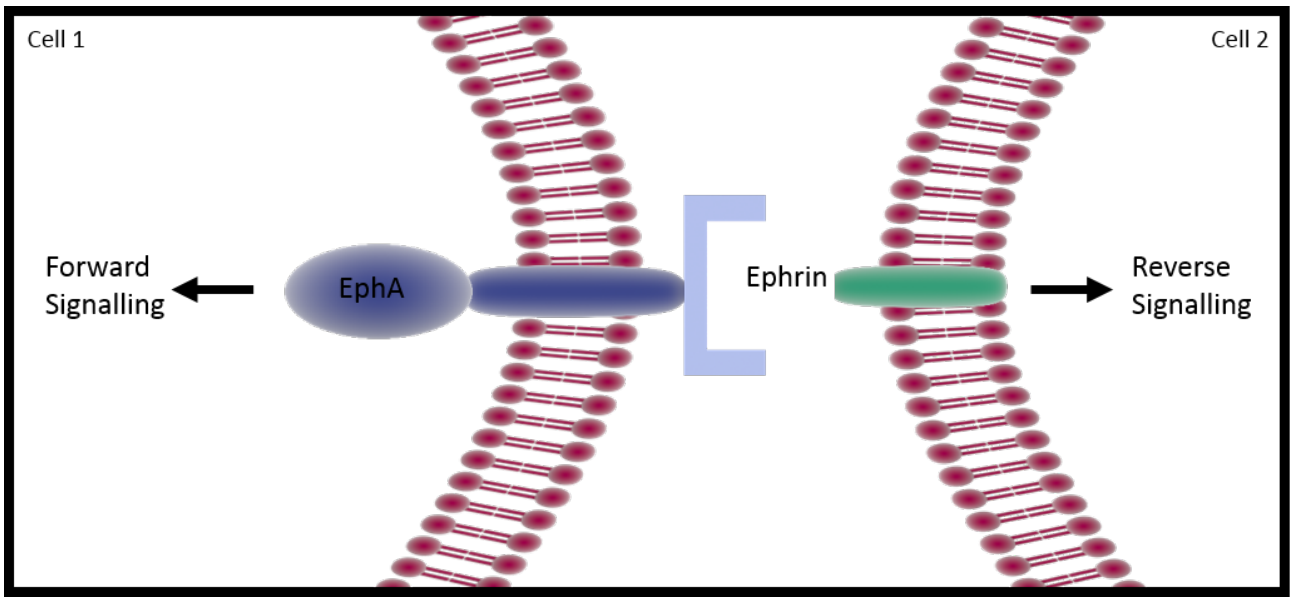

Figure 9 - Diagram showing EphA and Eprhin A signalling

EphA receptor and EphrinA ligand undergo contact dependent signalling where-by signalling can initiate from EphA or Ephrin A to undergo forward or reverse signalling. In forward signalling the signal is induced into the cell through the Eph receptor. In reverse signalling the signal is transduced into the cell through the Ephrin ligand. Activation of EphA or Ephrin can then activate down stream signalling pathways such as Rho GTPases.

1.13.1 EphA-EphrinA repulsive signalling

EphA signalling can lead to repulsive migratory behaviour mediated via EphA forward signalling into the cell. EphA-EprhinA interaction can mediate a process called CIL (contact inhibition of locomotion) whereby, the membrane bound ligand and receptor interaction between two cells causes a change in actin dynamics and a retraction of the actin cytoskeleton in the cell containing the EphA receptor (Batson et al. 2013; Mayor and Carmona-Fontaine 2010). This is followed by repolarisation, which allows the formation of a new lamellipodia and migration of the cell away from the site of contact. This behaviour is mediated through Rho GTPase which acts upon the actin cytoskeleton. EphA can activate RhoA by influencing the conversion of GTPases between a GDP bound (inactive) and a GTP bound (active) state through regulation of guanine nucleotide exchange factors and GTPase-activating proteins leading to activation of Rho (Shamah et al. 2001; Wahl et al. 2000) (**Figure 10)**. RhoA is found within stress fibres and focal adhesions within the actin cytoskeleton. RhoA GTPases activate stress fibre formation and acts at the rear of the cell to promote detachment which therefore allows for cell migration (Ridley 2006).

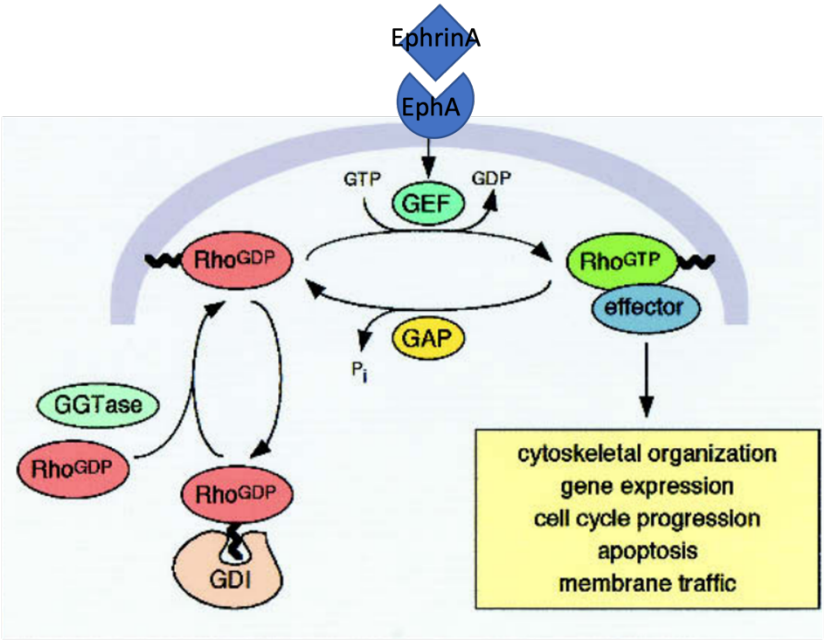

Figure 10 - EphA activation of the Rho GTPase pathway leading to cell migration

EphA5 is activated when it binds to EphrinA on another cell. This leads to the activation of GTP bound Rho which influence actin cytoskeleton dynamics and consequently cell migration. Image adapted from (Schmidt and Hall 2002).

EphA repulsive migratory behaviour have been extensively described in a range of biological systems. EphA2 and EphA4 have been shown to mediate CIL in PC-3 prostate cancer cells. Knock down of EphA2 and EphA4 using siRNA in these cells causes cells to migrate in the same direction and push past each other, rather than undergo CIL and repulsive signalling as seen in WT PC-3 cells (Astin et al. 2010). Repulsive signalling through EphA also directs axon migration through EphA-Ephrin mediated repulsion of the growth cone. In the CNS, EphA4-EphrinA3 have been described to play a role in the formation of postsynaptic dendritic spines in the hippocampus. In these experiments EphA4-EphrinA3 cross talk between astrocytes and neurones mediates the structure of excitatory synapses. Spines in EphA4 KO mice were irregular in shape and had a disorganized appearance (Murai et al. 2003). EphA2-EprhinA4 has been described to promote the migration of cortical interneurons through reverse repulsive signalling (Steinecke et al. 2014). In retinal ganglion cells

(RGC) EphrinA5 mediated growth cone collapse though RhoA. RGC grown in culture on laminin was treated with EphrinA5 which activated RhoA and lead to growth cone collapse which was strongly reduced upon the addition of a RhoA inhibitor (Wahl et al. 2000). EphrinA5 is essential for retinal axon guidance and topographic mapping in the visual system as although global EphrinA5 KO animals developed normally and showed normal anterior–posterior patterning in the mid brain, retinal axons in the superior colliculus showed incorrect topographic mapping (Frisen et al. 1998). During rat optic nerve injury an up-regulation of ephrin-A2 in the superior colliculus and EphA5 in the retina is observed and upregulation of both ligand and receptor may help guide optic nerve regeneration through repulsive signalling following injury (Rodger et al. 2001).

1.13.2 WDC antagonistic peptide

To help investigate the role of EphA5, an 12 amino acid antagonistic peptide (WDCNGPYCHWLG) called WDC with binding specificity for the ligand binding domain of EphA5 has been generated (Helmbacher et al. 2000; Huan et al. 2013). This allows the function of EphA5 to be investigated specifically rather than just the down stream signalling pathways. Phage display analysis was first used to identify WDC as antagonist for rat EphA5 (Helmbacher et al. 2000). Isothermal titration calorimetry experiments then went on to identify WDC as a binding partner to the ligand binding domain of rat EphA5. EphA5 is highly conserved between human, mouse and rat. The ligand binding domain of EphA5 is 179 amino acids in all three species, with human and rat sharing 98.3% identity, rat to mouse sharing 98.3% identity and mouse to human sharing 98.9% identity. The critical cysteines for binding to the WDC peptide are conserved between species which allows a disulphide bond

to form between WDC and the EphA5 LBD (ligand binding domain) (Helmbacher et al. 2000). This leads to WDC undergoing competitive binding which significantly inhibits EphA5 binding to EphrinA ligands. WDC peptide has not yet been used for any clinical or research based studies. The discovery of such a peptide does however allow the potential for the specific function of EphA5 to be investigated through its selective inhibition and will therefore be particularly useful in research studies. In addition to this it could also act to have future clinical implications for the treatment of disease pathways involving EphA5 overexpression and hyperactivation of signalling pathways downstream of EphA5. EphA5 expression in patients with pancreatic ductal adenocarcinoma have shorter survival times and consequently blockage of EphA5 with WDC could indicate a potential treatment for high grade metastatic tumours (Giaginis et al. 2010).

1.13.3 EphA5 knockout mice

Global EphA5 knock out (KO) mouse line C57BL/6NEpha5$^{m1b\ (NCOM)\ Mfgc}$/Tcp was generated by Cre excision of Epha5<tm1b(NCOM)Mfgc> allele (MGI:TBD) to remove the neo selection cassette and critical exons leaving behind the lacZ reporter cassette and a loxP site (Bradley et al. 2012; Mamiya et al. 2008). Using a tm1b0LacZ tagged deletion system the crucial exon and the neomycin cassette is deleted using a Cre recombinase that recognises loxP sites. LacZ is then expressed in the tissues where the deleted gene (EphA5) is expressed (Coleman et al. 2015). This global homozygous EphA5 KO line show no obvious developmental defects although did show increased body weight and decreased mean corpuscular volume (Mamiya et al. 2008). The limited effect of EphA5 KO may be a result of compensation from other EphA proteins. As previously described there are 9 EphA proteins with many of these

activating similar downstream signalling pathways. Therefore it is possible that KO of EphA5 may lead to a compensatory increase in other EphA proteins. These potential upregulation may mean that alternative EphA receptors are able to perform similar functions to that of EphA and consequently EphA5 global KO have a limited phenotype. Compensation through the upreguation of alternative EphA receptors can be investigated by observing the change in gene and protein expression of other EphA upon knock out of EphA5. Currently, it is not clear if EphA5 plays a role in functional recovery following peripheral nerve injury, this thesis acts to examine that.

2 Chapter 2 Materials and methods

2.1 Mice and surgery

All work involving animals was carried out according to Home Office regulations under the UK Animals Scientific Procedures Act 1986 (ASPA). Ethical approval for all experiments was granted by Plymouth University Animal Welfare and Ethical Review Board. Animals were housed in a specialised animal facility, where they were under a 12 hour light/dark daily cycle, 22 ± 2°C, 50–60% humidity and unlimited access to food and water.

For surgery, animals were firstly anesthetised using isoflurane. After loss of consciousness the skin was shaved and sterilised using an iodine solution. The skin and muscle of the right rear limb was then opened to reveal the sciatic nerve. Sciatic nerve cut and crush were carried out according to procedures detailed in Dun and Parkinson (2015). For a cut procedure the right sciatic nerve exposed and the nerve transected at approximately 0.5 cm distal to the sciatic notch, for a crush procedure the right nerve was exposed and the nerve crushed for 2 separate 30 second periods at the same site using a pair of fine tweezers. After procedures wounds were closed by suturing the muscle and the skin was then clipped with an autoclip applier. All animals undergoing surgery were given appropriate post-operative analgesia, 0.05% bupivacaine solution topically applied above the muscle suture before applying the surgical clip and meloxicam (5 mg/kg) injection (sub-cutaneous) just before recovery from anaesthetic. All animals undergoing surgery were given nesting material and enrichment in the cage to prevent autotomy. Mice were then given the appropriate post-operative care and checked daily to ensure no adverse effects were observed (e.g. weight loss or autotomy). At appropriate time points post-surgery, animals were euthanized humanely in accordance with UK Home Office regulations (Schedule 1) and samples were dissected out for further experimentation.

PLP-GFP (proteolipid protein-green fluorescent protein) are a transgenic mice strain. Myelin PLP drives the expression of GFP in the oligodendrocytes, Schwann cells and enteric glia of the gut. PLP-GFP expression is expressed in embryonic and postnatal cells and therefore allows lineage tracing of oligodendrocytes and Schwann cells as long as the PLP promotor is switched on. PLP-GFP mice are on a background strain of C57BL6. Mice were generated as described in Mallon et al, 2002 (Mallon et al. 2002). Briefly, using a pNEB193 vector restriction enzymes EGFP into the PLP promotor region of the construct. The DNA fragment was then injected into pronuclei of C57BL6 fertilized oocytes that were transferred to the oviducts of pseudopregnant mice. To identify transgenic mice genotyping was performed.

2.2 Cell culture:

2.2.1 Raw 264.7

Raw 264.7 cells were cultured in DMEM (Dulbecco's modified Eagle's medium) (Gibco #11965092) containing: 10% v/v FBS, 100U/ml penicillin/100U/ml streptomycin (Gibco #15140122), 2mM L-glutamine (Gibco #25030149) and 5g/L glucose (Gibco #A2494001). Cells were incubated at 37˚C in a humidified atmosphere with 5% CO_2.

2.2.2 Primary rat or mouse Schwann Cell Culture

Rat and mouse Schwann cells were prepared as described previously (Dun et al, 2019). Briefly, P1-P3 Sprague Dawley rat pups or P1-P3 mouse pups were humanely euthanized before the sciatic and brachial nerves were dissected out into L-15 media on ice. Any connective tissue was removed before nerves were cut up into small pieces. Nerves were digested in 2mg/ml collagenase for 30 minutes at 37˚c before being trypsinised in 1.25 mg/ml trypsin for around 10 minutes until all clumps of cells had broken up. Enzymes were inactivated in DMEM containing 6% FBS before cell suspension was centrifuged at 500 xg for 10 minutes. The pellet was resuspended in 1g/L glucose DMEM (Gibco #12320032) containing 6% FBS with 100U/ml penicillin/100U/ml streptomycin (Gibco #15140122), and cells were seeded on a 0.1mg/ml Poly-L-lysine hydrobromide (PLL) (Sigma #P6282) and laminin coated dish. Media was changed 24h later to 1g/L glucose DMEM (Gibco #12320032) containing 6% FBS and 10nM cytosine arabinoside to kill dividing fibroblasts. 48h later, media was changed to 1g/L glucose DMEM (Gibco #12320032) containing 3% FBS, 10ng/ml neuregulin (R&D, 396-HB-050) and 2μM forskolin (Sigma #344270) to allow Schwann cells to proliferate. Schwann cells were maintained and expanded on PLL coated plates in 1g/L glucose DMEM (Gibco #12320032) containing 3% FBS, 10ng/ml neuregulin (R&D, 396-HB-050) and 2μM forskolin (Sigma #344270).

2.2.3 Primary macrophage culture

Bone marrow was obtained from 6-8 week old male and female mice animals who were euthanized humanely in accordance with UK Home Office regulations (Schedule 1). The femur and tibia were dissected out into 1X PBS (Gibco #14190144) and muscle and connective tissue were removed before they were quickly washed in 70% ethanol and washed again in PBS. The joints were cut at both ends and the bone marrow was washed out with 1X PBS (Gibco #14190144) using a 19GA lancet inserted into one end. The bone marrow from 4 sets of femur and tibia bones containing the macrophage precursor cells were pelleted at 10000 xg for 5 minutes. Supernatant was discarded and the cells were re-suspended in Plutznik medium (DMEM medium (Gibco #11965092) supplemented with 20% v/v FBS, 20% v/v L-cell condition medium, 1mM sodium pyruvate (Gibco #11360070), 2mM L-glutamine (Gibco #25030149), 100U/ml penicillin/100U/ml streptomycin (Gibco #15140122). L-cell condition medium was produced by culturing L-929 fibroblasts. Fibroblasts were seeded at 1x105/ml in 175cm^2 tissue culture flasks in DMEM (Gibco #11965092) supplemented with 10% v/v FBS, 100U/ml penicillin/100U/ml streptomycin (Gibco #15140122), 2mM L-glutamine (Gibco #25030149), 5mM HEPES. Cells were cultured at 37^{o}C in 5% CO2 in a humidified atmosphere. After 7 days of culture the supernatant was collected, clarified by centrifugation at 10000 xg for 5 minutes and pooled with other supernatants. The pooled supernatants were sterile filtered, and stored in aliquots at -80^{o}c

Monocytes were counted and seeded in 75cm^2 flasks at 1x10^6 cells/ ml of Plutznik medium. Cells were cultured at for 10 days, with a complete medium change at day 7 to refresh medium and remove any remaining red blood cells. On day 10 more than

98% of the cells were macrophages and cells were used for experiments. (Freudenberg, et al., 1986).

2.2.4 Cell splitting

To split cells, medium was aspirated off, cells were washed in 1X PBS (Gibco #14190144) and the remaining adhered cells were detached using 0.05% Trypsin-EDTA (Gibco #25300054). Flasks was gently tapped to ensure all cells had detached and trypsin was inactivated using culture medium. Cell suspension was spun down at 10000 xg for 5 minutes. The supernatant was discarded and cells were re-suspended in fresh culture medium. Cells were counted and seeded at required density for maintenance or experiments in the appropriate size culture vessel. All cells were incubated at 37˚c in a humidified atmosphere with 5% CO2.

2.2.5 Co-culture

Schwann cells (rat or mouse) and macrophages (Raw 264.6 or primary mouse macrophages) were seeded together on PLL (Sigma #P6282) coated cover slips at a density of $9x10^4$ and $6x10^4$ respectively in 1g/L DMEM (Gibco #12320032) containing 3% FBS v/v and penicillin/100U/ml streptomycin (Gibco #15140122). 100 nM of WDC was added to the cell were appropriate before fixation in 4% PFA in 1xPBS (Gibco #14190144) for 10 minutes at 24h followed by 3x 10 minute PBS washes. The immunocytochemistry protocol was then followed for cover slip staining of cells (Section 2.10).

2.3 Migration assays

2.3.1 Scratch wound assay

Rat Schwann cells or Raw 264.7 cells were grown to confluency in a six well plate, for rat Schwann cells plates were coated with PLL using the same method previously

described for rat Schwann cells prior to the Scratch wound assay. Upon reaching confluency a scratch was introduced into the well using a 200μl pipette tip which removed cells from this area. Primary macrophages were seeded into a 24 well plate at confluency and a scratch was introduced using a 10μl pipette tip. Media was aspirated off and wells were washed with 1xPBS to wash off cell debris. Cell were then incubated in DMEM (Gibco #11965092) containing 0.5% FBS v/v and 2mM glutamine (Gibco #25030149) containing either 30ng A2 protein (R&D #603-A2) or 100nM WDC for 24h or 100nM WDC for 1h followed by 23h 30ng A2(R&D #603-A2). Images were taken of the scratch wound at 0h and 24h post wound and cells migrated into the wound were quantified to assess migration using ImageJ (available from https://imagej.nih.gov/ij/) by counting individual cells migrated or using the formula to assess migration rate = (D0 - D24)/D0 x100 (Qin et al. 2016).

2.3.2 Transwell migration assay

For Schwann cells 8.0μm pore Corning® Transwell® polycarbonate migration chambers (Merck # CLS3422) were coated with PLL for 30 minutes before being washed with 1x PBS (Gibco #14190144) and allowed to dry. Schwann cells were counted and seeded into the upper chambers cambers at a density of $3x10^5$ in 100μl of 1g/L glucose DMEM (Gibco #12320032) containing 3%FBS v/v. 600μl of Schwann cell media was added to the bottom chambers. 30ng A2 protein (R&D #603-A2) or 100nM WDC for 24h or 100nM WDC for 1h followed by 23h 30ng A2 (R&D #603-A2) were added as appropriate into the top chamber and cells were left to migrate for 24h. For macrophages (primary and Raw 264.7), cells were seeded at a density of $3x10^5$ in 100μl of DMEM (Gibco #11965092) into the upper chamber of a 8.0μm pore Corning® Transwell® polycarbonate migration chamber (Merck #CLS3422). 600μl of DMEM (Gibco #11965092) containing 10% FBS v/v and 2mM glutamine (Gibco #25030149)

cell media was added to the bottom chambers. 30ng A2 protein (R&D #603-A2) or 100nM WDC for 24h or 100nM WDC for 1h followed by 23h 30ng A2 (R&D #603-A2) were added as appropriate into the top chamber and cells were left to migrate for 24h. For both cell types, after 24h media was removed from the upper and lower chambers and washed in 1x PBS (Gibco #14190144) before being fixed 4% PFA in 1x PBS (Gibco #14190144) for 10 minutes. Cells were then stained with 0.1% crystal violet (Sigma #V5265) for 20 minutes and then. washed 3 times in 1xPBS (Gibco #14190144) to remove the excess stain. The cells in the upper chamber were wiped away using a cotton bud and chambers were left to air dry before being imaged on Leica IM8 microscope. Cells were counted using the counting function from ImageJ available from https://imagej.nih.gov/ij/.

2.4 Sciatic nerve peptide incubation

Intact mouse sciatic nerves or distal nerves at10 days post cut injury were dissected out, the epineurium was removed and nerves were teased. Nerves were then incubated in DMEM (Gibco #11965092) supplemented with 5% FBS v/v (control) or DMEM (Gibco #11965092) supplemented with 5% FBS v/v containing 100nM of VIP or PACAP peptides or receptor specific agonists (**Table 12**) for 24 hours. mRNA was then isolated from nerves following procedure detailed in Section 2.5 below.

2.5 mRNA extraction

2.5.1 Sciatic nerve mRNA extraction

mRNA was extracted using a miRNeasy Mini Kit (Qiagen #217004). Prior to extraction all equipment was treated with RNaseZAP™ (Thermo Fisher #AM9780) to prevent breakdown of mRNA by RNase. Samples were sonicated in 700µl of TRIzol® (Thermo Fisher #15596026) until no visible lumps of tissue could be seen. Following sonication,

a further 700µl of TRIzol® (Thermo Fisher #15596026) was added to sciatic nerve samples and samples were separated into two separate 1.5ml Eppendorf's. 140µl of chloroform per 700µl of sample was added and samples were shaken for 15 seconds and left to rest at RT for up to 3 minutes before being centrifuged at 4˚C at 12,000 xg for 15 minutes. The upper aqueous phase containing DNA/RNA was removed and combined together from both 1.5ml tubes. Following this, sciatic nerve samples underwent an addition chloroform extraction as previously described. Following chloroform extraction, 1.5 volumes of 100% ethanol were added to the upper aqueous phase. mRNA was then immediately purified in a RNeasy spin column (Qiagen #217004) with in column DNase digestion as per the manufacturer's instructions. mRNA concentration was then determined using a nanodrop machine.

2.5.2 Cell mRNA extraction

When investigating mRNA expression in Schwann cells, the medium was changed from expansion media (1g/L glucose DMEM (Gibco #12320032) containing 3% FBS, 10ng/ml neuregulin (R&D, 396-HB-050) and 2µM forskolin (Sigma #344270)) to 1g/mL glucose DMEM (Gibco #12320032) containing 3% FBS v/v and appropriate samples were either untreated (control) or treated with PolyI:C (10 mg/ml), LPS (100 ng/ml) or 100nM of VIP PACAP or receptor specific agonists and antagonists (**Table 12**) for differing times before mRNA extracted.

mRNA was extracted using a RNeasy plus Mini Kit (Qiagen #74134). Confluent cell layers were lysed in an appropriate volume of RLT buffer from the kit, based on the kit insert and culture vessel volume. The lysate was then transferred to a QIAshredder spin column (Qiagen #79654) for homogenisation. The homogenate was then run through a gDNA eliminator column via centrifugation and the flow through was

collected. Flow through was added to 70% ethanol in a 1:1 volume. Samples were then added to a mini spin column and washed with 700µl Buffer RW1. The column was then washed twice with 500µl of RPE. Sample was eluted with 30µl of RNAse free water. mRNA concentration was determined using a nanodrop machine.

2.6 cDNA preparation

mRNA is reverse transcribed to cDNA when then can be stored at -20˚C . This process is carried out as mRNA cannot be amplified by PCR where as cDNA can as it is more stable and less prone to degradation. For up to every 2µg of mRNA 1µl of random primers (Promega #C1181), 50U RNAse inhibitor (Promega #N2111), 10µl of 5x M-MLV reverse transcriptase reaction buffer (Promega #M531A), 2.5µl dNTP (Promega #U120A-U123A) and 1µl M-MLV reverse transcriptase (Promega #M368) were combined and made up to 50µl with RNAse free PCR water (Sigma #W4502). Table 2 shows a typical reverse transcription master mix and Table 3 shows the reaction steps.

Reagent	Volume	Concentration
M-MLV Reverse Transcriptase 5X Reaction Buffer (Promega #M531A)	10µL	0.5pM

ddH_2O (Sigma #W4502)	Various	
cDNA	Various	2µg
dNTPs (Promega #U120A-U123A)	2.5µL	200µM
Random Primers (Promega #C1181)	1µL	500ng
M-MLV RT (H–) Point Mutant (Promega #M170A)	1µL	400U
RNAse inhibitor (Promega #N2111)	1µL	50U

Table 1 – Reaction mixture for 2ug of cDNA in 50 µL reaction.

Table lists all the components used in a 50µl reaction. Various volumes of mRNA are used in each reaction and is dependent on sample concentration. Reaction volume is made up to 50µl using RNase free H_2O.

Step	Condition
1 Addition of mRNA and random primers	At room temperature
2 Denaturation of secondary structure and primer annealing	70˚C 5 minutes
3 Inhibition of secondary structure formation	Cool on ice 5 minutes
4 Addition of remainder of reagents (RNAse inhibitor, M-MLV reverse transcriptase 5x reaction buffer, dNTP and M-MLV reverse transcriptase)	On ice

5 Synthesis of cDNA strands	37˚C 60 minutes
6 Heat inactivation of enzymes	70˚C for 15 minutes
8	4˚C

Table 2 – Standard PCR program for the conversion of mRNA to cDNA.

Program is run on a thermal cycler before long term storage of cDNA products at -20˚C

2.7 RT-PCR

Specific primers recognizing desired genes were used to amplify DNA (**Table 8**). This enabled us to ensure primers were specific to genes of interest by the presence of a single band of the correct expected size compared to size markers run alongside the PCR products prior to qPCR. 2ul of cDNA was added to a reaction mix and run on a thermocycler, typical reaction mix and PCR steps shown in Tables 4 and 5. Amplification products were separated by electrophoresis on a 2% agarose gel. Agarose gel was made by dissolving agarose powder (Thermo Fisher Scientific #17852) in 1x Tris Acetate EDTA (TAE) buffer and heated in the microwave (50x TAE buffer: 242g of Tris-base (Mw = 121.14 g/mol), 57.1ml of 100 % glacial acid, 100mL of 0.5 M EDTA (pH 8.0) topped up to 1L using MiliQ H_2O). GelRed™ (Sigma #SCT123) was added at 1:50,000 and the set agarose gel was submerged in 1x TAE and run at 120v for 60-90 minutes to allow electrophoresis and separation of DNA. Gels were imaged using a UV box to reveal DNA bands using a SYNGENE PXI 4.

2.8 PCR Genotyping

Ear notches were used to extract DNA samples from weaned mice. DNA from ear notches were released from samples by submerging them in 75µl of alkaline lysis buffer (25 mM NaOH and 0.2 mM EDTA in H_2O) and heated to 95°C for 90 minutes in a thermal cycler as per the HotSHOT protocol (Truett et al. 2000). The solution was vortexed and 75 µL of neutralisation buffer (40 mM Tris-HCl in H_2O) was added, DNA was stored at 4°c short term or -20°c long term storage. 2.0µl of the DNA sample (or water for the negative control) was added to 23µl of a PCR master mix; a typical PCR reaction mix and PCR program are shown in Table 3 and 4. Amplification products were separated and visualised by electrophoresis as described in Section 2.7.

Reagent	Volume	Final concentration
5x Green GoTaq Buffer (Promega #M891A)	5µL	
RNAase free H_2O (Sigma #W4502)	14.9µL	
DNA	2µL	
dNTPs (Promega #U120A-U123A)	0.5µL	200µM
$MgCl_2$ (Promega #A351H)	1.5µL	1.5mM
Primers (Eurofins)	1µL	0.5µM each
Taq Polymerase (Promega #M740B)	0.1µL	1.25U

Table 3 - Components of polymerase chain reaction master mix used for both genotyping and semi-quantitative RT-PCR.

Table lists all the components used in a PCR master mix per 25µl reaction.

Step	Condition
1	95˚C 5 minutes
2	95˚C 30 seconds
3	55˚C 45 seconds
4	72˚C 60 seconds
5	Repeat 2-4, 38 times
6	72˚C 5 minutes
7	4˚C (infinite storage)

Table 4 - Standard PCR program.

For primer pairs, annealing temperature and product size see table 7.

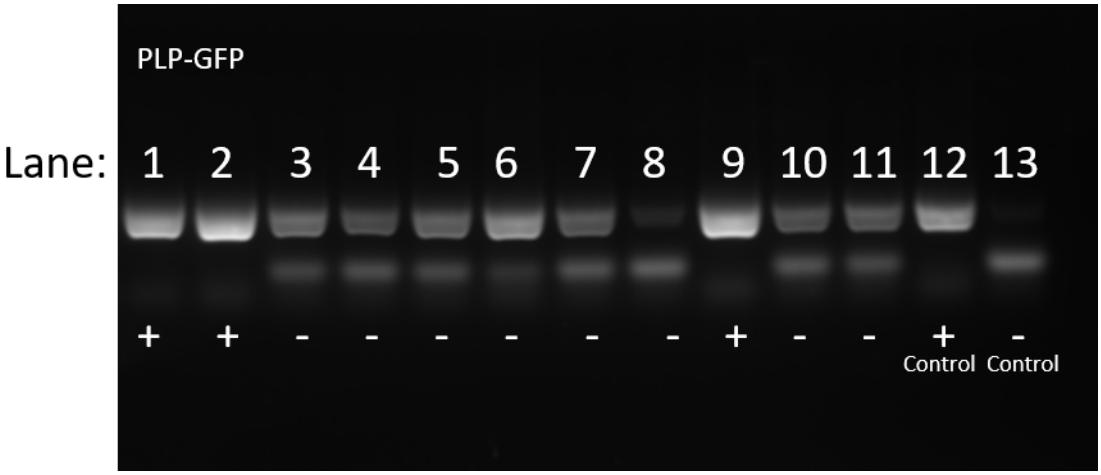

Figure 5- Example of a DNA gel for genotyping

2.9 Quantitative (q)PCR

cDNA samples were then prepared for qPCR analysis in a LightCycler® 480 (Roche Applied Science). A 10µl reaction was prepared on ice containing 1µL of cDNA combined with 1µl of 2.5pm/µl sequence specific forward and reverse primers (Table 8), 5µl of 2x SYBR™ green master mix (Roche #04707516001) and made up to volume with PCR water. Each 10µl sample was loaded into a 384 multiwell plate and sealed with LightCycler® 480 multiwell sealing foil before being centrifuged at 1500 x g for 1 minute. The multiwell plate was then loaded into a LightCycler® 480 instrument and the the program run as shown in Table 7. Cq and Tm values were produced using LightCycler® 480 software and additional data analysis was performed in Excel to determine ΔΔ-Ct (Livak and Schmittgen 2001). All primers were designed to have an annealing temperature of around 55˚C. This can be determined by the G and C content of the primers when designing them and the Tm can be determined using the equation Tm=((sum A+T) x2) + ((sum G+C) x4). qPCR analysis for target genes in each cDNA sample was carried out in triplicate.

Reagent	Volume	Concentration
2x SYBR green (Roche #04707516001)	5µL	1X
RNase free H_2O (Sigma #W4502)	2µL	
Forward primer (Eurofins)	1µL	2.5pm/µl
Reverse primer (Eurofins)	1µL	2.5pm/µl
cDNA	1µL	

Table 5 - Components of qPCR reaction

Table lists all the components used in a PCR master mix per 10µl reaction

Step	Condition
1 (Pre incubation)	95˚C for 4 minutes (Ramp rate ˚c/second 4.8)
2 (Amplification)	95˚C 30 seconds (Ramp rate ˚c/second 4.8)
3 (Annealing)	55˚C 1 minute (Ramp rate ˚c/second 2.5)
4 (Extension)	72˚C 1 minute (Ramp rate ˚c/second 4.8)
5	Repeat 2-4, 45 times
6 (cooling)	40˚C for 40 seconds

Table 6 - Standard qPCR program.

Primer	Forward: 5'---3'	Reverse: 5'---3'	Size (bp)
EphA5 KO	CCATTACCAGTTGGTCTGGTGTC	GAATGGGAGTAGAACTGATGACAAG	563
EphA5 WT	AACTTAGCCCAGCTTCTCTGCCACTG	ACAGTGCGCGAATCCAACAAATTCAC	619
Mouse Ephrin A1	CCGCGCTATGGAGTTCCTTT	CCTCACGGAACTTGGGATTTG	187
Mouse Ephrin A2	CGTAGCAACCCCAGGTTTCA	TCGTTGATGCTCACCTCCAC	137
Mouse Ephrin A4	CCCTTTCAGCCCTGTTCGAT	GAGTCGGCACCGAGATGTAG	166
Mouse Ephrin A5	CTGGTGCTCTGGATGTGTGT	CCCTCTGGAATCTGGGGTTG	154
Mouse EphA5	GGTACCTGCCAAGCTCCTTC	ATTCCATTGGGGCGATCTGG	170
Mouse GAPDH	AAGGTCATCCCAGAGCTGAA	CTGCTTCACCACCTTCTTGA	222
Mouse IL-10	GCTCTTGCACTACCAAAGCC	CTGCTGATCCTCATGCCAGT	112
Mouse IL-13	GGCAGCATGGTATGGAGTGT	CTTGCGGTTACAGAGGCCAT	132
Mouse IL-4	CCATATCCACGGATGCGACA	AAGCACCTTGGAAGCCCTAC	166
Mouse IL-6	AGTTGCCTTCTTGGGACTGA	TCCACGATTTCCCAGAGAAC	159
Mouse IL-α	GCAACGGGAAGATTCTGAAG	TGACAAACTTCTGCCTGACG	177
Mouse IL-β	GCCCATCCTCTGTGACTCAT	AGGCCACAGGTATTTTGTCG	230
Mouse MCP-1	AGGTCCCTGTCATGCTTCTG	TCTGGACCCATTCCTTCTTG	249
Mouse PAC1	CCGGACCAAGTCTGGATGAC	AGCCATCCTCAGTGCAGTTC	112
Mouse TNF-α	CGTCAGCCGATTTGCTATCT	CGGACTCCGCAAAGTCTAAG	206
Mouse VPAC1	GCCTCCACACAAGGCAAATG	GTGTTTCCAGGTAGGGCACA	160

Mouse VPAC2	ATAGGCGCGAGACTGAGGAA	CAACCAGCAGTAGCAGGTCA	135
Rat EphA5	ACTACATCAGAAAAGGGCTGACA	TCCCATGCAGTAGTGAAAGTCC	185
Rat Ephrin A1	TACACTGCGGAGCTTTCGTC	CTCCTCTCGGAACTTGGGAT	153
Rat Ephrin A4	TCCAGCCTCCGCCACTCTAT	TAATGCAAACGTTTCCGGGC	141
Rat Ephrin A5	AGGTGTTCGTGATCGTGTTT	CGGTGTCATCTGCTGGTTCT	156
Rat Ephrin A2	TACGTGCGTCCAACCAATGA	ACACTAGGAGCCCAGTAGGG	71
Rat GAPDH	AGTGCCAGCCTCGTCTCATA	GGTAACCAGGCGTCCGATAC	77
Rat IL-6	AGCGATGATGCACTGTCAGA	GGAACTCCAGAAGACCAGAGC	106
Rat IL-α	CCTCGTCCTAAGTCACTCGC	GGCTGGTTCCACTAGGCTTT	105
Rat IL-β	GACTTCACCATGGAACCCGT	GGAGACTGCCCATTCTCGAC	85
Rat Krox20	AGGAGCAAATGATGACCGCC	CATGCCATCTCCAGCCACTC	185
Rat Mbp	TGTGGGGGTAAGAGAAACGC	AAGGTCGGTCGTTCAGTCAC	126
Rat MCP-1	CAGGTCTCTGTCACGCTTCT	GGCATTAACTGCATCTGGCTG	87
Rat Mpz	ATGACCGAGGACCAATGACG	CTGTGCTCCAGAGTGGTCAG	102
Rat PAC1	AGCATTCACCCCCTTTCCTCA	GGAGAGAAGGCGAATACTGTGT	176
Rat TNF-α	CATCCGTTCTCTACCCAGCC	AATTCTGAGCCCGGAGTTGG	151
Rat VPAC1	GCTCCTTAAAACTGGCCCCT	TCAAACACCTCAGTGCCGTT	149
Rat VPAC2	GAAGGCAGAGAGGGCGATAG	CAACCAGCAGTAGCAGGTCA	152

Table 7 - Polymerase chain reaction conditions for each primer pair.

Table lists the species and the gene target to be amplified, the sequence of the forward and reverse primer and the fragment size in base pairs (bp). Primers were designed for an annealing temperature of 55˚c

2.10 Immunohistochemistry (IHC) and Immunocytochemistry (ICC):

For IHC sciatic nerves were dissected from mice and fixed in 4% paraformaldehyde (PFA) overnight at 4˚C. Following fixation samples were washed 3 times for 10 minutes in 1x PBS before dehydration in 30% sucrose for 48h at 4˚C. Post dehydration, samples were embedded into optimal cutting temperature (OCT) compound (Maxanim, #94-4583) and snap frozen using liquid nitrogen. Embedded samples were kept frozen at -80˚C until sectioned. OCT blocks were mounted onto a cryostat and sectioned at a thickness of 10 µm. Sections were placed onto SuperFrost®Plus slides (VWR, #631-0108P) and left to dry at room temperature before being stored at -20˚C. To begin the staining procedure slides were allowed to come up to room temperature. A hydrophobic ring using a liquid blocker pen (Sigma, #Z377821-1EA) was drawn around the OCT. 1x PBS was then added into the hydrophobic ring to dissolve the OCT.

For staining of tissue sections requiring antigen retrieval, the sections were first fixed in 4% PFA for 10 minutes followed by 3 x 10 minute 1x PBS washes. Slides were then placed in a box containing citrate buffer (Citrate buffer: Tri-sodium citrate (dihydrate) 2.94g in 1L of MiliQ H_2O. Adjusted to pH 6.0 with 1M HCl) and the box was heated to 95˚C in a water bath for 25 minutes. Slides were then allowed to cool in citrate buffer and the following experimental procedure was performed for all slides.

The following protocol was performed for antibody staining of tissue samples (IHC) and cells on coverslips (ICC):

Samples were permeabilised in 1% BSA w/v (Sigma, #126593) containing 0.25% Triton®X-100 (Sigma, #648462) for 45 minutes at room temperature. Permeabilisation solution was removed and replaced with 3% BSA (Sigma, #126593) containing 0.05% Triton®X-100 (Sigma, #648462) at room temperature for an hour to block samples.

Primary antibodies (**Table 10**) were appropriately diluted in 3% BSA (Sigma #126593) and applied to tissues samples before incubation at 4˚C overnight. Following primary antibody incubation slides or coverslips were washed 3x for at least 10 minutes in 1xPBS to remove any unbound antibody before application of secondary antibody (1:200 dilution) (**Table 11**) and Hoechst stain (1:500 dilution) diluted 3% BSA (Sigma, #126593) and incubated in the dark at room temperature for 1 hour. Slides or coverslips were washed 3x for 10 minutes in 1x PBS to remove any unbound antibody and mounted in glycerol PBS before sealing. Samples were then stored at 4˚C.

2.10.1 Three layer protocol

A three layer protocol was used in some cases to increase signals. This uses a three layer protocol where the a primary antibody is bound to the antigen of interest, a second antibody conjugated to streptavidin recognises the primary antibody and this boosts the signal and makes staining more specific. Finally, a third antibody that recognises the streptavidin and conjugated to a fluorophore is used. Tissue samples were permeabilised / blocked and incubated with primary antibody following the standard protocol. Following removal of primary antibodies, slides were washed 3x for 10 minutes in 1xPBS. Next a biotinylated secondary antibody, raised against the primary antibody species, diluted 1:250 in 3% BSA (Sigma, #126593) was added to slides and incubated for 60 minutes at room temperature. Samples were then washed 3 times for 10 minutes in 1x PBS before incubating with streptavidin conjugated to a fluorophore for the tertiary layer (1:1000) and Hoechst dye (1:500) diluted in 3% BSA (Sigma, #126593) for 45 minutes at room temperature. Tissue samples were washed 3 times for 10 minutes in 1x PBS, mounted and sealed as in the two layer protocol.

2.11 Whole mount staining

Whole mount staining is used to look at the whole sciatic nerve post injury and enables us the view axons regenerating into the nerve bridge and down through the distal stump. The protocol followed what that derived by Dun and Parkinson, 2015 (Dun and Parkinson 2015). Briefly, a sciatic nerve segment containing the proximal nerve, the nerve bridge and distal nerve stump was carefully dissected out with the surrounding muscle at appropriate time points post injury. This was fixed in 4% PFA at 4°C overnight. Following fixation, samples were washed 3 times for 10 minutes in 1x PBS and the muscle and connective tissue removed from the sciatic nerve under a dissection microscope. Sciatic nerves were then permeabilised and blocked in 1% Triton®X-100 (Sigma, #648462) in 10% FBS for 24h at 4°C. The following day nerves were incubated with neurofilament antibody (**Table 10**) in 0.1% Triton®X-100 (Sigma, #648462) in 10% FBS for 4-5 days at 4°C. Sciatic nerves were then washed in 1x PBS 5 hours, with the PBS being changed every hour before incubation with secondary antibody for 48h at 4°C. The staining was checked under a fluorescent microscope before samples underwent glycerol clearance. For glycerol clearance samples were left in 25% v/v glycerol for 24h followed by 50% v/v glycerol for 24h and finally 75% v/v glycerol for 24h (Sigma, #G6279). Finally, samples were mounted in glycerol PBS (Agar Scientific, #R1320) and cover slips were sealed with nail varnish. Whole mounts samples were imaged by z stack and separate images were compiled using photomerge on Adobe Photoshop CC 2018.

2.12 Electron microscopy and semithin section preparation

Adult mouse sciatic nerves were dissected out at appropriate time points post injury. The nerves were fixed in glutaraldehyde (2.5% pH 7.2, 0.1M) for at least 24 hours.

Next, the nerves were then processed for electron microscopy and semithin preparation by staff in the EM unit. Nerves were washed twice in sodium cacodylate buffer (pH 7.2, 0.1M) for 15 minutes. The nerves were secondary fixed with osmium tetroxide (1% w/v in buffer pH 7.2, 0.1M) for 1 hour. After two 15-minute washes with sodium cacodylate buffer, the nerves were dehydrated through an alcohol series of 30%, 50%, 70%, 90% and 100% v/v ethanol for 15 minutes per step. To ensure thorough dehydration the 100% ethanol step was repeated. The alcohol in the sample was then replaced by Agar low viscosity resin by placing the sample in increasing concentrations of resin for at least 12h per step. First 30% resin: 70% ethanol, followed by 50% resin: 50% alcohol, then 70% resin :30% ethanol and finally 100% resin. Again to ensure complete resin infiltration, the 100% resin step was repeated twice, leaving it overnight between changes. The tissue was placed in beem capsules which were then placed in an embedding oven and the resin polymerised at 60°C overnight. The resulting blocks were sectioned with a Leica Ultracut E ultra microtome using a diatome diamond knife. The sections were then stained using a saturated solution of uranyl acetate for 15 minutes and Reynold's lead citrate 15 minutes. The sections were examined using a JEOL 1400 TEM.

For Semithin section preparation after samples were embedded in resin, semithin sections were cut with a Reichert Jung ultra-cut E into 0.5μm sections, they were collected and placed on slides in drops of water. The drop was allowed to dry by heating it on a hot plate. They were then stained with Methylene blue for 1 minute. The methylene blue was removed from the slides through rinsing with tap water until the water ran clear. The sections were examined under a Leica IM8 microscope.

2.13 Western Blotting

Cells and sciatic nerves were lysed in an appropriate volume of radioimmunoprecipitation assay (RIPA) buffer in a microcentrifuge tube (50 mM Tris-HCl pH 7.4, 0.1% SDS, 1% NP-40, 150 mM NaCl, 1 mM EDTA, 0.5% sodium deoxycholate) and phosphatase inhibitor cocktails used at 1:100 (Santa Cruz Biotechnology, #sc-45045; #sc-45065) on ice then spun down at 16,000 x g for 15 minutes at 4°C. The supernatant was then transferred to fresh 1.5 ml microcentrifuge tubes and protein concentration determined using the Pierce™ BCA Protein Assay Kit (Thermo Fisher Scientific, #23225). An appropriate volume of sample was added to SDS sample buffer (50 mM Tris-HCl; 2% SDS; 10% glycerol; 1% β-mercaptoethanol; 12.5 mM EDTA and 0.02% bromophenol blue. Samples were boiled at 95ºC for 5 minutes prior to loading.

Samples were run on gel of appropriate percentage polyacrylamide gel (8%, 10%, 12% (w/v)) dependent on the protein of interest or on a 4-20% TGX precast gel (Bio-Rad, #4561086). Reagents to make polyacrylamide gels are listed in Table 9. Polyacrylamide gels were submerged in 1x running buffer (25 mM Tris base, 1.92 M glycine, 3.47 mM SDS) and proteins were separated at 150V for 90 minutes at RT. Proteins from the gel were transferred onto a polyvinylidene fluoride transfer membrane (PVDF) (Bio-Rad, #1620177) that was first activated in methanol using the wet transfer method. Proteins were transferred from gel to PVDF membrane in 1x transfer buffer (27.5 mM Tris base, 0.21 M glycine, 15% methanol) for 90 minutes at 300mA. Membranes were then reactivated in methanol, washed in MilliQ H_2O and equilibrated in Tris-buffered saline and 0.1% TWEEN (1x TBST). Membranes were blocked in blocking solution (5% w/v milk powder diluted in TBST) for one hour at RT

before primary antibodies (**Table 9**) were added to the blocking solution and membranes incubated in primary antibodies overnight at 4°C.

Following overnight antibody incubation, membranes were washed 3 times for 10 minutes per wash in 1x TBST to remove unbound primary antibody followed by incubation with appropriate species anti-mouse or anti-rabbit horseradish peroxidise (HRP)-conjugated secondary antibodies (**Table 10**) diluted 1:5000 in blocking solution for one hour at RT. Finally, membranes were washed 3 times for 10 minutes per wash in 1x TBST to remove unbound antibody before being slightly dried to remove excess TBST. Pierce® ECL western blotting substrate (Pierce, #32106) was added to the membranes as per the manufacturer's instructions to detect chemiluminescence from proteins of interest. GAPDH or β-Tubulin was used as a loading control for all samples (**Table 9**). The intensity of protein bands was quantified using the free ImageJ software available from https://imagej.nih.gov/ij/

Reagents	Resolving						Stacking
	5%	8%)	10%	12%	15%	18%	5%
H_2O	5.9 ml	5.3 ml	4.8 ml	4.5 ml	3.9 ml	3.6 ml	2.95 ml
Tris HCL 1.5M (pH 8.8)*	2.8 ml	2.5 ml	2.5 ml	2.3 ml	2 ml	1.8 ml	1.4 ml
40% Acrylamide	1.25 ml	2 ml	2.5 ml	3 ml	3.75 ml	4.5 ml	0.625 ml
10% SDS	100 µl	100 µl	100 µl	100 µl	100 µl	100 µl	50 µl
10% APS	75 µl	75 µl	75 µl	75 µl	75 µl	75 µl	37.5 µl
TEMED	10 µl	10 µl	10 µl	10 µl	10 µl	10 µl	5 µl

Table 8 - SDS-PAGE reagents.

Reagents used to make 1 SDS-Page gel of various resolving percentages for electrophoresis. *For stacking gel, Tris HCl pH was 6.8.

Antibody	Species	Company	Code	Application and dilution
CD206 (MMR)	Goat	R&D	AF2535	IHC (1/100)
CD68	Rat	Abcam	ab53444	IHC (1:100), ICC (1:100)
EphA5	Rabbit	Santa Cruz	SC1014	IHC (1:100), WB (1:500)
F480	Rat	Abcam	ab6640	IHC (1:100)
GAPDH	Mouse	Abcam	ab8245	WB (1:10, 000)
IBA1	Rabbit	WAKO	019-19741	IHC (1:500)
MBP	Rabbit	Abcam	ab40390	WB (1:500)
MPZ	Rabbit	Abcam	ab31851	WB (1:500)
NF	Chicken	Abcam	ab4680	IHC (1:10,000)
PAC1	Rabbit	Santa Cruz	sc-30018	IHC (1:100), WB (1:500)
PACAP	Rabbit	Abcam	Ab216627	IHC (1:100)
S100	Rabbit	DAKO	Z0311	ICC (1:200)
Tubulin	Mouse	Santa Cruz	2-RY22	WB (1:1000)
VIP	Rabbit	Abcam	ab78536	IHC (1:100)
VPAC1	Rabbit	Santa Cruz	sc-30019	IHC (1:100), WB (1:500)
VPAC2	Rabbit	Santa Cruz	sc-30020	IHC (1:100), WB (1:500)

Table 9 - Primary antibodies.

Table lists the primary antibodies used in this study, species, the source, which techniques they were used in.

Species/Conjugate	Company	Antibody	Application	Dilution
Chicken Alexa Fluor 488nm	Invitrogen	A-11039	ICC/IHC	1:200
Goat Alexa Fluor 488nm	Invitrogen	A-11055	ICC/IHC-F	1:200
Goat Alexa Fluor 568nm	Invitrogen	A -11957	ICC/IHC-F	1:200
Mouse HRP	Bio-Rad	1706516	WB	1:5000
Rabbit Alexa Fluor 488nm	Invitrogen	A-11008	ICC/IHC-F	1:200
Rabbit Alexa Fluor 568nm	Invitrogen	A-11011	ICC/IHC-F	1:200
Rabbit Biotinylated	Vector Laboratories	BA-1000	ICC/IHC-F	1:500
Rabbit HRP	Bio-Rad	1706515	WB	1:5000
Streptavidin Alexa Fluor 488nm	Invitrogen	S11223	ICC/IHC-F	1:1000
Streptavidin Alexa Fluor 568nm	Invitrogen	S11226	ICC/IHC-F	1:1000

Table 10 Secondary and tertiary antibodies

2.14 Functional tests.

Motor and sensory recovery of animals following injury was examined using various tests.

2.14.1 Sciatic static index (SSI)

SSI can be used to assess a mouse functional recovery following a sciatic nerve crush injury. Using video analysis of standing animals, parameters of toe spread taken from

the normal (control) and experimental (injured) hind paw are measured and used to calculate SSI (**Table 11**) (Bervar 2000).

SSI analysis was carried out on control (uninjured) mice and animals which had undergone sciatic nerve crush injury. Mice were placed into a clear Perspex box and videoed from below to assess toe spread and print length. Videos were then renamed to blind the analyst to phenotype and avoid bias. From these videos still images were taken when the mice had all 4 paws on the ground and the hind paw toes were spread. These images were used to calculate SSI. First toe spread factor (TSF) (measured from toe 1-5) and intermediate toe spread factor (ITSF) (measured from toe 2-4) was calculated. These were then used in the formula shown in Table 12to calculate the SSI. SSI was measured from each mouse before surgery (0 days), then 1, 7 and 11 days after surgery, thereafter measurements were taken 2-3 day intervals until the SSI measurement was back to that observed in the uninjured paw, at which point mice were said to have fully recovered.

TSF (toe 1-5)	OperatedTSF-normalTSF/normalTSF
ITSF (toe 2-4)	OperatedITSF-normalITSF/normalITSF
SSI	(108.44 × TSF) + (31.85 × ITSF) − 5.49

Table 11 - Equation for SSI calculation

2.14.2 Toe pinch test

Toe pinch testing is a method for measuring sensory function nerve injury. This technique involves using a pair of forceps to lightly pinch the toes of mice on the injury side and the generated response is assessed (Vogelaar et al. 2004).

Animals were gently scruffed and the most distal part of toe 3, 4 and 5 on the injured hindlimb were lightly pinched. A positive response was considered upon reflex withdrawal or the animal vocalising. Assessment of sensory recovery following peripheral nerve injury started at day 7 post cut injury and mice underwent assessment every day until recovery in toe 3, 4 and 5 has returned.

2.15 Molecules used for cell and nerve treatment

Chemical	Company	Catalogue number
db cAMP	Sigma	D0627
Ephrin A2	R&D	603-A2
Forskolin	Sigma	344270
LPS	Sigma	L3024
Neuregulin	R&D	396-HB-050
PACAP38	BACHEN	H-8430
PAC1 selective agonist (Maxadilan)	BACHEN	H-6734
PAC1 selective antagonist (M65)	BACHEN	H-6736
Poly I:C	Sigma	P0913
VIP	TOCRIS	1911
VPAC1	BACHEN	H-5802

VPAC2	TOCRIS	Bay 55-9837
VPAC2 antagonist	BACHEN	H-7292
WDC	BACHEN	Custom peptide

Table 12 - List of molecules used for cell and nerve treatment

Results

3 VIP and PACAP have distinct functions in the distal nerve stump during peripheral nerve regeneration

3.1 Introduction

The peripheral nervous system has a capacity to regenerate following both cut and crush injury. The up-regulation of regeneration-associated genes in neurons contributes significantly to the success of repair following injury. Studies have revealed that both VIP and PACAP are widely distributed peptides with a variety of biological activities (Waschek 2013). Many studies have reported that both VIP and PACAP are up-regulated in motor and sensory neurons after peripheral nerve injury and are secreted by regenerating axons to promote axon outgrowth and survival (Armstrong et al. 2003; H. S. Xiao et al. 2002; Zhou et al. 1999). Neurons up-regulate VIP and PACAP ligands but down-regulate receptors. The reason for this and the paracrine effect of VIP and PACAP in the injured peripheral nerve has not been investigated. Following peripheral nerve injury large numbers of macrophages infiltrate into the distal nerve stump. Both VIP and PACAP have well characterized immunomodulatory functions on macrophages in other tissues and act to regulate pro- and anti-inflammatory factor expression (Delgado et al. 1999c; Ganea and Delgado 2002; W. Sun et al. 2000). There is also some evidence in the literature to suggest that VIP and PACAP act on Schwann cells to promote the expression of laminin and myelin proteins (Castorina et al. 2014). This study investigates the role of VIP and PACAP paracrine effect on macrophage and Schwann cells following peripheral nerve injury.

3.2 Results

3.2.1 VIP and PACAP ligands are expressed from peripheral nerves following peripheral nerve injury.

Both VIP and PACAP are up-regulated in motor and sensory neurons after peripheral nerve injury (Armstrong et al. 2003; H. S. Xiao et al. 2002; Zhou et al. 1999). To confirm VIP and PACAP up-regulation in sensory neurons of C56BL6 mouse sciatic nerve transection injury model, a transection injury was performed and IHC on DRG tissue at 7DPI was stained for VIP and PACAP expression in sensory neurons. VIP and PACAP (red) co-localises with neuronal markers NeuN (green) showing VIP and PACAP are expressed in the sensory neurones of the DRG (**Figure 11 A-F**). Immunostaining also confirms PACAP expression in regenerating axons, where PACAP is shown to colocalise with NF which is expressed in the cytoplasm of neurones (green) in 7DPI axons (**Figure 11 G-I**).

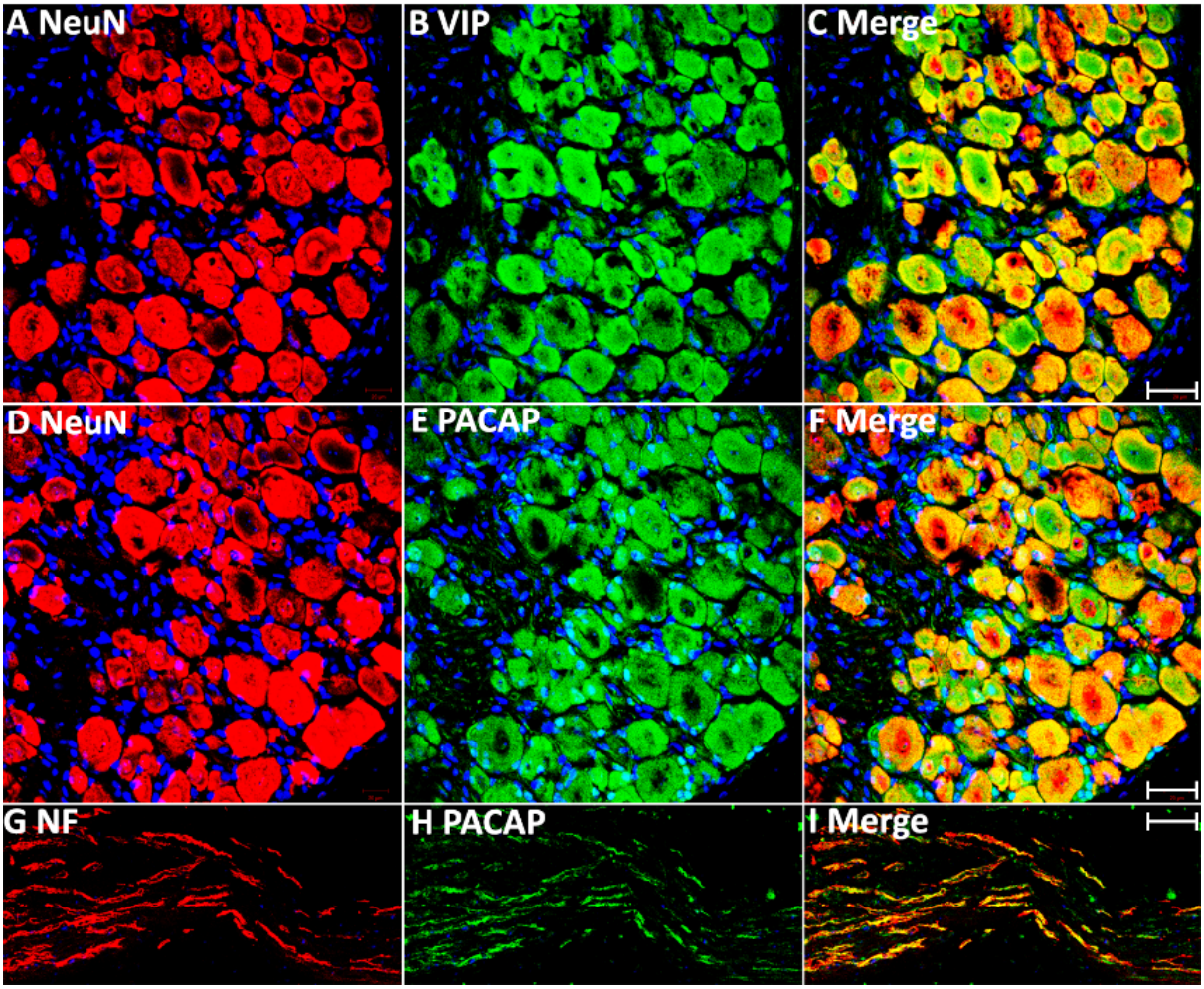

Figure 11 - Expression of VIP and PACAP in DRG sensory neurones and regenerating axons following peripheral nerve injury.

(A-C) Double staining of Vasoactive Intestinal Peptide (VIP) with the neuronal marker NeuN showing that sensory neurons in the DRG express VIP at 7 days after sciatic nerve transection injury. (D-F) Double staining of Pituitary Adenylyl Cyclase Activating Peptide (PACAP) with the neuronal marker NeuN showing that sensory neurons in the DRG express PACAP 7 days after sciatic nerve transection injury. (G–I) Double staining of PACAP with neurofilament (NF) showing that PACAP is present in leading regenerating axons in the nerve bridge 7 days after sciatic nerve transection injury. Ho (blue) staining marks nucleus. Scale bars in C and F 20 μm. Scale bar in I 40 μm.

3.2.2 VIP and PACAP receptors VPAC1, VPAC2 and PAC1 are expressed within peripheral nerves

VPAC1, VPAC2 and PAC1 have all been described to be expressed on rat Schwann cells in RT4-D6P2T cells, primary rat Schwann cells and schwannoma cell cultures (Castorina et al. 2008; Castorina et al. 2015; Lee et al. 2009). To investigate receptor expression and localisation of VPAC1, VPAC2 and PAC1 in intact and injured sciatic nerves of adult mice, immunohistochemistry, western blot and qRT-PCR analyses were performed.

3.2.2.1 VPAC1, VPAC2 and PAC1 are expressed in adult mouse intact peripheral nerves

To understand more clearly the cell-specific expression of VPAC1, VPAC2, and PAC1 proteins in intact adult mouse sciatic nerve, double staining of VPAC1, VPAC2, and PAC1 (green) with an axonal marker NF (red), on adult sciatic nerve transverse sections was performed. Double staining of VPAC1 with NF showed that VPAC1 strongly co-localised with NF indicating that VPAC1 is strongly expressed in axons of the peripheral nerve NF (**Figures 12 A–C**). VPAC1 also showed staining surrounding axons which did not co-localise with NF indicating that it is also expressed in Schwann cells (**Figures 12 A–C**). Similarly, double staining of VPAC2 with NF showed that VPAC2 is expressed in axons due to the co-localisation between VPAC2 and NF and Schwann cells, due to staining surrounding axons which did not co-localise with NF (**Figures 12 D–F**). In contrast, double staining of PAC1 with NF showed that PAC1 is only expressed in Schwann cells as no co-localisation between NF and PAC1 was observed (**Figures 12 G–I**). To confirm the expression of VPAC1, VPAC2, and PAC1 in Schwann cells staining for VPAC1, VPAC2, and PAC1 on sciatic nerve transverse sections from PLP-GFP, which label Schwann cells GFP-positive was performed.

Once again, the staining showed that VPAC1 is highly expressed in axons and weakly expressed in Schwann cells as weak co-localisation between the PLP-GFP signal and VPAC1 was observed along with axonal expression from in between the PLP-GFP Schwann cells (**Figures 13 A–I**). VPAC2 staining showed stronger staining and thus expression in Schwann cells than in axons with strong co-localisation observed between PLP-GFP signal and VPAC2 and weak axonal staining which does not co-localise with PLP-GFP (**Figures 13 D–M**). In contrast, PAC1 is only expressed in Schwann cells with weak colocalistion between PLP-GFP and PAC1 (**Figures 13 G–I**).

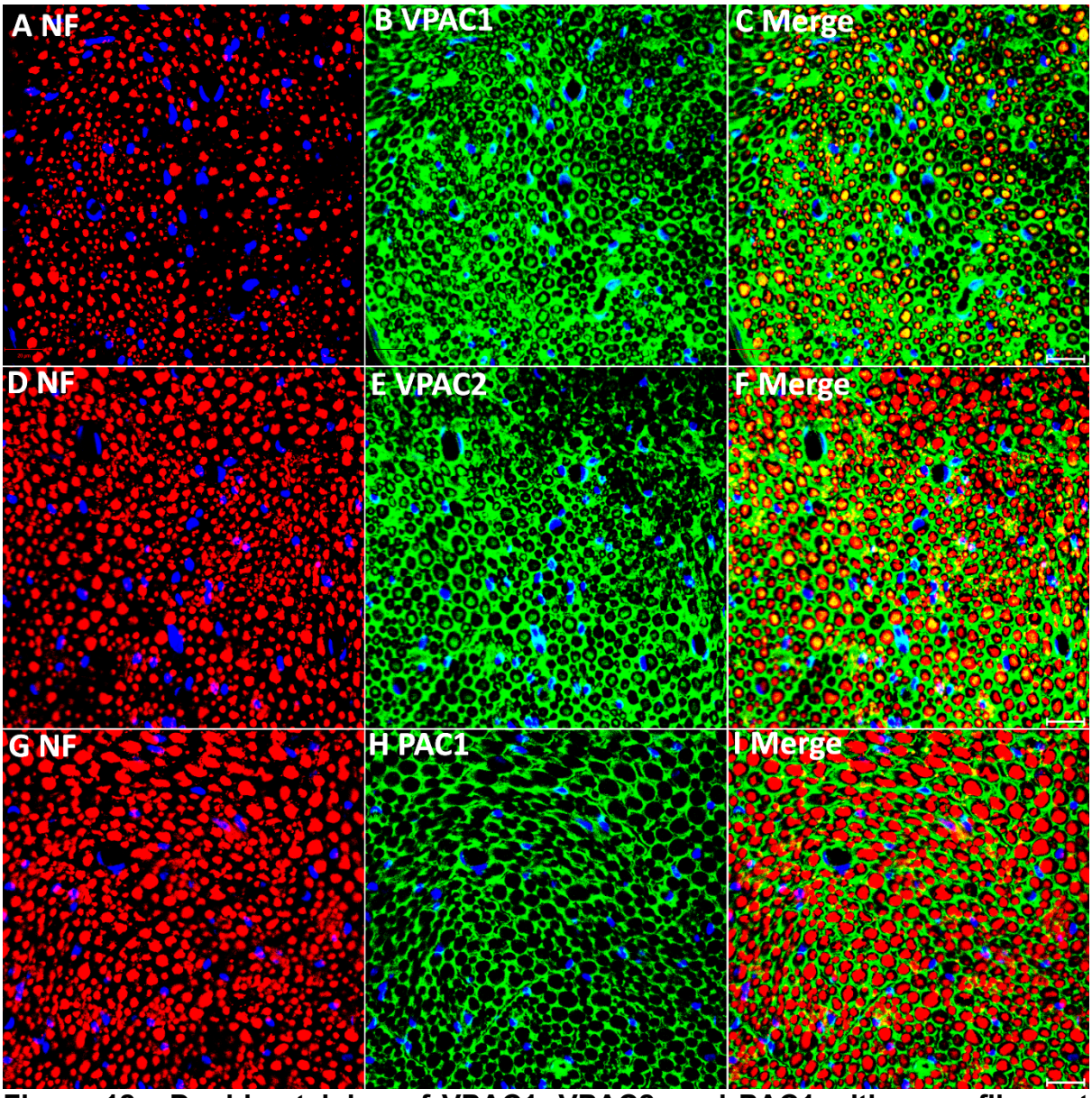

Figure 12 - Double staining of VPAC1, VPAC2, and PAC1 with neurofilament heavy chain (NF) on transverse sections from uninjured mouse sciatic nerve

VPAC1 (A–C) and VPAC2 (D–F) staining both show co-localization with neurofilament (NF) but PAC1 (G–I) does not. Yellow colour in (C,F) shows VPAC1 and VPAC2 co-localize with NF, respectively. VPAC1, VPAC2, and PAC1 also show positive staining in areas surrounding axons. Ho (blue) staining marks nucleus. Scale bars 20 μm.

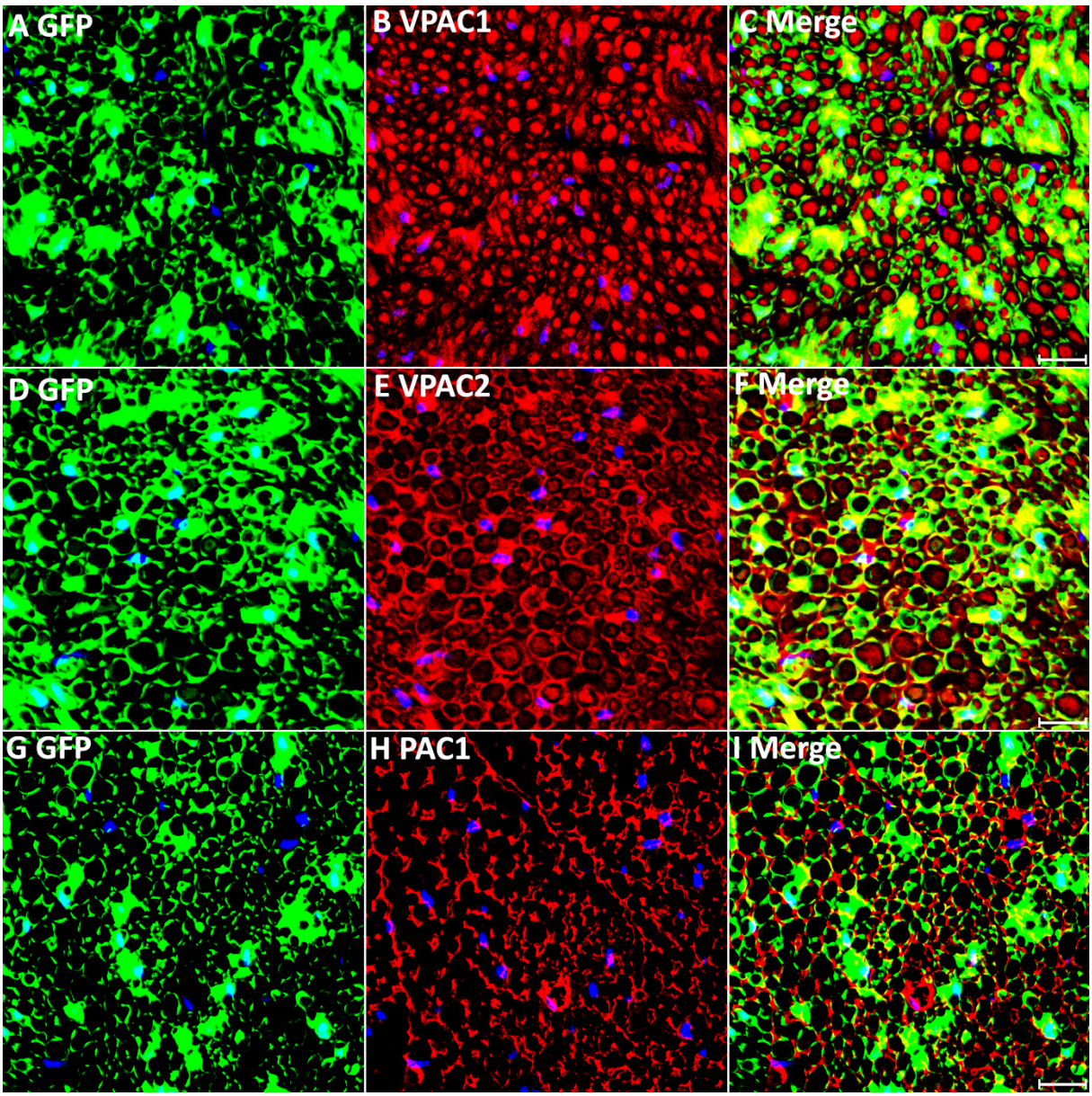

Figure 13 - VPAC1, VPAC2, and PAC1 staining on transverse sections from uninjured PLP-GFP mouse sciatic nerve.

VPAC1 (A–C), VPAC2 (D–F), and PAC1 (G–I) staining all co-localize with GFP-positive Schwann cells. VPAC1 and VPAC2 also show positive staining in axons but PAC1 (G–I) does not. Ho (blue) staining marks nucleus. Scale bars 20 μm.

3.2.2.2 VPAC1, VPAC2 and PAC1 expression is upregulated in injured peripheral nerves.

Following confirmation of VPAC1, VPAC2 and PAC1 expression in intact nerves, receptor expression within injured nerves was investigated.

An RT-PCR method was first used to detect expression of VPAC1, VPAC2, and PAC1 mRNAs in the intact mouse sciatic nerve and in the distal sciatic nerve stump at 7 days post transection injury. RT-PCR results showed that VPAC1, VPAC2, and PAC1 mRNAs are all present in the intact mouse sciatic nerve and expression of all receptors increase in the distal nerve stump following injury (**Figure 14A**). After confirming the presence of their mRNAs in the intact sciatic nerve and in the distal sciatic nerve stump, Quantitative (q) RT-PCR was used to investigate changes in mRNA expression at 4, 7, 10, and 14 days following sciatic nerve transection, using the contralateral intact sciatic nerve as control. VPAC1, VPAC2, and PAC1 mRNA levels are all significantly up-regulated in the distal nerve stump following injury compared to their expression in control uninjured nerves (**Figure 14B**). VPAC1 and VPAC2 show similar expression profiles and their expression becomes significantly elevated compared to control nerve at day 7 and peaks at day 10. PAC1 expression is significantly up-regulated at day 4 and peaks at day 10. Expression of VPAC1, VPAC2, and PAC1 begins to decrease at day 14 but remains significantly increased compared to control nerves (**Figure 14B**).

Next, changes in protein expression were investigated by western blot in the proximal and distal nerve stump at 7, 10, and 14 days following transection injury. Consistent with their mRNA up-regulation in the distal nerve stump at day 7, 10, and 14, western blot results confirmed the up-regulation of VPAC1, VPAC2, and PAC1 proteins in the

distal nerve stump at day 7, 10, and 14 post injury (**Figures 14C–F**). In contrast, there were no significant changes of their protein levels in the proximal nerve stump following injury (**Figures 14C–F**). Thus, RT-PCR, qRT-PCR, and western blot results not only confirmed the expression of VPAC1, VPAC2, and PAC1 in the mouse peripheral nerve but also revealed their up-regulation in the distal nerve stump following injury.

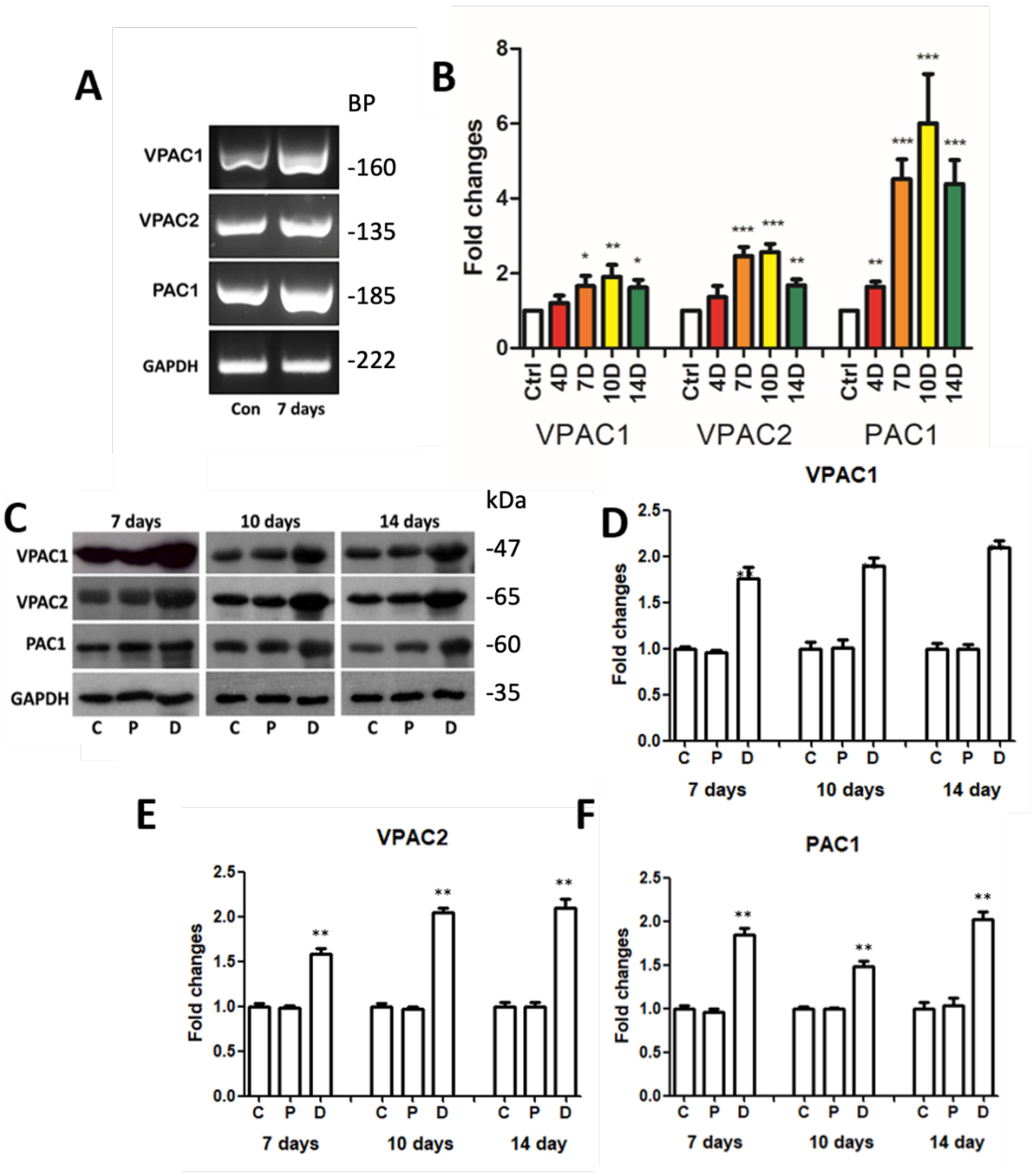

Figure 14 - Up-regulation of VPAC1, VPAC2, and PAC1 following injury in the mouse peripheral nerve

(A) RT-PCR showing the presence of VPAC1, VPAC2, and PAC1 mRNA in the intact (Con) mouse sciatic nerve and in the distal sciatic nerve 7 days after transection injury. (B) qRT-PCR showing VPAC1, VPAC2, and PAC1 mRNA up-regulation in the mouse distal sciatic nerve at 4, 7, 10 and 14 days following transection injury (C) Western blot showing VPAC1, VPAC2, and PAC1 protein expression in control uninjured (C), proximal (P), and distal (D) mouse sciatic nerve at 7, 10, and 14 days following transection injury. (D–F) Quantification of VPAC1 (D), VPAC2 (E), and PAC1 (F) protein levels from three independent western blot results showing VPAC1, VPAC2, and PAC1 protein up-regulation in the distal nerve stump. All samples were normalized to GAPDH and control samples were normalized to 1. (n=3) Data is presented as mean ± SEM. One way ANOVA followed by Tukey post hoc test. *P<0.05. **P<0.01. ***P<0.001 compared to control uninjured nerves.

Next, a transection injury on sciatic nerve in PLP-GFP mice was used to study VPAC1, VPAC2, and PAC1 expression in Schwann cells of the distal nerve stump. Immunostaining of VPAC1, VPAC2, and PAC1 on transverse sections of distal nerve at 7 days post injury showed that all GFP positive cells express VPAC1, VPAC2, and PAC1, due to co-localisation between PLP-GFP (green) and VPAC1, VPAC2 and PAC1 (red). This confirms that VPAC1, VPAC2, and PAC1 are all still expressed in Schwann cells of the distal sciatic nerve after transection injury (**Figures 15A–I**). However, axonal staining of VPAC1 and VPAC2 receptors is lost and this is due to both axonal breakdown and to receptors being downregulated in remaining axons following injury (Zhou et al. 1999). Thus, VIP and PACAP released from regenerating axons could diffuse through the distal nerve stump to interact with their receptors that are expressed in Schwann cells of the distal nerve stump to potentially regulate Schwann cell function during peripheral nerve regeneration.

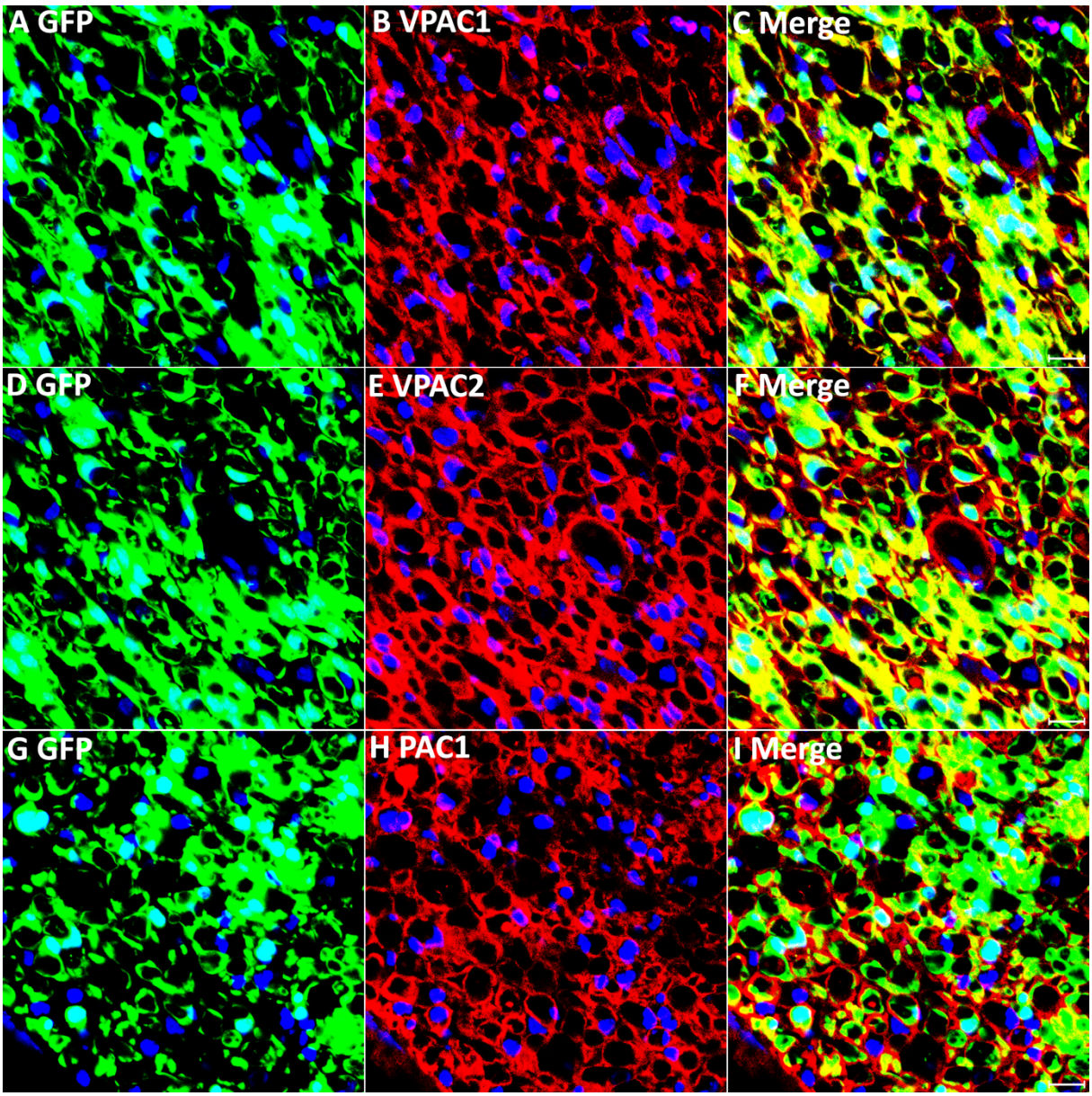

Figure 15 - VPAC1, VPAC2, and PAC1 expression in Schwann cells of the distal nerve stump 7 day post cut injury

VPAC1, VPAC2, and PAC1 staining on transverse sections from distal sciatic nerve of PLP-GFP mice 7 days after transection injury. VPAC1 (A–C), VPAC2 (D–F), and PAC1 (G–I) all co-localize with GFP in Schwann cells, confirming that VPAC1, VPAC2, and PAC1 are all expressed in Schwann cells of the distal nerve stump. Ho (blue) staining marks nucleus. Scale bars 20 μm.

3.2.3 VPAC1, VPAC2 and PAC1 are expressed on macrophages within injured peripheral nerve tissue.

In addition to Schwann cells, macrophages are the other major cell type in the distal nerve stump following injury; macrophages first act to assist Schwann cells in phagocytosis of myelin and axonal debris and then act to promote peripheral nerve regeneration (P. W. Chen et al. 2015; Martini et al. 2008). Macrophages can express both pro- and anti- inflammatory cytokines (Gaudet et al. 2011). Peripheral blood macrophages express both VIP and PACAP receptors and VIP and PACAP have well characterized functions on macrophages to promote anti-inflammatory cytokine expression (Delgado et al. 2004; Vaudry et al. 2009). Therefore, expression of VPAC1, VPAC2 and PAC1 on macrophages in the distal nerve stump was studied by immunohistochemistry on day 7 following mouse sciatic nerve transection injury. Double staining of VPAC1, VPAC2, or PAC1 (red) with well characterized pan macrophage marker F4/80 (green) on transverse sections was performed and co-localisation between the two channels was examined to investigate VPAC1, VPAC2 or PAC1 expression on macrophages. Staining revealed that VPAC1 (**Figures 16A–C**) and PAC1 (**Figures 16G–I**) are expressed by most macrophages of the distal nerve stump and that some macrophages also express VPAC2 (**Figures 16D–F** indicated by arrows). This co-expression was confirmed using an additional well characterized pan macrophage marker CD68 and the same pattern observed. Staining with CD68 revealed that VPAC1 (**Figures 17A–C**) and PAC1 (**Figures 17G–I**) are expressed by most macrophages of the distal nerve stump and that some macrophages also express VPAC2 (**Figures 17D–F** indicated by arrows) as shown by co-localisation between the two channels. Expression of VPAC1 VPAC2 and PAC1 on CD68+ and F480+ macrophages was further validated using longitudinal 7DPI sections and once

again staining for VPAC1, VPAC2 or PAC1 with CD68 or F480. Co-localisation between VPAC1, VPAC2 and PAC1 with CD68 and F480 confirmed receptor expression on macrophages (**Figures 18A-I, Figure 19A-I**). Using longitudinal sections, the strong Schwann cells expression of VPAC1, VPAC2 and particularly PAC1 does however make the weaker straining from macrophages more difficult to see. VIP and PACAP released from regenerating axons could potentially act in a paracrine manner to interact with receptors that are expressed on macrophages in the distal nerve stump to regulate the immune response within the nerve during regeneration.

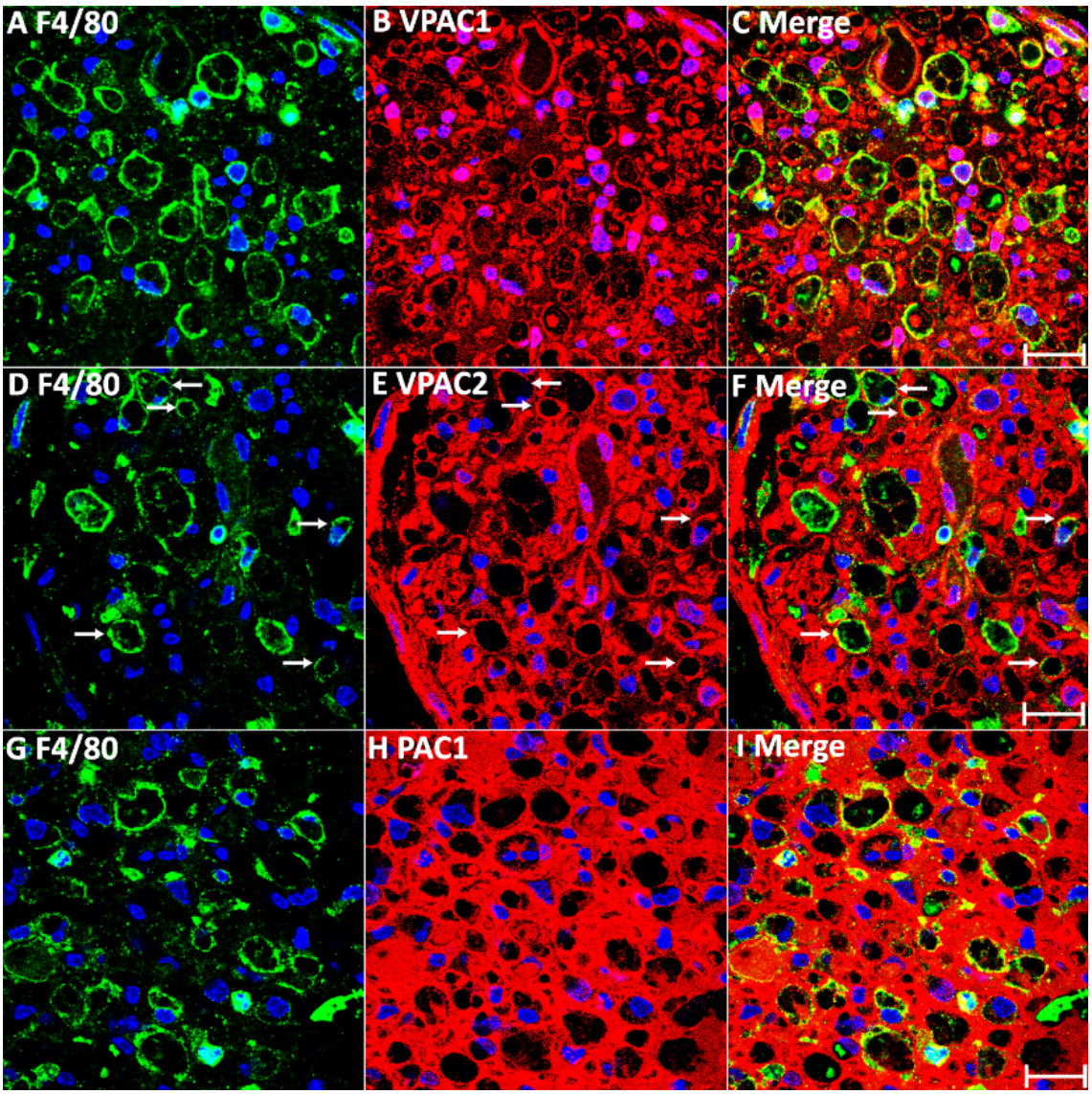

Figure 16 - VPAC1, VPAC2 and PAC1 are expressed in F4/80+ macrophages at 7 day post cut injury

(A–I) Double staining of VPAC1, VPAC2, and PAC1 (red) with macrophage marker F4/80 (green) on transverse sections from mouse distal sciatic nerve at 7 days post-transection injury. VPAC1 (A–C) and PAC1 (G–I) are expressed in most macrophages of the distal nerve stump. Macrophages expressing VPAC2 are indicated by arrows in (D–F). Ho (blue) staining marks nucleus. Scale bars 20 μm

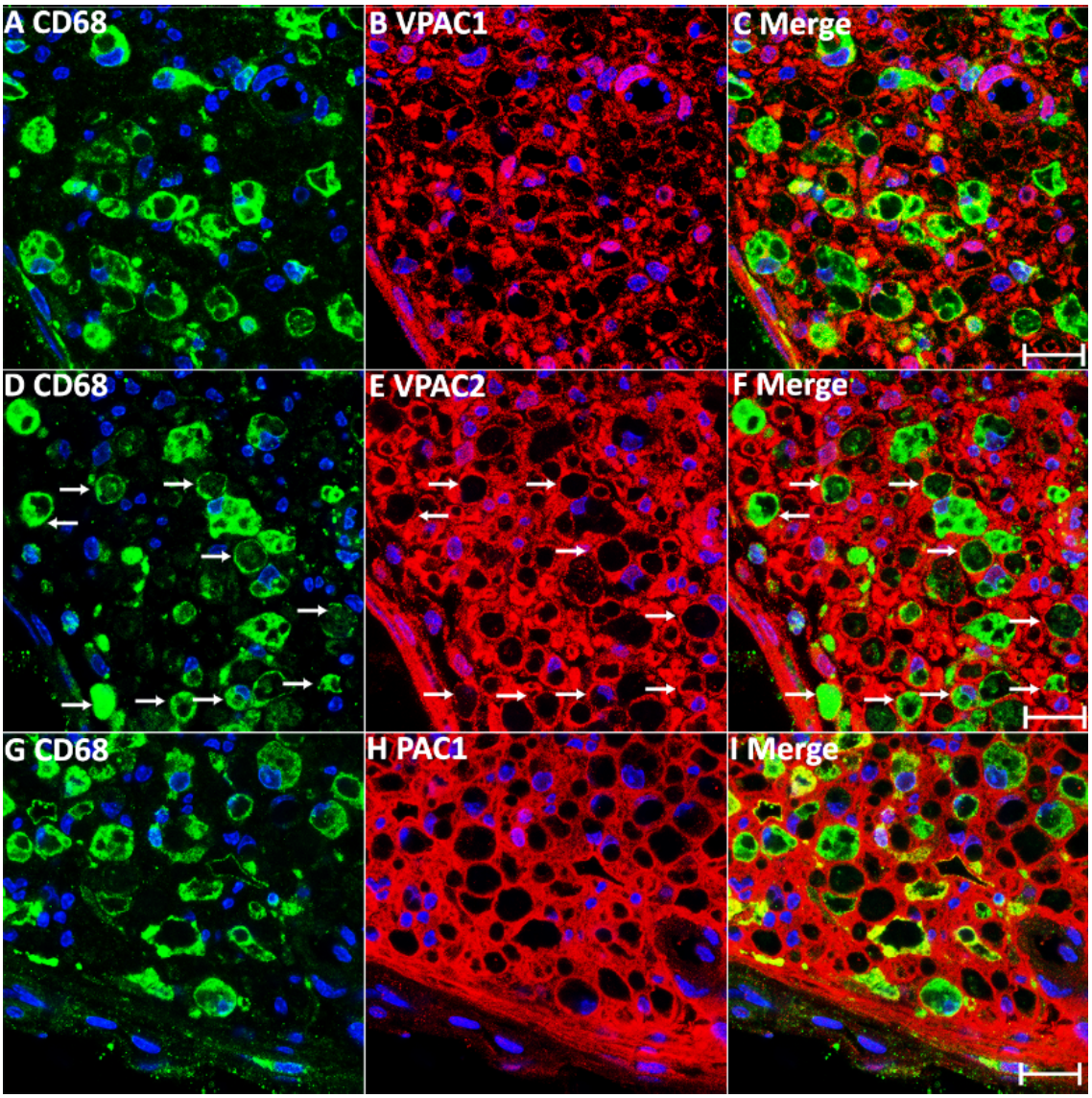

Figure 17 - VPAC1, VPAC2 and PAC1 are expressed in CD68+ macrophages at 7 day post cut injury

(A–I) Double staining of VPAC1, VPAC2, and PAC1 (red) with macrophage marker CD68 (green) on transverse sections from mouse distal sciatic nerve at 7 days post-transection injury. VPAC1 (A–C) and PAC1 (G–I) are expressed in most macrophages of the distal nerve stump. Macrophages expressing VPAC2 are indicated by arrows in (D–F). Ho (blue) staining marks nucleus. Scale bars 20 μm

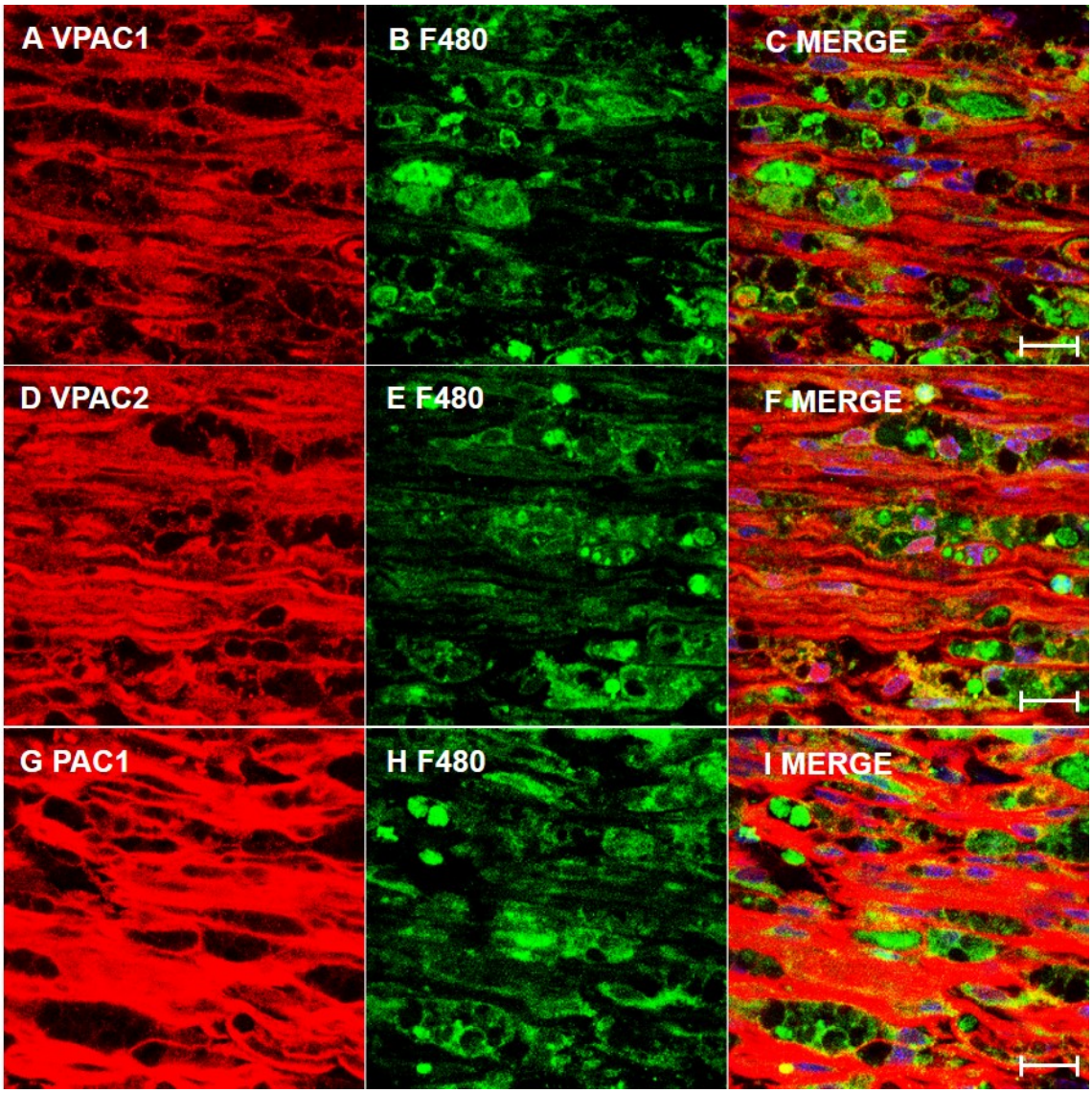

Figure 18 - VPAC1, VPAC2 and PAC1 staining colocalises with F480+ macrophages on longitudinal sections at 7 day post cut injury showing receptor expression on macrophages in the distal peripheral nerve.

(A–I) Double staining of VPAC1, VPAC2, and PAC1 (red) with macrophage marker F4/80 (green) on longitudinal sections from mouse distal sciatic nerve at 7 days post-transection injury. Ho (blue) staining marks nucleus. Scale bars 20 μm

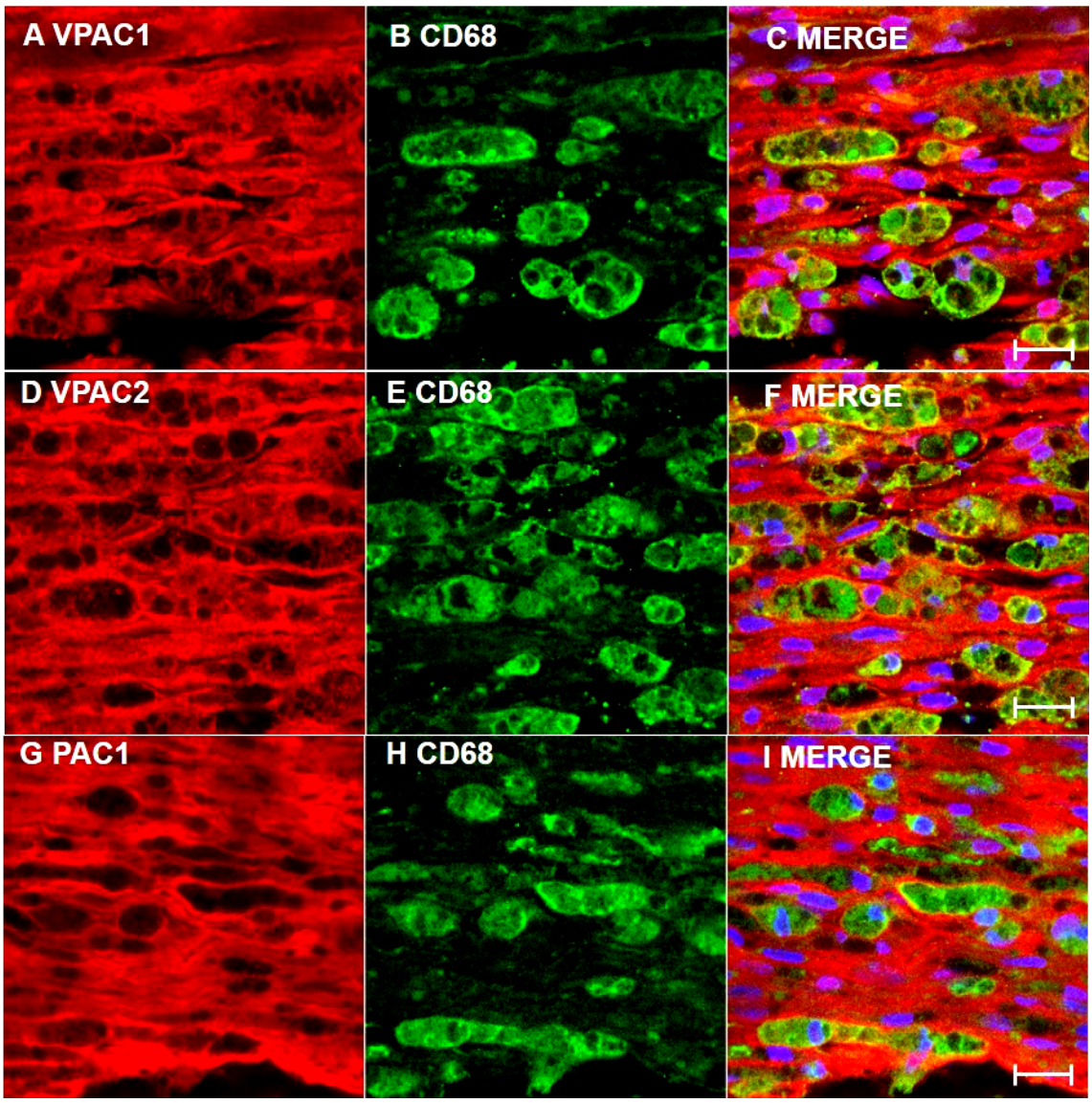

Figure 19 - Expression of VPAC1, VPAC2 and PAC1 colocalises with CD68+ macrophages on longitudinal sections at 7 day post cut injury showing receptor expression on macrophages in the distal nerve stump

(A–I) Double staining of VPAC1, VPAC2, and PAC1 (red) with macrophage marker CD68 (green) on longitudinal sections from mouse distal sciatic nerve at 7 days post-transection injury. Ho (blue) staining marks nucleus. Scale bars 20 μm

3.2.4 Receptor specific effects of VIP and PACAP regulates the expression of inflammatory cytokines following peripheral nerve injury

The relative expression levels of VPAC1, VPAC2 and PAC1 mRNA was compared in primary rat Schwann cells by qRT-PCR. This showed that VPAC1 mRNA has the lowest expression, with VPAC2 mRNA expression 3.0 fold and PAC1 mRNA expression 10.4 fold higher compared to VPAC1 (**Figure 20A**). Expression was confirmed at the protein level using western blot which showed VPAC1, VPAC2 and PAC1 to all be expressed on cultured rat Schwann cells (**Figure 20B**).

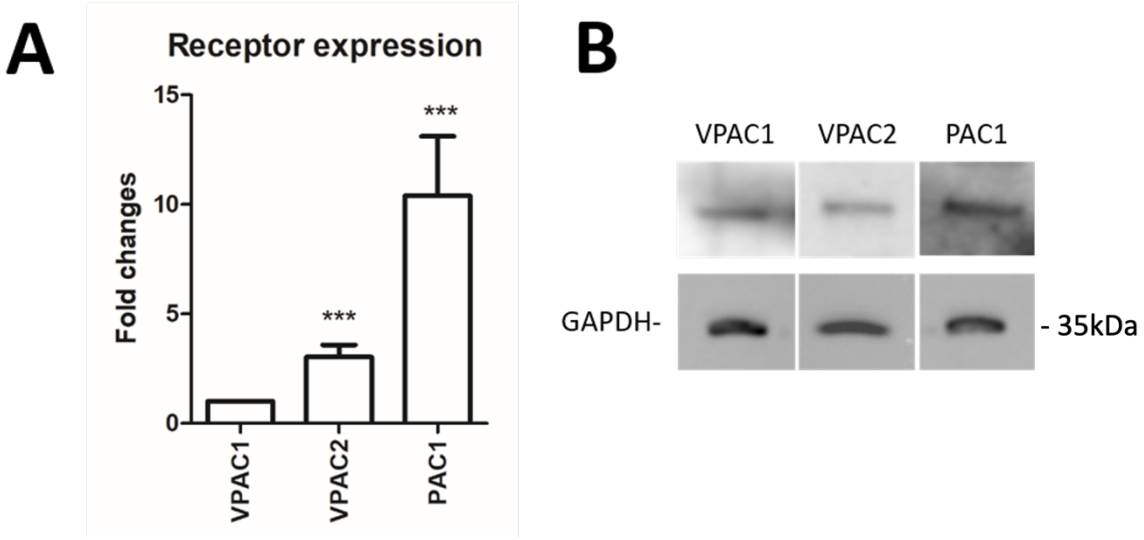

Figure 20 - VPAC1, VPAC2 and PAC1 are expressed from primary rat Schwann cells

(A) Relative expression level of VPAC1, VPAC2, and PAC1 mRNA in cultured primary rat Schwann cells, n = 3 (B) Protein expression of VPAC1, VPAC2 and PAC1 in cultured primary rat Schwann cells. GAPDH was used as a loading control. (n=3). Data is presented as mean ± SEM. One way ANOVA with Tukey post hoc test. ***P < 0.001 compared to VPAC1 levels.

3.2.4.1 VIP and PACAP acts to down regulate the expression of pro-inflammatory cytokines from Schwann cell in vitro.

Following confirmation of receptor expression Schwann cells within a primary rat Schwann cell culture, modulation of the inflammatory response was investigated in vitro. After peripheral nerve injury, Schwann cells in the distal nerve stump release pro-inflammatory cytokines such as tumour necrosis factor alpha (TNF-α), Interleukin 6 (IL-6), Interleukin 1 alpha (IL-1α), Interleukin 1 beta (IL-1β), and monocyte chemoattractant protein-1 (MCP-1) to recruit macrophages for clearance of both myelin and axonal debris (Martini et al. 2008; Zigrnond and Echevarria 2019) Pro-inflammatory cytokine production has to be carefully controlled in order to prevent excessive macrophage recruitment. The signals that control pro- and anti-inflammatory cytokines expression in the distal nerve stump are not known. VIP and PACAP have well characterized functions on macrophages to inhibit pro-inflammatory cytokine expression in other systems and so their ability to modulate cytokine expression in the distal nerve stump was investigated (Abad et al. 2016; Burian et al. 2010; Ganea and Delgado 2002).

To investigate if VIP and PACAP could inhibit pro-inflammatory cytokine expression in Schwann cells, polyinosinic-polycytidylic acid (Poly IC) and lipopolysaccharide (LPS) was used to induce pro-inflammatory cytokine expression in primary rat Schwann cells. Schwann cells express high levels of the toll-like receptors 3 (TLR3) and 4 (TLR4). Poly IC activates TLR3, while LPS activates TLR4 in Schwann cells to induce pro-inflammatory cytokine expression (Goethals et al., 2010).

First unstimulated Schwann cells were treated with VIP or PACAP to investigate if 24h VIP or PACAP treatment had any effect on TNF-α, IL-6, IL-1α, IL-1β and MCP-1 cytokine expression. Treatment of unstimulated Schwann cells with VIP and PACAP

showed that cytokine expression was not significantly altered, this is probably because in their unstimulated state Schwann cells do not express high levels of inflammatory cytokines (**Figure 21A**). Next, Schwann cells were treated with Poly IC and LPS (**Figure 21A**). As expected, Poly IC (10 mg/ml) and LPS (100 ng/ml) treatment significantly induced TNF-α, IL-6, IL-1α, IL-1β, and MCP-1 mRNA expression in primary rat Schwann cells compared to untreated Schwann cells; this created an in vitro model to simulate cytokine expression in Schwann cells in intact nerves and in injured nerves (**Figure 21A**). Treating Schwann cells with a combination of Poly IC and LPS, and VIP or PACAP significantly reduced the induction of TNF-α, IL-6, IL-1α, IL-1β and MCP-1 by Poly IC and LPS in Schwann cells (**Figure 21A**). In contrast, adding VPAC2 and PAC1 receptor antagonists 1 h before VIP and PACAP treatment inhibited the ability for VIP and PACAP to reduce pro-inflammatory cytokine expression (**Figures 21B,C**). VPAC2 and PAC1 receptor antagonists were used in these experiments where as VPAC1 receptor antagonist PG97-269 was excluded as it shows a low affinity and is less selective showing some selectivity for the PAC1 receptor (Gourlet et al. 1997). To investigate which receptors may be responsible for VIP and PACAP inhibiting pro-inflammatory cytokine expression in Schwann cells, Schwann cells were treated with receptor-specific agonists to activate selective signalling through just one receptor. Receptor-specific agonists together with Poly IC and LPS were used to treat Schwann cells and cytokine expression was investigated. qRT-PCR results showed that VPAC1 and VPAC2 specific agonists significantly inhibited Poly IC and LPS-induced TNF-α, IL-6, IL-1α, IL-1β, and MCP-1 expression (**Figure 21D**), but a PAC1 specific agonist had a more limited effect only inhibiting IL-6 and IL-1α (**Figure 21D**). Thus, VIP and PACAP appear to inhibit pro-inflammatory cytokine expression mainly through VPAC1 and VPAC2 receptors on Schwann cells.

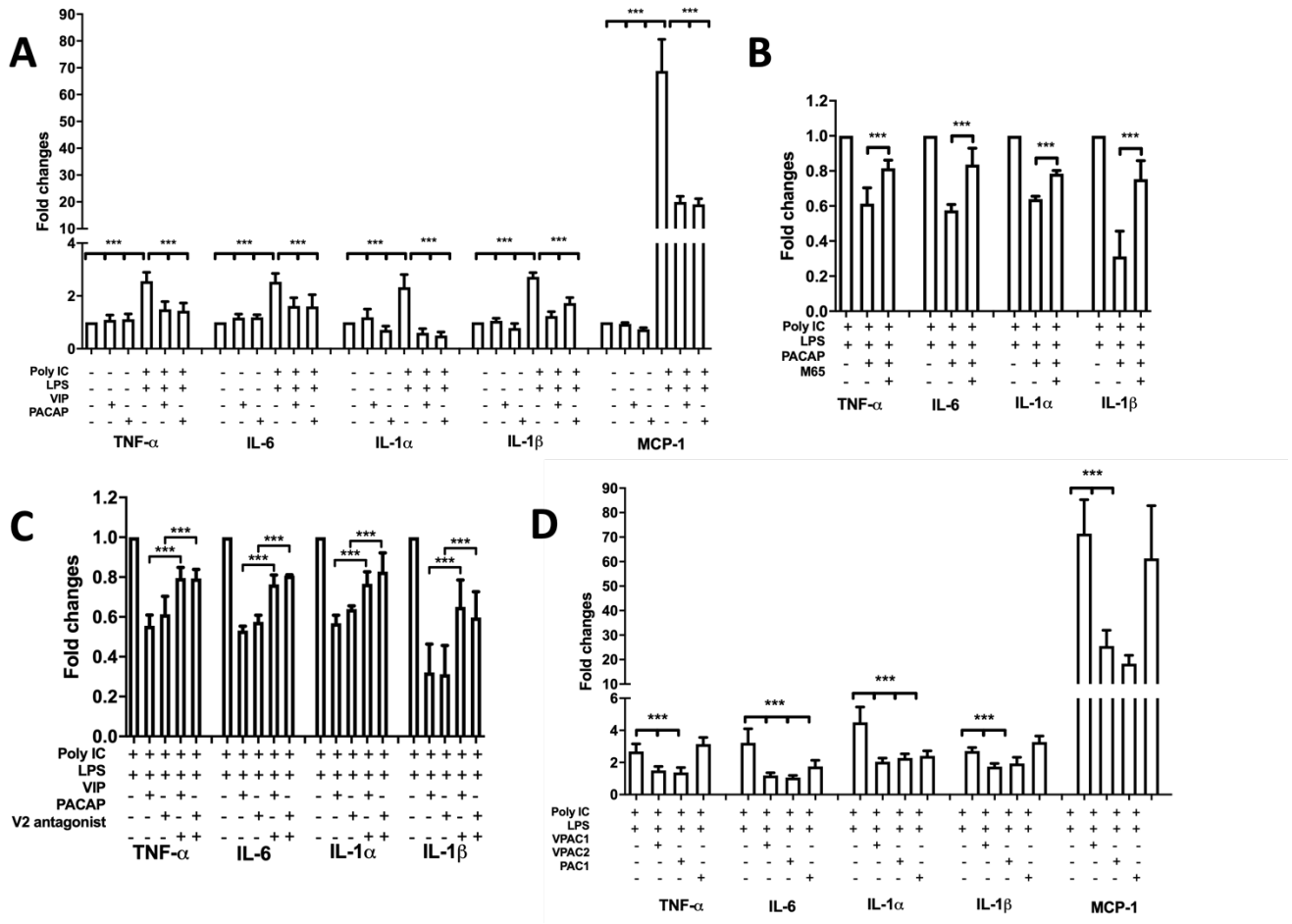

Figure 21 - VIP and PACAP inhibit pro-inflammatory cytokine expression in cultured Schwann cells

(A) VIP and PACAP inhibit Poly IC and lipopolysaccharide (LPS) induction of TNF-α, IL-6, IL-1α, IL-1β, and MCP-1 expression in Schwann cells. (B) PAC1 receptor antagonist (M65) pre-treatment (1h before adding PACAP) inhibits PACAP function. (C) VPAC2 receptor antagonist pre-treatment (1 h before adding VIP and PACAP) inhibits VIP and PACAP function. (D) VPAC1 and VPAC2 receptor specific agonist inhibits TNF-α, IL-6, IL-1α, IL-1β, and MCP-1 expression in Schwann cells induced by Poly IC and LPS stimulation. Note that PAC1 receptor specific agonist inhibits IL-6 and IL-1α but not TNF-α, IL-1β, and MCP-1 expression. All samples were normalized to GAPDH and control samples were normalized to 1. (n=4). Data is presented as mean ± SEM. One way ANOVA with Tukey post hoc test. ***P<0.001. A and D compare treated vs control samples, B compare PACAP vs M65 and C compare VIP vs V2 antagonist and PACAP vs V2 antagonist.

3.2.4.2 VIP and PACAP regulate expression of inflammatory cytokines in sciatic nerve explants

Peripheral nerve injury rapidly triggers secretion of pro-inflammatory cytokines from Schwann cells in the distal nerve stump to recruit macrophages for myelin and axonal debris clearance (Martini et al. 2008; Zigrnond and Echevarria 2019). Pro-inflammatory cytokine expression in the distal nerve peaks at 24 h following peripheral nerve injury (Rotshenker 2011). To test whether VIP and PACAP could inhibit pro-inflammatory cytokine secretion in the injured peripheral nerve, mouse adult sciatic nerve explants were incubated with VIP and PACAP. Previous experiments had shown the ability of VIP and PACAP to inhibit pro-inflammatory cytokine expression from Schwann cells in vitro. Consequently, this was further investigated using a ex vivo technique where the sciatic nerve is dissected out of the mouse and then treated in vitro so peptide effect on the whole nerve rather than just one cell type can be investigated. The adult mouse sciatic nerve dissection and explant culture triggers the injury response due to the axon being cut and induces TNF-α, IL-6, IL-1α, IL-1β and MCP-1 secretion from Schwann cells of the nerve explants. Epineurium was removed from the nerves and the nerves were pulled apart using fine needle tweezers to allow peptides to enter the peripheral nerves and act upon Schwann cells. After 24 h of VIP and PACAP incubation, mRNA was extracted for subsequent qRT-PCR analysis to measure TNF-α, IL-6, IL-1α, IL-1β, and MCP-1 expression. The experimental design for the explant experiments is shown in **Figure 22**. qRT-PCR results showed that both VIP and PACAP are both able to significantly inhibit TNF-α, IL-6, IL-1α, IL-1β, and MCP-1 mRNA expression in sciatic nerve explants (**Figure 23A**).

To determine which receptor VIP and PACAP may be acting through to decrease pro-inflammatory cytokine expression in the nerve explants, sciatic nerve explant culture was performed where nerve explants were plated and incubated with receptor-specific agonists. Treatment with receptor specific agonist showed that stimulation with VPAC1 and VPAC2 specific agonists significantly down-regulated the expression of pro-inflammatory cytokines investigated, with the VPAC2 specific agonist having the bigger inhibitory effect between the VPAC1 and VPAC2 agonists (**Figure 23B**). However, treatment with a PAC1-specific agonist had no effect upon TNF-α, IL-1α and MCP1 expression (**Figure 23B**), but significantly up-regulated the expression IL-6 and IL-1β in sciatic nerve explants (**Figure 23B**). PACAP expression reaches its peak on day 2 post injury, which is much earlier than the peak of VIP expression which occurs on day 7 (Armstrong et al. 2003; Zhou et al. 1999). The upregulation of IL-6 and IL-1α by PACAP in nerve explants suggests that PACAP may be able to promote early pro-inflammatory cytokine production in the sciatic nerve following injury. VIP and PACAP appear to act through VPAC1 and VPAC2 receptors in Schwann cells in the nerve explants to inhibit pro-inflammatory cytokine expression. This is in line with results seen in cultured Schwann cells, where pro inflammatory cytokine expression is primarily inhibited through VPAC1 and VPAC2 receptors with PAC1 having a more limited effect.

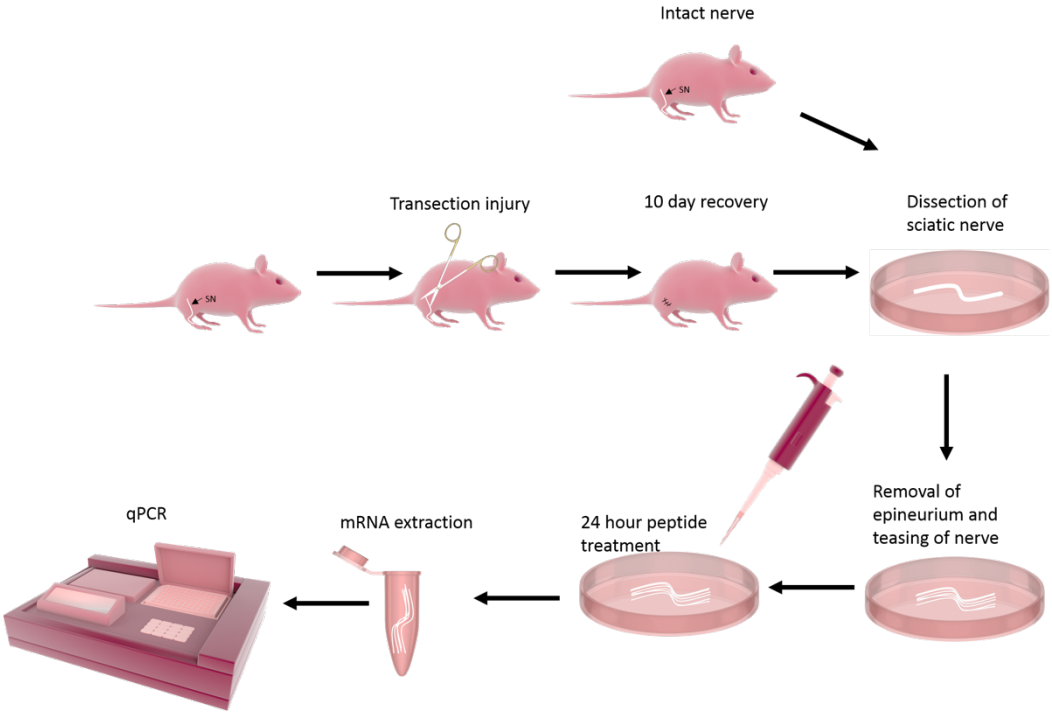

Figure 22 - Schematic for Sciatic nerve explant culture experiment

For sciatic nerve explant experiments an intact or 10DPI transacted distal nerve is dissected out. The epineurium of the nerve is removed and the nerve is teased. 100nm of VIP or PACAP is added to DMEM and incubated for 24h. At the end of this time, mRNA is extracted and inflammatory cytokines are measured using qRT-PCR.

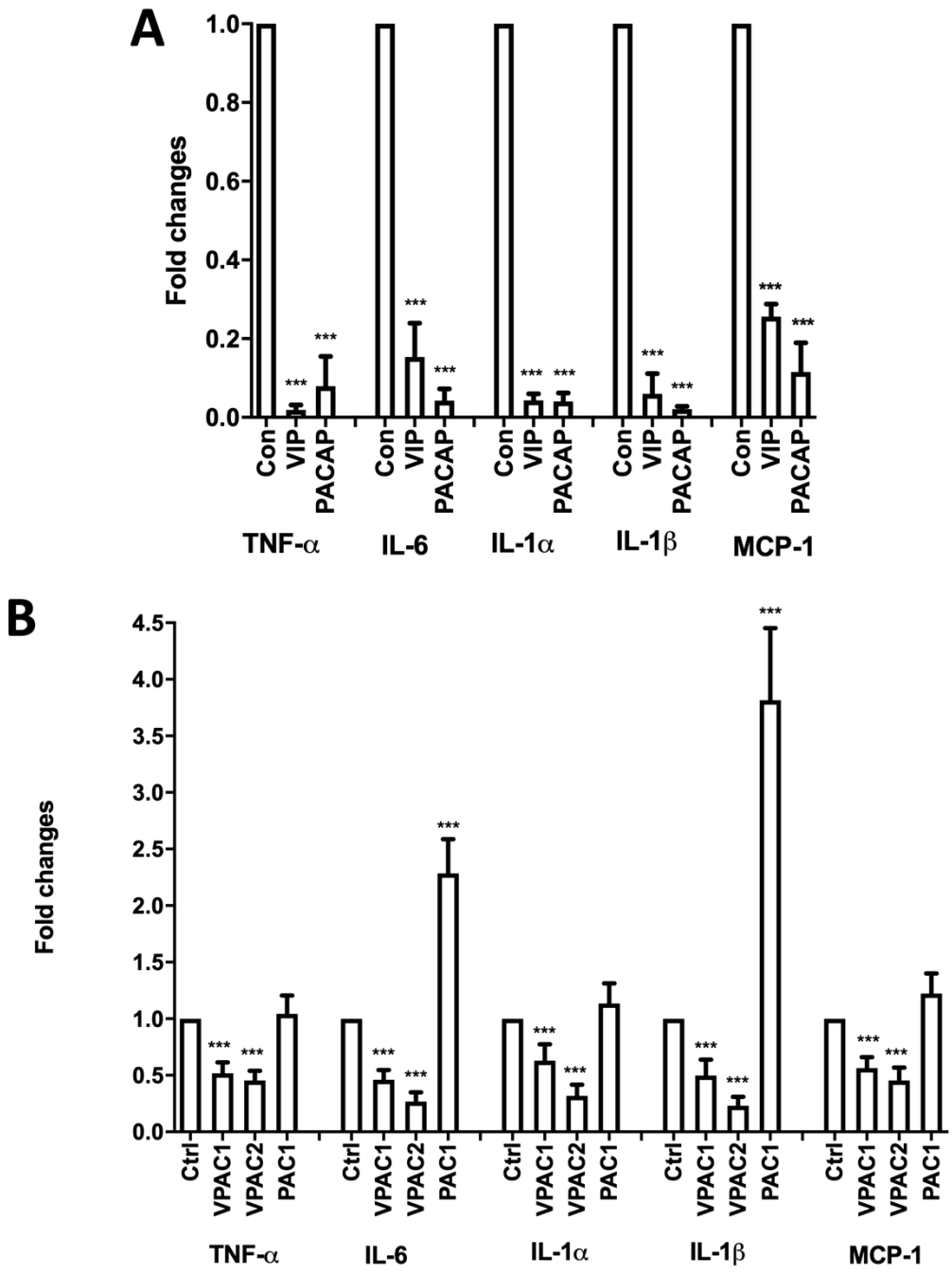

Figure 23 - VIP and PACAP decreases pro-inflammatory cytokine expression following peripheral nerve injury

(A) 24 h treatment with VIP or PACAP inhibit TNF-α, IL-6, IL-1α, IL-1β, and MCP-1 expression in cultured sciatic nerve explants. Sciatic nerve explants were cultured from uninjured mouse sciatic nerve. (B) 24 h treatment with VPAC1 or VPAC2 receptor-specific agonist treatment inhibits TNF-α, IL-6, IL-1α, IL-1β, and MCP-1 expression in cultured sciatic nerve explants. In contrast, PAC1 receptor specific agonist treatment induces IL-6 and IL-β expression. Sciatic nerve explants were cultured from uninjured mouse sciatic nerve. All samples were normalized to GAPDH and control samples were made relative to 1. n = 3. Data is presented as mean ± SEM. One way ANOVA with Tukey post hoc test. **P < 0.01, ***P < 0.001 compared to control untreated explants.

3.2.4.3 VIP AND PACAP promote the expression of anti-inflammatory cytokines from macrophages after peripheral nerve injury

Macrophages in the distal nerve stump secrete anti-inflammatory cytokines such as IL-4, IL-10, and IL-13 to promote peripheral nerve regeneration (Martini et al. 2008; Ydens et al. 2012; Zigrnond and Echevarria 2019). Macrophages infiltrate the injured nerves from day 3 and the total macrophage numbers within the injured nerve peaks between day 10 and day 14 post-injury (Martini et al. 2008; Zigrnond and Echevarria 2019). A previous study showed that 20.3% in the mouse distal sciatic nerve at 10 days post nerve transection are F480+ macrophages (Stierli et al. 2018).

The role of VIP and PACAP on macrophages in the distal nerve stump was investigated. VIP and PACAP have been previously described to act on macrophages to promote anti-inflammatory cytokine expression (Ganea and Delgado 2002). IL-10 production for example is enhanced in mouse macrophages treated with both VIP and PACAP (Delgado et al. 1999a). Previous staining had shown CD68 and F480+ macrophages to express VPAC1, VPAC2 and PAC1 7 days post cut injury, however macrophages in the distal nerve stump are able to change their phenotype from M1 to M2 around 10DPI and consequently could change receptor expression. Therefore, longitudinal adult mouse sciatic nerve sections were stained with VPAC1, VPAC2 and PAC1 and the macrophage markers F480 or CD68 to further confirm receptor expression on macrophages following peripheral nerve injury. Staining revealed that VPAC1 (**Figures 24A–C, 25A-C**) and PAC1 (**Figures 24G–I, 25G-I**) are expressed by most macrophages of the distal nerve stump and that some macrophages also express VPAC2 (**Figures 24D–F, 25D-F**) as shown by co-localisation between the two channels. VPAC1, VPAC2 and PAC1 expression on CD206 positive macrophages was also investigated at 10DPI. CD206 is strongly expressed on M2 macrophages,

macrophages in an anti-inflammatory state. VPAC1 (**Figure 26A-C)** and VPAC2 (**Figure 26D-F)** appeared to be strongly expressed on most CD206+ macrophages, whereas expression of PAC1 (**Figure 26G-I)** on CD206+ macrophages appeared to be weaker as less co-localisation between PAC1 and CD206 was observed.

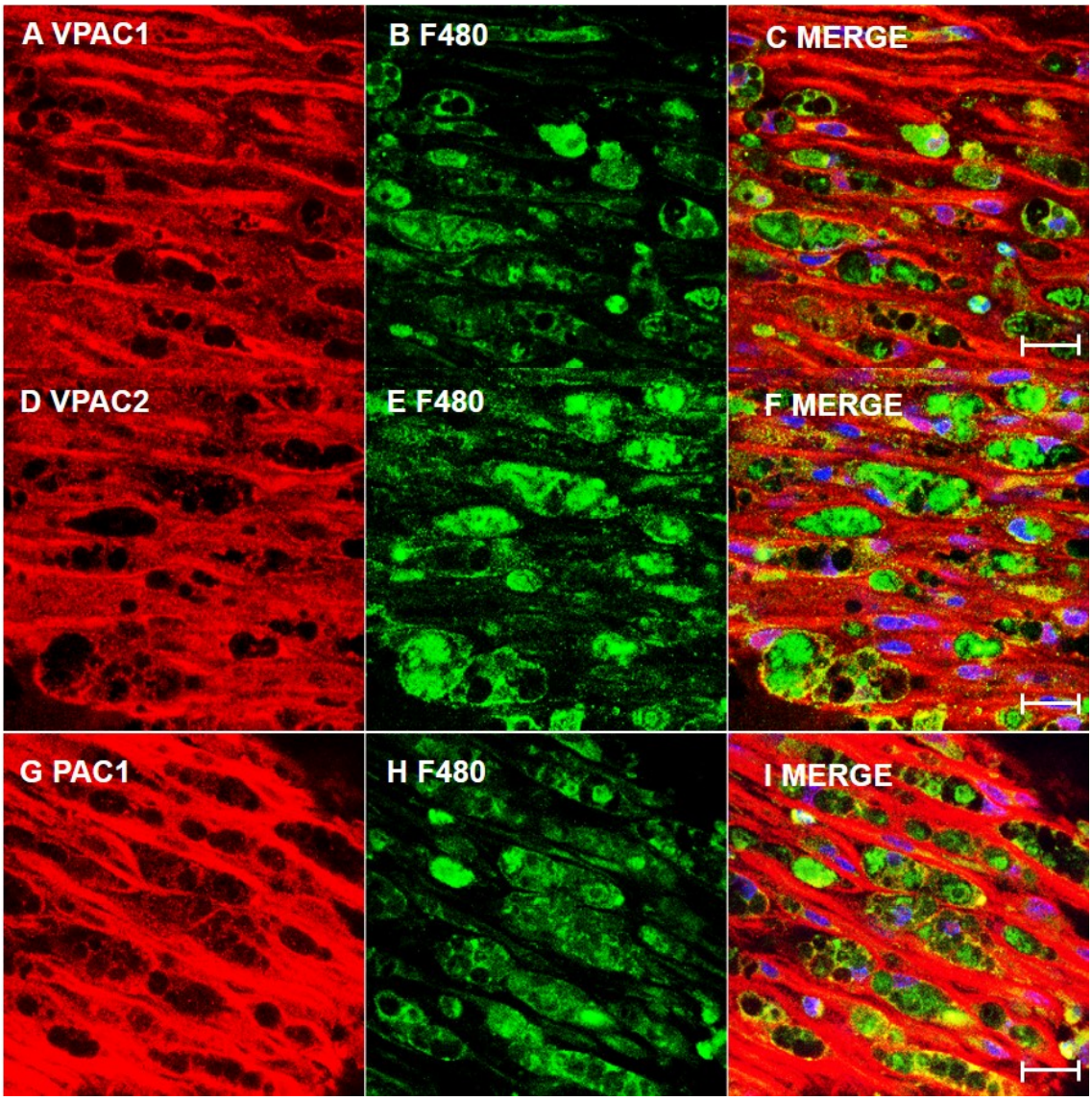

Figure 24 - VPAC1, VPAC2 and PAC1 staining colocalises with F480+ macrophages at 10 day post cut injury showing receptor expression on macrophages in the distal nerve

(A–I) Double staining of VPAC1, VPAC2, and PAC1 (red) with macrophage marker F480 (green) on longitudinal sections from mouse distal sciatic nerve at 10 days post-transection injury. Ho (blue) staining marks nucleus. Scale bars 20 μm

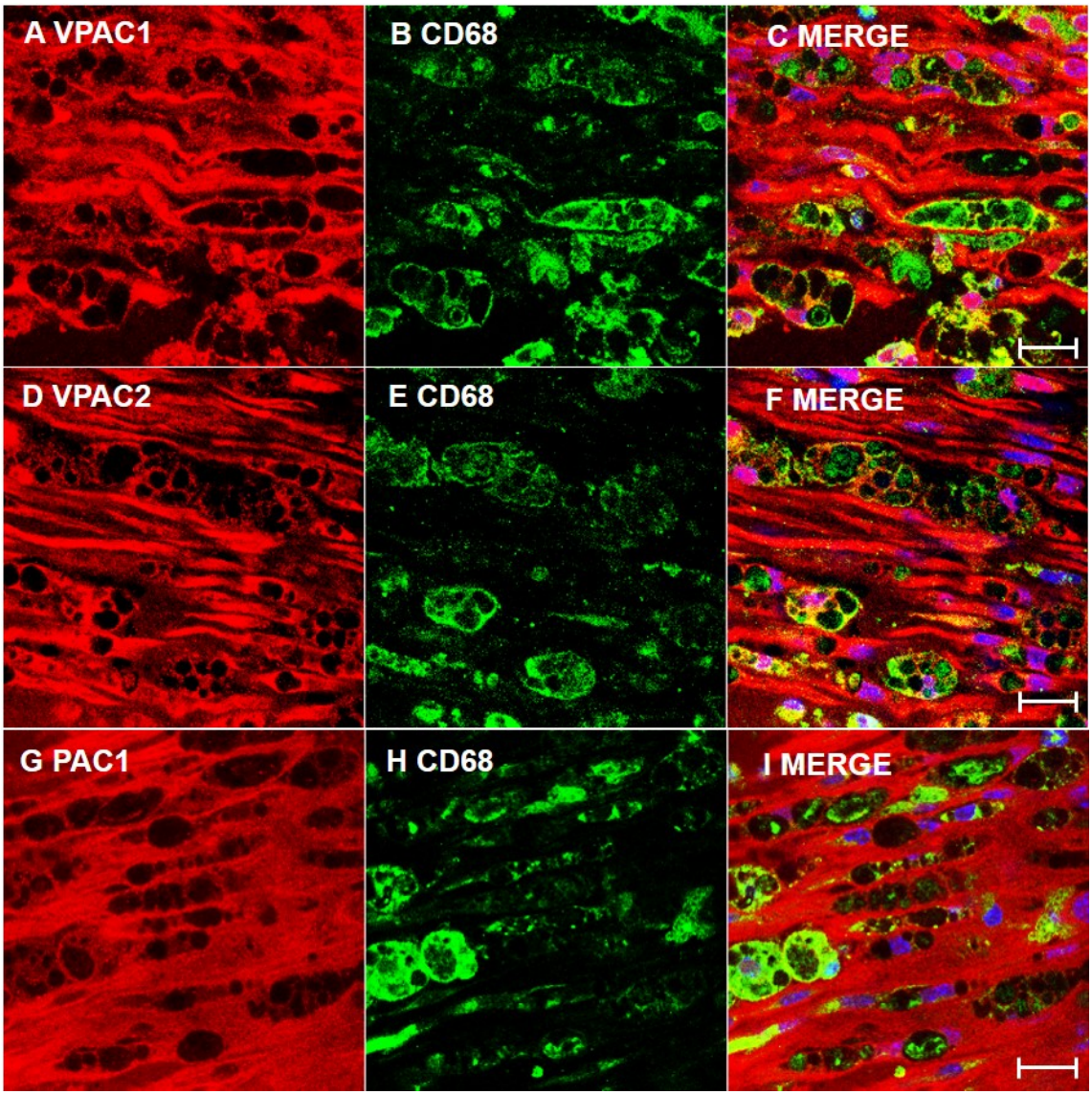

Figure 25 - VPAC1, VPAC2 and PAC1 staining colocalises with CD68+ macrophages at 10 day post cut injury showing receptor expression on macrophages in the distal nerve

(A–I) Double staining of VPAC1, VPAC2, and PAC1 (red) with macrophage marker CD68 (green) on longitudinal sections from mouse distal sciatic nerve at 10 days post-transection injury. Ho (blue) staining marks nucleus. Scale bars 20 μm

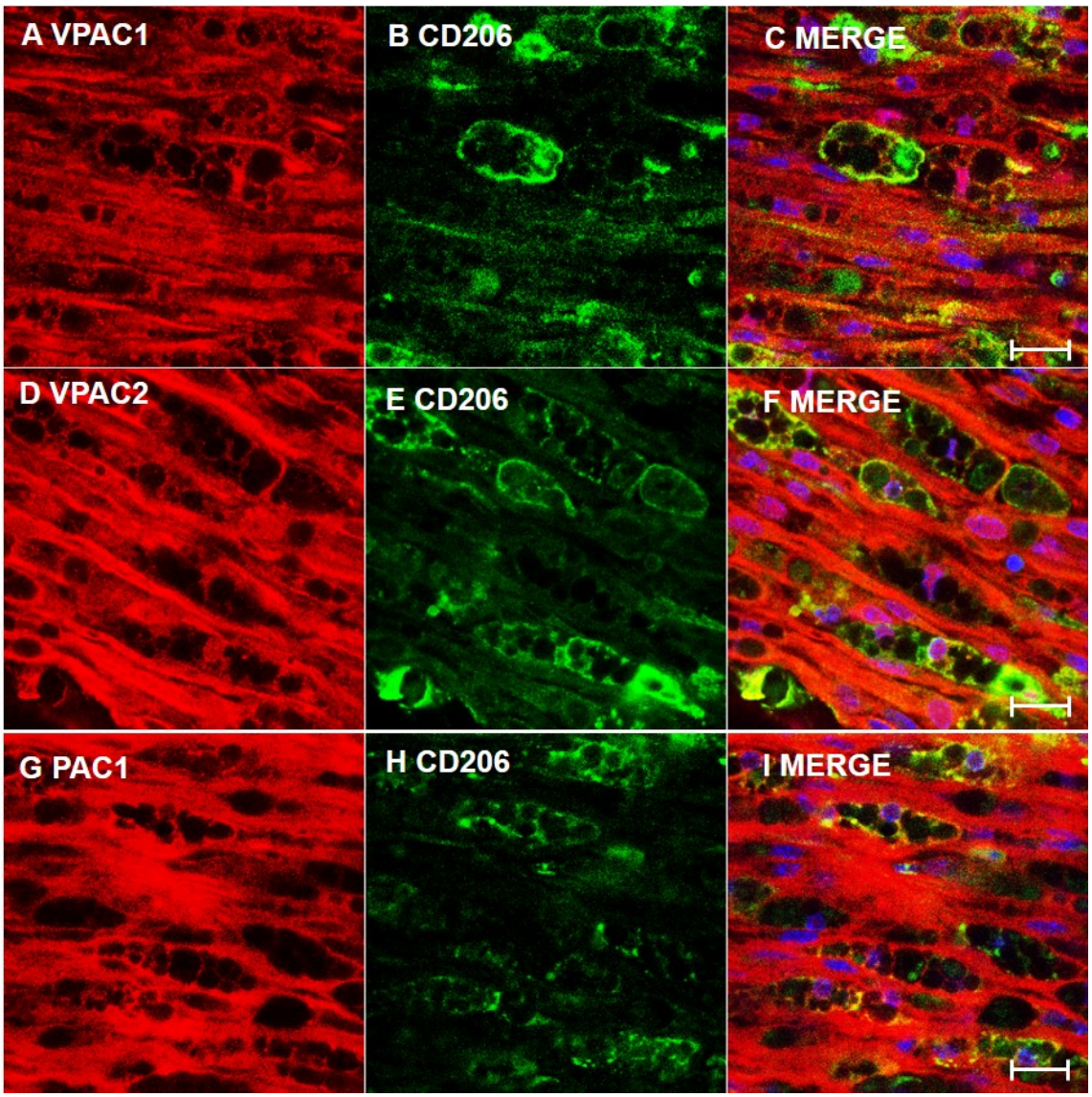

Figure 26 - VPAC1 and VPAC2 staining colocalises strongly with CD206+ macrophages at 10 day post cut injury whereas PAC1 staining colocalises weakly showing primary VPAC1 and VPAC2 receptor expression on macrophages in an M2 anti-inflammatory state in the distal nerve.

(A–I) Double staining of VPAC1, VPAC2, and PAC1 (red) with macrophage marker CD206 (green) on longitudinal sections from mouse distal sciatic nerve at 10 days post-transection injury. VPAC1 and CPAC2 appeared to be expressed from most CD206+ macrophages, whereas PAC1 was expressed from only some CD206+ macrophages. Ho (blue) staining marks nucleus. Scale bars 20 μm

To investigate if VIP and PACAP could act on mouse distal nerve and promote anti-inflammatory cytokine expression, sciatic nerve explants were taken from the distal nerve stump of 10 day post-cut injury mouse sciatic nerves, where large amounts of haematogenous cytokine expressing macrophages are present in the distal nerve stump(Gaudet et al. 2011; Mueller et al. 2003). Dissected distal nerve stumps were then incubated with VIP and PACAP for 24h followed by investigation of the expression of anti-inflammatory cytokines IL-4, IL-10, and IL-13 by qRT-PCR. qRT-PCR results showed that both VIP and PACAP are able to significantly increase the expression of anti-inflammatory cytokines IL-4, IL-10, and IL-13 in distal nerve explants following incubation (**Figure 27**). To determine which receptor VIP and PACAP may be acting through to increase IL-4, IL-10, and IL-13 expression in the nerve explants, the nerve explants were cultured with receptor specific agonists before expression of IL-4, IL-10, and IL-13 was again assessed using qRT-PCR. This revealed that both VPAC1 and VPAC2 activation was able to significantly upregulate the expression of IL-4, IL-10, and IL-13. However, PAC1 stimulation only up-regulated IL-13 and had no effect on IL-10 and IL-4 expression (**Figure 27**), indicating that VPAC1 and VPAC2 are the major receptors responsible for increasing anti-inflammatory cytokine expression in mouse distal nerve explants.

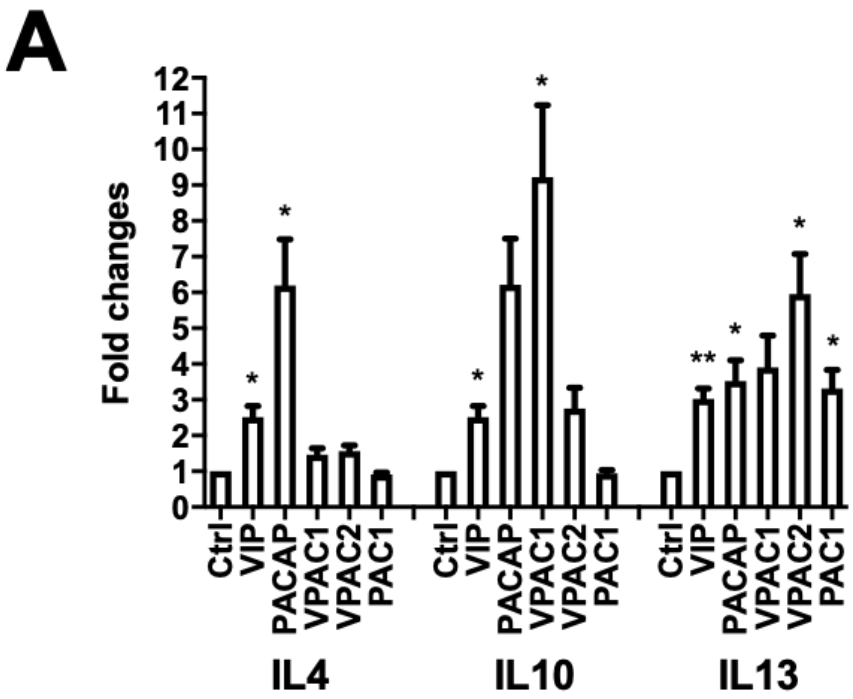

Figure 27 - VIP and PACAP increase anti-inflammatory cytokine expression in nerve explants

24 h treatment with VIP, PACAP or receptor specific agonists induce anti-inflammatory cytokines IL-4, IL-10, and IL-13 expression in nerve explants. Nerve explants were cultured from the distal nerve stump at 10 days post-transection injury. All samples were normalized to GAPDH and control samples were made relative to 1. n = 3. Data is presented as mean ± SEM One way ANOVA with Tukey post hoc test. *P < 0.05. **P < 0.01 compared to control untreated nerve explant.

3.2.5 VIP and PACAP can promote the expression of myelin proteins from Schwann cell

It has been previously described that VIP and PACAP treatment increases myelin protein expression in the rat RT4 schwannoma cell line (Castorina et al. 2014) but this has not been tested in primary Schwann cells. Therefore, the effect of VIP and PACAP on myelin gene expression in primary rat Schwann cells was investigated. It was first investigated as to whether VIP or PACAP treatment could induce mRNA expression of three key markers of myelinating Schwann cells, the transcription factor Krox20, and myelin proteins myelin protein zero (MPZ) and myelin basic protein (MBP) in primary rat Schwann cells (Martini et al. 1995; Topilko et al. 1994). Schwann cells were treated with VIP or PACAP (100 nM) every 24 h for 3 days with cyclic AMP (cAMP) treatment used as a positive control. The treatment of Schwann cells with cAMP mimics axonal contact as cAMP is able to bind to the cyclic AMP response element binding protein which leads to the induction of myelin protein expression (Monje et al. 2006; Morgan et al. 1991). At the mRNA level, both VIP and PACAP significantly increased the expression of Krox20, MPZ and MBP (**Figure 28A**). This indicates that both VIP and PACAP may function to induce signalling pathways that can promote remyelination during peripheral nerve regeneration. PACAP appears to have a much stronger ability than VIP in driving Krox20, MBP and MPZ expression (**Figure 28A**). To investigate which receptor may be responsible for promoting Schwann cell myelination, Schwann cells were treated with VPAC1, VPAC2, and PAC1 specific agonists every 24 h for 3 days. All three receptor-specific agonists significantly increased Krox20, MBP and MPZ mRNA levels, indicating that this VIP and PACAP function in Schwann cells may not be entirely receptor specific (**Figure 28B**). However, selective activation of PAC1 induced the biggest increase of Krox-20 and MBP

expression in Schwann cells (**Figure 28B**). Western blotting was used to measure MPZ and MBP protein levels in Schwann cells after VIP, PACAP or VPAC1, VPAC2, and PAC1 specific agonist treatment. This showed that VIP, PACAP, VPAC1, VPAC2, and PAC1 specific agonists are all able to increase MBP and MPZ protein expression (**Figures 28C-F**). The treatment showed that signalling through VPAC2 and PAC1 receptors has a much stronger ability to increase MPZ and MBP protein expression in Schwann cells (**Figures 28C-F**). Taken together, PACAP appears to have a much stronger ability than VIP in promoting Krox20, MBP, and MPZ expression which appears to act through VPAC2 and PAC1 receptors to carry out the function of inducing myelination in Schwann cells.

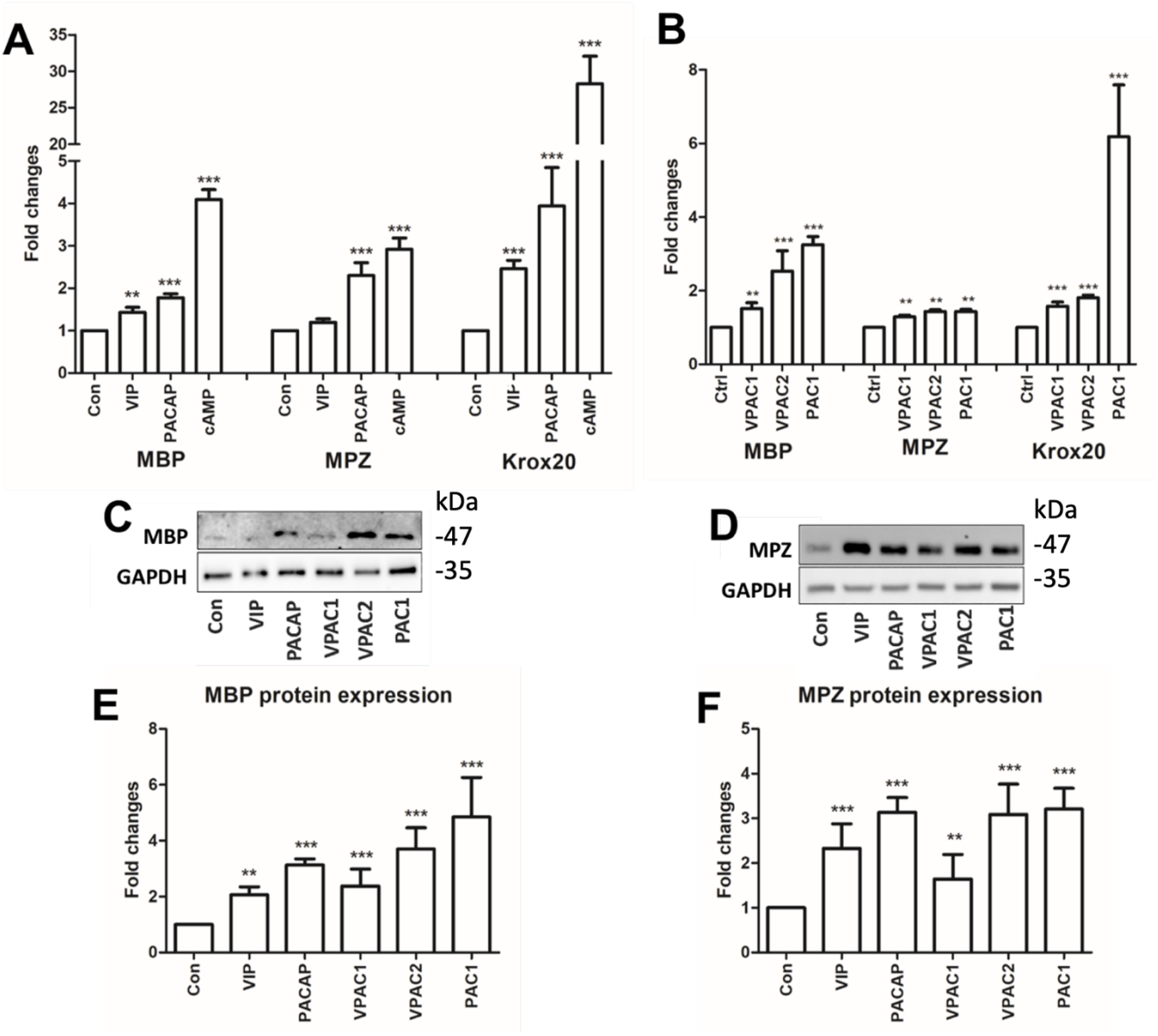

Figure 28 - VIP and PACAP increase myelin gene expression in cultured Schwann cells.

(A) qRT-PCR data showing VIP and PACAP increase the mRNA expression of myelinating Schwann cell markers myelin basic protein (MBP), myelin protein zero (MPZ), and Krox20 after 24 h treatment, n = 3. (B) VPAC1, VPAC2, and PAC1 receptor specific agonist treatment increases MBP, MPZ, and Krox20 mRNA expression in Schwann cells. (C, D) Western blot results show VIP, PACAP and receptor specific agonist up-regulation of MBP and MPZ protein expression in Schwann cells. (E, F) Quantification of MBP and MPZ levels from three independent western blot results. Data is presented as mean ± SEM. One way ANOVA with Tukey post hoc test. $*P < 0.05$, $**P < 0.01$, $***P < 0.001$ compared to a control of untreated cells.

3.3 Discussion

Previous studies have been focussed upon studying the autocrine effect of VIP and PACAP on neuronal survival and axon outgrowth during peripheral nerve regeneration; these studies revealed that increased VIP and PACAP expression in neurons was accompanied by a decrease in expression of their receptors (Zhou et al. 1999). This data provides a plausible reason for receptor down-regulation in neurons. Results suggest that this could be to allow VIP and PACAP secreted from neurones to act in a paracrine manner on Schwann cells and macrophages in the distal nerve stump during regeneration. Using qRT-PCR and western blot methods, VPAC1, VAPC2, and PAC1 up-regulation in the distal nerve stump after peripheral nerve injury was confirmed. By using immunohistochemistry of cell-specific markers, VIP and PACAP receptor proteins were shown to be highly expressed in Schwann cells and infiltrating macrophages of the distal nerve stump.

Previous reports have shown that VPAC1, VPAC2, and PAC1 are expressed in cultured primary rat Schwann cells and schwannoma cells (CRL-2768 schwannoma cell line) (Castorina et al. 2008; Lee et al. 2009; Q. L. Zhang et al. 1996). PAC1 was shown to be expressed at the highest level by both mRNA and protein levels in rat primary Schwann cell cultures, followed by VPAC2 and then VPAC1, this is in line with other studies where Lee et al 2009, showed that Schwann cell expression of VPAC2 mRNA level was 3 fold higher than VPAC1 mRNA expression. (**Figure 20**). VIP treatment on cultured mouse primary Schwann cells was first shown to have the effect of inducing laminin synthesis (Q. L. Zhang et al. 1996). VIP and PACAP treatment on rat RT4 schwannoma cells has also been shown to prevent cell apoptosis and induce myelin protein expression (Castorina et al. 2008; Castorina et al. 2014). VIP and

PACAP binding to their receptors is able to increase intracellular cAMP (Castorina et al. 2014; Harmar et al. 1998). cAMP is a key signalling molecule to induce Schwann cell myelination during peripheral nerve development. cAMP is thought to be produced through activity of the G-protein coupled receptor gpr126 and Schwann cell-specific knockout of this receptor in mice leads to Schwann cells arresting in the promyelination stage during development (Jessen and Mirsky 2005; Monk et al. 2009; Monk et al. 2011; Morgan et al. 1991). In vivo studies have shown that injection of VIP into the mouse sciatic nerve gap following nerve transection and delivery of VIP-expressing mesenchymal stem cells into a nerve guidance conduit for rat sciatic nerve gap repair accelerated Schwann cell re-myelination and nerve repair (Q. L. Zhang et al. 2002). VIP and PACAP could therefore be important signals to promote peripheral nerve remyelination during regeneration. Their effects on Schwann cell re-myelination could be mediated by increasing intracellular cAMP levels. Previous studies have shown that binding of PACAP to PAC1 had a much stronger ability to induce cAMP production than binding to VPAC1 and VPAC2 receptors (Vaudry et al. 2009). In light of this, then it is perhaps not surprising that PAC1 was observed as the most effective at inducing Krox20, MBP, and MPZ expression in Schwann cells in these experiments. It therefore appears that PACAP has a stronger ability to promote Schwann cell re-myelination.

After peripheral nerve injury, large numbers of macrophages infiltrate into the distal nerve stump to clear axonal and myelin debris; infiltrated macrophages also release pro-inflammatory cytokines to recruit more macrophages to the distal nerve (Zigmond 2012; Zigrnond and Echevarria 2019). The rapid inflammatory response after peripheral nerve injury must be carefully controlled in order to prevent prolonged and excessive macrophage recruitment and therefore unnecessary inflammation and

tissue damage. Currently, signals that are required to balance pro-inflammatory cytokines and anti-inflammatory cytokine production in the distal nerve stump have not been well established (Martini et al. 2008). Macrophages in the distal nerve stump undergo a stage transition to completely downregulate pro-inflammatory cytokines production and further up-regulate anti-inflammatory cytokines expression (Fry et al. 2007). Again, signals that regulate macrophage transition towards a repair phenotype in the peripheral nerves during regeneration have not been characterised.

There is a well characterised role of VIP and PACAP in macrophage stage transition in other tissues and organs (Abad et al. 2016; Armstrong et al. 2003; Burian et al. 2010; Delgado et al. 2001; Tan et al. 2009). VIP and PACAP could act as immunomodulators on infiltrating macrophages to balance pro-inflammatory and anti-inflammatory cytokines production in the distal nerve stump. In support of this idea, the time and the peak of VIP expression not only coincides with macrophage accumulation in the distal nerve stump during regeneration, but also matches with the kinetics of IL-10 production (a classic anti-inflammatory factor) in the distal nerve stump. IL-10 expression starts to increase considerably in the distal nerve stump 4 days post-injury, peaks at day 7 and remains elevated during the course of regeneration (Be'eri et al. 1997). Staining on mouse distal nerve, at 7 and 10 days post-injury, showed that macrophages within the distal nerve stump express VPAC1, VPAC2, and PAC1. Incubation of distal nerve explants taken at 10 days post-injury with VIP or PACAP for 24 h up-regulated the expression of anti-inflammatory cytokines IL-4, IL-10, and IL-13 expression. This is in line with a previous study by Armstrong et al, 2008 where PACAP knockout animals not only showed that axon regeneration following injury is reduced, but also found that pro-inflammatory cytokine down-

regulation is delayed and anti-inflammatory cytokine production is impaired in the distal nerve stump following injury (Armstrong et al. 2008). VIP and PACAP act as key signalling molecules to balance pro-inflammatory and anti-inflammatory cytokine production and potentially control macrophage stage transition in the distal nerve stump. These are key steps for the resolution of the inflammatory response of the injured peripheral nerve and re-establishment of tissue homeostasis.

Peripheral nerve injury triggers TNF-α, MCP-1, IL-1α, IL-1β, and IL-6 expression in Schwann cells and they peak at 24 h following injury (Rotshenker 2011). Increasing evidence shows that there are remarkable similarities between inherited peripheral neuropathies and peripheral nerve trauma in term of inflammatory response although the former is chronic and the latter is acute (Martini et al. 2013). In pathological situations such as Charcot-Marie-Tooth (CMT) disease, acute inflammatory demyelinating polyneuropathy (AIDP), and chronic inflammatory demyelinating polyneuropathy (CIDP), Schwann cells also release pro-inflammatory cytokines and recruit macrophages to the peripheral nerves. Macrophages are the major immune cells to be found in the peripheral nerves of animal models for CMT diseases (Fledrich et al. 2012; Martini et al. 2013). In CMT animal models, macrophages enter into the peripheral nerves in response to chemokines released by Schwann cells and phagocytose myelin to leave intact but demyelinated axons. This strongly contributes to the pathogenesis of CMT disorders. Investigations in human nerve biopsies have revealed that abnormal macrophage recruitment plays a key role in the demyelination process in neuropathies such as CMT, AIDP, and CIDP diseases (D. Klein and Martini 2016; Martini et al. 2013). Inherited peripheral neuropathies in humans are still incurable and lead to muscle wasting, sensory dysfunction and progressive disability

(Fledrich et al. 2012). As such, the development of novel therapeutic approaches is important. My experiments show that VIP and PACAP treatment not only inhibits TNF-α, MCP-1, IL-1α , IL-1β , and IL-6 expression in Schwann cells induced by Poly:IC and LPS stimulation but also significantly reduced TNF-α, MCP-1, IL-1α , IL-1β, and IL-6 expression in nerve explants. Findings from my studies indicate the potential for using exogenous VIP and PACAP to act through VPAC1 and VPAC2 receptors and inhibit the release of pro-inflammatory cytokines by Schwann cells in such pathological situations. Further investigation of VIP and PACAP immunomodulatory function on CMT mouse models could potentially develop VIP and PACAP as novel molecules for the treatment of peripheral neuropathies.

My data provides evidence that up-regulated VIP and PACAP could act on both Schwann cells and macrophages in the distal nerve stump and potentially regulate peripheral nerve regeneration. Although both VIP and PACAP were up-regulated in neurons following peripheral nerve injury, PACAP reaches its peak expression at day 2 while VIP reaches its peak expression at day 7 (Armstrong et al. 2003). The differences in peak expression times indicates that VIP and PACAP may execute distinct functions in the distal nerve stump at different time points during regeneration. Treatment with PAC1 specific agonist significantly up-regulated IL-6, IL1β and MCP-1 expression in sciatic nerve explants. This result indicated that PACAP may have the ability to promote early pro-inflammatory cytokine production in the sciatic nerve following injury. However, activation of PAC1 has limited effect on the release of pro-inflammatory cytokines in cultured Schwann cells, indicating that PACAP may act on a different cell type in the sciatic nerve explants to promote pro-inflammatory cytokine release. About 8% of cells in the peripheral nerves are known to be resident macrophages and their activation contributes significantly to the early release of pro-

inflammatory cytokine following peripheral nerve injury (Stierli et al. 2018; Zigrnond and Echevarria 2019). This data has shown that macrophages in the mouse sciatic nerve express the PAC1 receptor, thus, PACAP peaking at day 2 following injury may have an important function by acting on PAC1 expressed on resident macrophages to promote early pro-inflammatory cytokine production. In contrast, the peak expression of VIP on day 7 following peripheral nerve injury matches well with the time point of pro-inflammatory cytokine down-regulation. Therefore, VIP could have a more important function than PACAP in terms of the resolution of the distal nerve inflammatory response.

Taken together, in this study, VPAC1, VPAC2, and PAC1 are shown to be up-regulated in Schwann cells and macrophages of the distal nerve stump after peripheral nerve injury. In the early stage of peripheral nerve injury, VIP and PACAP could balance pro-inflammatory cytokine production and prevent unnecessary macrophage recruitment. In the later stages of regeneration, VIP and PACAP may downregulate the expression of pro-inflammatory cytokines and up-regulate the production of anti-inflammatory cytokines in macrophages to trigger the macrophage stage transition and eventually terminate the inflammatory response in the distal nerve stump. VIP and PACAP may also have important function in promoting Schwann cell re-myelination.

4 The role of EphA5 signalling in Schwann cell migration and macrophage clearance during peripheral nerve regeneration.

4.1 Introduction

The nerve bridge forms between the proximal and distal nerve stumps following transection; cells migrate from both nerve stumps to form this new tissue. Schwann cells and macrophages are two of the cell types with migratory behaviours that carry out distinct functions within the peripheral nerves. Schwann cells migrate into the nerve bridge from the proximal and distal nerve stump and act to provide both trophic support and provide a track that regenerating axons can migrate along (Min et al. 2021). Schwann cells have been shown to interact with other cell types within the peripheral nerves including axons, macrophages, endothelial cells and fibroblasts, which help guide cells and aid in determining the fate and function of some of these cells (Cattin et al. 2015; Dubovy et al. 2014; Parrinello et al. 2010). Macrophages infiltrate the distal nerve stump to carry out distinct functions such as myelin phagocytosis and secretion of cytokines and trophic factors (Rotshenker 2011). Once these functions have been carried out, macrophages are required to leave the distal nerve stump so the nerve can complete regeneration and tissue homeostasis can resume. Whilst the majority of macrophages are known to migrate out of peripheral nerves back into the blood stream, some macrophages are known to undergo apoptosis (Kuhlmann et al. 2001). Although macrophage efflux has been extensively described, the controlling mechanisms have not been characterised (Mueller et al. 2003). Currently only one macrophage efflux mechanism has been identified in the mouse distal nerve stump, mediated by the Nogo receptor 1. The Nogo receptor 1 interacts with myelin associated glycoprotein on remyelinated axons to induce

macrophage efflux from the regenerated nerve through the activation of RhoA (Fry et al. 2007). Signals that can initiate repulsive signalling and promote macrophage migration may be important players in macrophage clearance from the distal nerve stump during peripheral nerve regeneration.

EphA5 expression has been shown to be increased in the distal nerve stump in an Affymetrix dataset following injury suggesting EphA5 signalling may play a role in the nerve repair after injury (Stratton et al. 2018). Whilst EphA receptors play a major role in axon guidance during development of the nervous system, their role within peripheral nerve following injury have not yet been investigated (Caras 1997; Cooper et al. 2009; Helmbacher et al. 2000; Steinecke et al. 2014). The well characterised pathway of contact dependent repulsive signalling leading to contact inhibition of locomotion and cell migration mediated by EphA signalling may play a role in controlling migration, particularly macrophages and Schwann cells, within the nerve bridge and distal nerve stump following injury (Astin et al. 2010; Batson et al. 2013; Mayor and Carmona-Fontaine 2010). My data in this chapter identifies a new role for EphA5 upregulation and signalling within the nerve bridge and distal stump of peripheral nerves in both macrophages and Schwann cells following peripheral nerve injury. It also starts to elucidate which ligands may be important in inducing signalling through EphA5 expressing cells.

4.2 EphA5 expression in sciatic nerve

Expression of EphA5 was first confirmed in the mouse peripheral nerve following injury. qRT-PCR was performed with intact mouse peripheral nerves and injured sciatic nerves at 4, 7, 10, 14, 21 and 28 DPI **(Figure 29A).** This confirmed EphA5 up-regulation in the peripheral nerve following injury; EphA5 mRNA was significantly

upregulated from 7DPI, expression peaked at 14DPI and remained significantly upregulated up until at least 28DPI. EphA5 upregulation was confirmed at the protein level at 7DPI using western blot (**Figure 29B)**. Next, IHC staining of peripheral nerve sections post injury was used to start to elucidate which cell types may be expressing EphA5. A transection injury to the sciatic nerve in PLP-GFP mice was used to study EphA5 expression in the distal nerve stump. EphA5 co-localised with PLP-GFP expressing cells indicating EphA5 expression in Schwann cells (arrow heads) (**Figure 30A**).

However, expression of EphA5 could also be seen expressed on an undetermined cell type following injury in the nerve, presumably macrophages based upon the cell morphology (**Figure 30A** Arrows). To confirm if EphA5 was expressed by macrophages present in the peripheral nerve following injury, double staining of EphA5 with 3 macrophage markers CD206, F4/80 and CD68 was performed **(Figure 30B-D).** Double staining saw co-localisation of macrophage markers CD206+, F4/80+ and CD68+ (green) with EphA5 (red) (**Figure 30B-D** Arrow). This therefore confirmed EphA5 expression on Schwann cells and macrophages in the distal peripheral nerve at 7DPI.

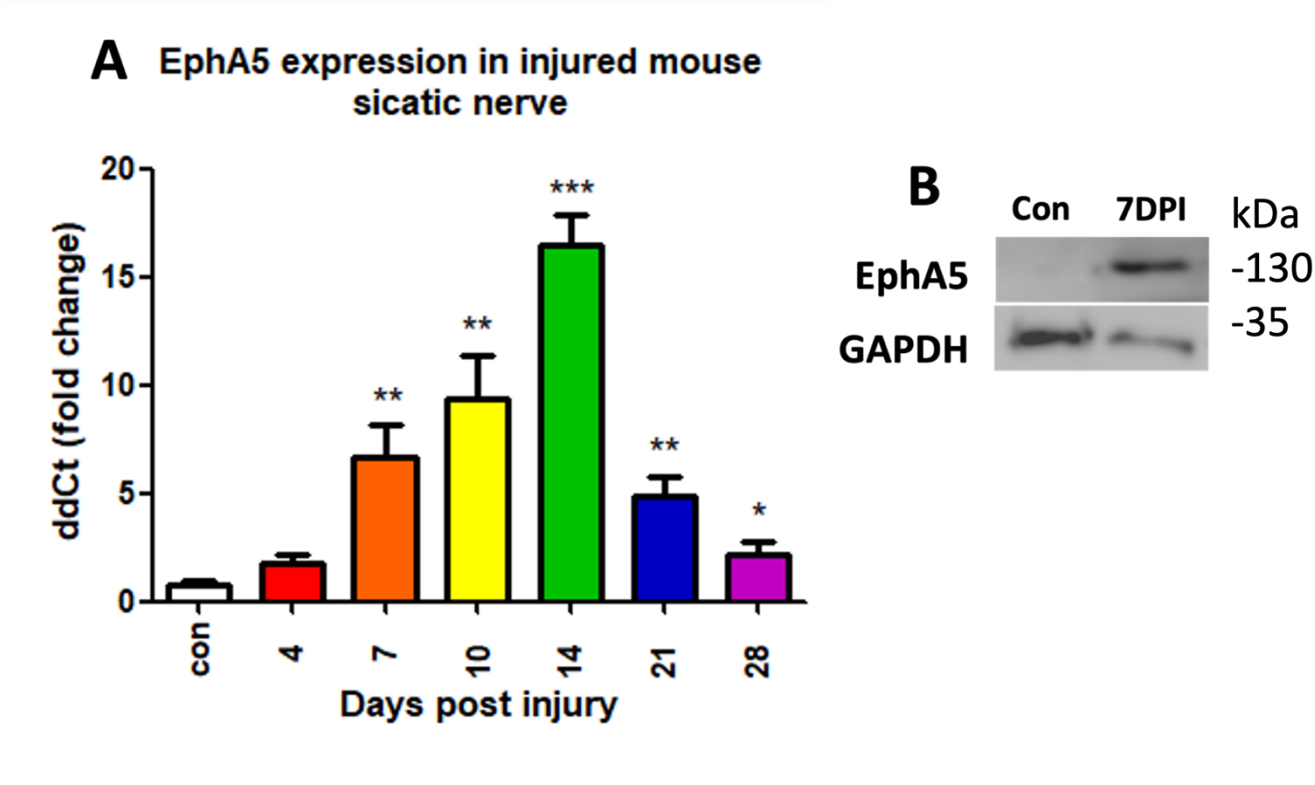

Figure 29- EphA5 expression is upregulated in mouse sciatic nerve following transection injury

A. qRT-PCR used to determine the fold change of EphA5 expression at the mRNA level. EphA5 expression is significantly up-regulated from 7-28DPI compared control levels. B. Western blot showing EphA5 in control nerve and distal nerve 7DPI. GAPDH was used as a loading control. (N3) Data is presented as mean ± SEM. Control uninjured contralateral nerve vs injured nerve. One way ANOVA with Tukey post hoc test *P<0.05. ** P<0.01. ***P<0.005.

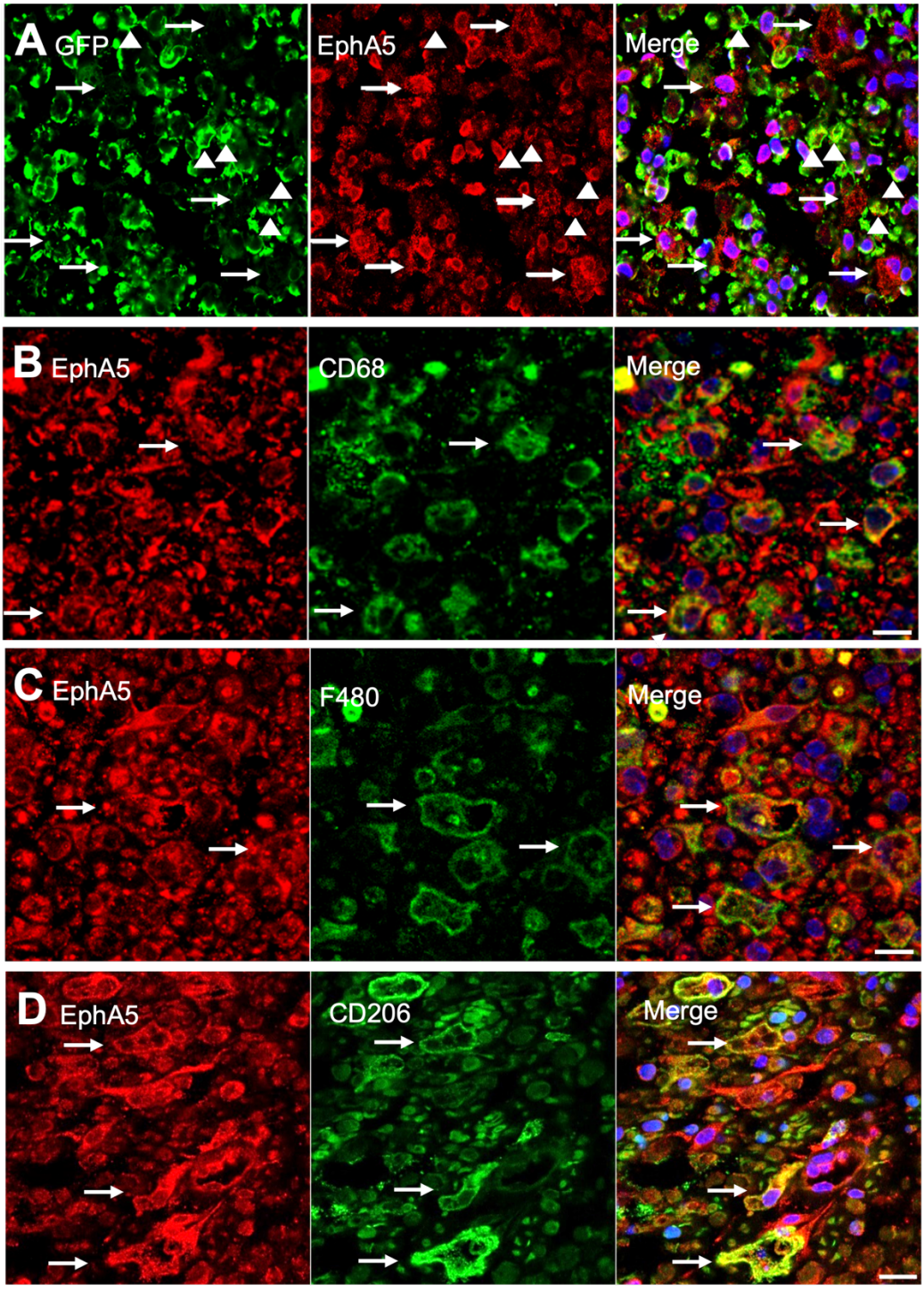

Figure 30 - EphA5 is expressed in Schwann cells and macrophages following peripheral nerve injury.

A. Immunostaining of EphA5 (red) on transverse sections from distal sciatic nerve from PLP-GFP mice at 7DPI. Schwann cells (green) express low levels of EphA5 (indicated by arrowheads). Other types of cells than Schwann cells express high levels of EphA5 (indicated by arrows). B-D Immunostaining on transverse sections from distal sciatic nerve from C57/BL6 mice 7DPI. EphA5 (red) is expressed on some CD68+ (B), F4/80+ (C) and CD206+ (D) macrophages as (green) indicated by the arrows. Ho (blue) staining marks nucleus. Scale bars 20 μm

4.3 EphrinA expression in sciatic nerve

The expression of EphA5 ligands, EphrinA1-5, within the sciatic nerve was next investigated. EphA5 receptor interacts with its EprhinA ligands to induce signalling throughout the cell (Batson et al. 2013; Lisabeth et al. 2013; Miao and Wang 2012; Steinecke et al. 2014). RT-PCR was first used to determine EphrinA1-5 expression in the mouse peripheral nerve in control nerves and nerves 7DPI **(Figure 31A).** Ephrin A1, A2, A4 and A5 were all expressed in control nerves and nerves 7DPI. Ephrin A3 however was not expressed in either conditionand was therefore not investigated further. qRT-PCR was used to determine relative gene expression in mouse distal sciatic nerve up to 28DPI compared to that in control nerves (**Figure 31B**). Expression of Ephrin A1 decreased significantly at 4DPI before remaining at around the expression level observed in control nerves from 7-28DPI. Ephrin A2 and A4 showed the same expression pattern. Ephrin A2 and A4 expression increased significantly at day 4 and continued to increase until day 10 where their expression peaked. Expression decreased from 10-28DPI but still remained significantly increased compared to that in control nerves. Ephrin A5 expression remained around control levels at 4DPI, expression then became significantly increased at 7DPI and peaked at 10DPI before decreasing but remaining elevated compared to expression levels seen in control nerves up until 28DPI.

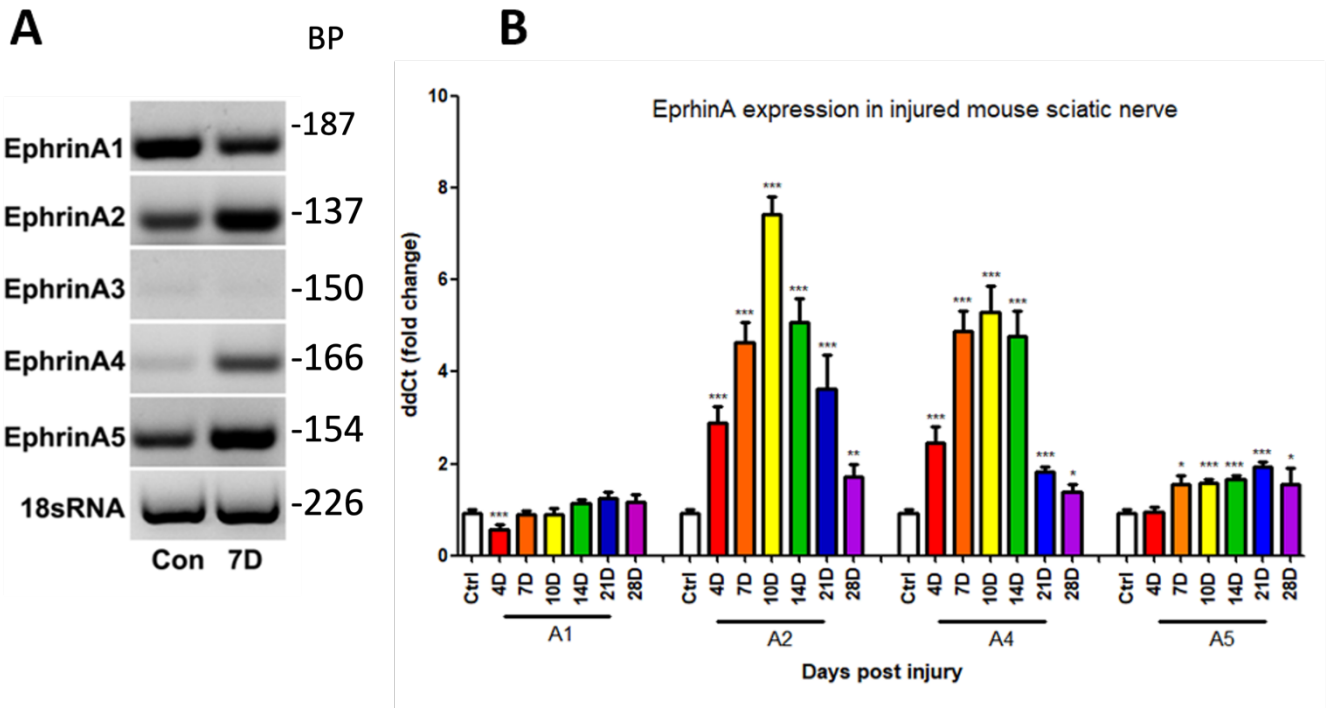

Figure 31 - EphrinA2, A4 and A5 expression is upregulated following peripheral nerve injury

A. RT-PCR showing expression of EphrinA in control and 7DPI mouse sciatic nerve. B. qRT-PCR used to determine the fold change of EphrinA ligand expression in mouse distal sciatic nerves following injury. A1 expression was significantly down regulated at day 4. A2 and A4 expression are upregulated from day 4, expression peaked at day 14 and remains significantly upregulated through to 28DPI. A5 expression was significantly upregulated from day 7 and remained significantly upregulated through to day 28. All samples were normalised to GAPDH and control uninjured samples were made relative to 1. (n=4) Data is presented as mean ± SEM for each group. DPI vs Ctrl One way ANOVA with Tukey post hoc test * P<0.05. ** P<0.01. ***P<0.005.

Next, IHC was used on intact and 7DPI sciatic nerves from PLP-GFP mice (GFP expressing Schwann cells, green) to confirm EphrinA (red) expression and investigate cell specific expression. Ephrin A staining was used to help identify cell type by the morphological structures stained and by colocalization of staining. A1 expression was detected primarily in non-myelinating Schwann cells which can be recognized by the strong GFP signalling and the morphology of Remak bundles. In injured nerves, EphrinA1 expression is seen in all Schwann cells as by 7DPI Schwann cells have differentiated into a repair-competent phenotype Schwann cells **(Figure 32A-B)**. A2 and A4 co-localised with the GFP and appears to be expressed weakly in areas of myelinating Schwann cells in intact nerves.

After injury, A2 and A4 are strongly expressed from all Schwann cells which have dedifferentiated by day 7 **(Figure 32C-F)**. A5 is expressed weakly on resident macrophages in intact nerves. Following injury A5 is primarily expressed from cells with a macrophage like morphology **(Figure 32G-H)**. EphrinA5 expression on macrophages was confirmed by double staining with CD206 where strong co-localisation between EphrinA5 and CD206 was observed **(Figure 33A-B)**. These results therefore show that EphA5 and EphrinA5 are expressed on macrophages, and Ephrin A1, A2, A4 and EphA5 are expressed on Schwann cells.

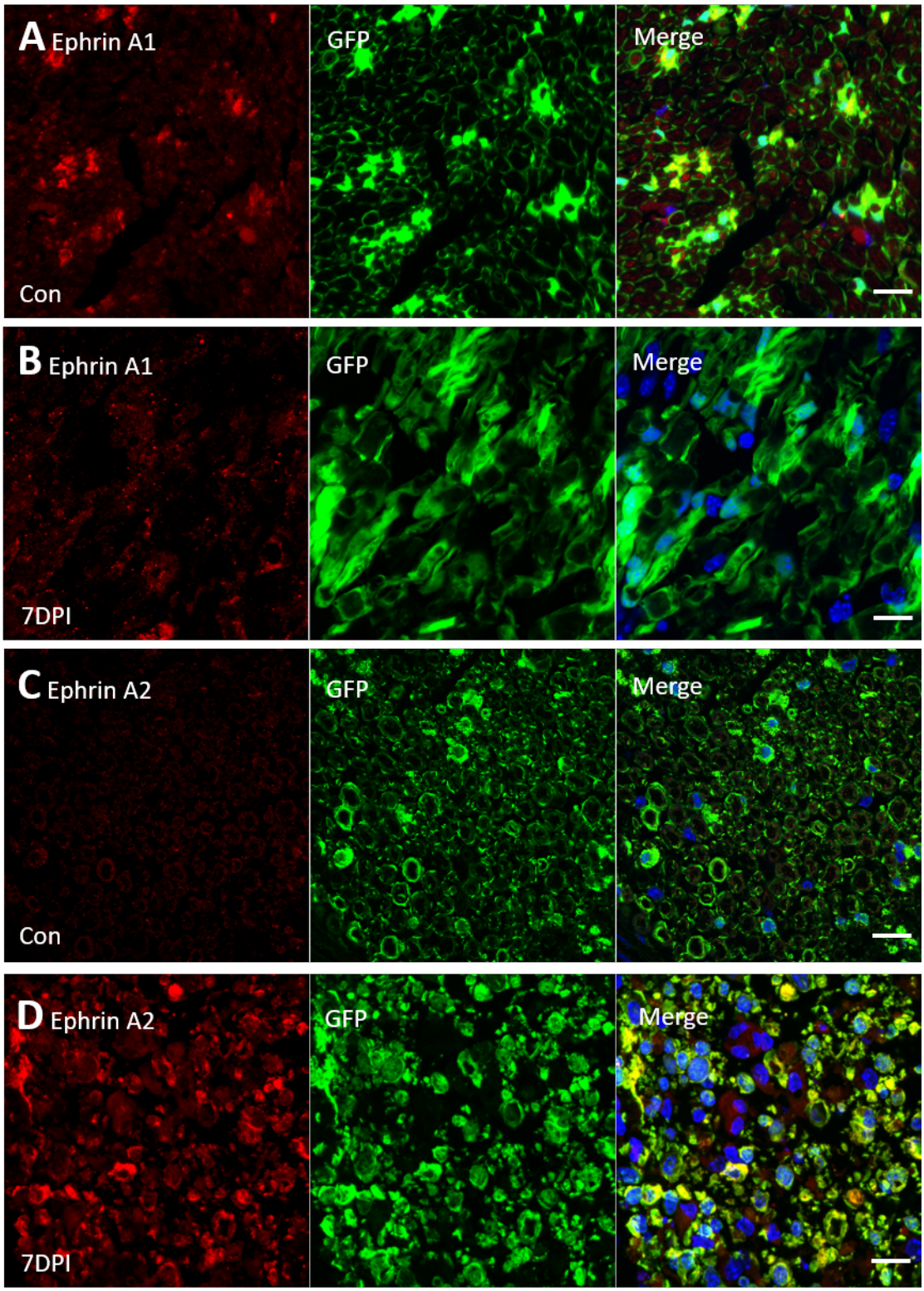
A Ephrin A1
GFP
Merge
Con
B Ephrin A1
GFP
Merge
7DPI
C Ephrin A2
GFP
Merge
Con
D Ephrin A2
GFP
Merge
7DPI

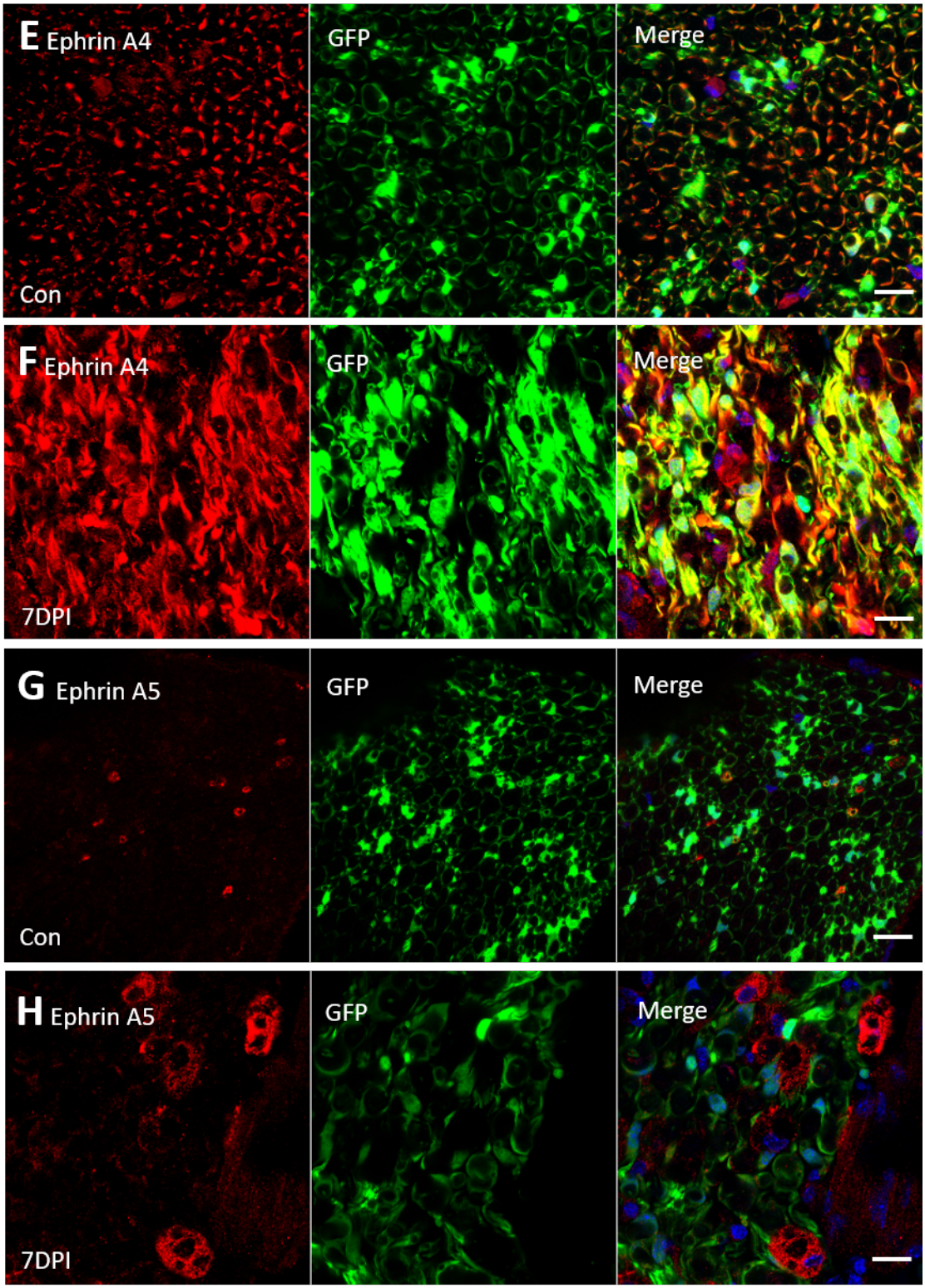

Figure 32 - EphrinA1, A2, A4 and A5 are expressed in intact and injured peripheral nerves

Immunostaining of EphrinA ligands (red) on transverse sections from intact sciatic nerve (A, C, E, G) and 7DPI (B, D, F, H) distal nerves from PLP-GFP mice. Ho (blue) staining marks nucleus. Scale bars 20 µm

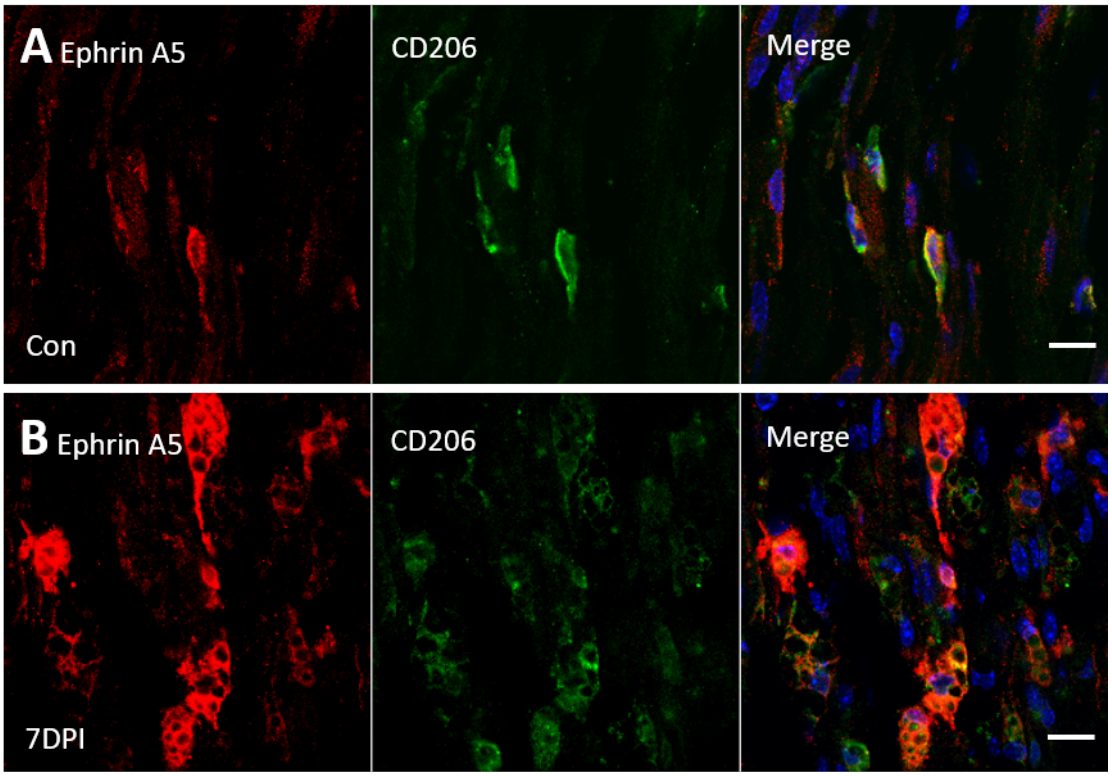

Figure 33 - EprhinA5 is expressed from resident and haematogenous macrophages

Immunostaining of EphrinA5 (red) and CCD206+ (green) macrophages on transverse sections from intact (A) and 7DPI (B) sciatic nerve in C57/BL6. Ho (blue) staining marks nucleus. Scale bars 20 μm

4.4 EphA5 KO peripheral nerve characterisation

For these experiments EphA5 WT and KO mice on C57BL6 background were used and EphA5 expression was confirmed using genotyping and IHC in both control and EphA5 KO animals (Mamiya et al. 2008). EphA5 KO mice have a global KO meaning EphA5 is not expressed in any cells. In WT mice distal transverse sections 7 days post cut sciatic nerve injury, EphA5 (red) expression is strongly colocalised with CD68, F4/80 and CD206 (green) and Schwann cells (**Figure 31A and 34A-C**). In EphA5 KO animals however no EphA5 signal is observed confirming the specificity of antibody we have used as well as EphA5 KO mice (**Figure 34D-F**).

EphA5 KO mice have been described to develop normally, although some KO mice did show increased weight and more aggressive behaviour than their WT counterparts (Mamiya et al. 2008). Intact sciatic nerve architecture in 6 week old EphA5 WT and KO mice was investigated. First transverse sections from WT and KO intact sciatic nerves were stained with NF (green) to mark axons and MBP (red) to mark myelinating Schwann cells. No difference could be observed in nerve structure between WT and KO animals using IHC (**Figure 35A-B**). Semithin sections were stained with methylene blue, and from these sections nerve architecture was examined and myelinated axon number counted (**Figure 35C-D**). From this work, no differences were observed between sciatic nerve structure and number of myelinated axons ($p=0.48$) in EphA5 WT and KO animals (**Figure 35E**).

Myelination status of EphA5 WT and KO sciatic nerves were also investigated in 6 week old animals. TEM images were taken and from this G ratios were calculated. There was no difference in G ratio between WT (0.65 ± 0.045) and KO (0.63 ± 0.07) animals indicating normal peripheral nerve development and myelination in EphA5 KO mouse sciatic nerves (**Figure 36A-C**). Western blot was also undertaken to investigate

levels of MPZ at 6 weeks of age; similarly to EM results, no difference was observed in the expression of myelin protein MPZ between EphA5 WT and KO animals (**Figure 36D**). This data combined shows that there are no visible differences in the peripheral nerves of intact EphA5 WT and KO 6 week old animals.

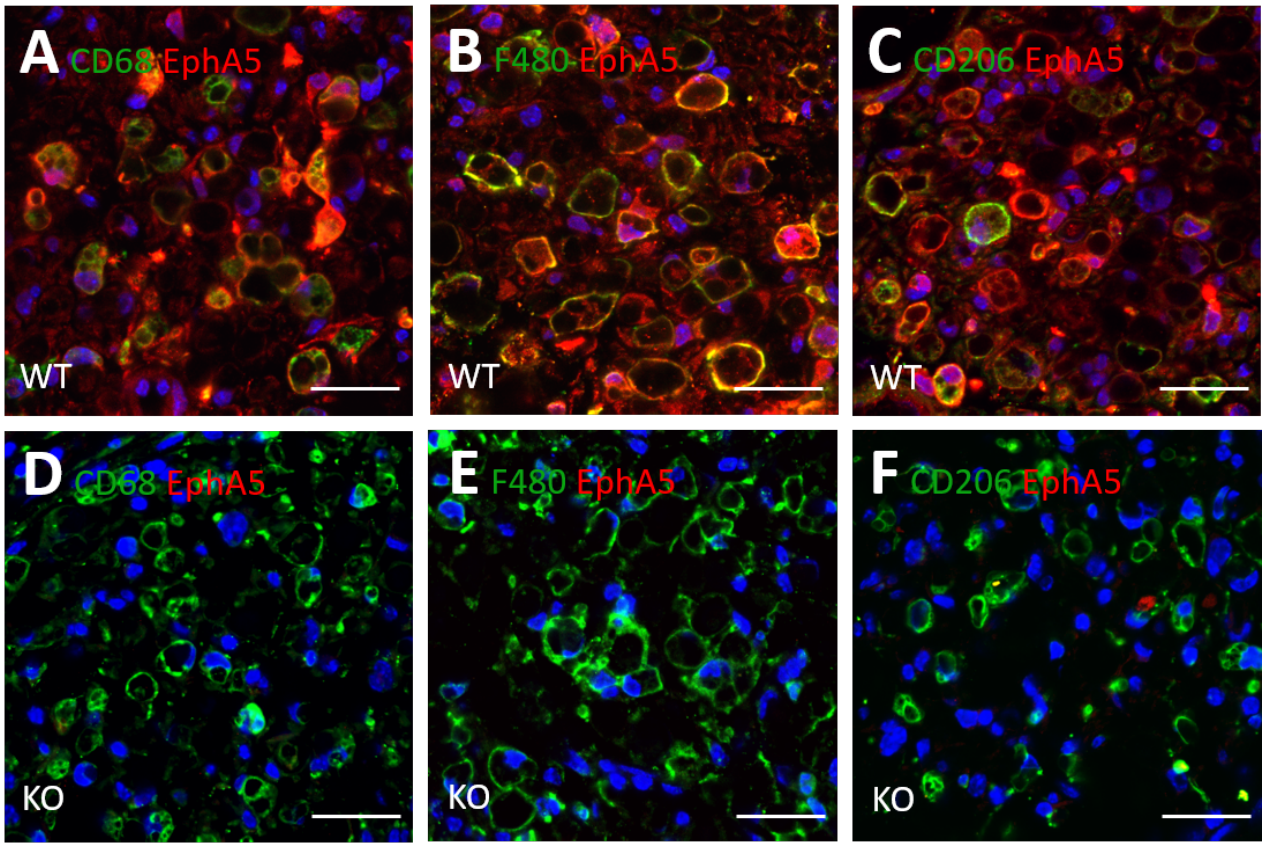

Figure 34 - EphA5 is not expressed in EphA5 KO animals

EphA5 KO was confirmed using immunostaining on transverse sections of 7DPI distal sciatic nerve. EphA5 and macrophage markers CD68 (A, D), F4/80 (B, E) and CD206 (C, F) in WT (A-C) and KO (D-F) mice. Fields were randomly selected throughout the nerve section and exposure was unchanged between both images and slides. Ho (blue) staining marks nucleus. Scale bars 25 µm

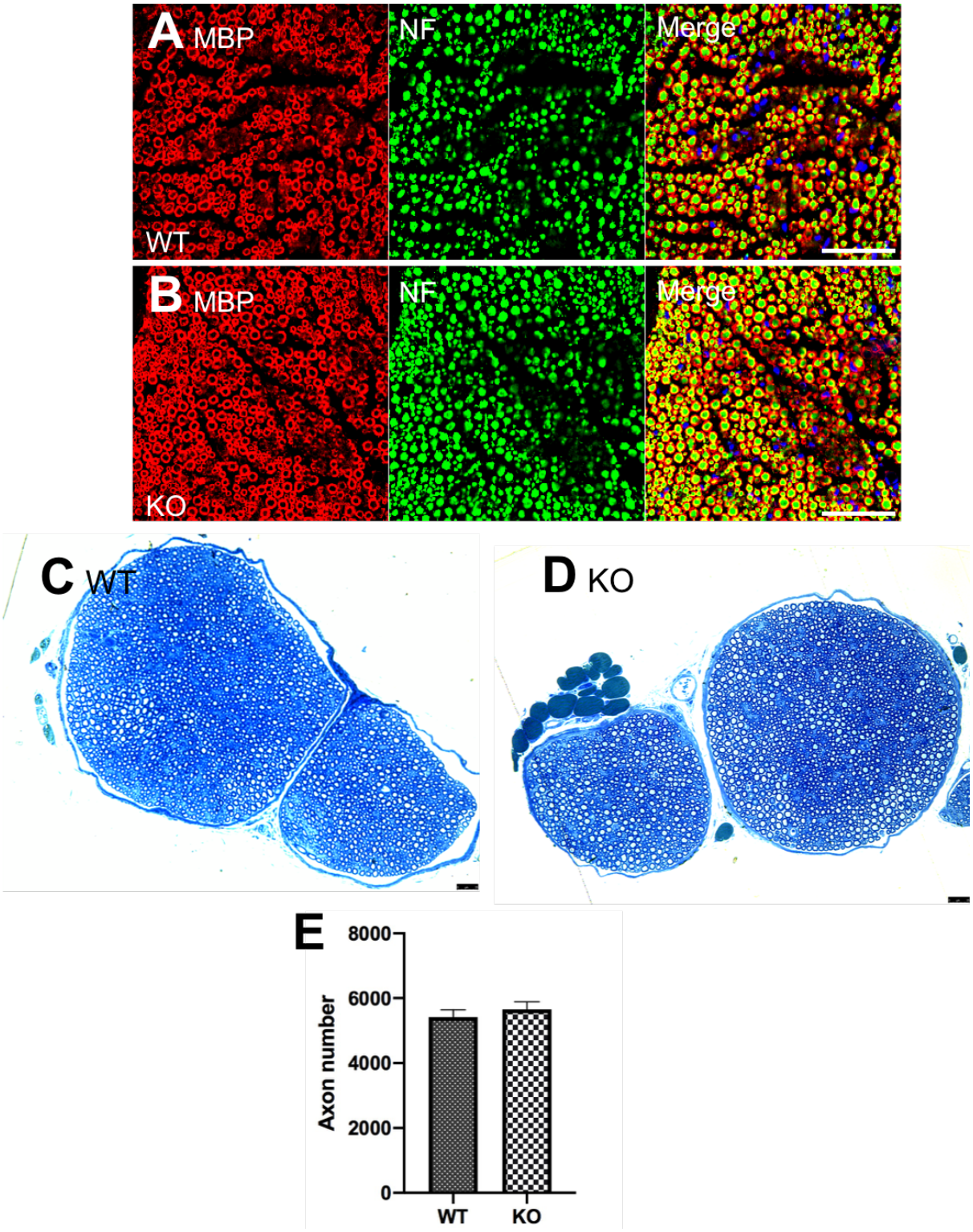

Figure 35 - There is no difference in EphA5 WT and KO intact sciatic nerve structure in 6 week old animals.

A, B. immunostaining transverse section of WT (A) and KO (B) sciatic nerve with MBP (red) and NF (green). Ho (blue) staining marks nucleus. C, D. methylene blue staining of intact sciatic nerve in WT (C) and KO (D) mice. Scale bars 50 μm (A, B) 25 μm (C, D) E. Myelinated axon number quantified using semithin sections from images shown in C and D. n=3. Student's T test compared to EphA5 WT nerves

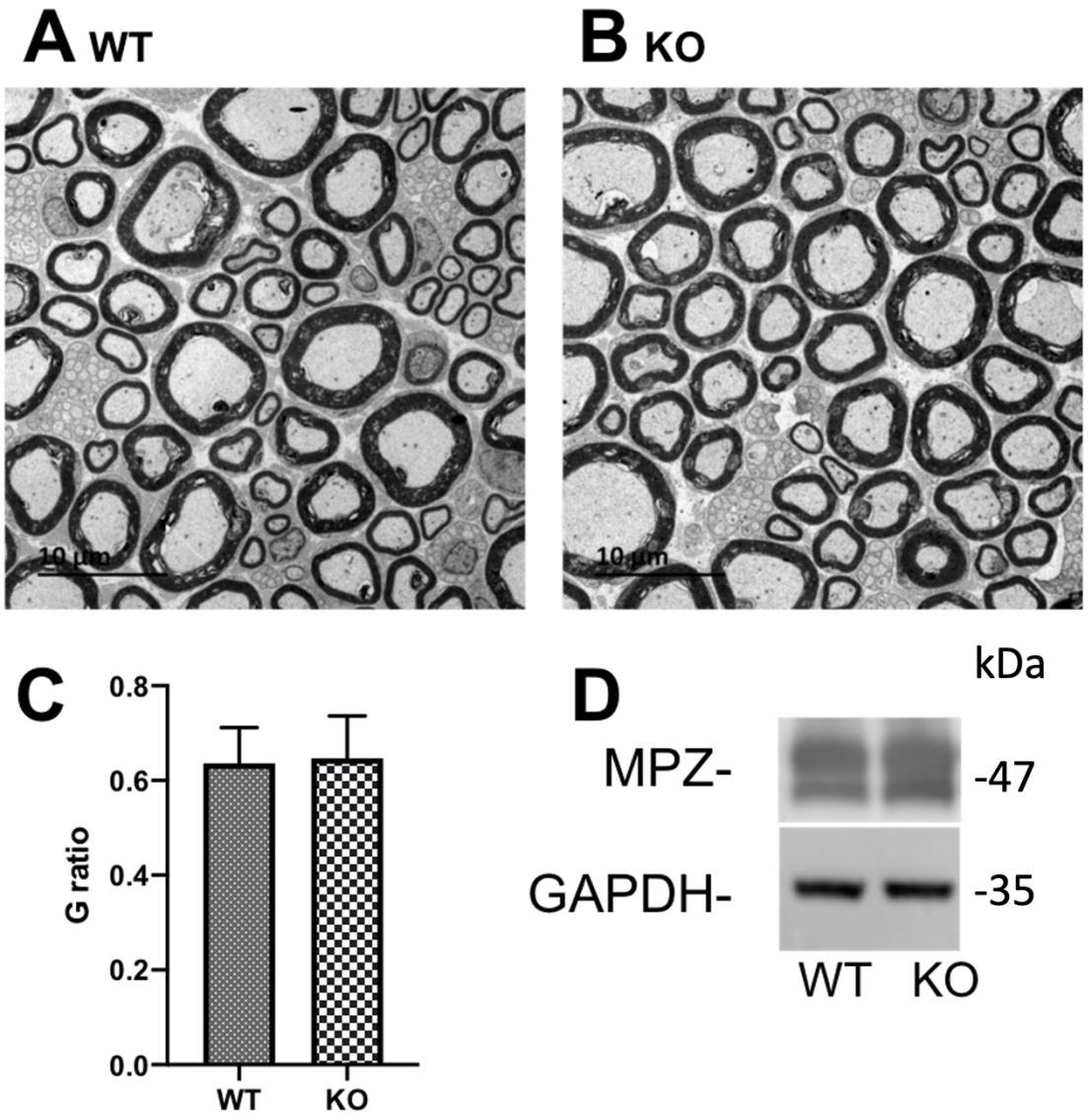

Figure 36 – There is no difference in peripheral nerve myelination of intact 6 week old sciatic nerves between EphA5 WT and EphA5 KO mice.

A, B. Representative TEM images from EphA5 WT and KO 6 week old animals. Scale bar 10μm C. G ratio calculated using TEM images. D. Western blot showing MPZ protein expression in EphA5 WT and KO sciatic nerve. GAPDH was used as a loading control. Student's T test compared to EphA5 WT nerves

4.5 Role of EphA5-Ephrin signalling in macrophage-Schwann cell sorting.

To start to determine if EphA-EphrinA signalling can occur between macrophages and Schwann cells as both receptor and ligand are expressed on these cell types, a macrophage (Raw 264.7)-Schwann cells (primary rat) co-culture experiment was performed. Raw 264.7 cells are a murine derived macrophage cell line (Russell et al. 1980). First, EphA5 and EphrinA expression was confirmed on rat Schwann cells and Raw 264.7 cells. EphA5 and EphrinA 1, 2, 4 and 5 were all expressed on both rat Schwann cells and Raw 264.7 cells (**Figure 37A**). As previously stated, EphA-EphrinA have well described functions in mediating cell migration and so it was hypothesised that EphA5-EphrinA signalling may function to activate contact inhibition of locomotion and repulsive signalling (Astin et al. 2010; Batson et al. 2013). This could be an important signalling mechanism for cell sorting and migration in the injured peripheral nerve.

To start to investigate Schwann cell and macrophage interaction through EphA5-EphrinA signalling pathway, Schwann cells and Raw 264.7 cells were seeded together and some samples were treated with 100nM WDC, an EphA5 inhibitor (Huan et al. 2013). WDC blocks EphA5 signalling by binding to the EphA5 binding site and stops it from interacting with EphrinA ligands expressed on other cells. Co-cultures were fixed at 24h post-plating and stained to visualise Schwann cells (S100, red) and macrophages (CD68, green). Schwann cells and macrophages in control samples group into distinct large clusters containing just one of the two cell types. Schwann cells are not seen to intermingle amongst macrophages but rather are observed to group together and form connecting chains around them (**Figure 37B**). In WDC treated samples however, Schwann cell clusters are smaller and less organised, the cell types are observed to be more mixed together with some Schwann cells growing

on top and within macrophage clusters (**Figure 37C**). Schwann cells in these samples no longer show the typical bipolar morphology and although they form small clusters, Schwann cells are clumped together rather than arranged in a chain like fashion as seen in control samples (Weiner et al. 2001). The Image J counting tool was used to quantify number of Schwann cells in a cluster. In control (untreated) co cultures, 60.92% (±6.92) of Schwann cells were clustered in clusters of more than 9 with the remaining 40% in smaller clusters (1-2 4.95% (±1.55), 3-4: 11.21% (±2.82), 5-6: 13.91 (±2.24), 7-8: 14.00 (±2.40)) . However, in WDC treated co-cultures Schwann cells are clustered in significantly smaller clusters compared to control co-cultures with only 17% (±2.94) of Schwann cells in clusters of more than 9 and the rest in smaller clusters (1-2 22.45% (±1.22), 3-4: 22.72.% (±2.92), 5-6: 23.09 (±1.81), 7-8: 17.15 (±0.49) (**Figure 37D**). The inhibition of EphA5 signalling through the use of WDC peptide treatment in these cell cultures leads to loss of organised cell sorting into distinct populations. In addition to this, Schwann cells' distinct bipolar morphology was also observed to be lost. EphA5 signalling therefore may be an important signalling mechanism for Schwann cell morphology and alignment, macrophage sorting and clearance in the peripheral nerve; however, further experiments needed to be undertaken to prove this idea.

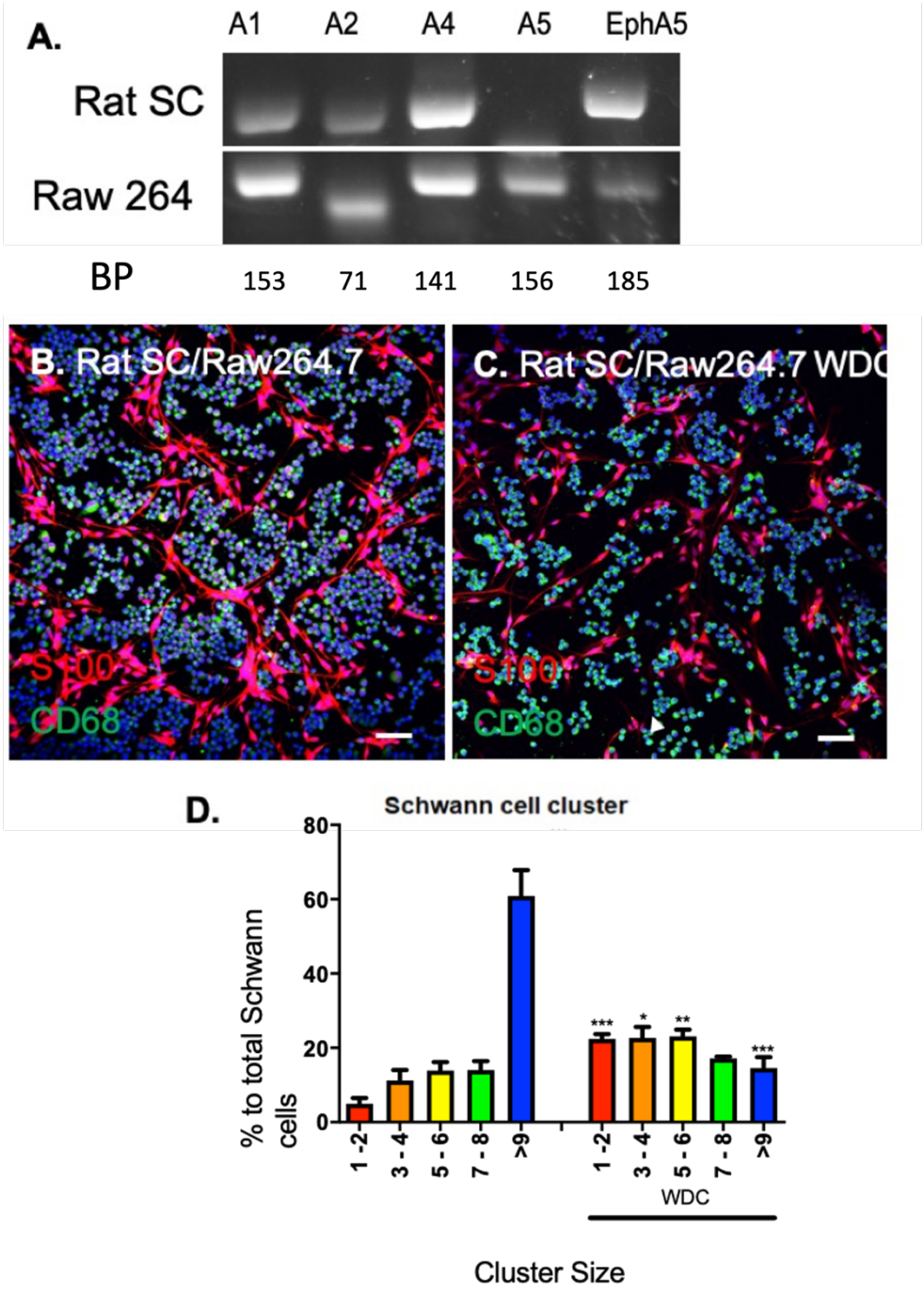

Figure 37 - Inhibition of EphA5 using WDC peptide causes significant disruption to cell sorting in Schwann cell-macrophage co-cultures

A. RT-PCR showing the presence of EphA5 and EphrinA on Schwann cells and Raw 264 cells. B-C. Macrophage and Schwann cells clustering in vitro. Representative images of ICC. Schwann cells and macrophages were seeded together in a co-culture for 24h in control (B) and WDC (C) treated samples prior to fixation and immunostaining Schwann cells (S100, red) and Macrophages (CD68, green). Cell nucleus stained using Hoechst in all samples. Scale bar 50µm D. Schwann cell cluster size was quantified based on number of Schwann cells per cluster in control and WDC treated samples. Random images across the slide were taken. Images were renumbered to blind the counter to avoid bias during analysis (n=3) Data is presented as mean ± SEM for each group. Cluster size compared in control and WDC treated samples. One way ANOVA with Tukey post hoc test * P<0.05. ** P<0.01. ***P<0.005

To further investigate the role of EphA5-EphrinA signalling between Schwann cells and macrophages, primary Schwann cells and macrophages were isolated from WT ($EphA5^{+/+}$) and KO ($EphA5^{-/-}$) mouse models. EphA5 expression was first confirmed using PCR. EphA5 was expressed in $EphA5^{+/+}$ Schwann cells and macrophages but was not expressed on $EphA5^{-/-}$ Schwann cells and macrophages (**Figure 38A**). Primary cells were then cultured together and stained with CD68 (green) and S100 (red) to further investigate the role of EphA5 in cell signalling between Schwann cells and macrophages. Primary Schwann cells and macrophage cultures were obtained from WT and KO mice giving four distinct cell types. $EphA5^{+/+}$ mouse macrophages, $EphA5^{-/-}$ mouse macrophages, $EphA5^{+/+}$ mouse Schwann cells, $EphA5^{-/-}$ mouse Schwann cells. These cells were then co-cultured together in combinations of WT and KO macrophage and Schwann cells to assess the function of EphA5 signalling between cell types.

Co-culturing $EphA5^{+/+}$ Schwann cells and $EphA5^{+/+}$ macrophages together for 24h shows, as previously described in Figure 38B, that Schwann cells and macrophages arrange themselves into distinct clusters (**Figure 38B**). In these co-cultures Schwann cells group together in clusters of varying sizes. 97% of Schwann cells cluster in groups for more than 3 (3-4: 20.03% (±3.63), 5-6: 24.32% (±3.82), 7-8: 21.68% (±2.4)) and 30.73% (±2.14) in clusters of 9 or more (**Figure 38E**). When $EphA5^{+/+}$ Schwann cells and $EphA5^{-/-}$ macrophages were co-cultured together for 24h a very similar pattern is observed (**Figure 38C**). Schwann cells arranged themselves around clusters of macrophages. 97.5% of Schwann cells formed into clusters of more than 3 (3-4: 16.87% (±1.85), 5-6: 21.73% (±3.32), 7-8: 22.61% (±2.88)), and 34.19% (±3.93) formed into clusters more than 9 (**Figure 38E**). In co-cultures of $EphA5^{+/+}$ Schwann

cells, Schwann cells showed a typical Schwann cell shape with bipolar morphology, regardless of whether they were co-cultured with EphA5$^{+/+}$ or EphA5$^{-/-}$ macrophages.

However, when co culturing EphA5$^{-/-}$ Schwann cells with EphA5$^{+/+}$ or EphA5$^{-/-}$ macrophages, Schwann cells clustering activity was not observed (**Figure 38D-E**). Schwann cells were all exclusively formed into groups of cluster sized 1-2 cells (WT 94.50% (±2.62), KO 94.66% (±3.17) or 3-4 (WT 5.50% (±2.62), KO 5.33% (±3.17)) (**Figure 38E**). Schwann cells do not exhibit bipolar processes and normal Schwann cells morphology (Weiner et al. 2001). This indicates that interruption of EphA5 signalling leads to dysregulation in the ability of Schwann cells and macrophages to signal and order themselves into groups of distinct cell types. This may have major consequences in the peripheral nerve during regeneration as Schwann cells and macrophages are the major cell types within the nerve bridge and distal nerve stump of the injured peripheral nerve. Crosstalk within and between these two cell types is required for structural re-organisation following injury. This will be particularly important within the nerve bridge where Schwann cell transverse across the site of injury in organised cords to join proximal and distal nerve stumps and in the distal nerve stump where migratory macrophages may use a EphA5-EphrinA signalling mechanism to enable contact-dependent crosstalk between macrophages and Schwann cells and allow macrophage migration out of the distal stump.

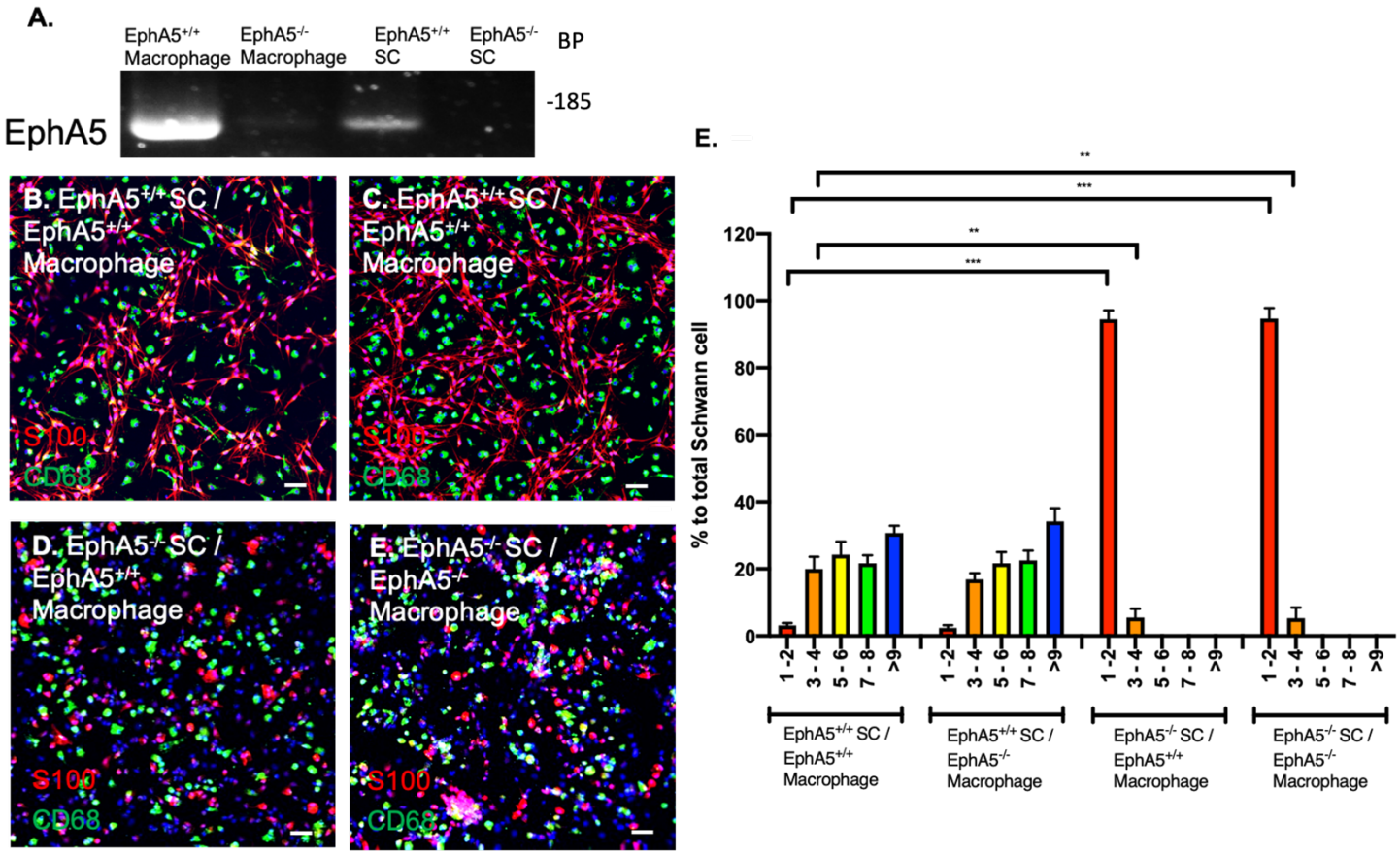

Figure 38 - EphA5 KO on Schwann cells leads to disrupted Schwann cell-macrophage cell sorting in co-cultures

A. RT-PCR showing the presence of EphA5 in WT primary Schwann cells and macrophage cells and lack of expression in KO primary SC and macrophage cells. B-C. Macrophage and Schwann cell clustering in vitro. Representative images of ICC. Schwann cells and macrophages were seeded together in a co-culture for 24h prior to fixation and immunostaining of Schwann cells (S100, red) and macrophages (CD68, green). Cell nucleus stained using Hoechst in all samples. Scale bar 50µm D. Schwann cell cluster size was quantified based on number of Schwann cells per cluster in control and WDC treated samples. Random images across the slide were taken. Images were renumbered to blind the counter to avoid bias (n=3) Data is presented as mean ± SEM for each group. Cluster size compared to equivalent cluster size in EphA5$^{+/+}$ Schwann cells/EphA5$^{+/+}$ macrophage. One way ANOVA with Tukey post hoc test ** P<0.01. ***P<0.005.

4.6 Macrophage numbers in the distal nerve stump of EphA5 WT and KO mice following injury.

I have shown that EphA5 is expressed on macrophages in the distal nerve stump and in vitro experiments have shown that EphA5-Ephrin signalling between Schwann cells and macrophages may control cell sorting and migration (**Figure 30B-D, Figure 37 and Figure 38**). Macrophages expressing EphA5 are present within the peripheral nerve following injury and EphrinA ligand expression is upregulated on Schwann cells up to at least 28DPI. Both Schwann cells and macrophages increase their migratory behaviour following peripheral nerve injury and throughout the regeneration process (Aberle 2019; Bendszus and Stoll 2003; B. Chen et al. 2019). EphA5 and EphrinA contact-dependent signalling can induce repulsive signalling and promote migratory behaviour within cells (Nguyen et al. 2017; Rodger et al. 2001). It was therefore hypothesised that activation of EphA5 on macrophages by interaction with an EphrinA ligand on Schwann cells may lead to repulsive signalling within macrophages and consequently leading to macrophage migration and efflux out of the peripheral nerve. Macrophage numbers in the sciatic nerve of WT and KO mice following peripheral nerve injury was investigated. Mice underwent a cut injury before being euthanized at the appropriate time point, the sciatic nerve was dissected out and longitudinal sections were taken. Macrophage markers IBA1 (red) and CD206 (green) was used to stain macrophages and the number of macrophages in the sciatic nerve following nerve injury per mm^2 was calculated at time points between 7 and 60DPI. IBA1 is highly expressed in M1 and M2 type macrophages and is therefore classed as a pan-macrophage marker, marking all macrophages (Kohler 2007). CD206 is highly expressed on the surface of M2 macrophages and therefore is a good marker of M2

macrophages (Roszer 2015). This study uses both IBA1 and CD206 macrophage markers, to investigate both the total number of macrophages and those in a M2 state. The first time point investigated was 7DPI. Macrophages migrate into injured nerves following injury and their number begin to peak around 7DPI (Bendszus and Stoll 2003; P. W. Chen et al. 2015; Gaudet et al. 2011). Longitudinal sections were stained with IBA1 (red) and CD206 (green) to visualise macrophages. Macrophage numbers were then counted. At 7DPI there was no difference in IBA1+ and CD206+ macrophage numbers in WT and KO distal nerves. Macrophage numbers in WT distal nerve stump were calculated to be 840/mm^2 ($\pm$31.22) and 663/mm^2 ($\pm$19.07) for IBA1+ and CD206+ respectively. Macrophage numbers in KO distal nerve stump were calculated to be 838/mm^2 ($\pm$34.23) and 676/mm^2 ($\pm$31.26) for IBA1+ and CD206+ macrophages respectively (**Figure 39A-J**). This indicates no difference in the number of macrophages recruited into the peripheral nerves of WT and KO mice at 7DPI (IBA1+ p=0.97 CD206+ p=0.72). There were significantly more IBA1+ macrophages than CD206+ macrophages in both WT and KO nerves indicating the likely presence of a small but significant number of M1 macrophages at 7DPI (**Figure 39K-L**).

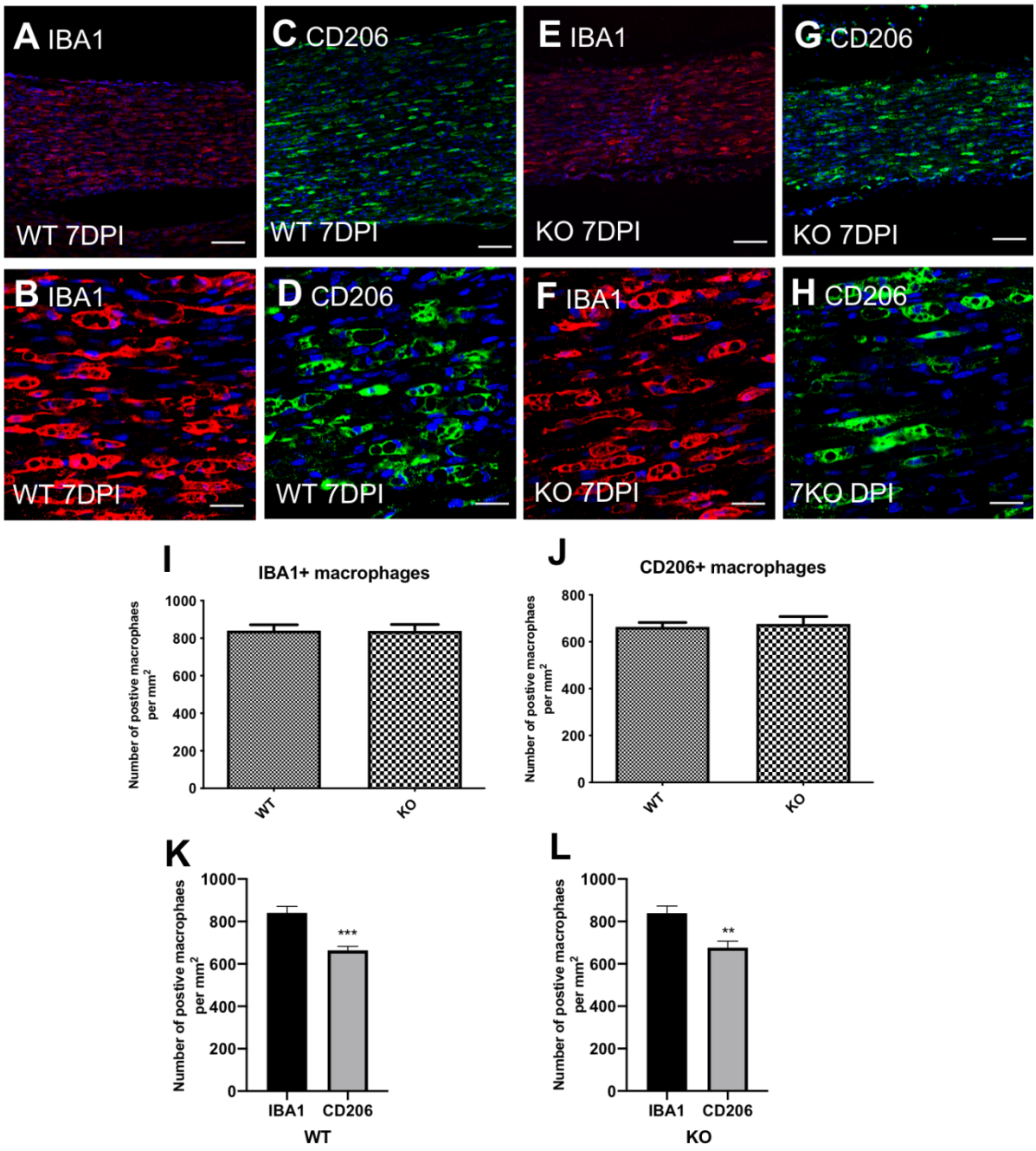

Figure 39 – Following transection injury, is no difference in the number of macrophages in the peripheral nerves between EphA5 WT and KO nerves 7 DPI , although both EphA5 WT and KO nerves showed significantly more IBA1+ macrophages then CD206+ macrophages

Staining longitudinal sections for IBA1+ (A, B, E, F) and CD206+ (C, D, G, H) macrophages in EphA5 WT (A-D) and KO (E-H) mouse distal sciatic nerve 7DPI. Representative images shown at x10 objective (A, C, E, G) and x40 objective (B, D, F, H). Ho (blue) staining marks nucleus. Scale bars A, C, E, G 100μm B, D, F, H 25μm . I-J. quantification of IBA1+ (I) and CD206+ (J) macrophages in WT and KO sciatic nerve sections 7DPI. K-L. Comparison of IBA1+ and CD206+ macrophages in WT and KO sciatic nerve sections. 5mm pieces of distal nerve stump were dissected out for staining. Images were taken from the injury site down though the distal nerve stump and macrophage numbers were counted in all these images (n=3) Data is presented as mean ± SEM for each group. Student's T test ** P<0.01. ***P<0.005 WT vs KO nerves.

The next time point investigated was 14DPI. Numbers of IBA1+ and CD206+ macrophages infiltrating into the distal nerve stump continues to increase. At 14DPI IBA1+ and CD206+ macrophage numbers in WT distal nerve are similar compared to 7DPI, to 883/mm^2 (±22.75) and 733/mm^2 (±19.41) for IBA1+ and CD206+ macrophages respectively. Macrophage numbers in KO distal nerve stump peak at 1042/mm^2 (±32.86) and 812/mm^2 (±24.83) for IBA1+ and CD206+ respectively (**Figure 40A-J**). At 14DPI there was a small but significant increase in the number of IBA1+ macrophages in the distal nerve stump in EphA5 KO mice compared to control ($p=0.0076$). A significant difference between EphA5 WT and KO was not however seen when staining for CD206+ macrophages ($p=0.059$). There are significantly more IBA1+ macrophages compared to CD206+ macrophages in both EphA5 WT and KO indicating that as expected a number of the macrophages are still in a M1 pro inflammatory state (**Figure 40K-L**).

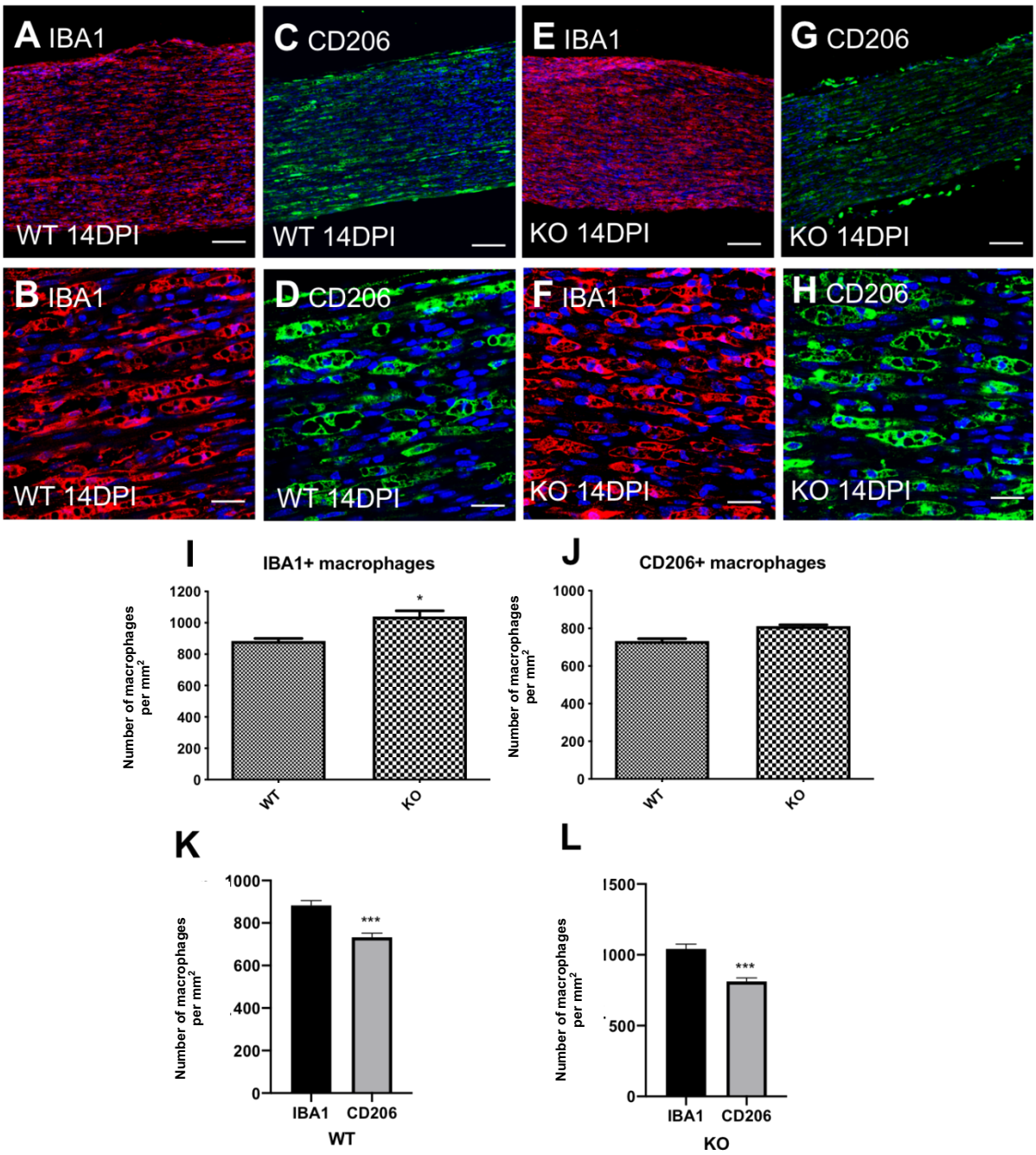

Figure 40 – Following transection injury, there is significantly more IBA1+ macrophages in EphA5 KO distal nerve stump compared to EphA5 WT at 14DPI

Staining longitudinal sections for IBA1+ (A, B, E, F) and CD206+ (C, D, G, H) macrophages in EphA5 WT (A-D) and KO (E-H) mouse distal sciatic nerve 14DPI. Representative images shown at x10 objective (A, C, E, G) and x40 objective (B, D, F, H). Ho (blue) staining marks nucleus. Scale bars A, C, E, G 100µm B, D, F, H 25µm . I-J. Quantification of IBA1+ (I) and CD206+ (J) macrophages in WT and KO sciatic nerve sections 14DPI. K-L. Comparison of IBA1+ and CD206+ macrophages in WT and KO sciatic nerve sections. 5mm pieces of distal nerve stump were dissected out for staining. Images were taken from the injury site down though the distal nerve stump and macrophage numbers were counted in all these images (n=3) Data is presented as mean ± SEM for each group. Student's T test * P<0.05. ***P<0.005 WT vs KO nerves.

At 21DPI the number of macrophages within the distal peripheral nerves begins to decrease as macrophages will have finished carrying out their phagocytic role and start to efflux out of the peripheral nerve (Hirata and Kawabuchi 2002; F. C. Zhang et al. 2020). This decrease in macrophage numbers is much bigger in EphA5 WT nerves compared to EphA5 KO. In normal nerves, by 21 day post crush injury macrophages efflux from the peripheral nerves and regenerated axons can start to become remyelinated by Schwann cells (Gomez-Sanchez et al. 2017; Grove et al. 2020; Mogha et al. 2016). At 21DPI IBA1+ and CD206+ macrophage numbers in WT distal nerve decreased in number, to 512/mm^2 ($\pm$22.22) and 458/mm^2 ($\pm$27.85) for IBA1+ and CD206+ macrophages respectively. Macrophage numbers in KO distal nerve stump decreased to 895/mm^2 ($\pm$30.98) and 720/mm^2 ($\pm$32.91) for IBA1+ and CD206+ respectively (**Figure 41A-J**). This meant that there were significantly more macrophages in the distal nerve stump of KO mice compared to WT. The number of macrophages remaining in EphA5 KO distal nerves may indicate that macrophages are less able to migrate out of the distal nerves post injury and may essentially be stuck within injured peripheral nerves. The numbers of IBA1+ and CD206+ cells per mm^2 in EphA5 WT nerves were similar, with no significant difference observed indicating that most macrophages in the peripheral nerves of EphA5 WT animals are in an M2 anti-inflammatory state ($p=0.066$). This is in line with previous data whereby macrophages in a crushed peripheral nerve at 21DPI were in a M2 regenerative state, which mediates tissue regeneration and restoration of tissue homeostasis (P. W. Chen et al. 2015; F. C. Zhang et al. 2020). However, EphA5 KO nerves showed a significant difference between the number of IBA1+ and CD206+ macrophages, indicating that not only are there more macrophages in KO nerves, a significant subset of these macrophages were still in a M1 inflammatory state which can impair regeneration as

it favours a pro-inflammatory phagocytic environment (p=0.0008) (Sindrilaru et al. 2011)(**Figure 41K-L**).

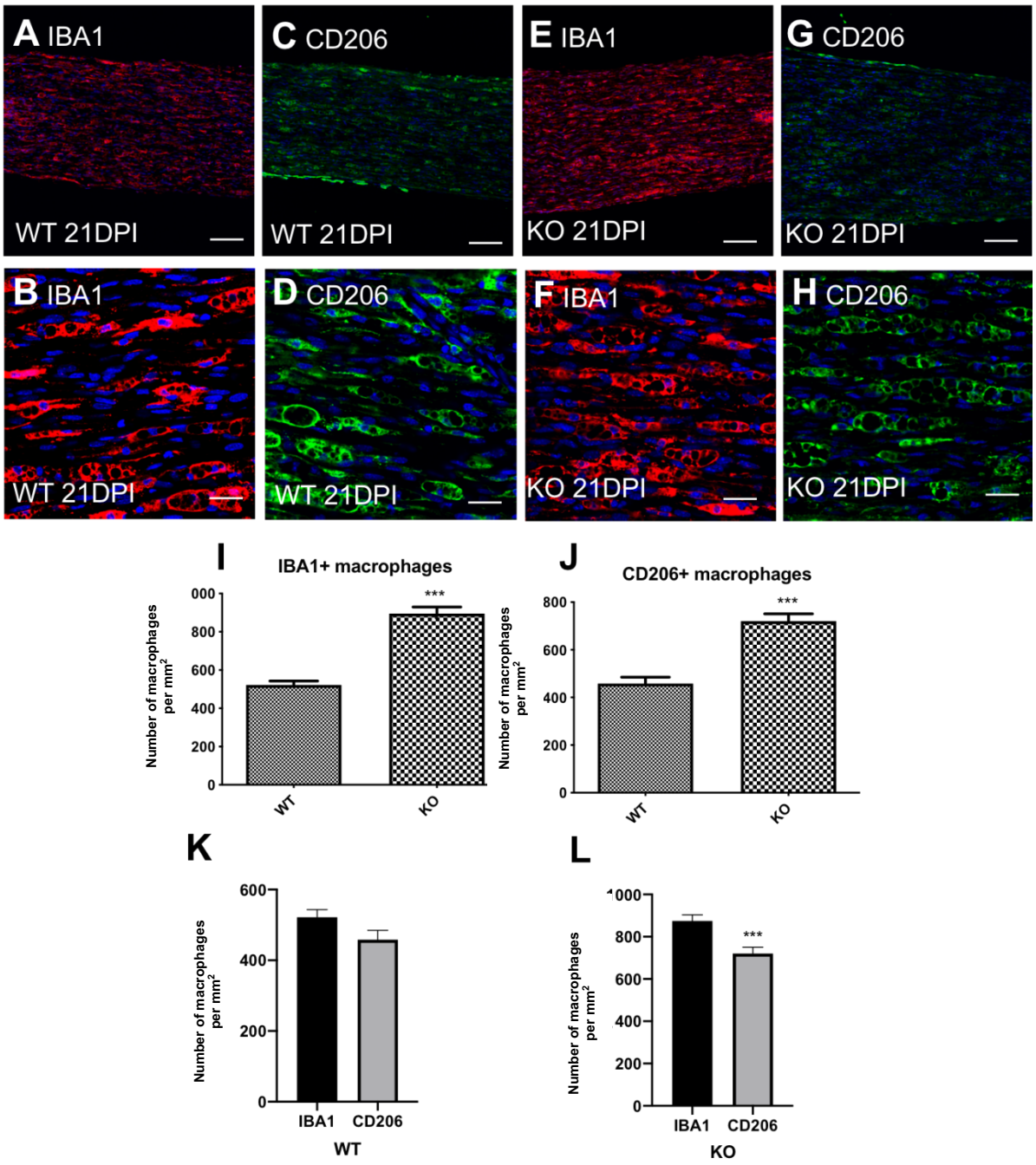

Figure 41 – Following transection injury, there are around double the number of macrophages in the distal nerve stump of EphA5 KO nerves compared to EphA5 WT nerves 21DPI

Staining longitudinal sections for IBA1+ (A, B, E, F) and CD206+ (C, D, G, H) macrophages in EphA5 WT (A-D) and KO (E-H) mouse distal sciatic nerve 21DPI. Representative images shown at x10 objective (A, C, E, G) and x40 objective (B, D, F, H). Ho (blue) staining marks nucleus. Scale bars A, C, E, G 100µm B, D, F, H 25µm . I, J. quantification of IBA1+ (I) and CD206+ (J) macrophages in WT and KO sciatic nerve sections 21DPI. K-L. Comparison of IBA1+ and CD206+ macrophages in WT and KO sciatic nerve sections. 5mm pieces of distal nerve stump were dissected out for staining. Images were taken from the injury site down though the distal nerve stump and macrophage numbers were counted in all these images (n=3) Data is presented as mean ± SEM for each group. Student's T test ***P<0.005 WT vs KO nerves.

At 28DPI in the distal nerve stump the largest difference in macrophage numbers between EphA5 WT and KO animals was observed. Macrophage numbers continued to decrease in WT animals. At 28DPI IBA1+ and CD206+ macrophage numbers in WT distal nerves decreased in number to 426/mm^2 (±26.82) and 404/mm^2 (±40.88) for IBA1+ and CD206+ macrophages respectively, showing a steady decrease from 21DPI, indicating that continued macrophage efflux from the peripheral nerve was occurring. Macrophage numbers in KO distal nerve stump decreased to 840/mm^2 (±41.72) and 547/mm^2 (±31.20) for IBA1+ and CD206+ respectively (**Figure 42A-J**). There is no significant difference between numbers of IBA1+ and CD206+ macrophages within the peripheral nerves of EphA5 WT, again indicating as expected and synonymous to what is seen in peripheral nerves of WT mice at 21DPI that macrophages are in a M2 regenerative state (p=0.69). In distal EphA5 KO nerves the number of CD206+ and IBA1+ macrophages also continued to decrease but numbers remained significantly increased compared to macrophages numbers in EphA5 WT distal nerves at the same time point (IBA1+ p=<0.0001, CD206+ p=0.0125). Not only were there significantly more IBA1+ and CD206+ macrophages within the peripheral nerves of EphA5 KO, but there were also significantly more IBA1+ macrophages compared to CD206+ macrophages, again suggesting that the distal nerve of EphA5 KO mice may be remaining in M1 pro inflammatory state (p=<0.0001) (**Figure 42K-L**). The small decrease in macrophage number in the distal nerves of EphA5 KO mice between 21DPI to 28DPI and the significant increase in macrophage number in nerve of EphA5 KO mice compared to WT further indicates that macrophages within the peripheral nerve may not be able to migrate out of the distal nerve back through the blood nerve barrier.

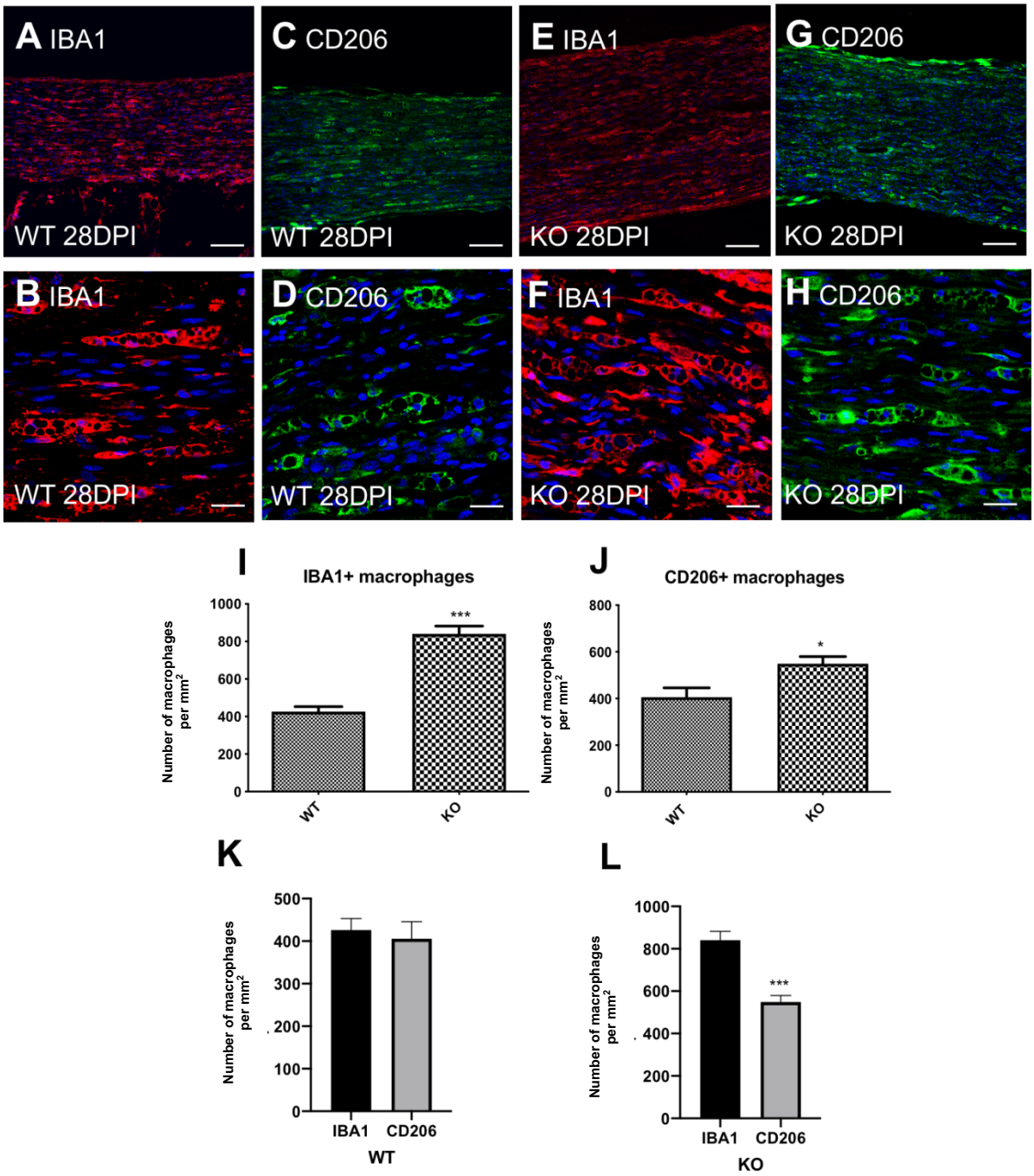

Figure 42 – Following transection injury, the number of macrophages in the distal nerve stump of EphA5 KO nerves is still significantly increased compared to EphA5 WT nerves at 28DPI.

Staining longitudinal sections for IBA1+ (A, B, E, F) and CD206+ (C, D, G, H) macrophages in EphA5 WT (A-D) and KO (E-H) mouse distal sciatic nerve 28DPI. Representative images shown at x10 objective (A, C, E, G) and x40 objective (B, D, F, H). Ho (blue) staining marks nucleus. Scale bars A, C, E, G 100µm B, D, F, H 25µm . I, J. quantification of IBA1+ (I) and CD206+ (J) macrophages in WT and KO sciatic nerve sections 28DPI. K-L. Comparison of IBA1+ and CD206+ macrophages in WT and KO sciatic nerve sections. 5mm pieces of distal nerve stump were dissected out for staining. Images were taken from the injury site down though the distal nerve stump and macrophage numbers were counted in all these images (n=3) Data is presented as mean ± SEM for each group. Student's T test * $P<0.05$. ***$P<0.005$ WT vs KO nerves.

At 35DPI macrophage numbers in the distal nerve stump of EphA5 WT and KO animals continue to decrease. At 35DPI IBA1+ and CD206+ macrophage numbers in WT distal nerve decreased in number to 252/mm^2 ($\pm$13.87) and 238/mm^2 ($\pm$15.62) for IBA1+ and CD206+ macrophages respectively, showing a continuous steady decrease from 28DPI. Macrophage numbers in KO distal nerve stump at 35DPI also showed a decrease in number compared to 28DPI. Macrophage number in distal EphA5 nerve reduced to 410/mm^2 ($\pm$16.46) and 376/mm^2 ($\pm$17.57) for IBA1+ and CD206+ respectively (**Figure 43A-J**). However, numbers of IBA1+ and CD206+ macrophages within the distal nerve of KO animals still remained significantly increased compared to WT (IBA1+ p=<0.0001, CD206+ p=<0.0001). Further suggesting that macrophages in the distal nerves of EphA5 KO mice were unable to efficiently efflux out of the nerve. At this timepoint, however, there was no significant difference between IBA1+ and CD206+ macrophage numbers counted in EphA5 KO nerves, suggesting that these macrophages in the peripheral nerves of KO animals may have undergone the stage transition to an a predominantly M2 phenotype (p=0.16) (**Figure 43K-L**).

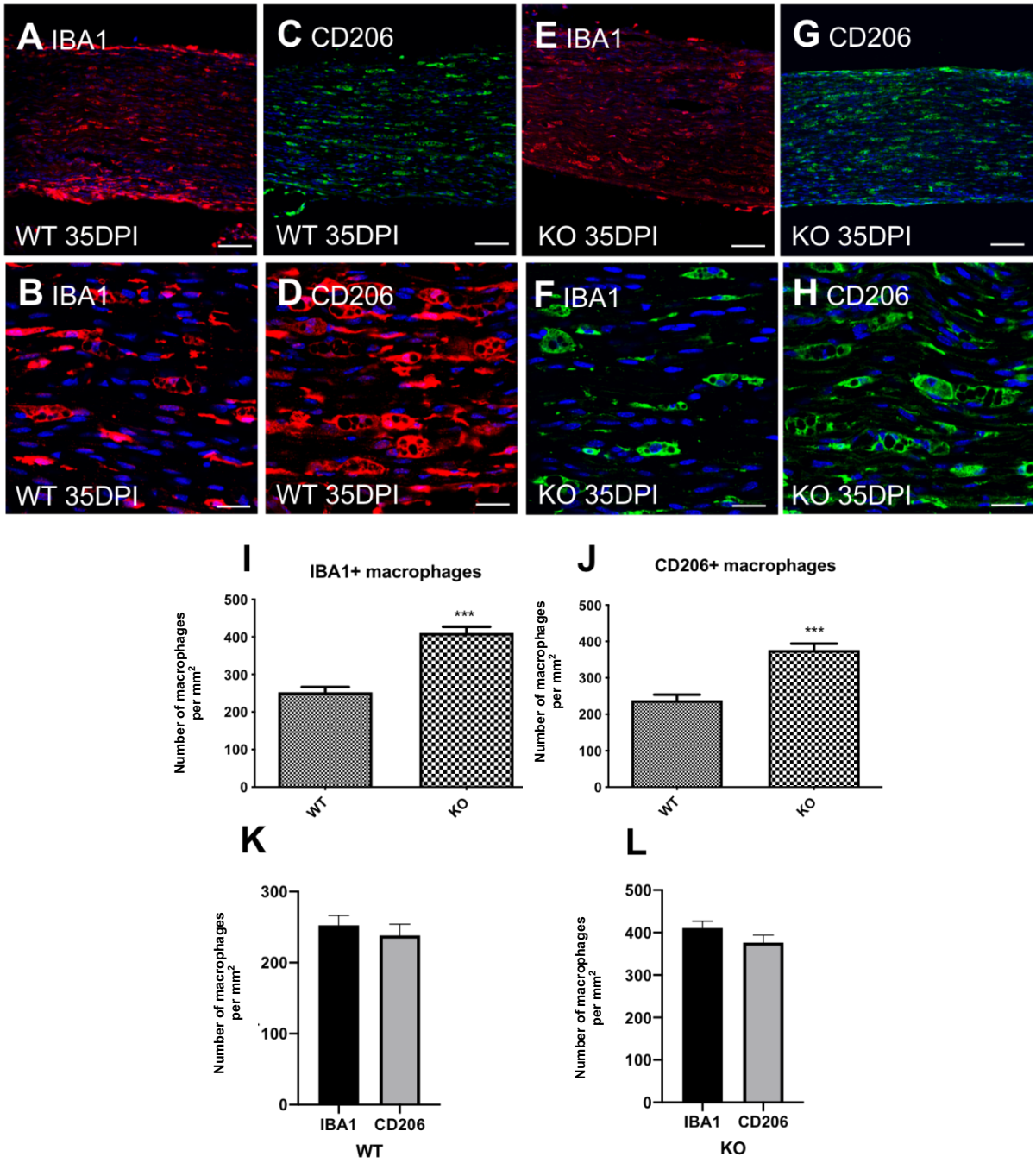

Figure 43 - Following transection injury, the number of macrophages in the distal nerve stump of EphA5 KO nerves is still significantly increased compared to EphA5 WT nerves at 35DPI.

Staining longitudinal sections for IBA1+ (A, B, E, F) and CD206+ (C, D, G, H) macrophages in EphA5 WT (A-D) and KO (E-H) mouse distal sciatic nerve 35DPI. Representative images shown at x10 objective (A, C, E, G) and x40 objective (B, D, F, H). Ho (blue) staining marks nucleus. Scale bars A, C, E, G 100µm B, D, F, H 25µm . I, J. quantification of IBA1+ (I) and CD206+ (J) macrophages in WT and KO sciatic nerve sections 35DPI. K-L. Comparison of IBA1+ and CD206+ macrophages in WT and KO sciatic nerve sections. 5mm pieces of distal nerve stump were dissected out for staining. Images were taken from the injury site down though the distal nerve stump and macrophage numbers were counted in all these images (n=3) Data is presented as mean ± SEM for each group. Student's T test ** P<0.01. ***P<0.005 WT vs KO nerves.

At 60DPI macrophage numbers in the distal nerve stump of EphA5 WT and KO animals continued to decrease. At 60DPI IBA1+ and CD206+ macrophage numbers in WT distal nerve decreased in number to 166/mm^2 (±19,62) and 149/mm^2 (±21.21) for IBA1+ and CD206+ macrophages respectively. Most macrophages leave the distal nerve following regeneration and remyelination, although some macrophages stay within the distal nerve stump post-injury. Macrophage numbers in KO distal nerve stump also show a decrease from 35DPI to 298/mm^2 (±39.90) and 260/mm^2 (±44.50) for IBA1+ and CD206+ respectively (**Figure 44A-J**). Numbers of both IBA1+ and CD206+ macrophages within the distal nerve of KO animals were significantly increased compared to WT (IBA1+ p=0.0057, CD206+ p=0.026). There was however no significant difference seen between the numbers IBA1+ and CD206+ macrophages in both EphA5 WT and KO animals, suggesting that most macrophages in the distal nerves of both EphA5 WT and KO animals are in an M2 state (WT p=0.57, KO p=0.53) (**Figure 44K-L**). Macrophage numbers in WT distal nerves were vastly decreased compared to numbers at 7DPI indicating that the well described process of pro-inflammatory events followed by axon regeneration, resolution of the inflammatory response and macrophage efflux leading was tissue homeostasis had taken place. Significantly more macrophages were still present within the distal nerves of KO animals. Large numbers of macrophages can lead to chronic inflammation if inappropriately present within a tissue (Sindrilaru et al. 2011). Increased numbers of macrophages still present within the nerves of KO animals suggests that EphA5 KO may reduce macrophages migratory capacity out of peripheral nerves following injury and may also lead to delayed resolution of the inflammatory response and incomplete tissue homeostasis. Macrophages remaining within peripheral nerves following injury and peripheral nerve repair can lead to neuropathic pain and further tissue damage,

particularly if these macrophages were to transition back into an M1 state (Kiguchi et al. 2010).

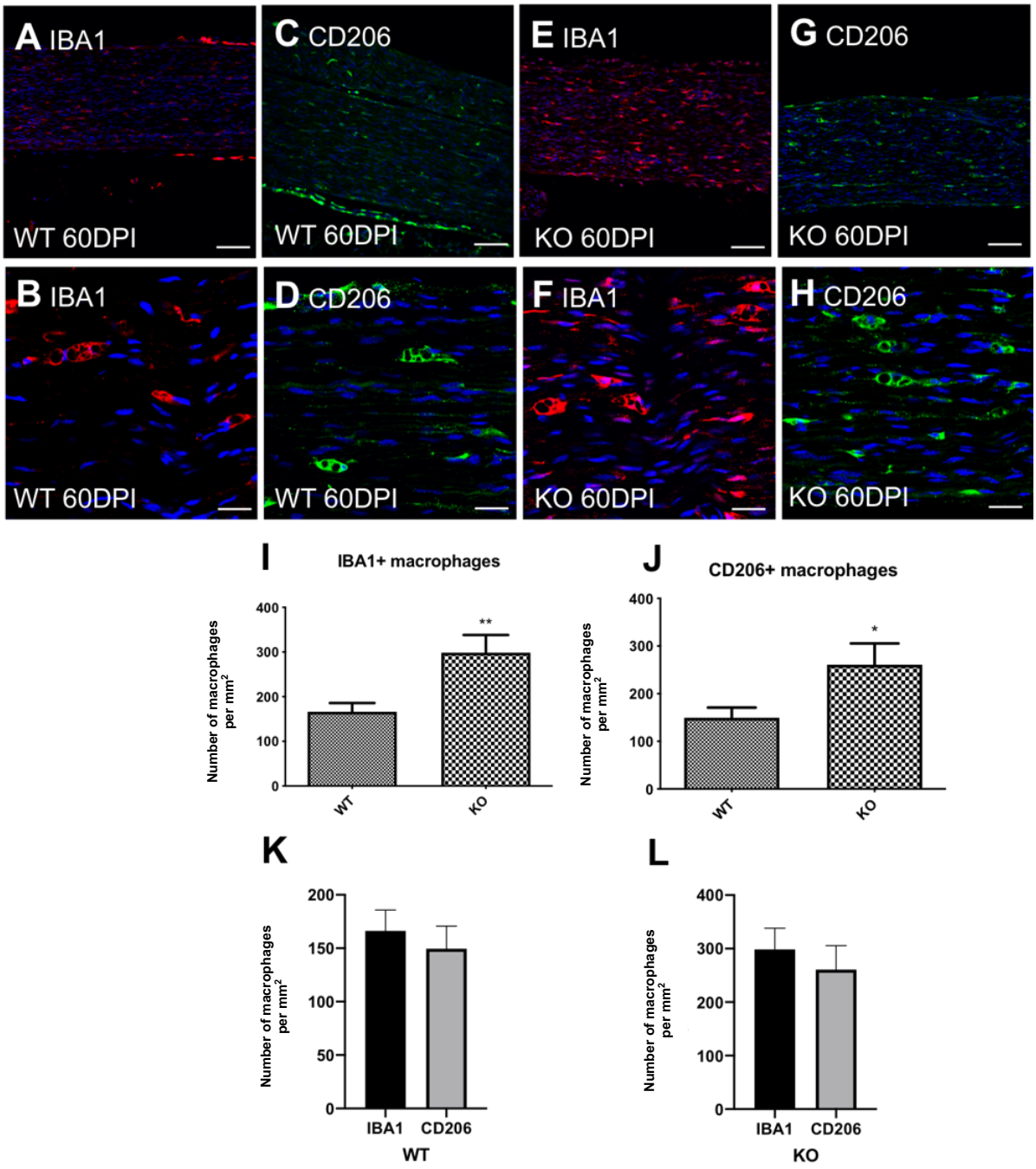

Figure 44 - Following transection injury, the number of macrophages in the distal nerve stump of EphA5 KO nerves is still significantly increased compared to EphA5 WT nerves at 60DPI.

Staining longitudinal sections for IBA1+ (A, B, E, F) and CD206+ (C, D, G, H) macrophages in EphA5 WT (A-D) and KO (E-H) mouse distal sciatic nerve 60DPI. Representative images shown at x10 objective (A, C, E, G) and x40 objective (B, D, F, H). Ho (blue) staining marks nucleus. Scale bars A, C, E, G 100µm B, D, F, H 25µm I, J. quantification of IBA1+ (I) and CD206+ (J) macrophages in WT and KO sciatic nerve sections 60DPI. K-L. Comparison of IBA1+ and CD206+ macrophages in WT and KO sciatic nerve sections. 5mm pieces of distal nerve stump were dissected out for staining. Images were taken from the injury site down though the distal nerve stump and macrophage numbers were counted in all these images (n=3) Data is presented as mean ± SEM for each group. Student's T test * $P<0.05$. ** $P<0.01$ WT vs KO nerves.

The final time point investigated was 90DPI. Macrophage numbers in the distal nerve stump of EphA5 WT and KO animals continued to decrease, with almost all macrophages having left the peripheral nerves. At 90DPI IBA1+ and CD206+ macrophage numbers in WT distal nerve decreased in number to 30/mm^2 ($\pm$13.40) and 26/mm^2 ($\pm$13.40) for IBA1+ and CD206+ macrophages respectively. Macrophage numbers in KO distal nerve stump also show a decrease to 19/mm^2 ($\pm$7.42) and 19/mm^2 ($\pm$7.42) for IBA1+ and CD206+ respectively. There was no difference in macrophage numbers between EphA5 WT and KO mice (IBA1+ p=0.43, CD206+ p=0.28) (**Figure 45A-L**). Most macrophages leave the distal nerve following regeneration and remyelination although some undergo apoptosis (Kuhlmann et al. 2001). Macrophage numbers in WT and KO distal nerves are vastly decreased compared to numbers at the peak of recruitment following initial injury, this further indicates that an inflammatory response has occurred, followed by inflammatory response resolution and tissue homeostasis, albeit significantly delayed in EphA5 KO mice.

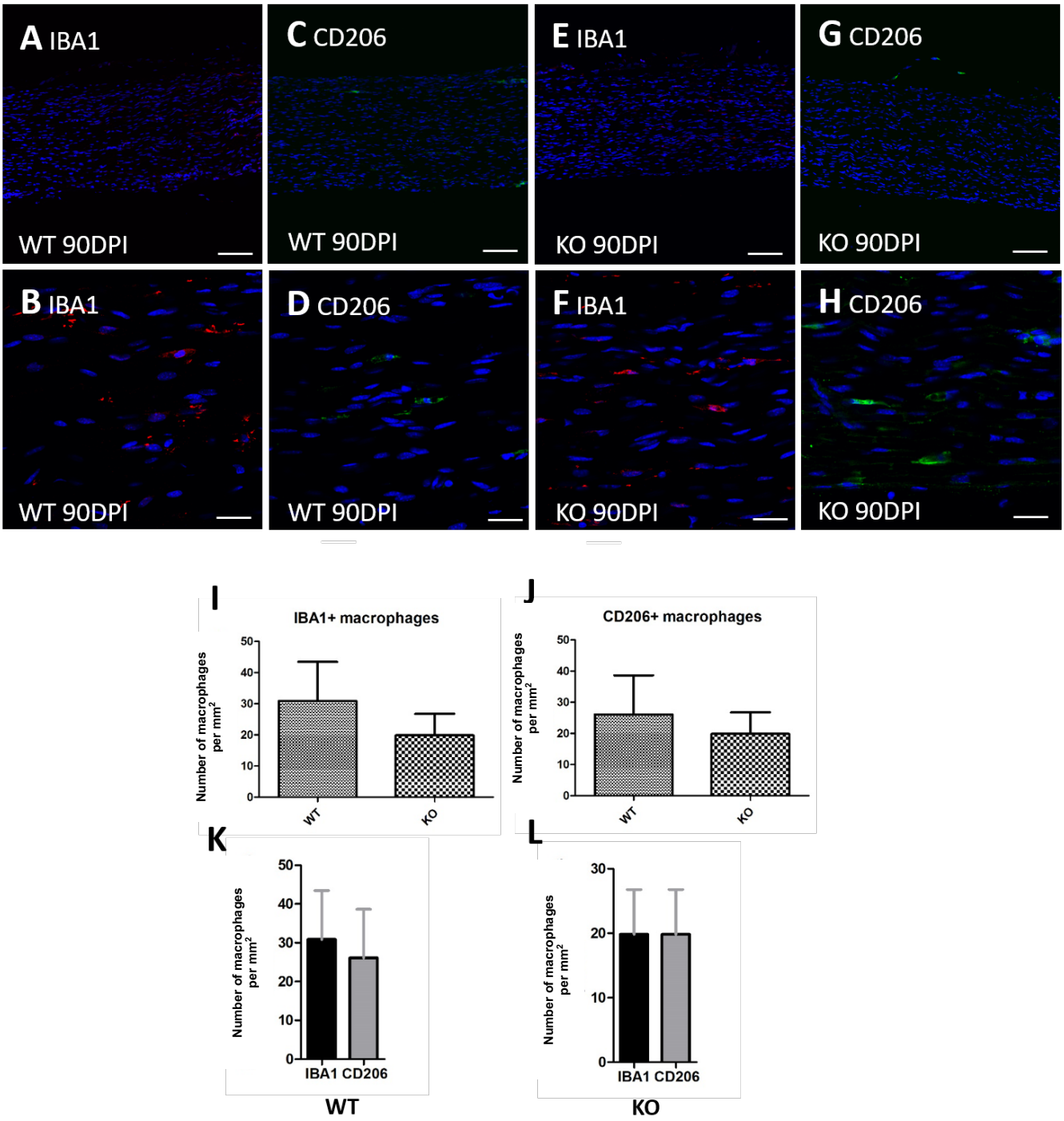

Figure 45 – Following transection injury at 90DPI there is no significant difference in the number of macrophages in the distal nerve stump between WT and EphA5 KO nerves.

Staining longitudinal sections for IBA1+ (A, B, E, F) and CD206+ (C, D, G, H) macrophages in EphA5 WT (A-D) and KO (E-H) mouse distal sciatic nerve 60DPI. Representative images shown at x10 objective (A, C, E, G) and x40 objective (B, D, F, H). Ho (blue) staining marks nucleus. Scale bars A, C, E, G 100µm B, D, F, H 25µm I, J. quantification of IBA1+ (I) and CD206+ (J) macrophages in WT and KO sciatic nerve sections 90DPI. K-L. Comparison of IBA1+ and CD206+ macrophages in WT and KO sciatic nerve sections. 5mm pieces of distal nerve stump were dissected out for staining. Images were taken from the injury site down though the distal nerve stump and macrophage numbers were counted in all these images (n=3) Data is presented as mean ± SEM for each group. Student's T test WT vs KO nerves.

4.7 Inflammatory cytokine expression in the distal nerve stump of EphA5 WT and KO mice

Macrophages enter the peripheral nerves after injury and during neuropathic diseases in response to expression of pro-inflammatory cytokines. They then express both pro- and anti- inflammatory cytokines within the peripheral nerves. IHC showed macrophage numbers within the peripheral nerves of EphA5 KO mice were increased and that macrophages in EphA5 WT nerves were polarised into an M2 state at an earlier time point than EphA5 KO. Consequently, inflammatory cytokine expression in the distal nerve was investigated at 10 and 28DPI. Pro-inflammatory cytokines IL-1α, IL-1β, MCP-1, TNF-α and IL-6 and anti-inflammatory cytokines IL-10, IL-4 and IL-13 were investigated in WT and KO animals using qRT-PCR.

Cytokine expression at 10DPI was first investigated. Expression of IL1-α, MCP-1, TNF-α, IL-10 and IL-13 between EphA5 WT and KO 10DPI peripheral nerves was unaffected, no significance difference in cytokine expression was observed (**Figure 46A, C, D, F, H**). However, IL-1β, IL-6 and IL-4 expression were significantly upregulated in EphA5KO compared to WT indicating that there may be some dysregulation in cytokine expression in EphA5 KO mice although there was no difference in macrophage numbers at a similar time point of 7DPI (**Figure 46, B, E, G**).

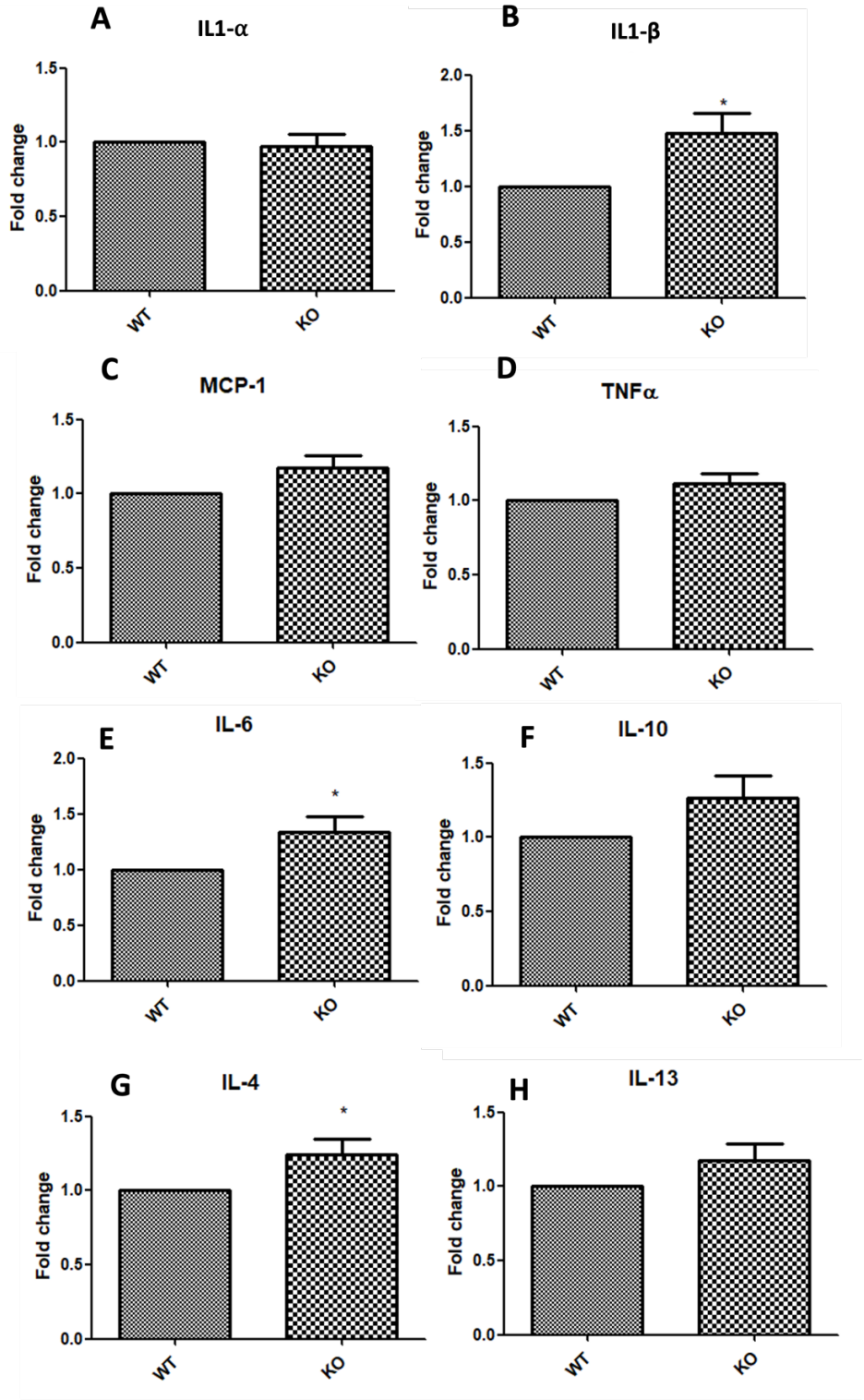

Figure 46 – The expression of cytokines IL-β, IL-6 and IL-4 is dysregulated in the distal nerve stump following a transection injury in EphA5 KO mice compared to EphA5 WT mice at 10DPI

qRT-PCR of pro-inflammatory (A-E) and anti inflammatory (F-H) cytokine expression in EphA5 WT and KO distal sciatic nerve 10DPI. IL-β (B), IL-6 (E) and IL-4 (G) are significantly increased in EphA5 KO compared to EphA5 WT. (n=3). Data is presented as mean ± SEM for each group. Student's T test *P <0.005 WT compared to KO nerves.

The next timepoint investigated was 28DPI, where the largest difference in macrophage numbers in the distal nerve stump between EphA5WT and KO animals and the largest difference between IBA1+ and CD206+ macrophages within EphA5 KO nerves was observed. Again, expression of pro-inflammatory cytokines IL-α, IL-β, MCP-1, TNF-α and IL-6 and anti-inflammatory cytokines IL-10, IL-4 and IL-13 was investigated. Expression of anti-inflammatory cytokines IL-10, IL-4 and IL-13 remained unchanged between EphA5 WT and KO distal nerve stumps (**Figure 47-H**). Pro-inflammatory cytokine expression of TNF-α and IL-6 remained unchanged between EphA5 WT and KO, whereas expression of IL-1α, IL-1β and MCP-1 were significantly upregulated in EphA5 KO mice 28DPI (**Figure 47A-E**). This indicates that in addition to increased macrophages in the peripheral nerves of EphA5 KO distal stumps at 28DPI, they are also expressing higher levels of some pro-inflammatory cytokines. The upregulated expression of pro-inflammatory cytokines shows that the peripheral nerves in EphA5 KO animals are still in a pro-inflammatory state and the inflammatory response is yet to be resolved. This may consequently lead to an increased regeneration time in peripheral nerves of EphA5 KO mice.

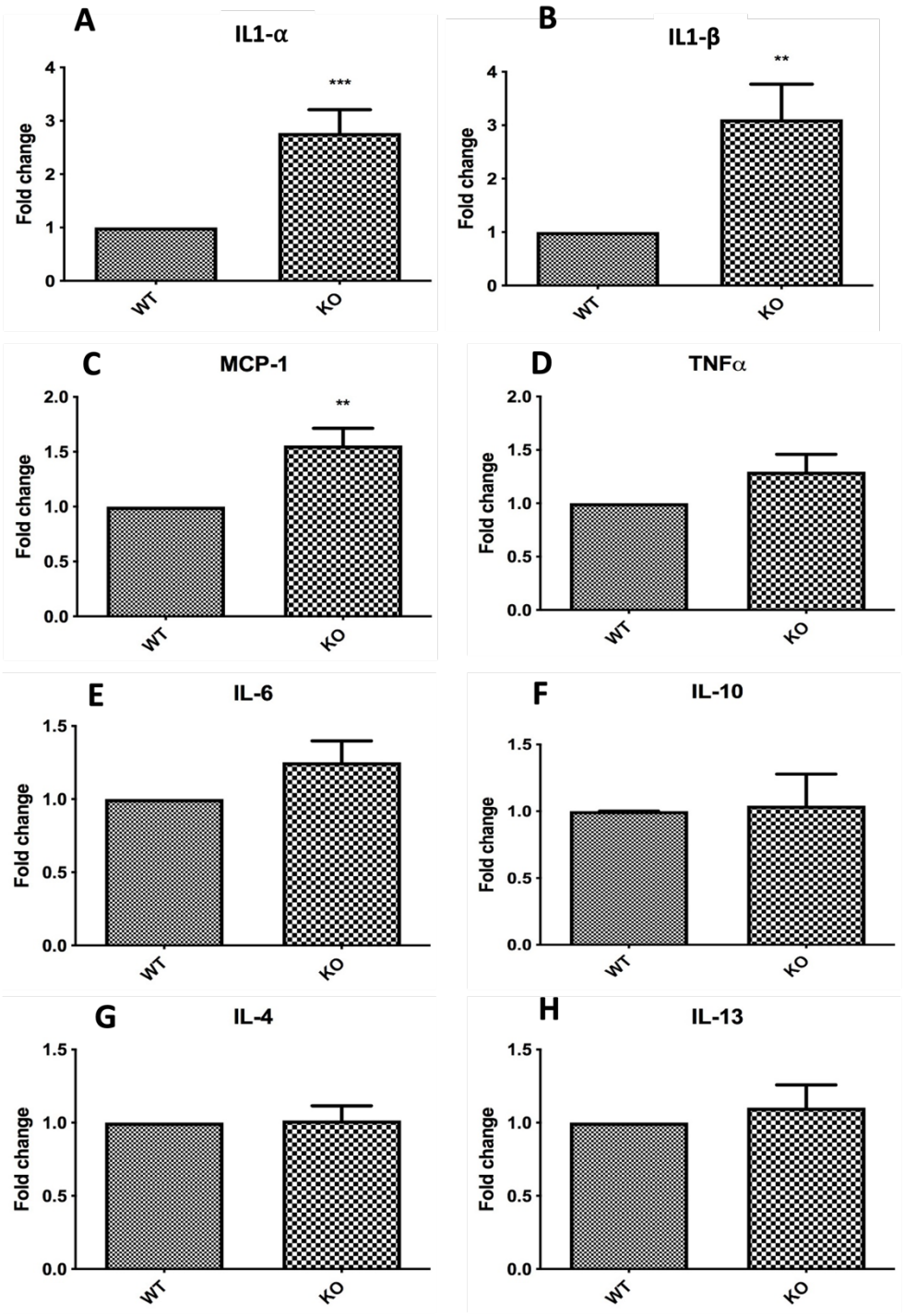

Figure 47 – Pro-inflammatory cytokine expression in the distal transacted peripheral nerve is upregulated in EphA5 KO mice compared to EphA5 WT mice at 28 DPI

qRT-PCR of pro-inflammatory (A-E) and anti-inflammatory (F-H) cytokine expression in EphA5 WT and KO distal sciatic nerve 10DPI. IL-1β (B), IL-6 (E) and IL-4 (G) are significantly increased in EphA5 KO compared to EphA5 WT. (n=3). Data is presented as mean ± SEM for each group. Student's T test *P <0.005 WT compared to KO nerves,

4.8 Effect of EphA5 KO on migration in vitro

To further investigate the suspected function of EphA5 on macrophage migration, in vitro migration assays were performed. Both the macrophage cell line Raw 264.7 and primary mouse macrophages were used in a scratch wound migration assay to investigate the role of EphA5 in macrophage migration (EphA5 expression in both cells lines has previously been confirmed in both cell types) (**Figure 34A, 35A**)). In vitro migration assay were also used to try to determine which Ephrin ligand may be important for EphA5 macrophage migratory signalling. EprhinA2 is highly expressed on Schwann cells following peripheral nerve injury with expression levels peaking at 10DPI but remaining significantly upregulated up to at least 28DPI (**Figure 30, 31D**). EphrinA2 expression from Schwann cells may interact with EphA5 on macrophages and promote contact-dependent reverse signalling through EphA5 expressing macrophages, leading to repulsive signalling through macrophages and an increase in macrophage migratory behaviour.

Raw 264.7 cells were grown to confluency on a 6 well plate before a 'wound' in the cell monolayer is introduced using a 200μl pipette tip. Cells were then incubated with 100nM EphA5 inhibitor WDC or 30ng EphA5 ligand Ephrin A2. Cell migration into the scratch wound was then assessed at 24h using phase contrast microscopy and migrated cells were counted using ImageJ. In control samples an average of 682 (±74.21) cells migrate into the wound area, when samples are treated with EphrinA2 an EphA5 ligand this is increased to 802 (±64.20), although this increase is not statistically significant increase and suggested EphrinA2 was not the main EphA5 ligand (**Figure 48A-B, E-F, I**). The number of migrated macrophages is reduced to 478 (±45.28) in WDC treated samples and samples where cells were pre-treated with WDC for 1 hour followed by treatment with Ephrin A2, again leading to a decrease in

the number of migratory macrophages to 468 (±31.77) (**Figure 48C-D, G-I**). This suggests activation of EphA5 signalling may induce contact-dependent repulsive signalling, leading to macrophage migration and that inhibition of EphA5 leads to an inhibitory effect on macrophage migration in this assay

To further assess the role of EphA5 in macrophage migration, primary macrophages differentiated from bone marrow monocytes from EphA5 WT and KO mice were collected and used for scratch wound assays. Cells were grown to confluency in a 24 well plate before a wound in the cell monolayer is introduced using a 10μl pipette tip. Cells were then left untreated or incubated with 30ng Ephrin A2 for 23h. Cell migration into the scratch wound was then assessed at 24h using phase contrast microscopy and migrated cells were counted using ImageJ.

In WT control scratch wound assays an average of 149 (±12.70) macrophages migrated into the wound, upon the addition of Ephrin A2 to WT macrophages this increased to 159 (±14.77) although this was not a significant increase and therefore again suggested EphrinA2 was not the main EphA5 ligand for macrophage repel signalling (**Figure 49A-B, E-F, I**). The number of EphA5 KO macrophages migrating into the scratch wound is significantly reduced to an average of 92 (±7.94) for control sample and 106 (±6.27) for Ephrin A2 treated samples compared to WT control (**Figure 49C-D, G-I**). This therefore indicates that EphA5 signalling may play a crucial role in macrophage migration although EphrinA2 does not appear to be the ligand EphA5 interacts with as addition of exogenous recombinant EphrinA2 did not significantly increase macrophage migration.

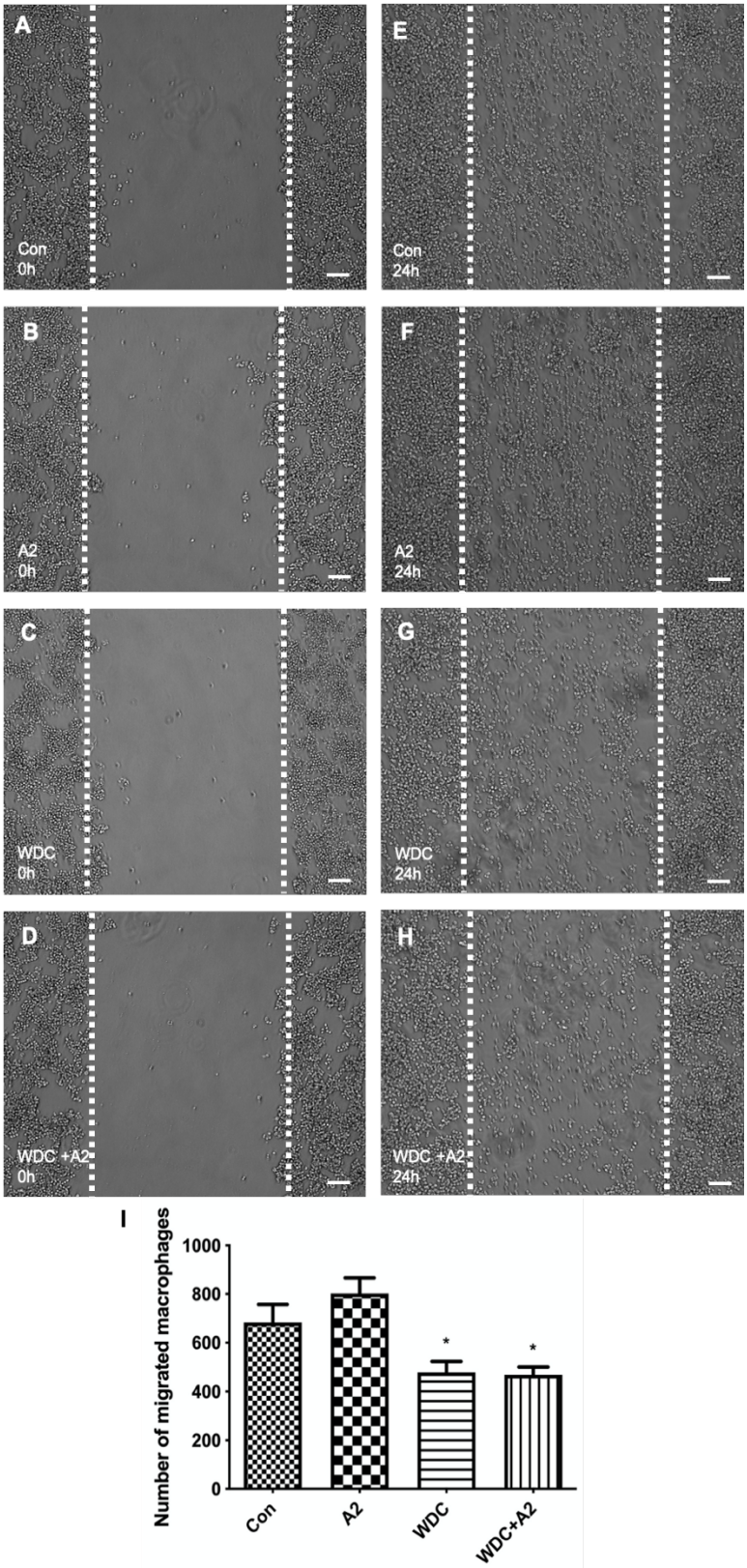

Figure 48 - Migration of Raw 264.7 into a scratch wound is decreased when EphA5 is inhibited

A-H. The migration of Raw 264.7 cells was analysed using a scratch wound assay and cells were left untreated (A, E) or treated with 30ng EphrinA2 (B, F), 100nM WDC (C, G) or 100nM WDC for 1h followed by 30ng EphrinA2 for 23h(D, H). Images were taken at 0h (A-D) and 24h (E-H) and migration into the scratch area was quantified I. Quantification of migrated Raw 264.7 cells. Migrated cells were counted using ImageJ counting tool. Scale bar 75μm. (n=3) Data is presented as mean ± SEM for each group. One way ANOVA with Tukey post hoc test * P<0.05. ** P<0.01. ***P<0.001 compared to control untreated cells.

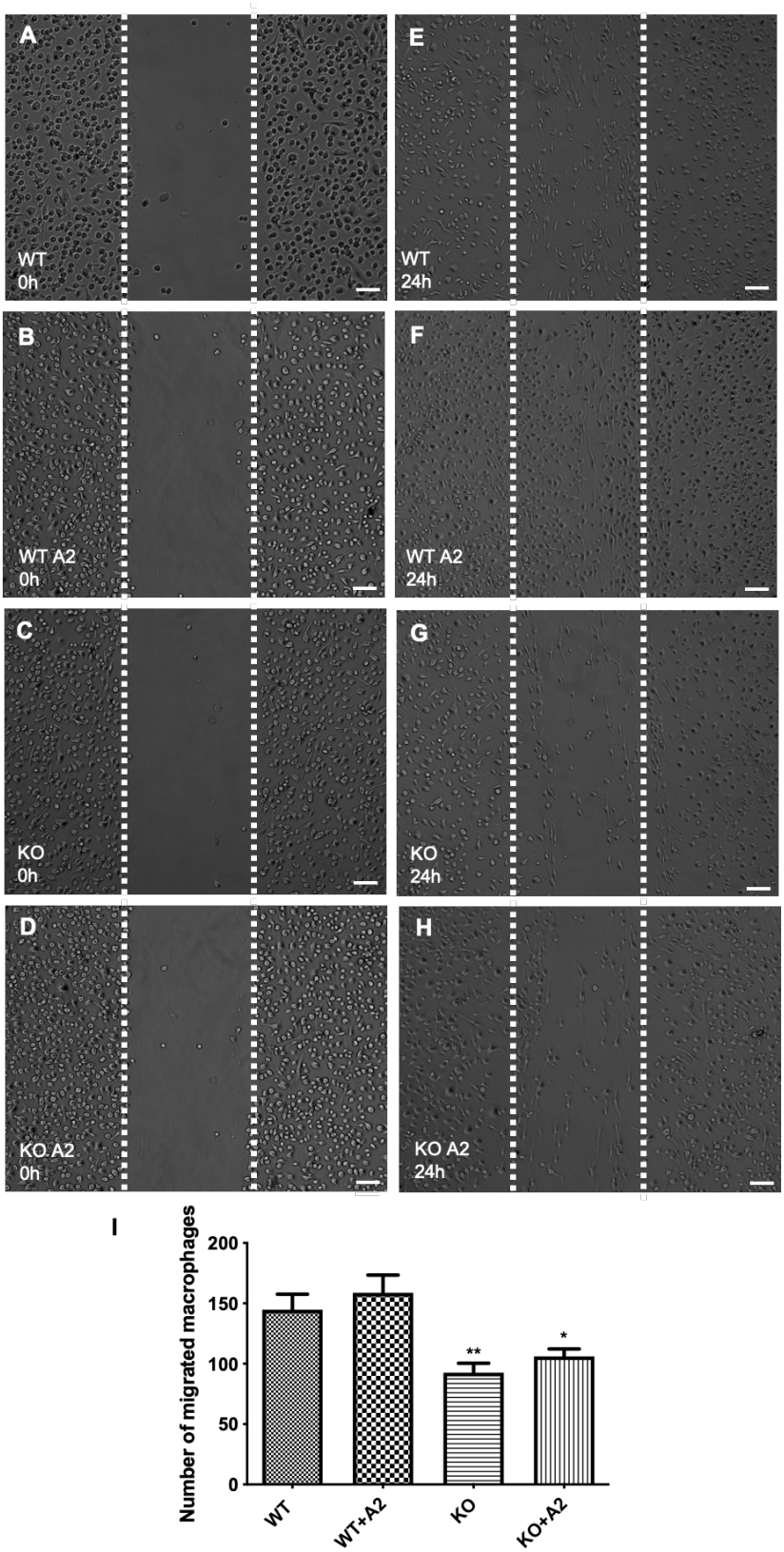

Figure 49 - Macrophage migration is decreased in EphA5 KO macrophages

A-H. The migration of EphA5 WT (A, B, E, F) and KO (C, D, G, H) primary macrophage cells was analysed using scratch wound assay, and cells were left untreated (A, E, C, G) or with 30ng EphrinA2 (B, F, D, H). Images were taken at 0h (A-D) and 24h (E-H) and migration into the scratch area was quantified I. Quantification of migrated macrophage cells. Migrated cells were counted using ImageJ counting tool. Scale bar 75μm. (n=3) Data is presented as mean ± SEM for each group. One way ANOVA with Tukey post hoc test * $P<0.05$. ** $P<0.01$ compared to WT control untreated cells

An additional migration assay, a transwell migration assay was also used to investigate the role of EphA5 in macrophage migration. Macrophages were seeded into the top chamber and treated with EphA5 inhibitor WDC or ligand and migration into the lower chamber was investigated. Cells migrated into the lower chamber were stained with crystal violet and counted using the Image J counting tool. First the macrophage cell line Raw 264.7 was used to investigate the role of EphA5 in macrophage migration. In control wells an average of 148 (±11.34) macrophages migrated into the chamber below. The EphA5 ligand, EphrinA2, did not increase macrophage migration into the lower chamber, an average of 167 (±5.57) macrophages migrated into the lower chamber, further showing that EphA5 interaction with EphrinA2 does not induce contact dependent repulsive migration (**Figure 50A-B, E**). WDC was used to inhibit EphA5 and this inhibited cell migration, decreasing the number of macrophages migrating into the lower chamber to an average of 75 (±4.45) (**Figure 50B, E**). This trend was also observed when cells were pre-treated with WDC followed by treatment with EphrinA2 and an average number of 77 (±7.43) macrophages migrated into the lower chamber further confirming a role for EphA5 in promoting macrophage migration (**Figure 50D-E**).

The migratory behaviour of primary macrophages differentiated from bone marrow monocytes from EphA5 WT and KO mice was also investigated using transwell migration assay. Cells were differentiated and then seeded into the upper chamber of migration chambers. Cells were left untreated or treated with EphrinA2 before migration into the lower chambers was assessed. An average of 92 (±8.14) WT macrophages migrated into the lower chamber. Treatment with EphrinA2 did not increase the number of migrated macrophage, with an average of 93 (±9.25) macrophages migrated into lower chambers (**Figure 51A-B, E**). KO macrophage

migration was significantly reduced compared to WT with an average of 47 (±7.78) macrophage migrating into the lower chamber. Similarly to what was observed previously the addition of EphrinA2 ligand, this did not increase migration with macrophage migration numbers at an average of 55 (±1) (**Figure 51C-E**).

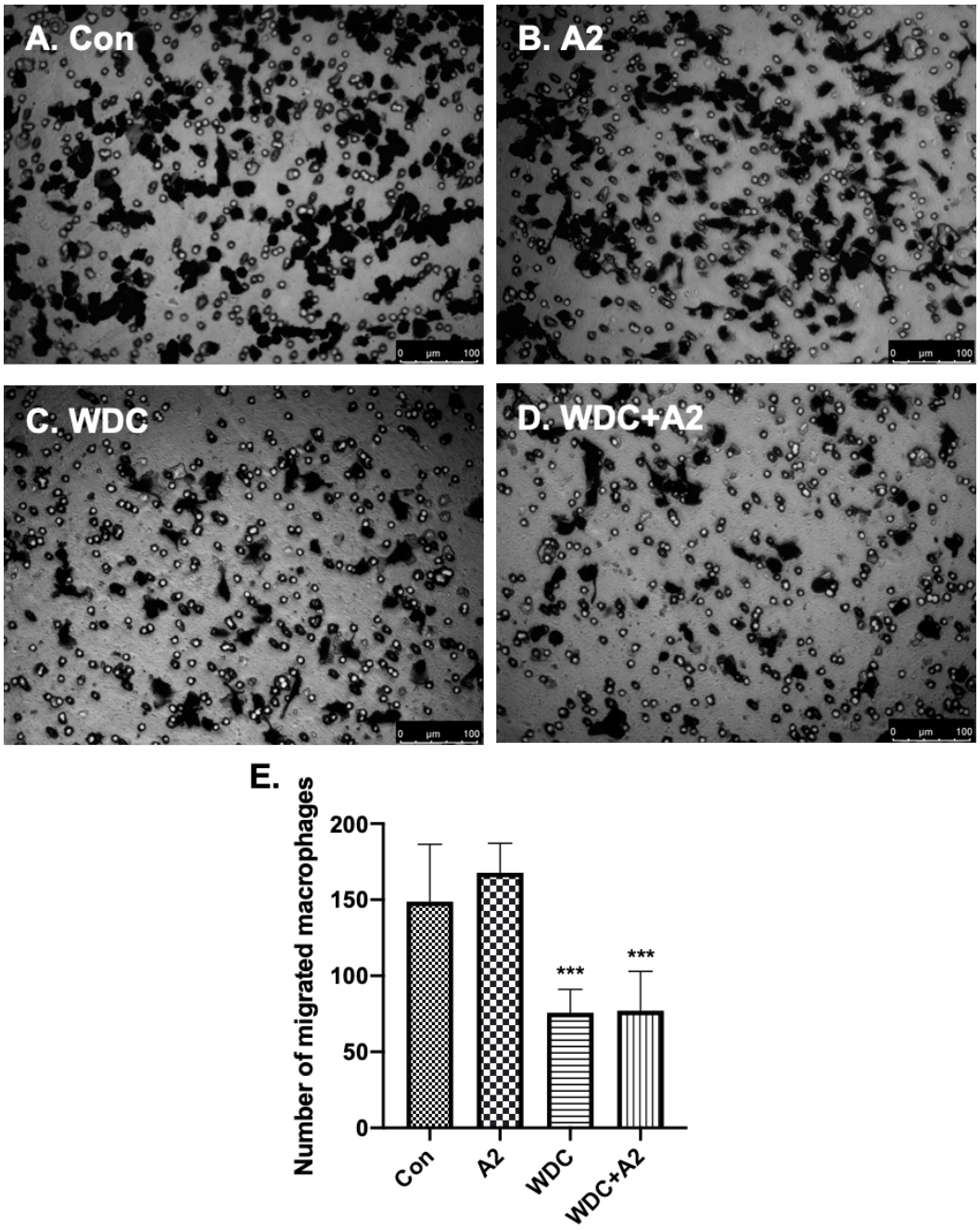

Figure 50 - Raw264.7 migration is decreased when EphA5 is inhibited

A-D. Migration of RAW 264.7 cells into the lower chamber of a transwell migration assay. Cells were seeded into the upper chamber of a transwell migration chamber and untreated (A), treated with 30ng EphrinA2 (B), 100nM WDC (C) or 30ng EprhinA2 for 1h followed by 100nM WDC (D). Cells were fixed, stained using crystal violet and cells in the top chamber were wiped away. Cells migrated into the lower chamber were counted using the ImageJ counting tool. E. Quantification of migrated macrophages. Scale bar 100μm. (n=3) Data is presented as mean ± SEM for each group. One way ANOVA with Tukey post hoc test *** P<0.001 compared to control untreated cells.

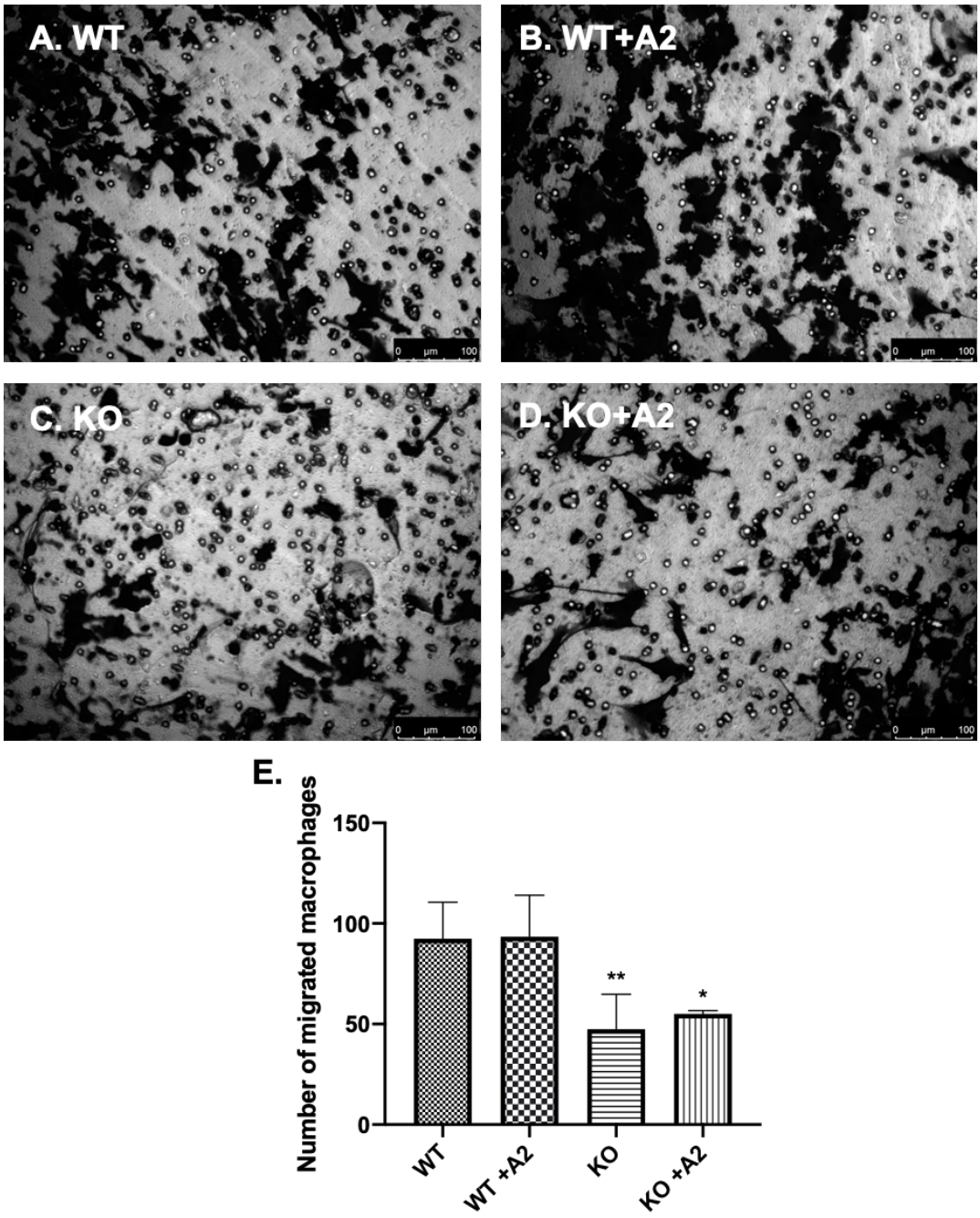

Figure 51 - Migration is reduced in EphA5 KO macrophages

A-D. Migration of WT (A, B) and KO (C, D) macrophages into the lower chamber of a transwell migration assay. Cells were seeded into the upper chamber of a transwell migration chamber and untreated (A, C), treated with 30ng EphrinA2 (B, D). Cells were fixed, stained using crystal violet and cells in the top chamber were wiped away. Cells migrated into the lower chamber were counted using the ImageJ counting tool. E. Quantification of migrated macrophage cells. Scale bar 100μm. (n=3) Data is presented as mean ± SEM for each group. One way ANOVA with Tukey post hoc test *P<0.05. **P<0.005 compared to WT untreated cells.

4.9 Schwann cell migration into the nerve bridge in EphA5 WT and KO following transection injury.

EphA5 and its ligands EphrinA 1, 2 and 4 have been shown to be expressed on Schwann cells and my in vitro experiments showed that EphA5-Ephrin signalling may play a role in Schwann cell sorting, migration and morphology when cultured with macrophages. Smaller Schwann cell clusters and a change in schwann cell morphology was observed upon inhibition of EphA5 in these co-cultures and therefore its function in Schwann cells after peripheral nerve injury was investigated. Schwann cells have been well described to be highly motile and migrate into the nerve bridge following transection injury (Cattin et al. 2015; B. Chen et al. 2019; Min et al. 2021; Parrinello et al. 2010; Qin et al. 2016). Schwann cell migration into the nerve bridge at 5.5DPI was investigated through whole nerve preparation using PLP-GFP EphA5 WT and PLP-GFP EphA5 KO animals. Schwann cells in PLP-GFP mice are labelled with GFP which can be detected through fluorescence microscopy (Dun et al. 2019). PLP-GFP animals were crossed with EphA5 WT and KO mice to obtain PLP-GFP EphA5 WT and PLP-GFP EphA5 KO animals.

Animals underwent a sciatic nerve cut injury and 5.5DPI the proximal, nerve bridge and distal nerve stump were dissected out. After fixing and tissue clearing with 25%, 50% and 75% glycerol, a series of z stack of images was taken along the nerve, a single flattened image was processed and images montaged together. The length of the nerve bridge and Schwann cell migration distance from the cut site from both the proximal and distal end were measured. There was no significant difference in nerve bridge length between EphA5 WT and KO mice, the average bridge length in WT and KO animals were 1.44mm (±0.19) and 1.56mm (±0.16) respectively (P=0.64).

Schwann cell migration however did appear to be affected in PLP-GFP EphA5 KO mice. Schwann cell migration from both the proximal and distal stumps was significantly decreased in PLP-GFP EphA5 KO mice compared to control animals Schwann cell migration distance from the proximal end was reduced from 0.54mm (±0.02) in EphA5 WT sciatic nerves to 0.42mm (±0.05) in EphA5 KO animals (p=0.047). Migration distance from the distal end was reduced from 0.57mm (±0.03) to 0.33mm (±0.03) in EphA5 WT and KO sciatic nerve respectively (P=<0.001) (**Figure 52A-E**).

This indicated that EphA5 may play a role in Schwann cell migration into the nerve bridge following peripheral nerve injury. The more time that is required for cords of Schwann cells from the proximal and distal stumps to connect within the bridge increases the time that axon regeneration will take through the nerve bridge and into the distal nerve stump, thus delaying re-innervation and functional recovery.(B. Chen et al. 2019).

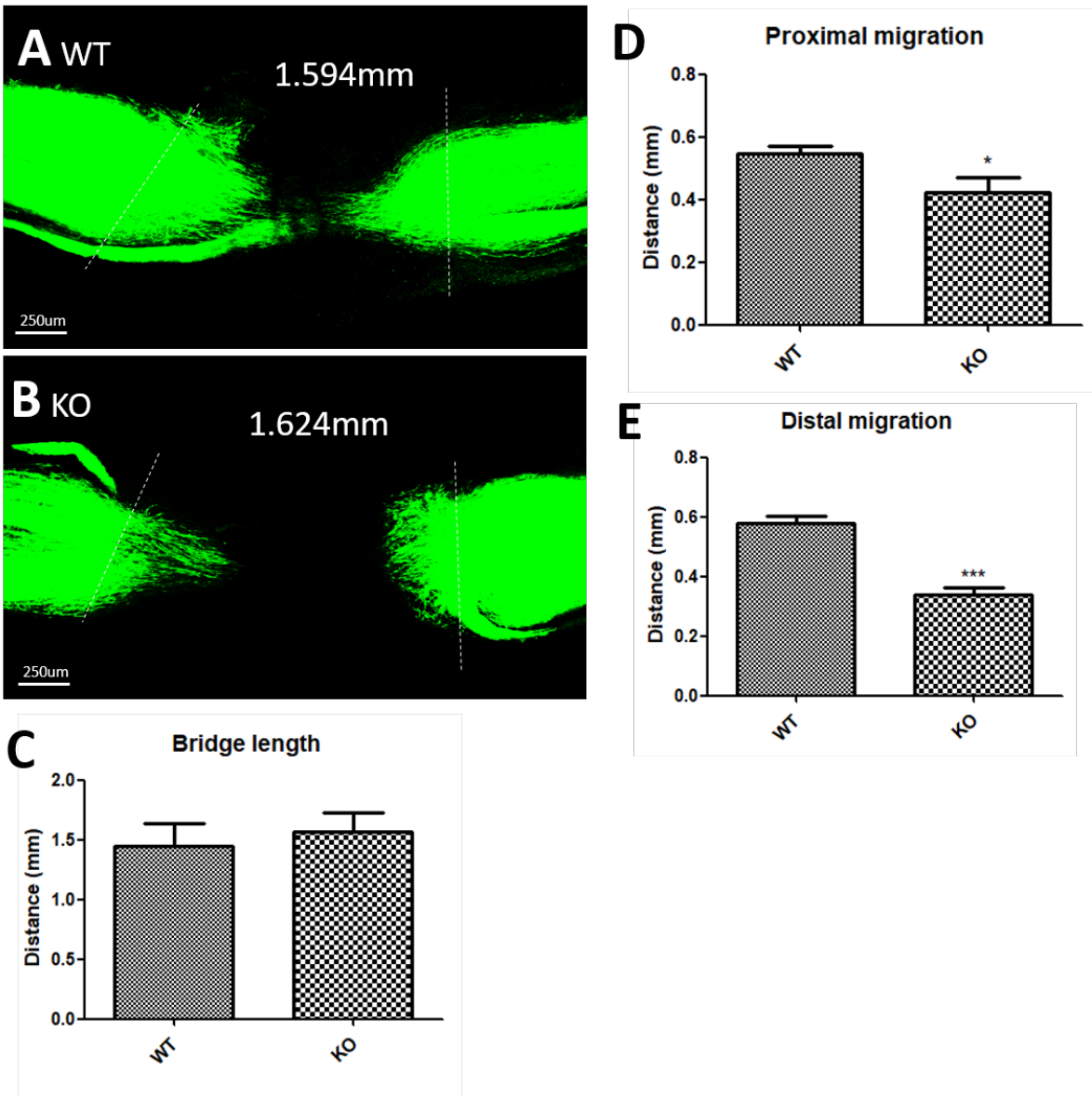

Figure 52 - Schwann cell migration into the nerve bridge in EphA5 KO mice is reduced compared to Schwann cell migration in EphA5 WT nerves at 5.5DPI

(A, B) Schwann cell (GFP+) migration from both proximal and distal nerve stumps in EphA5 WT (A) and KO (B) mice 5.5 days after sciatic nerve transection injury. Several z series were captured on a Leica SPE confocal microscope covering the entire field of interest. The individual series were then flattened into a single image for each location and combined into one image using Adobe Photoshop software (Adobe Systems) C. quantification of average nerve bridge distance. D, E. quantification of GFP+ Schwann cell migration from the proximal (D) and distal (E) nerve stump. (n=3) Student's T test $*P < 0.05$, $**P < 0.01$, $***P < 0.001$ EphA5 WT compared to EphA5 KO nerves

4.10 Migration of EphA5 KO Schwann cells in vitro

Having shown that in vivo Schwann cell migration into the nerve bridge was reduced in EphA5 KO animals, we next investigated the effects of EphA5 KO on Schwann cell migration and began to investigate which EphrinA5 ligands may interact with EphA5 to initiate Schwann cell migration; to do this, in vitro migration assays scratch wound and transwell migration assays were performed. Primary Rat Schwann cells were treated with WDC peptide or recombinant Ephrin A2. Ephrin A2 was highly expressed on Schwann cells following injury and consequently was chosen for investigation as the EphA5 ligand that could induce contact-dependent, migratory signalling in Schwann cells.

To assess Schwann cell migration, rat Schwann cells were seeded into a 6 well plate and grown to confluency. A scratch was introduced using a 200μl pipette tip and cells were incubated in DMEM containing 3% FBS alone to limit cell proliferation. 100nM WDC EphA5 inhibitor to block the receptor, 30ng of Ephrin A2 ligand which could activate EphA5 receptor or a combination of both EphA5 inhibitor followed by Ephrin A2 was added to cells to assess the effect on Schwann cell migration and elucidate if EphrinA2 contact with EphA5 receptor was responsible for cell migration in Schwann cells. Images were taken at 0h and 24h and the percentage of gap closure was determined to investigate cell migration rate. Schwann cells migrated into the scratch wound in control samples and the percentage gap closure was 16.57% (±1.85). Upon addition of Ephrin A2, the number of cells migrating into the wound was not significantly increased compared to control (18.7 ±1.55) . Upon addition of WDC Schwann cell migration was significantly decreased (10.92% ±1.28); this was also the case when cells were pre-treated with WDC followed by treatment with Ephrin A2 (10.90% ± 1.17) (**Figure 53A-I**).

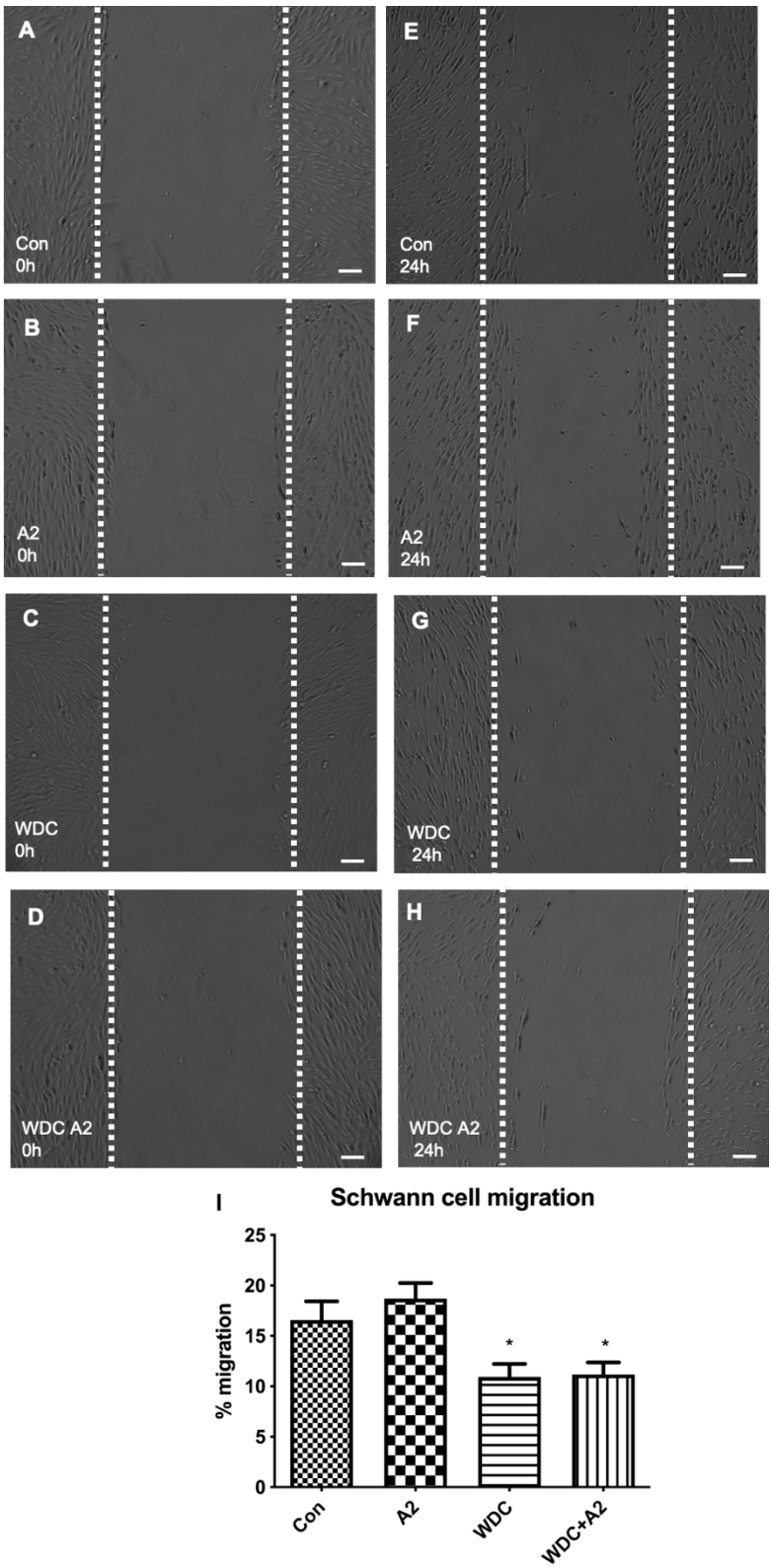

Figure 53 - Schwann cell migration into the scratch of a scratch wound assay is decreased when EphA5 is inhibited

A-H. The migration of Schwann cells were analysed using scratch wound assay, and cells were left untreated (A, E) or treated with 30ng EphrinA2 (B, F), 100nM WDC (C, G) or 100nM WDC for 1h followed by 30ng EphrinA2 (D, H). Images were taken at 0h (A-D) and 24h (E-H) and migration into the scratch area was quantified I. Quantification of migrated Schwann cells. Migration rate of Schwann cells and closure of scratch wound gap was determined using the equation migration rate = $(D_0 - D_{24})/D_0 \times 100$. Scale bar 75μm. (n=3) Data is presented as mean ± SEM for each group. One way ANOVA with Tukey post hoc test * $P<0.05$ compared to control untreated cells.

To further assess Schwann cell migration an additional migration assay, a transwell migration assay was used. Rat Schwann cells were seeded in the upper chamber with WDC or Ephrin A2 media and cells were left to migrate through a permeable membrane the upper to the lower chamber. Schwann cells migrating into the bottom chamber were then counted to assess migration. Migration was seen in control samples, with an average of 257 (±16.82) Schwann migrating into the lower chamber (**Figure 54A, E**). Surprisingly, as this has not been seen in previous assays, migration through the permeable membrane was significantly increased upon the addition of Ephrin A2 to the upper chamber and an average of 327 (±17.37) cell migrated into the lower chamber (**Figure 54B, E**). Addition of WDC significantly reduced migration of Schwann cells through the permeable membrane to 187 (±14.40) cells (**Figure 54C, E**). To confirm that the increase of migration was due to contact dependent repulsive signalling between EphA5 and Ephrin A2, Schwann cells were pre-treated with WDC to inhibit EphA5 activity followed by treatment with Ephrin A2. Pre-treatment with WDC inhibited Ephrin A2 induced Schwann cell migration as the number of migratory Schwann cells in the lower chambers reduced to an average of 160 (±14.45) (**Figure 54D-E**). This indicates that EphA5 signalling may play a crucial role in Schwann cell migration as inhibition of EphA5 decreased Schwann cell migration whereas addition of Ephrin A2 ligand acted to increase migration of Schwann cells into the lower chamber.

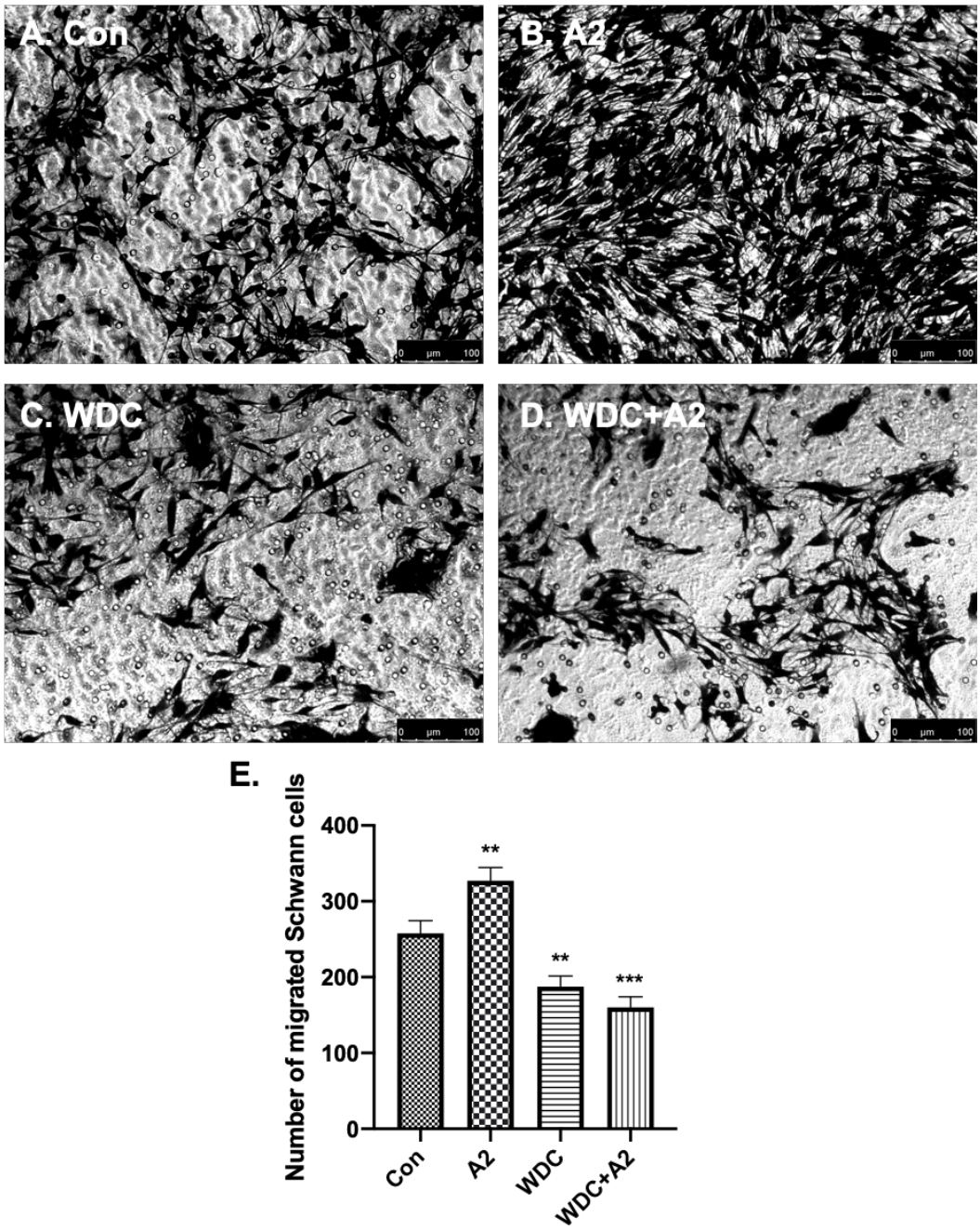

Figure 54 - Schwann cell migration is increased upon the addition of Ephrin A2 and decreased when EphA5 is inhibited.

A-D. Migration of Schwann cells into the lower chamber of a transwell migration assay. Cells were seeded into the upper chamber of a transwell migration chamber and untreated (A), treated with 30ng EphrinA2 (B), 100nM WDC (C) or 30ng EprhinA2 for 1h followed by 100nM WDC (D). Cells were fixed, stained using crystal violet and cells in the top chamber were wiped away. Cells migrated into the lower chamber were counted using the ImageJ counting tool. E. Quantification of migrated Schwann cells. Scale bar 100μm. (n=3) Data is presented as mean ± SEM for each group. One way ANOVA with Tukey post hoc test ** $P<0.005$. *** $P<0.001$ compared to control untreated cells.

4.11 Axon regeneration in EphA5 WT and KO mice.

EphA5 has been previously described as an axon guidance molecule during development and therefore we decided to examine its role in axon regeneration (Caras 1997; Rodger et al. 2001). Schwann cell migration at 5.5DPI into the nerve bridge was reduced in EphA5 KO mice, which could consequently lead to an additional effect on axon regeneration through the sciatic nerve and into the tibial nerve at 14DPI. A nerve crush injury was performed and the tibial nerve was dissected out and fixed in 4% PFA. Following fixation and dehydration in sucrose, tibial nerves were embedded in OCT. Each nerve was dissected out at the same point and sectioned in the same orientation (from closest to the cut site). This allowed tibial nerves from different samples to be sectioned a similar distance into the nerves and number of axons entering the nerve to be assessed. Samples were stained with neurofilament (NF) and the number of NF positive axons were counted per section. The number of axons entering into the tibial nerve was significantly reduced from 880 (±39.4) in EphA5 WT to 518 (±50) in EphA5 KO mice ($p=<0.0001$) (**Figure 55A-C**). This indicated that axon regeneration into the tibial nerve is delayed in EphA5 KO animals following nerve crush injury.

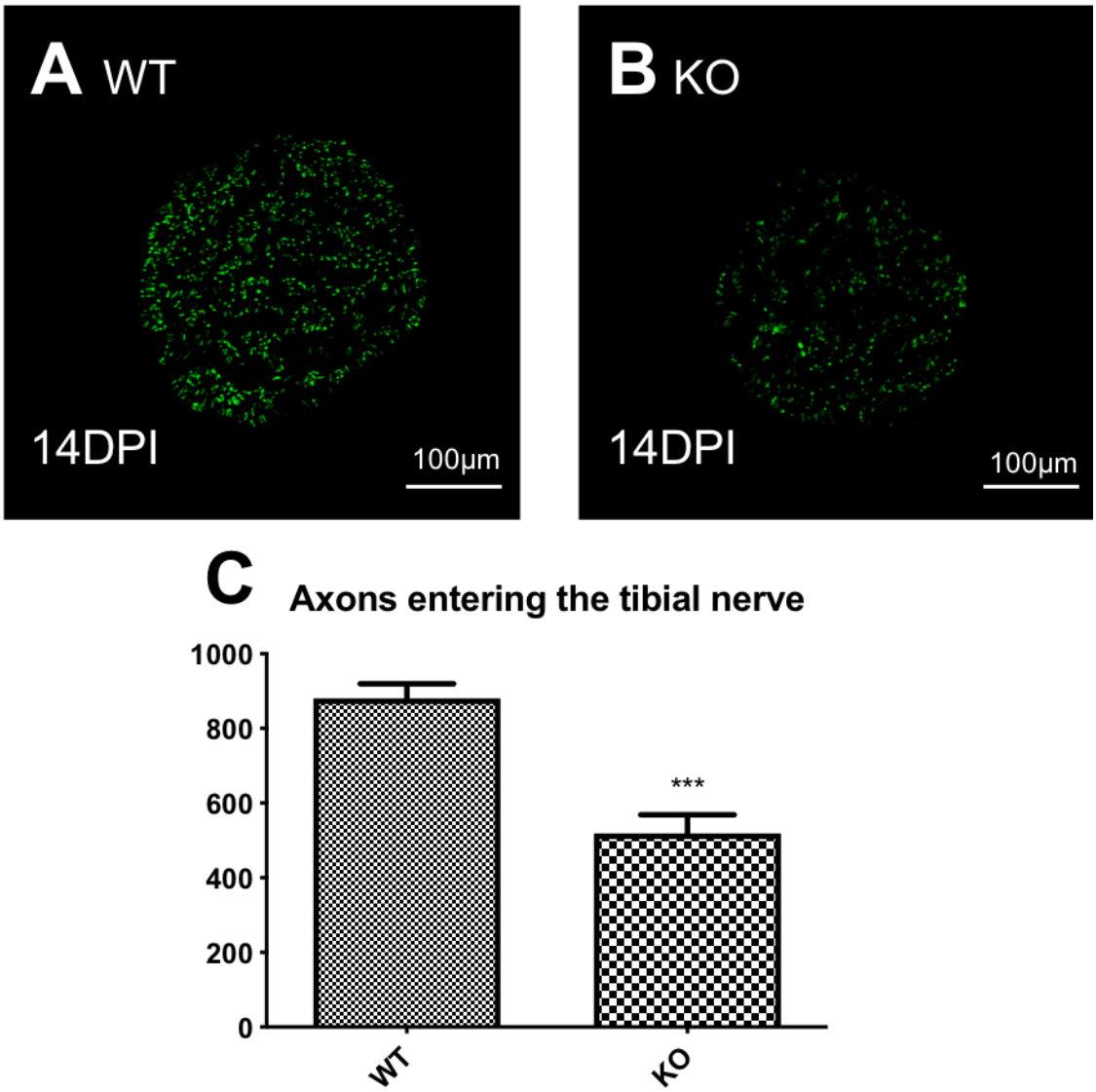

Figure 55 - Axon regeneration into the tibial nerve is impaired in EphA5 KO mice

A, B. Neurofilament antibody staining on tibial nerve transverse sections from EphA5 WT (A) and KO (B) mice 14 days post injury. C. Quantification of regenerated axon numbers in the tibial nerve of EphA5 WT and KO mice. n=3. Data is presented as mean ± SEM for each group. Student's T test *** $P<0.001$ compared to EphA5 WT nerves

4.12 Effect of EphA5 KO on Schwann cell remyelination following peripheral nerve injury.

As a result of the phenotype observed in EphA5 KO animals; decreased Schwann cell migration into the bridge, increased number of macrophages in the peripheral nerve and decreased axon regeneration into the tibial nerve. Schwann cell remyelination, a crucial step in peripheral nerve regeneration and for functional recovery, was next investigated. We've previously shown that 6 week old EphA5 KO mice have no difference in myelination and G ratio quantification in intact uninjured nerves, suggesting there is no developmental defect in myelination in the peripheral nerves of EphA5 KO mice (**Figure 35**), but, we next wanted to assess the effect of EphA5 KO on remyelination following nerve crush injury.

Distal sciatic nerves from EphA5 WT and KO mice were processed for TEM at 14 and 28 DPI. In order to determine whether myelin thickness and axon diameter were altered in the regenerating nerves of EphA5 WT and EphA5 KO mice at 14DPI, these two parameters were quantified on TEM images. At 14DPI there was no difference in the G ratio between EphA5 WT and EphA5 KO sciatic nerves, with an average G ratio of 0.77 and 0.80 respectively ($p=0.125$) (**Figure 56A-C**). The average axon diameter was slightly reduced in EphA5 KO regenerating nerves, 2.55μm in EphA5 WT mice compared to 2.33in EphA5 KO mice although this was not significant (**Figure 56D**). By these measures, this data suggested that there was no differences in axon diameter and remyelination in the peripheral nerve of EphA5 KO mice compared to EphA5 WT at 14DPI.

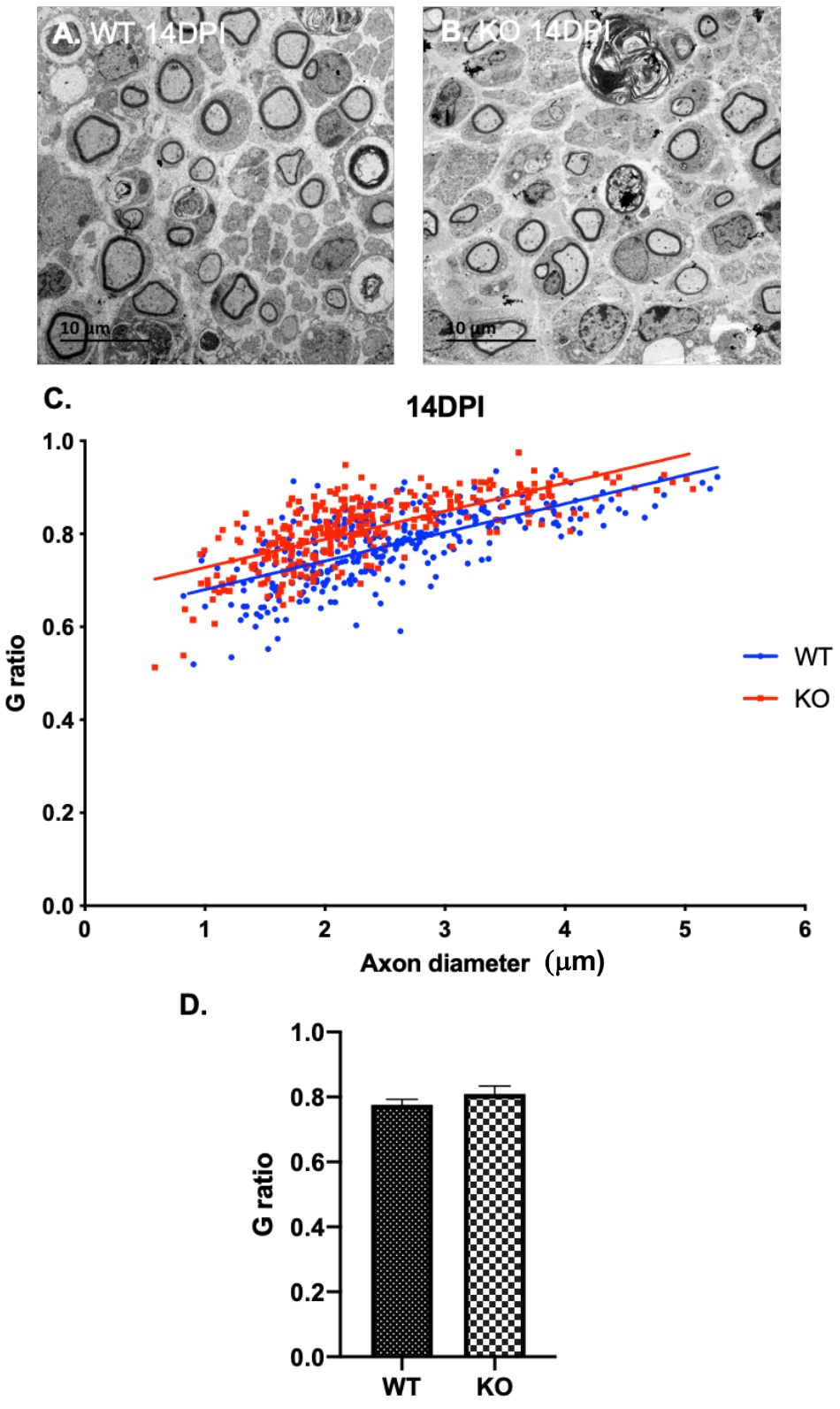

Figure 56 - No difference in remyelination between WT and KO mice 14DPI

A, B. Transmission electron micrographs of 14DPI distal sciatic nerve sections from EphA5 WT(A) and KO(B) mice. Scale bar 10µm C. Scatter plot displaying the g-ratio of individual axons in relation to axon diameter D. Graph showing the average g-ratio of EphA5 WT and KO nerves at 14 DPI. (n=3). Data is presented as mean ± SEM for each group. Student's T test compared to EphA5 WT nerves

Next, a later stage in regeneration, 28DPI was assessed. Typically, at this timepoint most injured nerves show a large degree of remyelination in WT animals (Rawlins et al. 1972; Song et al. 2006). Nerves from EphA5 WT and KO mice 28DPI were processed for TEM and myelin thickness and axon diameter was quantified in the regenerating nerves of EphA5 WT and EphA5 KO mice. At 28DPI, the G ratio was significantly lower in EphA5 WT nerves compared to EphA5 KO nerves, 0.65 and 0.71 respectively ($p=0.0125$) (**Figure 57A-D**). Similarly to 14DPI, the average axon diameter in 28DPI mice was reduced in EphA5 KO nerves, 2.68μm in EphA5 WT mice compared to 2.54μm in EphA5 KO mice although this was not significant. This data shows that axon regeneration may not be impaired due to no significant difference in axon diameter but myelin thickness is decreased in EphA5 KO animal. This suggests that EphA5 KO may cause injured sciatic nerves to remyelinate more slowly and produce thinner myelin sheaths at 28DPI.

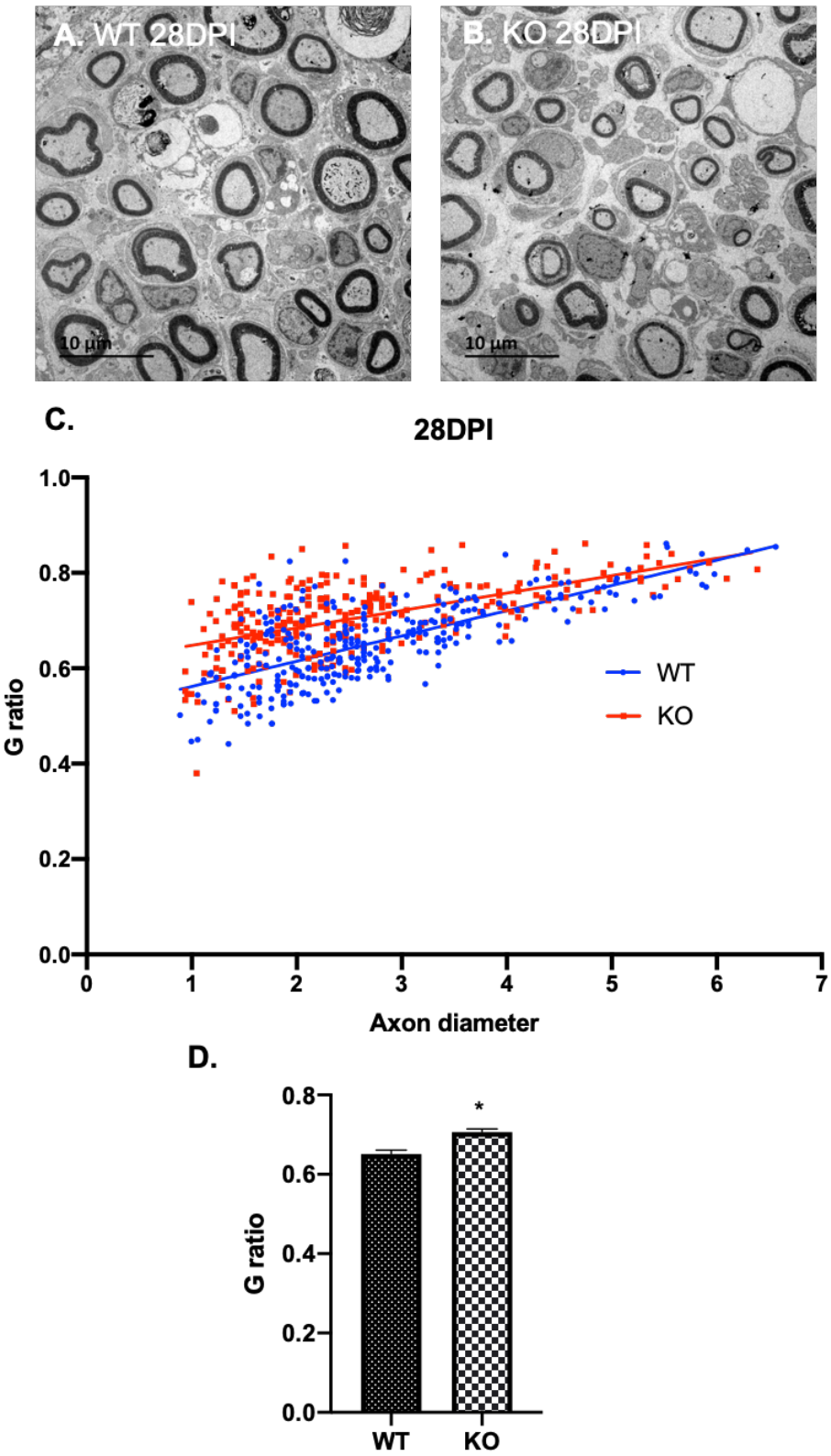

Figure 57 - Decreased myelination following a transection injury in EphA5 KO mice at 28DPI

A, B. Transmission electron micrographs of 28DPI distal sciatic nerve sections from EphA5 WT(A) and KO(B) mice. Scale bar 10μm C. Scatter plot displaying the g-ratio of individual axons in relation to axon diameter D. Graph showing the average g-ratio of EphA5 WT and KO nerves at 28 DPI. (n=3). Data is presented as mean ± SEM for each group. Student's T test * P<0.005 compared to EphA5 WT nerves

4.13 Functional recovery of WT and EphA5 KO mice following peripheral nerve injury

Peripheral nerve injury leads to loss of both motor and sensory function. Function can however be regained after Wallerian degeneration, axon regeneration and remyelination has taken place. Nerves are able to repair and re-innervate their target tissue leading to full functional recovery being seen in rodents between 3-4 weeks after crush injury (Jeub et al. 2020; Serpe et al. 2002). EphA5 KO mice have increased macrophage numbers in their peripheral nerves. Decreasing macrophage numbers in the peripheral nerve following injury through CXCR3 led to increased function recovery (Jeub et al. 2020). Therefore, an increase in macrophage numbers could lead to delayed functional recovery in the EphA5 KO animals. This coupled with a decrease in axons regenerating into the tibial nerve at 14DPI and a reduced myelination at 28DPI lead us to assess motor and sensory recovery in EphA5 WT and KO mice following injury.

To assess motor function recovery sciatic static index (SSI) measurements were taken. SSI is a method for assessing functional loss and recovery after peripheral nerve injury in mice over a duration of time (Bervar 2000). Using video analysis, toe spread measurements can were taken from the rear paws and these measurements were used to obtain SSI measurements. Measurements were taken from each animal before surgery (0 days), 1 day post-surgery and thereafter at 2-3 day intervals over a 28 day period post injury, until SSI measurements were back to pre-surgery values.

SSI measurements between EphA5 WT and KO animals show motor function recovery takes significantly longer in EphA5 KO mice. EphA5 KO show significantly lower SSI measurements from day 11 to day 15 and from day 19 to day 23 (**Figure**

58A). EphA5 WT animals regain full functional recovery to pre surgery level at 21DPI, whereas EphA5 KO animals take up to 27DPI to regain functional recovery comparable to pre surgery levels.

To assess sensory recovery, a toe pinch experiment was undertaken on toes 3, 4 and 5 (Vogelaar et al. 2004). Sensory recovery was also delayed in EphA5 KO compared to WT animals. Toe 3 regained sensory function on around day 20 (average 19.7) whereas this was significantly later in EphA5 KO animals which regained sensation at around day 22. Toes 4 and toe 5 regained sensation around day 20 (average 20.4) and 22 (average 21.5) in EphA5 WT animals compared to day 24 (average 24.4) and 27 (average 26.6) respectively in EphA5 KO animals (**Figure 58B**). This data showed that both motor and sensory recovery was delayed in EphA5 mice.

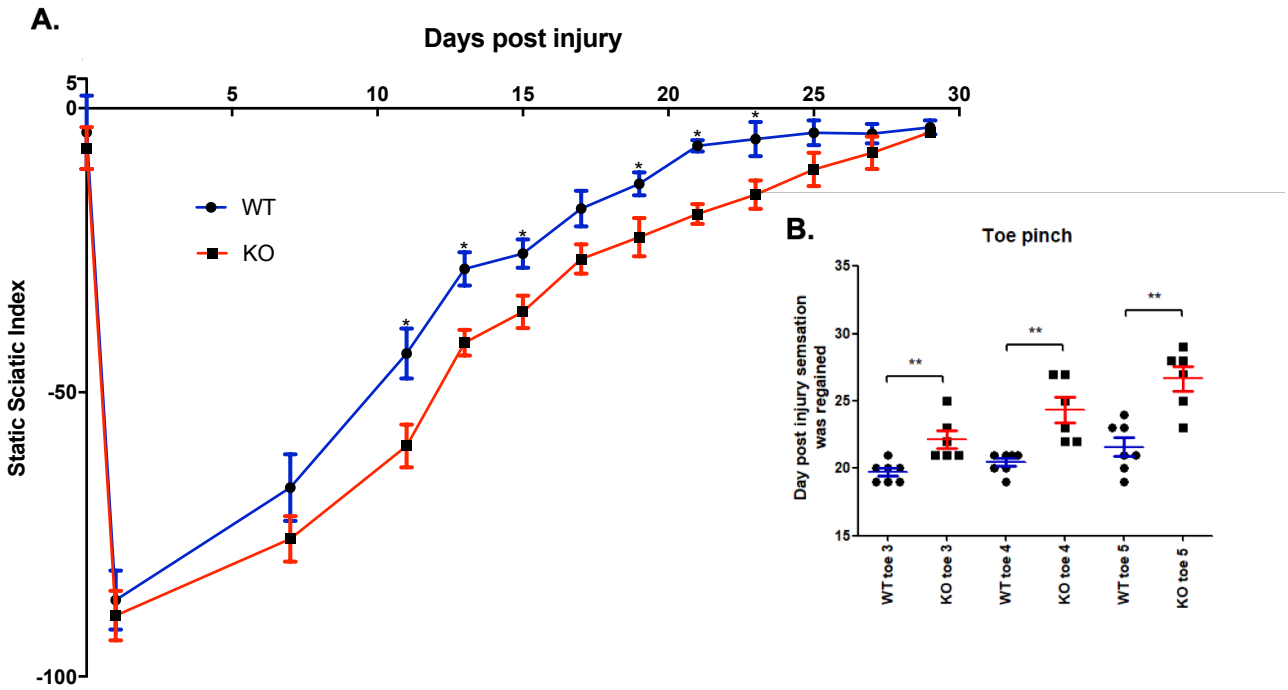

Figure 58 - Functional recovery is reduced in EphA5 KO mice

A. Sciatic static measurements to assess motor recovery taken from EphA5 WT and EphA5 KO mice starting at day 0 (pre surgery) up to 29 DPI. Measurements were obtained from still images taken from films of the mice move around a Perspex box. The images were renumbered to blind the analysis and avoid bias during the quantification process. B. Toe pinch measurements taken to assess sensory recovery in EphA5 WT and EphA5 KO mice. (n=3). Data is presented as mean ± SEM for each group. A. Student's T test B. One way ANOVA with Tukey post hoc test *P<0.005. **P<0.001 compared to EphA5 WT nerves

4.14 Discussion

EphA5-ephrin signalling has been extensively described in the literature to play a role in axon guidance during development and regulates axon guidance in retinal ganglion cells and the spinal cord (Caras 1997; J. B. Wang et al. 2016). Eph-ephrin are cell surface receptors and ligands which upon interaction lead to intracellular signalling and cell migration. My experiments show the expression patterns of EphA5 and EphrinA ligands within intact and injured mouse peripheral nerves and I then went on to examine the role(s) EphA5 may play during peripheral nerve regeneration. EphA5-ephrin signalling within haemopoietic stem cells has been described and signalling through this pathway can lead to cell migration through forward signalling and activation of Rac1 (Nguyen et al. 2017). Macrophages and Schwann cells are two cell types of which are known to interact with one another and migrate following peripheral nerve injury (Dun et al. 2019; Martini et al. 2008; Qu et al. 2021).My data shows for the first time that EphA5 is expressed on macrophages and Schwann cells in injured peripheral nerves. It also outlined for the first time the expression patterns of EphrinA ligands up to 28DPI. Ephrin A2 and A4 ligand was expressed on Schwann cells and Ephrin A5 was expressed on macrophages.

EphA5 has previously been shown to be expressed on neurons during development and in the rat optic nerve but its expression in adult mouse sciatic nerves and injured sciatic nerves has not been reported before(Caras 1997; Rodger et al. 2001; J. B. Wang et al. 2016) . My data confirmed EphA5 expression in peripheral nerves, revealed the cell types expressing EphA5was expressed on and identified a potential reason for its upregulation and role within peripheral nerve regeneration. This data has also helped determine which ephrin A ligands may interact with EphA5 to induce signalling through the cell types. qRT-PCR and western blot methods showed EphA5

up-regulation in the distal nerve stump after peripheral nerve injury. IHC using cell-specific markers revealed EphA5 was expressed in Schwann cells and infiltrating macrophages of the distal nerve stump. qRT-PCR and IHC was also used to elucidate ephrinA receptor expression and cell type expression in the peripheral nerve pre- and post- sciatic nerve injury.

Eph-ephrin interaction between Schwann cells and fibroblasts following peripheral nerve injury has already been documented, where EphB2 signalling between fibroblasts and Schwann cells directs Schwann cell sorting and migration into the nerve bridge (Parrinello et al. 2010). Co-cultures of macrophages and Schwann cells helped to determine whether EphA5-EprinA signalling occurs between these cell types and what its importance may be. In macrophage-Schwann cell co-cultures, distinct cell populations could be identified where Schwann cells and macrophages did not intermingle. A similar phenomenon is seen when culturing Schwann cells and astrocytes together, in control samples Schwann cells and astrocytes do not intermingle, however, upon the inhibition of EphA4 Schwann cells appear to migrate into the astrocyte population (Afshari et al. 2010). When EphA5 was either knocked out in primary cells or inhibited using WDC, macrophage-Schwann cell co-cultures were no longer able to form into distinct populations but instead formed intermingled populations where cells of different cell types were grouped together and were often seen on top of one another. This suggested that signalling through EphA5 may play a role in function and migration of Schwann cells and macrophages in the distal nerve following peripheral nerve injury.

Eph-Ephrin has a well documented function of increasing receptor tyrosine kinase (RTK) activity activation and regulating cell migration; however, Eph-Ephrin

expression on migratory cells within the peripheral nerve environment following nerve injury had not yet been investigated (Kullander and Klein 2002). Thus far, EphA5 knock out has only been documented to play a role within changes in attack behaviours seen in mice whereby they become more aggressive (Mamiya et al. 2008). In an adult mouse, the peripheral nerves are usually a largely transcriptionally inactive and maintain in a quiescent environment. However, following peripheral nerve injury, the distal nerve stump becomes a highly active environment. High levels of migratory cells move throughout the peripheral nerve, this includes the migration of macrophages into the distal nerve stump and migration of Schwann cells, macrophages and endothelial cells into the nerve bridge to aid peripheral nerve regeneration (Cattin et al. 2015; B. Chen et al. 2019; Mueller et al. 2003; Yamauchi et al. 2008). This therefore indicates the need for multiple mechanisms to induce and control cell migration.

My data showed an increase in macrophage numbers present within the distal nerve stump of sciatic nerves following peripheral nerve injury in EphA5 KO mice compared to WT between 14-60 DPI. In vitro data which showed reduced migration of primary EphA5$^{-/-}$ macrophages or macrophage cell line RAW 264 treated with WDC to inhibit EphA5 when assessed using the scratch and transwell migration assays. This in vivo and in vitro data taken together with the documented function of EphA5-ephrin signalling suggests that signalling through EphA5 could play a role in the modulation of macrophage migration out of the peripheral nerve following injury. As there was no difference in macrophage numbers at the peak of macrophage recruitment 7-14 DPI it suggests that macrophages are able to enter the nerves normally in EphA5 KO mice but there is a delay in their efflux.

Currently there is only one known signalling mechanism that acts to modulate the migration of macrophages out of distal nerves. The Nogo receptor interacts with myelin proteins on regenerating Schwann cells which leads to RhoA activation in macrophages, reduced macrophage-myelin binding and repulsion of macrophages (Fry et al. 2007). In similarity to this mechanism, my data suggests that EphA5 expressed on macrophages within the distal nerve stump interacts with an ephrinA ligand expressed on Schwann cells. Specifically which ephrinA ligand is yet to become clear, my data shows by IHC and qRT-PCR that EphrinA1/A2/A4/A5 ligands are all expressed within the peripheral nerve following injury with Ephrin A1, A2 and A4 being expressed on Schwann cells. Treating macrophages with recombinant EphrinA2 did not increase macrophage migration, indicating that EphrinA2 is not the ligand that interacts with EphA5 and induces macrophage efflux out of the peripheral nerves. Therefore, further investigation into the role of EphrinA1 and EphrinA4 and its interaction with EphA5 expressed on macrophages within the peripheral nerves is required.

Macrophage efflux from the distal nerve stump is a requirement for the resolution of the inflammatory response and successful peripheral nerve regeneration (Gaudet et al. 2011). EphA5 KO animals not only showed an increase in macrophage numbers within the distal nerve stump up to 60 DPI compared to control mice but they also showed an upregulation of pro-inflammatory cytokines IL-1α, IL-1β and MCP at 28DPI. This suggests that macrophages persisting within the peripheral nerve at 28DPI are remaining in a pro-inflammatory state which is detrimental to the regeneration process. Although macrophages play an important role in the first stages of peripheral nerve regeneration, where the act to clear myelin and cell debris following injury, a prolonged presence of macrophages and the expression pro-inflammatory cytokines can be

detrimental to regeneration as chronic inflammation and further tissue damage can occur (P. W. Chen et al. 2015; Gaudet et al. 2011; Hirata and Kawabuchi 2002). My identification of EphA5-Ephrin signalling pathways as a potential macrophage efflux mechanism, whereby EphA5 expressed on infiltrated macrophages interacts with EphrinA on Schwann cells on remyelinating axons to induce migration and efflux out of peripheral nerves will help restore homeostasis and complete peripheral nerve regeneration.

In patients with peripheral neuropathy, macrophages enter the peripheral nerves and begin to phagocytose myelin leaving intact demyelinated axons (Martini et al. 2008; Park et al. 2020). In CMT and CDIP for instance, high numbers of macrophages within the peripheral nerves are major contributors to the pathology seen within these diseases. Degradation of myelin leads to dysfunctional Schwann cells. My data shows a mechanism whereby EphA5 interacts with EphrinA receptor on Schwann cells to induce a migratory mechanism out of the injured peripheral nerves. Due to the demyelination, CDIP and CMT patients have dysfunctional Schwann cells in their peripheral nerves (Berger et al. 2006; Maier et al. 2002). It could be suggested that CDIP and CMT patients then aren't able to express the appropriate Ephrin receptors on their Schwann cells and migratory macrophages accumulating within the peripheral nerves of these patients may not be able to undergo this Eph-ephrin interaction. Consequently, macrophages are stuck within peripheral nerves creating a pro-inflammatory, phagocytic environment. Currently there are limited therapies available to patients with CDIP and CMT, if this mechanism is shown to be playing a role in the accumulation of macrophages within the peripheral nerves and consequently the pathogenesis of these types of diseases, recombinant ephrin ligand could potentially be introduced to help induce migration of macrophages out of the peripheral nerves

which could allow remyelination of these demyelinated axons. Both studies into EphrinA ligand expression in models of peripheral neuropathy and into the downstream signalling pathways activated during this process could open up the opportunity for pharmacological intervention in patients with peripheral nerve damage or peripheral neuropathies.

Cultured Schwann cells have a distinctive bipolar morphology when cultured on PLL substrates and co-cultured with macrophages. However, when WDC is used to block EphA5 or EphA5$^{-/-}$ Schwann cells are cultured with macrophages, this distinct bipolar morphology is lost (**Figure 38)** (Weiner et al. 2001). The effect of EphA5 KO on Schwann cell migration was investigated in vivo and in vitro. EphA is thought to stimulate RhoA activation, which causes cell de-adhesion/repulsion via increased stress fibre formation (A. Singh et al. 2012). Schwann cells in EphA5 KO mice show less migration into the nerve bridge compared to WT animals. Scratch wound and transwell migration assays also show that inhibition of EphA5 using WDC in rat Schwann cells or EphA5 KO mouse Schwann cells leads to decreased migration. EphA5 KO animals show decreased regeneration into the tibial nerve due to decreased neurofilament staining; corresponding sensory and motor function recovery is also delayed in EphA5 KO animals compared to controls.

Using lineage tracing following injury repair-competent Schwann cells, also known as Bungner cells have been shown to have a distinct morphology where they elongate up to 7 times the length of a myelinating Schwann cell (Arthur-Farraj et al. 2012; Gomez-Sanchez et al. 2017). If EphA5 KO Schwann cells are not able to elongate or migrate properly to generate these tracts due to EphA5 not being expressed, then this may slow regeneration into the distal nerve. Slower axon regeneration and re-

innervation through the distal nerve stump will lead to delayed functional recovery as also seen in my experiments.

Remyelination in WT and EphA5 KO mice was investigated through EM and was seen to be reduced in EphA5 KO nerves at 28DPI. Remyelination is the final stage of peripheral nerve regeneration. Schwann cells remyelinate axons, allowing rapid impulse transmission through the peripheral nerves and recovery of sensory and motor function (Jessen and Mirsky 2019).

My work showed that there was no significant difference in remyelination at 14DPI, but at 28DPI EphA5 KO animals have an increased G ratio compared to the WT controls. This shows that axons from EphA5 KO animals are remyelinating slower than in WT animals or the myelin sheath produced is thinner. This delay in remyelination is somewhat in line with the delayed functional recovery observed in EphA5 KO mice during motor and sensory recovery tests. However, this delay in functional recovery is also observed at 14DPI and so it is surprising that a significant difference in G ratio and consequently remyelination is not observed.

Depleting macrophages has been shown to both accelerate peripheral nerve regeneration and function recovery and reduce neuropathic pain (T. Liu et al. 2000; Mert et al. 2009) Therefore, increased macrophage numbers may act to delay regeneration. Decreased remyelination may be due to the elevated expression of pro-inflammatory cytokines IL-1α, IL-1β and MCP-1 in the peripheral nerves of EphA5 KO mice. IL-β has been described to promote Schwann cell differentiation and myelin break down during Wallerian degeneration. IL-1β shows two expression peaks in WT injured peripheral nerves, one at 24hour post-injury and one at 14DPI where it promotes myelin collapse and phagocytosis through Phospholipase A_2 (Shamash et al. 2002; Trigueros et al. 2003). Although IL-1β promotes rapid Wallerian degeneration

at early time point following injury, its elevated levels may inhibit efficient Schwann cell remyelination and lead to the decreased g-ratios observed in EphA5 KO mice at 28DPI. In addition to this, both MCP-1 and IL-1β have been described to have play an instrumental role in the breakdown of myelin at early time points following injury, therefore its increased production may inhibit remyelination in the regenerating nerve accounting for these reduced g-ratio (Opree and Kress 2000). Another pro-inflammatory cytokine, IL-17, has been shown to impede myelination; IL-17 expression was not investigated in this study, but other pro-inflammatory cytokines were upregulated and this expression therefore may account for the increased g-ratio seen in EphA5 KO nerves (Stettner et al. 2014).

It is unknown why macrophages in EphA5 KO mice have increased expression of pro-inflammatory cytokines. One reason for this however could be that as macrophages are unable to leave the distal nerve stump; persisting macrophages may start to again to express pro-inflammatory cytokines and this could lead to further tissue damage as seen in patients with peripheral neuropathies and exhibiting neuropathic pain (Opree and Kress 2000; Uceyler et al. 2007). An increase in the expression of pro-inflammatory cytokines is seen in EphA5 KO mice at 28DPI so this could suggest that this mechanism of chronic inflammation is indeed occurring. As discussed previously this is also the mechanism seen within acute demyelinating neuropathies where macrophages produce pro-inflammatory cytokines and promotes the phagocytosis of myelin from peripheral nerves. Consequently, this generates a cycle where upon nerve damage macrophages are recruited into the peripheral nerves in response to pro-inflammatory cytokines to phagocytose myelin and axonal debris, this is followed by a stage transition of macrophages from pro-inflammatory to anti-inflammatory and acts to help promote macrophage clearance, axon regeneration and remyelination.

Therefore, macrophage efflux from the peripheral nerves is crucial in the later time points of peripheral nerve regeneration.

Overall this data shows a novel role for EphA5-EphrinA signalling within macrophages and Schwann cells in the distal peripheral nerve with further experiments required to confirm which EphrinA ligands are interacting with EphA5 and determination which downstream signalling pathways are activated.

5 Discussion.

Peripheral nerves have a remarkable ability to regenerate following injury unlike nerves in the central nervous system. Macrophages and inflammatory cytokine expression play a crucial role in the events that occur following peripheral nerve injury and their actions and expression must be tightly controlled to ensure chronic inflammation does not occur. Exactly how their actions are controlled is not yet entirely understood. The research in this thesis has helped to clarify how macrophage stage transition is controlled and identified a novel macrophage clearance mechanism within injured peripheral nerves. Macrophages play a pivotal role in the early stages of regeneration where they act during Wallerian degeneration to phagocytose myelin and axonal debris (Gaudet et al. 2011). Macrophages enter the peripheral nerves in a M1 pro-inflammatory state where they express pro-inflammatory cytokines which act to recruit additional macrophages, promote debris clearance and Schwann cell survival and inhibit axon outgrowth. This aids in generating a pro-regenerative environment (Gillen et al. 1998). Macrophages are also suggested to play a role in initiating angiogenesis which acts to prevent hypoxia within injured nerves but also acts to create a track through the nerve bridge that Schwann cells and axons can migrate along connecting the proximal and distal stumps (Cattin et al. 2015). A recent paper by Stratton et al., 2018 have gone on to further outline the importance of macrophages at the early stages following injury whereby removing macrophages in the peripheral nerves 1 week post injury, caused an aberrant Schwann cell response and compromised remyelination (Stratton et al. 2018). This therefore highlights the need to understand the mechanisms that will allow macrophages to transition from a M1

state into an anti-inflammatory pro-regenerative M2 state and then allow macrophages to leave the peripheral nerves once their appropriate roles have been performed. The data in this thesis showed that the neuropeptides VIP and PACAP, which have been described to modulate cytokine expression in macrophages, are able to modulate cytokine expression from both macrophages and Schwann cells in the peripheral nerves. This mechanism has been previously described but my data shows that VIP is a potent regulator of inhibiting pro-inflammatory cytokine expression and promoting the expression of anti-inflammatory cytokines. This could potentially be revolutionary for the treatment of patients with chronic pain and inflammation following peripheral nerve injury and in patients with inflammatory peripheral neuropathies as this signalling pathway could be manipulated to polarise macrophages into an M2 state (Mokarram et al. 2012). It could allow macrophages to then leave the peripheral nerves and consequently promote healing and tissue homeostasis.

In addition to this, both VIP and PACAP are able to induce the expression of myelin proteins from Schwann cells. This is the final step in peripheral nerve regeneration and patients who have previously suffered a peripheral nerve injury often have thinner myelin sheathes than that in uninjured nerve (Duncan et al. 2017). Therefore, if remyelination could be enhanced, this could lead to better functional outcomes for patients. CIDP is a debilitating condition where macrophages act to phagocytose myelin from peripheral nerves leaving intact but demyelinated axons; if macrophages can be promoted to leave the peripheral nerves, then treatment with VIP or PACAP may be also able to promote remyelination and tissue homeostasis in these patients.

As described previously macrophages are able to migrate in and out of the peripheral nerves in response to signals such as cytokines. The migration of macrophages is a crucial step in peripheral nerve regeneration and allows regenerated axons to

remyelinate. If this step does not occur, macrophages can persist in the peripheral nerves and this can lead to chronic inflammation, pain and a decreased quality of life. Currently only one mechanism for macrophage clearance is known and little investigation has been carried out in this area. My research identified EphA5 to be expressed in peripheral nerves following injury and elucidated one of its main functions is to interact with EphrinA ligand on Schwann cells to induce macrophage migration. In EphA5 KO mice macrophages persist within the peripheral nerves longer than that in WT animals suggesting that this mechanism could be responsible for macrophage migration out of the peripheral in the later stages of regeneration. In EphA5 KO animals where macrophages persist increased expression of pro-inflammatory cytokines was also observed. Expression of pro-inflammatory cytokines is observed in patients with chronic inflammatory disease and patients with peripheral neuropathies, again highlighting the need for macrophage clearance at the appropriate time points during regeneration.

5.1 Future experiments

There were two aspects to this project, VIP and PACAP as immunomodulators in the peripheral nerve and EphA5-EphrinA as a regulator of macrophage clearance and Schwann cell migration, both of which show the need for further investigation and future application. Therefore, future aims will be split into two.

VIP and PACAP have been shown to modulate the inflammatory response and induce myelination on vitro. However, their role in vivo needs to be further investigated and this could be performed through the construction and injection of VIP, PACAP or receptor specific adeno-associated viruses at different time points following injury. This would lead to constitutive expression of these peptides and aid the understanding of

how VIP and PACAP act as immunomodulators within peripheral nerves following injury and which receptors are responsible. VPAC1, VPAC2 and PAC1 deficient mice have all been generated by other labs and may be available to purchase (Abad et al. 2016; Jamen et al. 2000; Tan et al. 2015). These could be used to further investigate and clarify their functions using these in vivo models Further understanding could open the door to use these peptides therapeutically in patients with chronic inflammation following injury or with inflammatory peripheral neuropathies. In addition to this, the capacity of VIP and PACAP to induce remyelination needs to be further assessed. Again, this could be done in vivo using adeno associated viruses to treat injured nerves and assess myelination through EM and assessment of motor and sensory recovery . The use of VIP and PACAP in treating peripheral neuropathies could also be measured by using CMT or CDIP mice models and treating with VIP and PACAP at the onset of disease and when disease is well progressed.

EphA5 has been described to activate multiple downstream signalling pathways to induce actin cytoskeleton re-arrangement and cell migration. To further understand how EphA5 induces macrophage and Schwann cell migration and which specific signalling pathways are activated, proteomics and phospho-proteomics together with pathway analysis could be performed on peripheral nerves and macrophage or Schwann cell cultures to help elucidate which proteins and thus signalling pathways are activated. Further investigation and confirmation of the EphrinA ligand also responsible for the mechanism needs to be undertaken and could be performed by using additional exogenous EphrinA ligands. To further identify if this pathway has roles in inflammatory peripheral neuropathies EphA5 and EphrinA expression can be determined on sections from human patient and models of CDIP and CMT. Additionally, once the EphrinA ligand suspected to interact with EphA5 to induce

migration has been determined, this ligand could be then injected into injured peripheral nerves or the nerves in inflammatory neuropathy models to determine if macrophage clearance can be further induced.

5.2 Conclusion

This data highlights novel signalling pathways involved within the peripheral nerves helping to promote peripheral nerve repair. This interplay of first VIP and PACAP acting to promote anti-inflammatory cytokine expression, followed by the novel EphA5-Ephrin signalling pathway promoting macrophage migration out of the peripheral nerves highlights some new pathways within some of the crucial steps required for effective peripheral nerve repair. This is then followed by Schwann cell remyelination which can be induced again using neuropeptides VIP and PACAP. These novel signalling pathways have identified areas that could be further investigated and targeted therapeutically to help resolve damage and promote tissue homeostasis following peripheral neve injury.

6 References

1. Abad, C., et al. (2016), 'VPAC1 receptor (Vipr1)-deficient mice exhibit ameliorated experimental autoimmune encephalomyelitis, with specific deficits in the effector stage', Journal of Neuroinflammation, 13.
2. Aberle, H. (2019), 'Axon Guidance and Collective Cell Migration by Substrate-Derived Attractants', Frontiers in Molecular Neuroscience, 12.
3. Afshari, F. T., Kwok, J. C., and Fawcett, J. W. (2010), 'Astrocyte-Produced Ephrins Inhibit Schwann Cell Migration via VAV2 Signaling', Journal of Neuroscience, 30 (12), 4246-55.
4. Armstrong, B. D., et al. (2008), 'Impaired nerve regeneration and enhanced neuroinflarnmatory response in mice lacking pituitary adenylyl cyclase activating peptide', Neuroscience, 151 (1), 63-73.
5. Armstrong, B. D., et al. (2003), 'Lymphocyte regulation of neuropeptide gene expression after neuronal injury', Journal of Neuroscience Research, 74 (2), 240-47.
6. Arthur-Farraj, P. J., et al. (2017), 'Changes in the Coding and Non-coding Transcriptome and DNA Methylome that Define the Schwann Cell Repair Phenotype after Nerve Injury', Cell Reports, 20 (11), 2719-34.
7. Arthur-Farraj, P. J., et al. (2012), 'c-Jun Reprograms Schwann Cells of Injured Nerves to Generate a Repair Cell Essential for Regeneration', Neuron, 75 (4), 633-47.
8. Arvanitis, D. And Davy, A. (2008), 'Eph/ephrin signaling: networks', Genes & Development, 22 (4), 416-29.
9. Astin, J. W., et al. (2010), 'Competition amongst Eph receptors regulates contact inhibition of locomotion and invasiveness in prostate cancer cells', Nature Cell Biology, 12 (12), 1194-U175.
10. Avellino, A. M., et al. (1995), 'Differential macrophage responses in the peripheral and central-nervous-system during Wallerian degeneration of axons', Experimental Neurology, 136 (2), 183-98.
11. Bacallao, K. And Monje, P. V. (2015), 'Requirement of camp Signaling for Schwann Cell Differentiation Restricts the Onset of Myelination', Plos One, 10 (2).
12. Barde, Y. A., Edgar, D., and Thoenen, H. (1982), 'Purification of a new neurotrophic factor from mammalian brain', Embo Journal, 1 (5), 549-53.
13. Barras, F. M., et al. (2002), 'Glial cell line-derived neurotrophic factor released by synthetic guidance channels promotes facial nerve regeneration in the rat', Journal of Neuroscience Research, 70 (6), 746-55.
14. Barrette, B., et al. (2010), 'Transcriptional profiling of the injured sciatic nerve of mice carrying the Wld(S) mutant gene: Identification of genes involved in neuroprotection, neuroinflammation, and nerve regeneration', Brain Behavior and Immunity, 24 (8), 1254-67.
15. Barrette, B., et al. (2008), 'Requirement of myeloid cells for axon regeneration', Journal of Neuroimmunology, 203 (2), 245-45.
16. Batson, J., Astin, J. W., and Nobes, C. D. (2013), 'Regulation of contact inhibition of locomotion by Eph-ephrin signalling', Journal of Microscopy, 251 (3), 232-41.
17. Be'eri, H., et al. (1997), 'The cytokine network of wallerian degeneration: IL-10 & GM-CSF', Neuroscience Letters, S8-S8.
18. Beauchamp, A. And Debinski, W. (2012), 'Ephs and ephrins in cancer: Ephrin-A1 signalling', Seminars in Cell & Developmental Biology, 23 (1), 109-15.

19. Beirowski, B., et al. (2014), 'Metabolic regulator LKB1 is crucial for Schwann cell-mediated axon maintenance', Nature Neuroscience, 17 (10), 1351-61.
20. Bendszus, M. And Stoll, G. (2003), 'Caught in the act: In vivo mapping of macrophage infiltration in nerve injury by magnetic resonance imaging', Journal of Neuroscience, 23 (34), 10892-96.
21. Bentley, C. A. And Lee, K. F. (2000), 'p75 is important for axon growth and Schwann cell migration during development', Journal of Neuroscience, 20 (20), 7706-15.
22. Berger, P., Niemann, A., and Suter, U. (2006), 'Schwann cells and the pathogenesis of inherited motor and sensory neuropathies (Charcot-Marie-Tooth disease)', Glia, 54 (4), 243-57.
23. Bermingham, J. R., et al. (1996), 'Tst-1/Oct-6/SCIP regulates a unique step in peripheral myelination and is required for normal respiration', Genes & Development, 10 (14), 1751-62.
24. Bervar, M. (2000), 'Video analysis of standing - an alternative footprint analysis to assess functional loss following injury to the rat sciatic nerve', Journal of Neuroscience Methods, 102 (2), 109-16.
25. Bhatheja, K. And Field, J. (2006), 'Schwann cells: Origins and role in axonal maintenance and regeneration', International Journal of Biochemistry & Cell Biology, 38 (12), 1995-99.
26. Bieker, J. J. (2001), 'Kruppel-like factors: Three fingers in many pies', Journal of Biological Chemistry, 276 (37), 34355-58.
27. Bienfait, H. M. E., et al. (2006), 'Comparison of CMT1A and CMT2: similarities and differences', Journal of Neurology, 253 (12), 1572-80.
28. Bin, J. M., et al. (2015), 'Complete Loss of Netrin-1 Results in Embryonic Lethality and Severe Axon Guidance Defects without Increased Neural Cell Death', Cell Reports, 12 (7), 1099-106.
29. Birgbauer, E., et al. (2000), 'Kinase independent function of ephb receptors in retinal axon pathfinding to the optic disc from dorsal but not ventral retina', Development, 127 (6), 1231-41.
30. Blanchard, A. D., et al. (1996), 'Oct-6 (SCIP/Tst-1) is expressed in Schwann cell precursors, embryonic Schwann cells, and postnatal myelinating Schwann cells: Comparison with Oct-1, Krox-20, and Pax-3', Journal of Neuroscience Research, 46 (5), 630-40.
31. Boivin, A., et al. (2007), 'Toll-like receptor signaling is critical for Wallerian degeneration and functional recovery after peripheral nerve injury', Journal of Neuroscience, 27 (46), 12565-76.
32. Bosse, F., et al. (2006), 'Gene expression profiling reveals that peripheral nerve regeneration is a consequence of both novel injury-dependent and reactivated developmental processes', Journal of Neurochemistry, 96 (5), 1441-57.
33. Boyer, N. P. And Gupton, S. L. (2018), 'Revisiting Netrin-1: One Who Guides (Axons)', Frontiers in Cellular Neuroscience, 12.
34. Bradley, A., et al. (2012), 'The mammalian gene function resource: the international knockout mouse consortium', Mammalian Genome, 23 (9-10), 580-86.
35. Bremer, M., et al. (2011), 'Sox10 Is Required for Schwann-Cell Homeostasis and Myelin Maintenance in the Adult Peripheral Nerve', Glia, 59 (7), 1022-32.
36. Britsch, S., et al. (2001), 'The transcription factor Sox10 is a key regulator of peripheral glial development', Genes & Development, 15 (1), 66-78.

37. Brose, K., et al. (1999), 'Slit proteins bind robe receptors and have an evolutionarily conserved role in repulsive axon guidance', Cell, 96 (6), 795-806.
38. Brown, T. J., Sedhom, R., and Gupta, A. (2019), 'Chemotherapy-Induced Peripheral Neuropathy', Jama Oncology, 5 (5), 750-50.
39. Bruck, W., Huitinga, I., and Dijkstra, C. D. (1996), 'Liposome-mediated monocyte depletion during Wallerian degeneration defines the role of hematogenous phagocytes in myelin removal', Journal of Neuroscience Research, 46 (4), 477-84.
40. Bunge, R. P. (1994), 'The role of the Schwann-cell in trophic support and regeneration', Journal of Neurology, 242 (1), S19-S21.
41. Burian, B., et al. (2010), 'Vasoactive intestinal peptide (VIP) receptor expression in monocyte-derived macrophages from COPD patients', Peptides, 31 (4), 603-08.
42. Calvo, J. R., et al. (1994), 'Expression of VIP receptors in mouse peritoneal-macrophages - functional and molecular characterization', Journal of Neuroimmunology, 50 (1), 85-93.
43. Campbell, W. W. (2008), 'Evaluation and management of peripheral nerve injury', Clinical Neurophysiology, 119 (9), 1951-65.
44. Campenot, R. B. (1977), 'Local control of neurite development by nerve growth-factor', Proceedings of the National Academy of Sciences of the United States of America, 74 (10), 4516-19.
45. Caras, I. W. (1997), 'A link between axon guidance and axon fasciculation suggested by studies of the tyrosine kinase receptor epha5/REK7 and its ligand Ephrin-A5/AL-1', Cell and Tissue Research, 290 (2), 261-64.
46. Carr, L., Parkinson, D. B., and Dun, X. P. (2017), 'Expression patterns of Slit and Robo family members in adult mouse spinal cord and peripheral nervous system', Plos One, 12 (2).
47. Carrion, M., et al. (2016), 'VIP impairs acquisition of the macrophage proinflammatory polarization profile', Journal of Leukocyte Biology, 100 (6), 1385-93.
48. Castorina, A., et al. (2014), 'PACAP and VIP increase the expression of myelin-related proteins in rat schwannoma cells: Involvement of PAC1/VPAC2 receptor-mediated activation of PI3K/Akt signaling pathways', Experimental Cell Research, 322 (1), 108-21.
49. Castorina, A., et al. (2015), 'PACAP Interacts with PAC(1) Receptors to Induce Tissue Plasminogen Activator (tpa) Expression and Activity in Schwann Cell-Like Cultures', Plos One, 10 (2).
50. Castorina, A., et al. (2008), 'PACAP and VIP prevent apoptosis in schwannoma cells', Brain Research, 1241, 29-35.
51. Cattin, A. L., et al. (2015), 'Macrophage-Induced Blood Vessels Guide Schwann Cell-Mediated Regeneration of Peripheral Nerves', Cell, 162 (5), 1127-39.
52. Cervellini, I., et al. (2018), 'Sustained MAPK/ERK Activation in Adult Schwann Cells Impairs Nerve Repair', Journal of Neuroscience, 38 (3), 679-90.
53. Chan, J. R., et al. (2001), 'Neurotrophins are key mediators of the myelination program in the peripheral nervous system', Proceedings of the National Academy of Sciences of the United States of America, 98 (25), 14661-68.
54. Chance, P. F., et al. (1992), 'Analysis of the DNA duplication 17p11.2 in Charcot-Marie-Tooth neuropathy type-1 pedigrees - additional evidence for a 3rd autosomal cmt1 locus', Neurology, 42 (10), 2037-41.

55. Chen, B., et al. (2019), 'Analysis of Schwann Cell Migration and Axon Regeneration Following Nerve Injury in the Sciatic Nerve Bridge', Frontiers in Molecular Neuroscience, 12.
56. Chen, P. W., Piao, X. H., and Bonaldo, P. (2015), 'Role of macrophages in Wallerian degeneration and axonal regeneration after peripheral nerve injury', Acta Neuropathologica, 130 (5), 605-18.
57. Chen, S., et al. (2006), 'Neuregulin 1-erbb signaling is necessary for normal myelination and sensory function', Journal of Neuroscience, 26 (12), 3079-86.
58. Choi, B. O., et al. (2011), 'MPZ mutation in an early-onset Charcot-Marie-Tooth disease type 1B family by genome-wide linkage analysis', International Journal of Molecular Medicine, 28 (3), 389-96.
59. Ciaramitaro, P., et al. (2010), 'Traumatic peripheral nerve injuries: epidemiological findings, neuropathic pain and quality of life in 158 patients', Journal of the Peripheral Nervous System, 15 (2), 120-27.
60. Cisterna, B. A., Arroyo, P., and Puebla, C. (2019), 'Role of Connexin-Based Gap Junction Channels in Communication of Myelin Sheath in Schwann Cells', Frontiers in Cellular Neuroscience, 13.
61. Clements, M. P., et al. (2017), 'The Wound Microenvironment Reprograms Schwann Cells to Invasive Mesenchymal-like Cells to Drive Peripheral Nerve Regeneration', Neuron, 96 (1), 98-+.
62. Coleman, J. L. J., et al. (2015), 'Rapid knockout and reporter mouse line generation and breeding colony establishment using EUCOMM conditional-ready embryonic stem cells: a case study', Frontiers in Endocrinology, 6.
63. Cooper, M. A., Kobayashi, K., and Zhou, R. P. (2009), 'Ephrin-A5 Regulates the Formation of the Ascending Midbrain Dopaminergic Pathways', Developmental Neurobiology, 69 (1), 36-46.
64. Cosgaya, J. M., Chan, J. R., and Shooter, E. M. (2002), 'The neurotrophin receptor p75(NTR) as a positive modulator of myelination', Science, 298 (5596), 1245-48.
65. David, S. And Kroner, A. (2011), 'Repertoire of microglial and macrophage responses after spinal cord injury', Nature Reviews Neuroscience, 12 (7), 388-99.
66. Deal, D. N., Griffin, J. W., and Hogan, M. V. (2012), 'Nerve Conduits for Nerve Repair or Reconstruction', Journal of the American Academy of Orthopaedic Surgeons, 20 (2), 63-68.
67. Decker, L., et al. (2006), 'Peripheral myelin maintenance is a dynamic process requiring constant Krox20 expression', Journal of Neuroscience, 26 (38), 9771-79.
68. Deiner, M. S., et al. (1997), 'Netrin-1 and DCC mediate axon guidance locally at the optic disc: Loss of function leads to optic nerve hypoplasia', Neuron, 19 (3), 575-89.
69. Delgado, M. And Ganea, D. (2000), 'Vasoactive intestinal peptide and pituitary adenylate cyclase activating polypeptide inhibit the MEKK1/MEK4/JNK signaling pathway in LPS-stimulated macrophages', Journal of Neuroimmunology, 110 (1-2), 97-105.
70. --- (2001a), 'Inhibition of endotoxin-induced macrophage chemokine production by vasoactive intestinal peptide and pituitary adenylate cyclase-activating polypeptide in vitro and in vivo', Journal of Immunology, 167 (2), 966-75.
71. --- (2001b), 'Vasoactive intestinal peptide and pituitary adenylate cyclase-activating polypeptide inhibit nuclear factor-kappa B-dependent gene activation

at multiple levels in the human monocytic cell line THP-1', Journal of Biological Chemistry, 276 (1), 369-80.
72. Delgado, M., Jonakait, G. M., and Ganea, D. (2002), 'Vasoactive intestinal peptide and pituitary adenylate cyclase-activating polypeptide inhibit chemokine production in activated microglia', Glia, 39 (2), 148-61.
73. Delgado, M., Pozo, D., and Ganea, D. (2004), 'The significance of vasoactive intestinal peptide in immunomodulation', Pharmacological Reviews, 56 (2), 249-90.
74. Delgado, M., et al. (1999a), 'Vasoactive intestinal peptide and pituitary adenylate cyclase-activating polypeptide enhance IL-10 production by murine macrophages: In vitro and in vivo studies', Journal of Immunology, 162 (3), 1707-16.
75. Delgado, M., et al. (1999b), 'VIP and PACAP differentially regulate the costimulatory activity of resting and activated macrophages through the modulation of B7.1 and B7.2 expression', Journal of Immunology, 163 (8), 4213-23.
76. Delgado, M., et al. (1999c), 'VIP and PACAP inhibit IL-12 production in LPS-stimulated macrophages. Subsequent effect on IFN gamma synthesis by T cells', Journal of Neuroimmunology, 96 (2), 167-81.
77. Delgado, M., et al. (2001), 'Vasoactive intestinal peptide prevents experimental arthritis by downregulating both autoimmune and inflammatory components of the disease', Nature Medicine, 7 (5), 563-68.
78. Deretzi, G., et al. (1999), 'Local effects of recombinant rat interleukin-6 on the peripheral nervous system', Immunology, 97 (4), 582-87.
79. Dickson, B. J. And Gilestro, G. F. (2006), 'Regulation of commissural axon pathfinding by slit and its robo receptors', Annual Review of Cell and Developmental Biology, 22, 651-75.
80. Dong, Z., et al. (1995), 'Neu differentiation factor is a neuron-glia signal and regulates survival, proliferation, and maturation of rat Schwann-cell precursors', Neuron, 15 (3), 585-96.
81. Dubovy, P., Klusakova, I., and Svizenska, I. H. (2014), 'Inflammatory Profiling of Schwann Cells in Contact with Growing Axons Distal to Nerve Injury', Biomed Research International.
82. Dun, X. P. And Parkinson, D. B. (2015), 'Visualizing Peripheral Nerve Regeneration by Whole Mount Staining', Plos One, 10 (3).
83. --- (2017), 'Role of Netrin-1 Signaling in Nerve Regeneration', International Journal of Molecular Sciences, 18 (3).
84. Dun, X. P., et al. (2019), 'Macrophage-Derived Slit3 Controls Cell Migration and Axon Pathfinding in the Peripheral Nerve Bridge', Cell Reports, 26 (6), 1458-+.
85. Duncan, I. D., et al. (2017), 'Thin myelin sheaths as the hallmark of remyelination persist over time and preserve axon function', Proceedings of the National Academy of Sciences of the United States of America, 114 (45), E9685-E91.
86. Egea, J. And Klein, R. (2007), 'Bidirectional Eph-ephrin signaling during axon guidance', Trends in Cell Biology, 17 (5), 230-38.
87. Ernfors, P., et al. (1990), 'Molecular-cloning and neurotrophic activities of a protein with structural similarities to nerve growth-factor - developmental and topographical expression in the brain', Proceedings of the National Academy of Sciences of the United States of America, 87 (14), 5454-58.

88. Fazal, S. V., et al. (2017), 'Graded Elevation of c-Jun in Schwann Cells In Vivo: Gene Dosage Determines Effects on Development, Remyelination, Tumorigenesis, and Hypomyelination', Journal of Neuroscience, 37 (50), 12297-313.
89. Figlia, G. (2018), 'c-Jun in Schwann Cells: Stay Away from Extremes', Journal of Neuroscience, 38 (14), 3388-90.
90. Figlia, G., et al. (2017), 'Dual function of the PI3K-Akt-mtorc1 axis in myelination of the peripheral nervous system', Elife, 6.
91. Finsterer, J., et al. (2018), 'CMT2 due to homozygous MFN2 variants is a multiorgan mitochondrial disorder', European Journal of Paediatric Neurology, 22 (5), 889-91.
92. Fledrich, R., Stassart, R. M., and Sereda, M. W. (2012), 'Murine therapeutic models for Charcot-Marie-Tooth (CMT) disease', British Medical Bulletin, 102 (1), 89-113.
93. Fletcher, A. (2016), 'Action potential: generation and propagation', Anaesthesia and Intensive Care Medicine, 17 (4), 204-08.
94. Fontana, X., et al. (2012), 'c-Jun in Schwann cells promotes axonal regeneration and motoneuron survival via paracrine signaling', Journal of Cell Biology, 198 (1), 127-41.
95. Fricker, F. R., et al. (2011), 'Axonally Derived Neuregulin-1 Is Required for Remyelination and Regeneration after Nerve Injury in Adulthood', Journal of Neuroscience, 31 (9), 3225-33.
96. Frisen, J., et al. (1998), 'Ephrin-A5 (AL-1/RAGS) is essential for proper retinal axon guidance and topographic mapping in the mammalian visual system', Neuron, 20 (2), 235-43.
97. Frostick, S. P., Yin, Q., and Kemp, G. J. (1998), 'Schwann cells, neurotrophic factors, and peripheral nerve regeneration', Microsurgery, 18 (7), 397-405.
98. Fry, E. J., Ho, C., and David, S. (2007), 'A role for Nogo receptor in macrophage clearance from injured peripheral nerve', Neuron, 53 (5), 649-62.
99. Ganea, D. And Delgado, M. (2002), 'Vasoactive intestinal peptide (VIP) and pituitary adenylate cyclase-activating polypeptide (PACAP) as modulators of both innate and adaptive immunity', Critical Reviews in Oral Biology & Medicine, 13 (3), 229-37.
100. Garbay, B., et al. (2000), 'Myelin synthesis in the peripheral nervous system', Progress in Neurobiology, 61 (3), 267-304.
101. Gaudet, A. D., Popovich, P. G., and Ramer, M. S. (2011), 'Wallerian degeneration: Gaining perspective on inflammatory events after peripheral nerve injury', Journal of Neuroinflammation, 8.
102. Ghazvini, M., et al. (2002), 'A cell type-specific allele of the POU gene Oct-6 reveals Schwann cell autonomous function in nerve development and regeneration', Embo Journal, 21 (17), 4612-20.
103. Ghislain, J. And Charnay, P. (2006), 'Control of myelination in Schwann cells: a Krox20 cis-regulatory element integrates Oct6, Brn2 and Sox10 activities', Embo Reports, 7 (1), 52-58.
104. Giaginis, C., et al. (2010), 'Clinical Significance of Ephrin (Eph)-A1,-A2,-A4,-A5 and-A7 Receptors in Pancreatic Ductal Adenocarcinoma', Pathology & Oncology Research, 16 (2), 267-76.
105. Gillen, C., Jander, S., and Stoll, G. (1998), 'Sequential expression of mrna for proinflammatory cytokines and interleukin-10 in the rat peripheral

nervous system: Comparison between immune-mediated demyelination and Wallerian degeneration', Journal of Neuroscience Research, 51 (4), 489-96.
106. Goethals, S., et al. (2010), 'Toll-Like Receptor Expression in the Peripheral Nerve', Glia, 58 (14), 1701-09.
107. Gomez-Sanchez, J. A., et al. (2017), 'After Nerve Injury, Lineage Tracing Shows That Myelin and Remak Schwann Cells Elongate Extensively and Branch to Form Repair Schwann Cells, Which Shorten Radically on Remyelination', Journal of Neuroscience, 37 (37), 9086-99.
108. Gomez-Sanchez, J. A., et al. (2015), 'Schwann cell autophagy, myelinophagy, initiates myelin clearance from injured nerves', Journal of Cell Biology, 210 (1), 153-68.
109. Gomis-Coloma, C., et al. (2018), 'Class iia histone deacetylases link camp signaling to the myelin transcriptional program of Schwann cells', Journal of Cell Biology, 217 (4), 1249-68.
110. Gonzalez-Rey, E., et al. (2006a), 'Vasoactive intestinal peptide induces CD4+,CD25+T regulatory cells with therapeutic effect in collagen-induced arthritis', Arthritis and Rheumatism, 54 (3), 864-76.
111. Gonzalez-Rey, E., et al. (2006b), 'Therapeutic effect of vasoactive intestinal peptide on experimental autoimmune encephalomyelitis - Down-regulation of inflammatory and autoimmune responses', American Journal of Pathology, 168 (4), 1179-88.
112. Gordon, T. (2014), 'Neurotrophic factor expression in denervated motor and sensory Schwann cells: Relevance to specificity of peripheral nerve regeneration', Experimental Neurology, 254, 99-108.
113. Gourlet, P., et al. (1997), 'In vitro properties of a high affinity selective antagonist of the VIP1 receptor', Peptides, 18 (10), 1555-60.
114. Graham, J. B. And Muir, D. (2016), 'Chondroitinase C Selectively Degrades Chondroitin Sulfate Glycosaminoglycans that Inhibit Axonal Growth within the Endoneurium of Peripheral Nerve', Plos One, 11 (12).
115. Greenfield, S., et al. (1973), 'Protein composition of myelin of peripheral nervous-system', Journal of Neurochemistry, 20 (4), 1207-+.
116. Griffin, J. W. And Thompson, W. J. (2008), 'Biology and Pathology of Nonmyelinating Schwann cells', Glia, 56 (14), 1518-31.
117. Grinsell, D. And Keating, C. P. (2014), 'Peripheral Nerve Reconstruction after Injury: A Review of Clinical and Experimental Therapies', Biomed Research International, 2014.
118. Groh, J., et al. (2010), 'Attenuation of MCP-1/CCL2 expression ameliorates neuropathy in a mouse model for Charcot-Marie-Tooth 1X', Human Molecular Genetics, 19 (18), 3530-43.
119. Grove, M., et al. (2020), 'Axon-dependent expression of YAP/TAZ mediates Schwann cell remyelination but not proliferation after nerve injury', Elife, 9.
120. Guo, L., et al. (2012), 'Rac1 Controls Schwann Cell Myelination through camp and NF2/merlin', Journal of Neuroscience, 32 (48), 17251-61.
121. Hadden, R. D. M., et al. (1998), 'Electrophysiological classification of Guillain-Barre syndrome: Clinical associations and outcome', Annals of Neurology, 44 (5), 780-88.
122. Hall, S. (2005), 'The response to injury in the peripheral nervous system', Journal of Bone and Joint Surgery-British Volume, 87B (10), 1309-19.

123. Hallbook, F. (1999), 'Evolution of the vertebrate neurotrophin and Trk receptor gene families', Current Opinion in Neurobiology, 9 (5), 616-21.
124. Hanemann, C. O. And Muller, H. W. (1998), 'Pathogenesis of Charcot-Marie-Tooth IA (CMTIA) neuropathy', Trends in Neurosciences, 21 (7), 282-86.
125. Harmar, A. J., et al. (1998), 'International Union of Pharmacology. XVIII. Nomenclature of receptors for vasoactive intestinal peptide and pituitary adenylate cyclase-activating polypeptide', Pharmacological Reviews, 50 (2), 265-70.
126. Harrisingh, M. C., et al. (2004), 'The Ras/Raf/ERK signalling pathway drives Schwann cell dedifferentiation', Embo Journal, 23 (15), 3061-71.
127. Hartung, H. P. And Toyka, K. V. (1990), 'T-cell and macrophage activation in experimental autoimmune neuritis and guillain-barre-syndrome', Annals of Neurology, 27, S57-S63.
128. Helmbacher, F., et al. (2000), 'Targeting of the epha4 tyrosine kinase receptor affects dorsal/ventral pathfinding of limb motor axons', Development, 127 (15), 3313-24.
129. Heumann, R., et al. (1987), 'Differential regulation of messenger-rna encoding nerve growth-factor and its receptor in rat sciatic-nerve during development, degeneration, and regeneration - role of macrophages', Proceedings of the National Academy of Sciences of the United States of America, 84 (23), 8735-39.
130. Hirai, H., et al. (1987), 'A novel putative tyrosine kinase receptor encoded by the eph gene', Science, 238 (4834), 1717-20.
131. Hirata, K. And Kawabuchi, M. (2002), 'Myelin phagocytosis by macrophages and nonmacrophages during Wallerian degeneration', Microscopy Research and Technique, 57 (6), 541-47.
132. Huan, X. L., et al. (2013), 'Unique Structure and Dynamics of the epha5 Ligand Binding Domain Mediate Its Binding Specificity as Revealed by X-ray Crystallography, NMR and MD Simulations', Plos One, 8 (9).
133. Huang, E. J. And Reichardt, L. F. (2001), 'Neurotrophins: Roles in neuronal development and function', Annual Review of Neuroscience, 24, 677-736.
134. Huang, L. L., et al. (2018), 'A compound scaffold with uniform longitudinally oriented guidance cues and a porous sheath promotes peripheral nerve regeneration in vivo', Acta Biomaterialia, 68, 223-36.
135. Huang, Z., et al. (2020), 'Perspective on Schwann Cells Derived from Induced Pluripotent Stem Cells in Peripheral Nerve Tissue Engineering', Cells, 9 (11).
136. Ikeda, M., et al. (2014), 'Acceleration of peripheral nerve regeneration using nerve conduits in combination with induced pluripotent stem cell technology and a basic fibroblast growth factor drug delivery system', Journal of Biomedical Materials Research Part A, 102 (5), 1370-78.
137. Ip, C. W., et al. (2006), 'Role of immune cells in animal models for inherited peripheral neuropathies', Neuromolecular Medicine, 8 (1-2), 175-89.
138. Jamen, F., et al. (2000), 'PAC1 receptor-deficient mice display impaired insulinotropic response to glucose and reduced glucose tolerance', Journal of Clinical Investigation, 105 (9), 1307-15.
139. Jang, S. W., et al. (2010), 'Locus-wide identification of Egr2/Krox20 regulatory targets in myelin genes', Journal of Neurochemistry, 115 (6), 1409-20.

140. Jen, J. C., et al. (2004), 'Mutations in a human ROBO gene disrupt hindbrain axon pathway crossing and morphogenesis', Science, 304 (5676), 1509-13.
141. Jessen, K. R. And Mirsky, R. (2005), 'The origin and development of glial cells in peripheral nerves', Nature Reviews Neuroscience, 6 (9), 671-82.
142. --- (2016), 'The repair Schwann cell and its function in regenerating nerves', Journal of Physiology-London, 594 (13), 3521-31.
143. --- (2019), 'The Success and Failure of the Schwann Cell Response to Nerve Injury', Frontiers in Cellular Neuroscience, 13.
144. Jessen, K. R. And Arthur-Farraj, P. (2019), 'Repair Schwann cell update: Adaptive reprogramming, EMT, and stemness in regenerating nerves', Glia, 67 (3), 421-37.
145. Jessen, K. R., Mirsky, R., and Lloyd, A. C. (2015), 'Schwann Cells: Development and Role in Nerve Repair', Cold Spring Harbor Perspectives in Biology, 7 (7).
146. Jeub, M., et al. (2020), 'Reduced inflammatory response and accelerated functional recovery following sciatic nerve crush lesion in CXCR3-deficient mice', Neuroreport, 31 (9), 672-77.
147. Jing, W., et al. (2018), 'Constructing conductive conduit with conductive fibrous infilling for peripheral nerve regeneration', Chemical Engineering Journal, 345, 566-77.
148. Jung, J., et al. (2011), 'Actin Polymerization Is Essential for Myelin Sheath Fragmentation during Wallerian Degeneration', Journal of Neuroscience, 31 (6), 2009-15.
149. Kalluri, R. And Weinberg, R. A. (2009), 'The basics of epithelial-mesenchymal transition', Journal of Clinical Investigation, 119 (6), 1420-28.
150. Kawasaki, T., et al. (2003), 'Oct6, a transcription factor controlling myelination, is a marker for active nerve regeneration in peripheral neuropathies', Acta Neuropathologica, 105 (3), 203-08.
151. Keleman, K. And Dickson, B. J. (2001), 'Short- and long-range repulsion by the Drosophila Unc5 netrin receptor', Neuron, 32 (4), 605-17.
152. Keynes, R. And Cook, G. M. W. (1995), 'Axon guidance molecules', Cell, 83 (2), 161-69.
153. Kigerl, K. A., et al. (2009), 'Identification of Two Distinct Macrophage Subsets with Divergent Effects Causing either Neurotoxicity or Regeneration in the Injured Mouse Spinal Cord', Journal of Neuroscience, 29 (43), 13435-44.
154. Kiguchi, N., et al. (2010), 'Macrophage inflammatory protein-1 alpha mediates the development of neuropathic pain following peripheral nerve injury through interleukin-1 beta up-regulation', Pain, 149 (2), 305-15.
155. Kitsukawa, T., et al. (1997), 'Neuropilin-semaphorin III/D-mediated chemorepulsive signals play a crucial role in peripheral nerve projection in mice', Neuron, 19 (5), 995-1005.
156. Klein, D. And Martini, R. (2016), 'Myelin and macrophages in the PNS: An intimate relationship in trauma and disease', Brain Research, 1641, 130-38.
157. Klein, R. (2004), 'Eph/ephrin signaling in morphogenesis, neural development and plasticity', Current Opinion in Cell Biology, 16 (5), 580-89.
158. Klein, S., et al. (2016), 'Collagen Type I Conduits for the Regeneration of Nerve Defects', Materials, 9 (4).

159. Knoferle, J., et al. (2010), 'Mechanisms of acute axonal degeneration in the optic nerve in vivo', Proceedings of the National Academy of Sciences of the United States of America, 107 (13), 6064-69.
160. Kobayashi, H., et al. (2008), 'mmps initiate Schwann cell-mediated MBP degradation and mechanical nociception after nerve damage', Molecular and Cellular Neuroscience, 39 (4), 619-27.
161. Kobsar, I., et al. (2005), 'Evidence for macrophage-mediated myelin disruption in an animal model for Charcot-Marie-Tooth neuropathy type 1A', Journal of Neuroscience Research, 81 (6), 857-64.
162. Kohler, C. (2007), 'Allograft inflammatory factor-1/Ionized calcium-binding adapter molecule 1 is specifically expressed by most subpopulations of macrophages and spermatids in testis', Cell and Tissue Research, 330 (2), 291-302.
163. Koncina, E., et al. (2007), 'Role of semaphorins during axon growth and guidance', Axon Growth and Guidance, 621, 50-64.
164. Krajewski, K. M., et al. (2000), 'Neurological dysfunction and axonal degeneration in Charcot-Marie-Tooth disease type 1A', Brain, 123, 1516-27.
165. Kuhlmann, T., et al. (2001), 'Macrophages are eliminated from the injured peripheral nerve via local apoptosis and circulation to regional lymph nodes and the spleen', Journal of Neuroscience, 21 (10), 3401-08.
166. Kullander, K. And Klein, R. (2002), 'Mechanisms and functions of EPH and ephrin signalling', Nature Reviews Molecular Cell Biology, 3 (7), 475-86.
167. Le, N., et al. (2005), 'Analysis of congenital hypomyelinating Egr2(Lo/Lo) nerves identifies Sox2 as an inhibitor of Schwann cell differentiation and myelination', Proceedings of the National Academy of Sciences of the United States of America, 102 (7), 2596-601.
168. Leblanc, S. E., et al. (2006), 'Direct regulation of myelin protein zero expression by the Egr2 transactivator', Journal of Biological Chemistry, 281 (9), 5453-60.
169. Lee, H., et al. (2009), 'Vasoactive Intestinal Peptide Inhibits Toll-Like Receptor 3-Induced Nitric Oxide Production in Schwann Cells and Subsequent Sensory Neuronal Cell Death In Vitro', Journal of Neuroscience Research, 87 (1), 171-78.
170. Leimeroth, R., et al. (2002), 'Membrane-bound neuregulin1 type III actively promotes Schwann cell differentiation of multipotent progenitor cells', Developmental Biology, 246 (2), 245-58.
171. Lemke, G., Lamar, E., and Pafterson, J. (2008), 'Isolation and Analysis of the Gene Encoding Peripheral Myelin Protein Zero', Neuron, 60 (3), 403-03.
172. Leonhard, S. E., et al. (2020), 'Guillain-Barre syndrome related to Zika virus infection: A systematic review and meta-analysis of the clinical and electrophysiological phenotype', Plos Neglected Tropical Diseases, 14 (4).
173. Leonhard, S. E., et al. (2019), 'Diagnosis and management of Guillain-Barre syndrome in ten steps', Nature Reviews Neurology, 15 (11), 671-83.
174. Li, G. C., et al. (2014a), 'Porous chitosan scaffolds with surface micropatterning and inner porosity and their effects on Schwann cells', Biomaterials, 35 (30), 8503-13.
175. Li, R. J., et al. (2014b), 'Peripheral Nerve Injuries Treatment: a Systematic Review', Cell Biochemistry and Biophysics, 68 (3), 449-54.
176. Lioudyno, M., et al. (1998), 'Pituitary adenylate cyclase-activating polypeptide (PACAP) protects dorsal root ganglion neurons from death and

induces calcitonin gene-related peptide (CGRP) immunoreactivity in vitro', Journal of Neuroscience Research, 51 (2), 243-56.
177. Lisabeth, E. M., Falivelli, G., and Pasquale, E. B. (2013), 'Eph Receptor Signaling and Ephrins', Cold Spring Harbor Perspectives in Biology, 5 (9).
178. Liu, G. F., et al. (2009), 'DSCAM functions as a netrin receptor in commissural axon pathfinding', Proceedings of the National Academy of Sciences of the United States of America, 106 (8), 2951-56.
179. Liu, T., van Rooijen, N., and Tracey, D. J. (2000), 'Depletion of macrophages reduces axonal degeneration and hyperalgesia following nerve injury', Pain, 86 (1-2), 25-32.
180. Livak, K. J. And Schmittgen, T. D. (2001), 'Analysis of relative gene expression data using real-time quantitative PCR and the 2(T)(-Delta Delta C) method', Methods, 25 (4), 402-08.
181. Lodish, H. F. (2000), 'Molecular Cell Biology. 4th edition. Section 21.2 The Action Potential and Conduction of Electric Impulses', (New York).
182. Long, H., et al. (2004), 'Conserved roles for slit and robo proteins in midline commissural axon guidance', Neuron, 42 (2), 213-23.
183. Lundborg, G., et al. (1982), 'Nerve regeneration in silicone chambers - influence of gap length and of distal stump components', Experimental Neurology, 76 (2), 361-75.
184. Madison, R. D., Zomorodi, A., and Robinson, G. A. (2000), 'Netrin-1 and peripheral nerve regeneration in the adult rat', Experimental Neurology, 161 (2), 563-70.
185. Maier, M., Berger, P., and Suter, U. (2002), 'Understanding Schwann cell-neurone interactions: the key to Charcot-Marie-Tooth disease?', Journal of Anatomy, 200 (4), 357-66.
186. Maisonpierre, P. C., et al. (1991), 'Human and rat brain-derived neurotrophic factor and neurotrophin-3 - gene structures, distributions, and chromosomal localizations', Genomics, 10 (3), 558-68.
187. Mallon, B. S., et al. (2002), 'Proteolipid promoter activity distinguishes two populations of NG2-positive cells throughout neonatal cortical development', Journal of Neuroscience, 22 (3), 876-85.
188. Mamiya, P. C., et al. (2008), 'Changes in attack behavior and activity in epha5 knockout mice', Brain Research, 1205, 91-99.
189. Mantovani, A., et al. (2004), 'The chemokine system in diverse forms of macrophage activation and polarization', Trends in Immunology, 25 (12), 677-86.
190. Marillat, V., et al. (2002), 'Spatiotemporal expression patterns of slit and robo genes in the rat brain', Journal of Comparative Neurology, 442 (2), 130-55.
191. Martens, W., et al. (2014), 'Human dental pulp stem cells can differentiate into Schwann cells and promote and guide neurite outgrowth in an aligned tissue-engineered collagen construct in vitro', Faseb Journal, 28 (4), 1634-43.
192. Martinez, C., et al. (2002), 'Anti-inflammatory role in septic shock of pituitary adenylate cyclase-activating polypeptide receptor', Proceedings of the National Academy of Sciences of the United States of America, 99 (2), 1053-58.
193. Martini, R., Klein, D., and Groh, J. (2013), 'Similarities between Inherited Demyelinating Neuropathies and Wallerian Degeneration An Old Repair

Program May Cause Myelin and Axon Perturbation under Non lesion Conditions', American Journal of Pathology, 183 (3), 655-60.
194. Martini, R., et al. (2008), 'Interactions Between Schwann Cells and Macrophages in Injury and Inherited Demyelinating Disease', Glia, 56 (14), 1566-77.
195. Martini, R., et al. (1995), 'Mice doubly deficient in the genes for P0 and myelin basic-protein show that both proteins contribute to the formation of the major dense line in peripheral-nerve myelin', Journal of Neuroscience, 15 (6), 4488-95.
196. Maurel, P. And Salzer, J. L. (2000), 'Axonal regulation of Schwann cell proliferation and survival and the initial events of myelination requires PI 3-kinase activity', Journal of Neuroscience, 20 (12), 4635-45.
197. Mayor, R. And Carmona-Fontaine, C. (2010), 'Keeping in touch with contact inhibition of locomotion', Trends in Cell Biology, 20 (6), 319-28.
198. Mccarthy, N. And Giesecke, J. (2001), 'Incidence of Guillain-Barre syndrome following infection with Campylobacter jejuni', American Journal of Epidemiology, 153 (6), 610-14.
199. Mckerracher, L., et al. (1994), 'Identification of myelin-associated glycoprotein as a major myelin-derived inhibitor of neurite growth', Neuron, 13 (4), 805-11.
200. Menorca, R. M. G., Fussell, T. S., and Elfar, J. C. (2013), 'Nerve Physiology Mechanisms of Injury and Recovery', Hand Clinics, 29 (3), 317-+.
201. Mert, T., et al. (2009), 'Macrophage depletion delays progression of neuropathic pain in diabetic animals', Naunyn-Schmiedebergs Archives of Pharmacology, 379 (5), 445-52.
202. Meyer, D. And Birchmeier, C. (1995), 'Multiple essential functions of neuregulin in development', Nature, 378 (6555), 386-90.
203. Miao, H. And Wang, B. C. (2009), 'Eph/ephrin signaling in epithelial development and homeostasis', International Journal of Biochemistry & Cell Biology, 41 (4), 762-70.
204. --- (2012), 'epha receptor signaling-Complexity and emerging themes', Seminars in Cell & Developmental Biology, 23 (1), 16-25.
205. Michailov, G. V., et al. (2004), 'Axonal neuregulin-1 regulates myelin sheath thickness', Science, 304 (5671), 700-03.
206. Mietto, B. S., et al. (2015), 'Role of IL-10 in Resolution of Inflammation and Functional Recovery after Peripheral Nerve Injury', Journal of Neuroscience, 35 (50), 16431-42.
207. Min, Q., Parkinson, D. B., and Dun, X. P. (2021), 'Migrating Schwann cells direct axon regeneration within the peripheral nerve bridge', Glia, 69 (2), 235-54.
208. Mindos, T., et al. (2017), 'Merlin controls the repair capacity of Schwann cells after injury by regulating Hippo/YAP activity', Journal of Cell Biology, 216 (2), 495-510.
209. Miranda, G. E. And Torres, R. Y. (2016), 'Epidemiology of Traumatic Peripheral Nerve Injuries Evaluated with Electrodiagnostic Studies in a Tertiary Care Hospital Clinic', Puerto Rico Health Sciences Journal, 35 (2), 76-80.
210. Misko, A. L., et al. (2012), 'Mitofusin2 Mutations Disrupt Axonal Mitochondrial Positioning and Promote Axon Degeneration', Journal of Neuroscience, 32 (12), 4145-55.

211. Miyata, A., et al. (1989), 'Isolation of a novel-38 residue-hypothalamic polypeptide which stimulates adenylate-cyclase in pituitary-cells', Biochemical and Biophysical Research Communications, 164 (1), 567-74.
212. Mizisin, A. P. And Weerasuriya, A. (2011), 'Homeostatic regulation of the endoneurial microenvironment during development, aging and in response to trauma, disease and toxic insult', Acta Neuropathologica, 121 (3), 291-312.
213. Mogha, A., et al. (2013), 'Gpr126 Functions in Schwann Cells to Control Differentiation and Myelination via G-Protein Activation', Journal of Neuroscience, 33 (46), 17976-85.
214. Mogha, A., et al. (2016), 'Gpr126/Adgrg6 Has Schwann Cell Autonomous and Nonautonomous Functions in Peripheral Nerve Injury and Repair', Journal of Neuroscience, 36 (49), 12351-67.
215. Mokarram, N., et al. (2012), 'Effect of modulating macrophage phenotype on peripheral nerve repair', Biomaterials, 33 (34), 8793-801.
216. Monje, P. V., Bunge, M. B., and Wood, P. M. (2006), 'Cyclic AMP synergistically enhances neuregulin-dependent ERK and Akt activation and cell cycle progression in Schwann cells', Glia, 53 (6), 649-59.
217. Monk, K. R., et al. (2011), 'Gpr126 is essential for peripheral nerve development and myelination in mammals', Development, 138 (13), 2673-80.
218. Monk, K. R., et al. (2009), 'A G Protein-Coupled Receptor Is Essential for Schwann Cells to Initiate Myelination', Science, 325 (5946), 1402-05.
219. Morgan, L., Jessen, K. R., and Mirsky, R. (1991), 'The effects of camp on differentiation of cultured schwann-cells - progression from an early phenotype (04+) to a myelin phenotype (P0+, GFAP-, N-CAM-, NGF-receptor-) depends on growth-inhibition', Journal of Cell Biology, 112 (3), 457-67.
220. Morris, J. K., et al. (1999), 'Rescue of the cardiac defect in erbb2 mutant mice reveals essential roles of erbb2 in peripheral nervous system development', Neuron, 23 (2), 273-83.
221. Muangsanit, P., et al. (2020), 'Rapidly formed stable and aligned dense collagen gels seeded with Schwann cells support peripheral nerve regeneration', Journal of Neural Engineering, 17 (4).
222. Mueller, M., et al. (2003), 'Macrophage response to peripheral nerve injury: The quantitative contribution of resident and hematogenous macrophages', Laboratory Investigation, 83 (2), 175-85.
223. Muppirala, A. N., et al. (2021), 'Schwann cell development: From neural crest to myelin sheath', Wiley Interdisciplinary Reviews-Developmental Biology, 10 (5).
224. Murai, K. K., et al. (2003), 'Control of hippocampal dendritic spine morphology through ephrin-A3/epha4 signaling', Nature Neuroscience, 6 (2), 153-60.
225. Murphy, P. G., et al. (1999), 'Endogenous interleukin-6 contributes to hypersensitivity to cutaneous stimuli and changes in neuropeptides associated with chronic nerve constriction in mice', European Journal of Neuroscience, 11 (7), 2243-53.
226. Muscella, A., et al. (2020), 'TGF-beta 1 activates RSC96 Schwann cells migration and invasion through MMP-2 and MMP-9 activities', Journal of Neurochemistry, 153 (4), 525-38.
227. Napoli, I., et al. (2012), 'A Central Role for the ERK-Signaling Pathway in Controlling Schwann Cell Plasticity and Peripheral Nerve Regeneration In Vivo', Neuron, 73 (4), 729-42.

228. Neukomm, L. J. And Freeman, M. R. (2014), 'Diverse cellular and molecular modes of axon degeneration', Trends in Cell Biology, 24 (9), 515-23.
229. Newbern, J. And Birchmeier, C. (2010), 'Nrg1/erbb signaling networks in Schwann cell development and myelination', Seminars in Cell & Developmental Biology, 21 (9), 922-28.
230. Ng, T., et al. (2013), 'Class 3 Semaphorin Mediates Dendrite Growth in Adult Newborn Neurons through Cdk5/FAK Pathway', Plos One, 8 (6).
231. Nguyen, T. M., et al. (2017), 'epha5 and epha7 forward signaling enhances human hematopoietic stem and progenitor cell maintenance, migration, and adhesion via Rac 1 activation', Experimental Hematology, 48, 72-78.
232. Nicoletti, F., et al. (2005), 'Macrophage migration inhibitory factor (MIF) seems crucially involved in Guillain-Barre syndrome and experimental allergic neuritis', Journal of Neuroimmunology, 168 (1-2), 168-74.
233. Nocera, G. And Jacob, C. (2020), 'Mechanisms of Schwann cell plasticity involved in peripheral nerve repair after injury', Cellular and Molecular Life Sciences, 77 (20), 3977-89.
234. Norrmen, C., et al. (2014), 'mtorc1 Controls PNS Myelination along the mtorc1-RXR gamma-SREBP-Lipid Biosynthesis Axis in Schwann Cells', Cell Reports, 9 (2), 646-60.
235. Novak, M. L. And Koh, T. J. (2013), 'Phenotypic Transitions of Macrophages Orchestrate Tissue Repair', American Journal of Pathology, 183 (5), 1352-63.
236. Ogata, T., et al. (2004), 'Opposing extracellular signal-regulated kinase and Akt pathways control Schwann cell myelination', Journal of Neuroscience, 24 (30), 6724-32.
237. Olsson, Y. And Kristensson, K. (1973), 'Perineurium as a diffusion barrier to protein tracers following trauma to nerves', Acta Neuropathologica, 23 (2), 105-11.
238. Opal, S. M. And depalo, V. A. (2000), 'Anti-inflammatory cytokines', Chest, 117 (4), 1162-72.
239. Opree, A. And Kress, M. (2000), 'Involvement of the proinflammatory cytokines tumor necrosis factor-alpha, IL-1 beta,and IL-6 but not IL-8 in the development of heat hyperalgesia: Effects on heat-evoked calcitonin gene-related peptide release from rat skin', Journal of Neuroscience, 20 (16), 6289-93.
240. Ozkaynak, E., et al. (2010), 'Adam22 Is a Major Neuronal Receptor for Lgi4-Mediated Schwann Cell Signaling', Journal of Neuroscience, 30 (10), 3857-64.
241. Pan, B., et al. (2017), 'Gene expression analysis at multiple time-points identifies key genes for nerve regeneration', Muscle & Nerve, 55 (3), 373-83.
242. Pareek, S., et al. (1993), 'Detection and processing of peripheral myelin protein pmp22 in cultured Schwann-cells', Journal of Biological Chemistry, 268 (14), 10372-79.
243. Park, H. T., et al. (2020), 'Behind the pathology of macrophage-associated demyelination in inflammatory neuropathies: demyelinating Schwann cells', Cellular and Molecular Life Sciences, 77 (13), 2497-506.
244. Parkinson, D. B., et al. (2004), 'Krox-20 inhibits Jun-NH(2)-terminal kinase/c-Jun to control Schwann cell proliferation and death', Journal of Cell Biology, 164 (3), 385-94.

245. Parkinson, D. B., et al. (2008), 'c-Jun is a negative regulator of myelination', Journal of Cell Biology, 181 (4), 625-37.
246. Parrinello, S., et al. (2010), 'EphB Signaling Directs Peripheral Nerve Regeneration through Sox2-Dependent Schwann Cell Sorting', Cell, 143 (1), 145-55.
247. Pasquale, E. B. (2008), 'Eph-ephrin bidirectional signaling in physiology and disease', Cell, 133 (1), 38-52.
248. Peltonen, Sirkku, Alanne, Maria, and Peltonen, Juha (2013), 'Barriers of the peripheral nerve', Tissue barriers, 1 (3), e24956-e56.
249. Perlin, J. R. And Talbot, W. S. (2007), 'Putting the glue in glia: Necls mediate Schwann cell-axon adhesion', Journal of Cell Biology, 178 (5), 721-23.
250. Perrin, F. E., et al. (2005), 'Involvement of monocyte chemoattractant protein-1, macrophage inflammatory protein-1 alpha and interleukin-1 beta in Wallerian degeneration', Brain, 128, 854-66.
251. Perry, V. H., Brown, M. C., and Gordon, S. (1987), 'The macrophage response to central and peripheral-nerve injury - a possible role for macrophages in regeneration', Journal of Experimental Medicine, 165 (4), 1218-23.
252. Qin, J., et al. (2016), 'Concentrated growth factor promotes Schwann cell migration partly through the integrin beta 1-mediated activation of the focal adhesion kinase pathway', International Journal of Molecular Medicine, 37 (5), 1363-70.
253. Qu, W. R., et al. (2021), 'Interaction between Schwann cells and other cells during repair of peripheral nerve injury', Neural Regeneration Research, 16 (1), 93-98.
254. Raasakka, A., et al. (2017), 'Membrane Association Landscape of Myelin Basic Protein Portrays Formation of the Myelin Major Dense Line', Scientific Reports, 7.
255. Radic, B., Radic, P., and Durakovic, D. (2018), 'Peripheral nerve injury in sports', Acta Clinica Croatica, 57 (3), 561-69.
256. Ran, W. Z., et al. (2015), 'Vasoactive intestinal peptide suppresses macrophage-mediated inflammation by downregulating interleukin-17A expression via PKA- and PKC-dependent pathways', International Journal of Experimental Pathology, 96 (4), 269-75.
257. Rawlins, F. A., et al. (1972), 'Fine-structural localization of cholesterol-1,2-3h in degenerating and regenerating mouse sciatic nerve', Journal of Cell Biology, 52 (3), 615-+.
258. Reichert, F., Levitzky, R., and Rotshenker, S. (1996), 'Interleukin 6 in intact and injured mouse peripheral nerves', European Journal of Neuroscience, 8 (3), 530-35.
259. Ridley, A. J. (2006), 'Rho gtpases and actin dynamics in membrane protrusions and vesicle trafficking', Trends in Cell Biology, 16 (10), 522-29.
260. Riethmacher, D., et al. (1997), 'Severe neuropathies in mice with targeted mutations in the erbb3 receptor', Nature, 389 (6652), 725-30.
261. Roa, B. B., et al. (1993), 'Charcot-Marie-Tooth disease type-1a - association with a spontaneous point mutation in the pmp22 gene', New England Journal of Medicine, 329 (2), 96-101.
262. Robinson, L. R. (2000), 'Traumatic injury to peripheral nerves', Muscle & Nerve, 23 (6), 863-73.

263. Rodger, J., et al. (2001), 'Expression of ephrin-A2 in the superior colliculus and epha5 in the retina following optic nerve section in adult rat', European Journal of Neuroscience, 14 (12), 1929-36.
264. Rosenberg, A. F., et al. (2012), 'In Vivo Nerve-Macrophage Interactions Following Peripheral Nerve Injury', Journal of Neuroscience, 32 (11), 3898-909.
265. Roszer, T. (2015), 'Understanding the Mysterious M2 Macrophage through Activation Markers and Effector Mechanisms', Mediators of Inflammation, 2015.
266. Rotshenker, S. (2011), 'Wallerian degeneration: the innate-immune response to traumatic nerve injury', Journal of Neuroinflammation, 8.
267. Rotshenker, S., Aamar, S., and Barak, V. (1992), 'Interleukin-1 activity in lesioned peripheral-nerve', Journal of Neuroimmunology, 39 (1-2), 75-80.
268. Russell, S. W., Gillespie, G. Y., and Pace, J. L. (1980), 'Comparison of responses to activating agents by mouse peritoneal-macrophages and cells of the macrophage line Raw-264', Journal of the Reticuloendothelial Society, 27 (6), 607-19.
269. Sagane, K., et al. (2005), 'Ataxia and peripheral nerve hypomyelination in ADAM22-deficient mice', Bmc Neuroscience, 6.
270. Said, S. I. And Mutt, V. (1970), 'Polypeptide with broad biological activity - isolation from small intestine', Science, 169 (3951), 1217.
271. Said, S. I. And Mutt, V. (1972), 'Isolation from porcine intestinal wall of a vasoactive octacosapeptide related to secretin and to glucagon', European Journal of Biochemistry, 28 (2), 199.
272. Sanen, K., et al. (2017), 'Engineered neural tissue with Schwann cell differentiated human dental pulp stem cells: potential for peripheral nerve repair?', Journal of Tissue Engineering and Regenerative Medicine, 11 (12), 3362-72.
273. Santoro, L., et al. (2004), 'A novel mutation of myelin protein zero associated with an axonal form of Charcot-Marie-Tooth disease', Journal of Neurology Neurosurgery and Psychiatry, 75 (2), 262-65.
274. Saporta, A. S. D., et al. (2011), 'Charcot-Marie-Tooth Disease Subtypes and Genetic Testing Strategies', Annals of Neurology, 69 (1), 22-33.
275. Schlaepfer, W. W. (1974), 'Calcium-induced degeneration of axoplasm in isolated segments of rat peripheral-nerve', Brain Research, 69 (2), 203-15.
276. Schmidt, A. And Hall, A. (2002), 'Guanine nucleotide exchange factors for Rho gtpases: turning on the switch', Genes & Development, 16 (13), 1587-609.
277. Serafini, T., et al. (1996), 'Netrin-1 is required for commissural axon guidance in the developing vertebrate nervous system', Cell, 87 (6), 1001-14.
278. Serpe, C. J., et al. (2002), 'Functional recovery after facial nerve crush is delayed in severe combined immunodeficient mice', Brain Behavior and Immunity, 16 (6), 808-12.
279. Shamah, S. M., et al. (2001), 'epha receptors regulate growth cone dynamics through the novel guanine nucleotide exchange factor ephexin', Cell, 105 (2), 233-44.
280. Shamash, S., Reichert, F., and Rotshenker, S. (2002), 'The cytokine network of Wallerian degeneration: tumour necrosis factor-alpha, interleukin-1 alpha, and interleukin-1 beta', Journal of Neuroscience, 22 (8), 3052-60.

281. Sharief, M. K., mclean, B., and Thompson, E. J. (1993), 'Elevated serum levels of tumor-necrosis-factor-alpha in guillain-barre-syndrome', Annals of Neurology, 33 (6), 591-96.
282. Sharma, A., Verhaagen, J., and Harvey, A. R. (2012), 'Receptor complexes for each of the Class 3 Semaphorins', Frontiers in Cellular Neuroscience, 6.
283. Shen, D. H., et al. (2018), 'Beneficial or Harmful Role of Macrophages in Guillain-Barre Syndrome and Experimental Autoimmune Neuritis', Mediators of Inflammation.
284. Sherman, D. L., et al. (2012), 'Arrest of Myelination and Reduced Axon Growth When Schwann Cells Lack mtor', Journal of Neuroscience, 32 (5), 1817-25.
285. Sheu, J. Y., Kulhanek, D. J., and Eckenstein, F. P. (2000), 'Differential patterns of ERK and STAT3 phosphorylation after sciatic nerve transection in the rat', Experimental Neurology, 166 (2), 392-402.
286. Shibata, A., et al. (2003), 'Peripheral nerve induces macrophage neurotrophic activities: regulation of neuronal process outgrowth, intracellular signaling and synaptic function', Journal of Neuroimmunology, 142 (1-2), 112-29.
287. Shubayev, V. I. And Myers, R. R. (2000), 'Upregulation and interaction of TNF alpha and gelatinases A and B in painful peripheral nerve injury', Brain Research, 855 (1), 83-89.
288. Shubayev, V. I., et al. (2006), 'TNF alpha-induced MMP-9 promotes macrophage recruitment into injured peripheral nerve', Molecular and Cellular Neuroscience, 31 (3), 407-15.
289. Siebert, H., et al. (2000), 'The chemokine receptor CCR2 is involved in macrophage recruitment to the injured peripheral nervous system', Journal of Neuroimmunology, 110 (1-2), 177-85.
290. Sindrilaru, A., et al. (2011), 'An unrestrained proinflammatory M1 macrophage population induced by iron impairs wound healing in humans and mice', Journal of Clinical Investigation, 121 (3), 985-97.
291. Singh, A., Winterbottom, E., and Daar, I. O. (2012), 'Eph/ephrin signaling in cell-cell and cell-substrate adhesion', Frontiers in Bioscience-Landmark, 17, 473-97.
292. Singh, R., Kishore, L., and Kaur, N. (2014), 'Diabetic peripheral neuropathy: Current perspective and future directions', Pharmacological Research, 80, 21-35.
293. Song, X. Y., et al. (2006), 'Knockout of p75(NTR) impairs re-myelination of injured sciatic nerve in mice', Journal of Neurochemistry, 96 (3), 833-42.
294. Spiegel, I., et al. (2007), 'A central role for Necl4 (syncam4) in Schwann cell- axon interaction and myelination', Nature Neuroscience, 10 (7), 861-69.
295. Stein, E. And Tessier-Lavigne, M. (2001), 'Hierarchical organization of guidance receptors: Silencing of netrin attraction by slit through a Robo/DCC receptor complex', Science, 291 (5510), 1928-38.
296. Steinecke, A., et al. (2014), 'epha/ephrin A reverse signaling promotes the migration of cortical interneurons from the medial ganglionic eminence', Development, 141 (2), 460-71.
297. Stettner, M., et al. (2014), 'Interleukin-17 impedes Schwann cell-mediated myelination', Journal of Neuroinflammation, 11.

298. Stierli, S., et al. (2018), 'The regulation of the homeostasis and regeneration of peripheral nerve is distinct from the CNS and independent of a stem cell population', Development, 145 (24).
299. Stino, A. M. And Smith, A. G. (2017), 'Peripheral neuropathy in prediabetes and the metabolic syndrome', Journal of Diabetes Investigation, 8 (5), 646-55.
300. Storka, A., et al. (2013), 'VPAC1 receptor expression in peripheral blood mononuclear cells in a human endotoxemia model', Journal of Translational Medicine, 11.
301. Stratton, J. A., et al. (2018), 'Macrophages Regulate Schwann Cell Maturation after Nerve Injury', Cell Reports, 24 (10), 2561-+.
302. Sullivan, R., et al. (2016), 'Peripheral Nerve Injury: Stem Cell Therapy and Peripheral Nerve Transfer', International Journal of Molecular Sciences, 17 (12).
303. Sun, C. X., et al. (2017), 'IL-17 contributed to the neuropathic pain following peripheral nerve injury by promoting astrocyte proliferation and secretion of proinflammatory cytokines', Molecular Medicine Reports, 15 (1), 89-96.
304. Sun, W., et al. (2000), 'Vasoactive intestinal peptide (VIP) inhibits TGF-beta 1 production in murine macrophages', Journal of Neuroimmunology, 107 (1), 88-99.
305. Tan, Y. V., et al. (2015), 'VPAC2 (vasoactive intestinal peptide receptor type 2) receptor deficient mice develop exacerbated experimental autoimmune encephalomyelitis with increased Th1/Th17 and reduced Th2/Treg responses', Brain Behavior and Immunity, 44, 167-75.
306. Tan, Y. V., et al. (2009), 'Pituitary adenylyl cyclase-activating polypeptide is an intrinsic regulator of Treg abundance and protects against experimental autoimmune encephalomyelitis', Proceedings of the National Academy of Sciences of the United States of America, 106 (6), 2012-17.
307. Taylor, C. A., et al. (2008), 'The incidence of peripheral nerve injury in extremity trauma', American Journal of Physical Medicine & Rehabilitation, 87 (5), 381-85.
308. Topilko, P., et al. (1994), 'Krox-20 controls myelination in the peripheral nervous-system', Nature, 371 (6500), 796-99.
309. Trigueros, S. D. A., Kalyvas, A., and David, S. (2003), 'Phospholipase A(2) plays an important role in myelin breakdown and phagocytosis during Wallerian degeneration', Molecular and Cellular Neuroscience, 24 (3), 753-65.
310. Truett, G. E., et al. (2000), 'Preparation of PCR-quality mouse genomic DNA with hot sodium hydroxide and tris (hotshot)', Biotechniques, 29 (1), 52-+.
311. Ubogu, E. E. (2020), 'Biology of the human blood-nerve barrier in health and disease', Experimental Neurology, 328.
312. Uceyler, N., et al. (2007), 'Differential expression of cytokines in painful and painless neuropathies', Neurology, 69 (1), 42-49.
313. Uncini, A., et al. (1999), 'Effect of rhtnf-alpha injection into rat sciatic nerve', Journal of Neuroimmunology, 94 (1-2), 88-94.
314. Van den Berg, B., et al. (2014), 'Guillain-Barre syndrome: pathogenesis, diagnosis, treatment and prognosis', Nature Reviews Neurology, 10 (8), 469-82.

315. Van Rossum, D., et al. (2008), 'Myelin-phagocytosing macrophages in isolated sciatic and optic nerves reveal a unique reactive phenotype', Glia, 56 (3), 271-83.
316. Vaudry, D., et al. (2009), 'Pituitary Adenylate Cyclase-Activating Polypeptide and Its Receptors: 20 Years after the Discovery', Pharmacological Reviews, 61 (3), 283-357.
317. Vellozzi, C., Iqbal, S., and Broder, K. (2014), 'Guillain-Barre Syndrome, Influenza, and Influenza Vaccination: The Epidemiologic Evidence', Clinical Infectious Diseases, 58 (8), 1149-55.
318. Viader, A., et al. (2011), 'Schwann Cell Mitochondrial Metabolism Supports Long-Term Axonal Survival and Peripheral Nerve Function', Journal of Neuroscience, 31 (28), 10128-40.
319. Vogelaar, C. F., et al. (2004), 'Sciatic nerve regeneration in mice and rats: recovery of sensory innervation is followed by a slowly retreating neuropathic pain-like syndrome', Brain Research, 1027 (1-2), 67-72.
320. Wagner, R. And Myers, R. R. (1996), 'Schwann cells produce tumor necrosis factor alpha: Expression in injured and non-injured nerves', Neuroscience, 73 (3), 625-29.
321. Wahl, S., et al. (2000), 'Ephrin-A5 induces collapse of growth cones by activating Rho and Rho kinase', Journal of Cell Biology, 149 (2), 263-70.
322. Waller, A (1850), 'Experiments on the section of the glossopharyngeal and hypoglossal nerves of the frog, and observations of the alterations produced thereby in the structure of their primitive fibres.', (Philosophical
323. Transactions of the Royal Society of London).
324. Wang, J. B., et al. (2016), 'Novel Roles and Mechanism for Kruppel-like Factor 16 (KLF16) Regulation of Neurite Outgrowth and Ephrin Receptor A5 (epha5) Expression in Retinal Ganglion Cells', Journal of Biological Chemistry, 291 (35), 18084-95.
325. Wang, Y. And Yin, F. (2016), 'A Review of X-linked Charcot-Marie-Tooth Disease', Journal of Child Neurology, 31 (6), 761-72.
326. Waschek, J. A. (2013), 'VIP and PACAP: neuropeptide modulators of CNS inflammation, injury, and repair', British Journal of Pharmacology, 169 (3), 512-23.
327. Weiner, J. A., et al. (2001), 'Regulation of Schwann cell morphology and adhesion by receptor-mediated lysophosphatidic acid signaling', Journal of Neuroscience, 21 (18), 7069-78.
328. Willison, H. J., Jacobs, B. C., and van Doorn, P. A. (2016), 'Guillain-Barre syndrome', Lancet, 388 (10045), 717-27.
329. Woodhoo, A. And Sommer, L. (2008), 'Development of the Schwann Cell Lineage: From the Neural Crest to the Myelinated Nerve', Glia, 56 (14), 1481-90.
330. Xiao, H. S., et al. (2002), 'Identification of gene expression profile of dorsal root ganglion in the rat peripheral axotomy model of neuropathic pain', Proceedings of the National Academy of Sciences of the United States of America, 99 (12), 8360-65.
331. Xiao, J. H., Kilpatrick, T. J., and Murray, S. S. (2009), 'The Role of Neurotrophins in the Regulation of Myelin Development', Neurosignals, 17 (4), 265-76.

332. Xing, Z., et al. (1998), 'IL-6 is an antiinflammatory cytokine required for controlling local or systemic acute inflammatory responses', Journal of Clinical Investigation, 101 (2), 311-20.
333. Xu, N. J. And Henkemeyer, M. (2012), 'Ephrin reverse signaling in axon guidance and synaptogenesis', Seminars in Cell & Developmental Biology, 23 (1), 58-64.
334. Yamauchi, J., et al. (2008), 'erbb2 directly activates the exchange factor Dock7 to promote Schwann cell migration', Journal of Cell Biology, 181 (2), 351-65.
335. Ydens, E., et al. (2012), 'Acute injury in the peripheral nervous system triggers an alternative macrophage response', Journal of Neuroinflammation, 9.
336. Yu, T. W. And Bargmann, C. I. (2001), 'Dynamic regulation of axon guidance', Nature Neuroscience, 4, 1169-76.
337. Yuan, W. L., et al. (1999), 'The mouse SLIT family: Secreted ligands for ROBO expressed in patterns that suggest a role in morphogenesis and axon guidance', Developmental Biology, 212 (2), 290-306.
338. Yue, Y., et al. (2002), 'Mistargeting hippocampal axons by expression of a truncated Eph receptor', Proceedings of the National Academy of Sciences of the United States of America, 99 (16), 10777-82.
339. Zhang, F. C., et al. (2020), 'Changes of pro-inflammatory and anti-inflammatory macrophages after peripheral nerve injury', Rsc Advances, 10 (64), 38767-73.
340. Zhang, H. H., et al. (2018), 'Toll-Like Receptor 4 (TLR4) Expression Affects Schwann Cell Behavior in vitro', Scientific Reports, 8.
341. Zhang, Q. L., et al. (2002), 'Local administration of vasoactive intestinal peptide after nerve transection accelerates early myelination and growth of regenerating axons', Journal of the Peripheral Nervous System, 7 (2), 118-27.
342. Zhang, Q. L., et al. (1996), 'Vasoactive intestinal peptide: Mediator of laminin synthesis in cultured Schwann cells', Journal of Neuroscience Research, 43 (4), 496-502.
343. Zhou, X. R., et al. (1999), 'Axotomy-induced changes in pituitary adenylate cyclase activating polypeptide (PACAP) and PACAP receptor gene expression in the adult rat facial motor nucleus', Journal of Neuroscience Research, 57 (6), 953-61.
344. Zigmond, R. E. (2012), 'Cytokines that promote nerve regeneration', Experimental Neurology, 238 (2), 101-06.
345. Zigrnond, R. E. And Echevarria, F. D. (2019), 'Macrophage biology in the peripheral nervous system after injury', Progress in Neurobiology, 173, 102-21.